INFORMATION TO USERS

This manuscript has been reproduced from the microfilm master. UMI films the text directly from the original or copy submitted. Thus, some thesis and dissertation copies are in typewriter face, while others may be from any type of computer printer.

The quality of this reproduction is dependent upon the quality of the copy submitted. Broken or indistinct print, colored or poor quality illustrations and photographs, print bleedthrough, substandard margins, and improper alignment can adversely affect reproduction.

In the unlikely event that the author did not send UMI a complete manuscript and there are missing pages, these will be noted. Also, if unauthorized copyright material had to be removed, a note will indicate the deletion.

Oversize materials (e.g., maps, drawings, charts) are reproduced by sectioning the original, beginning at the upper left-hand corner and continuing from left to right in equal sections with small overlaps. Each original is also photographed in one exposure and is included in reduced form at the back of the book.

Photographs included in the original manuscript have been reproduced xerographically in this copy. Higher quality 6" x 9" black and white photographic prints are available for any photographs or illustrations appearing in this copy for an additional charge. Contact UMI directly to order.

UMI

A Bell & Howell Information Company
300 North Zeeb Road, Ann Arbor MI 48106-1346 USA
313/761-4700 800/521-0600

Université d'Ottawa · University of Ottawa

Abstract

A number of dienophiles and ketones have been prepared and the resultant π-facial selectivity of these substrates in Diels-Alder and nucleophilic additions have been investigated. The ketene equivalent dienophile **46** gave all four possible cycloadducts when reacted with cyclopentadiene under thermal conditions. The resultant π-facial selectivity was in accord with the calculated electrostatic potential surface of **46**. The π-facial selectivity of the double bond isomer of dienophile **46** was also in accord with the electrostatic potential model. The use of boron trichloride at low temperatures resulted in the isolation of a single *endo* cycloadduct with complete π-facial selectivity in the Diels-Alder reaction of **46** with cyclopentadiene. The Cieplak model was not followed in either thermal or Lewis acid-catalyzed conditions employed. The π-facial selectivity of a number of cyclic ketones containing adjacent heteroatoms using organometallic and reducing agents was examined. The π-facial selectivity was independant of the size of reducing agent, contrary to results using cyclohexanones. The use of diisobutylaluminum hydride produced a reversal of π-facial selectivity in cyclopentanones **97**, **108**, **114**, but no reversal was observed with spiro-ketones **129** and **133**. The failure of the Cieplak model in many of the reduction reactions indicates that transition state stabilization by hyperconjugation is not an important factor. In many of the cases, electrostatic potential surfaces correctly predicted π-facial selectivity. Carbon nucleophiles such as methyllithium added to give the major diastereomer predicted by the Cieplak model in all cases examined except tetrahydrofuran **129**. The levels of π-facial selectivity for both carbon nucleophile addition and reduction reactions were at synthetically useful levels for most reagents with the exception of zinc borohydride.

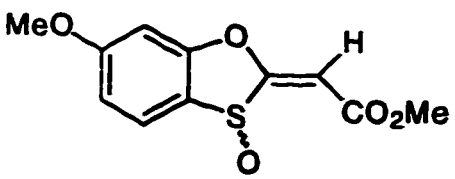

46

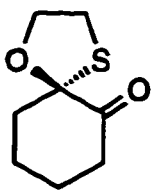

97

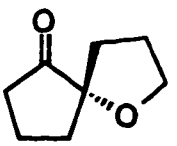

129

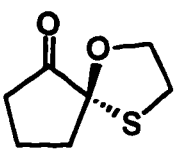

108

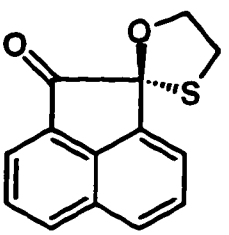

114

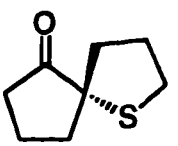

133

Acknowledgments

I would first like to extend my sincere thanks to Professor Alex Fallis for providing an environment that was not only scientifically rewarding, but also allowed for the development of a strong friendship. Professor Fallis' patience and his policy of scientific freedom is a unique combination that will be difficult to find elsewhere. I would also like to thank the faculty members and staff of the chemistry department of the University of Ottawa, especially Professor Howard Alper, Professor Tony Durst and Professor Bob Fraser for invaluable help over the course of my studies in Ottawa. I am indebted to Lise Maisonneuve for taking care of the administration side of things. I have been fortunate to have had the pleasure of meeting and working with very talented people over the years and thank them also.

Thanks: Mike "I'm watching you" T., Curt "Dinkboy" H., Tham "Tammy" P., KG, Sardine, Bogdan, Scoot, Pete, Helene (KB), Helen, Ronnie, Stevie, Jim, Ron, Irina, Clauido, Jodi, Mike, Jon, Simon, David, Tim O, The Mrs., Miguel, Isaac, Fung, Tim, Wesely, Agent 35, Hang-Ten, Chuckles, Karen, Sherissa, Anne, the Killer, no thanks to the BFH. Thanks also Peter, Jane, Cindy, Bob, John K., Don and John, Jacqueline and Leslie, Frank, Mick Pickwick.

Contents

Acknowledgements iii

List of Schemes viii

List of Figures x

List of Tables xiv

Chapter 1 π-Facial Selectivity in Diels-Alder Cycloadditions 1

1.1 Introduction 1

1.2 Previous Studies 3

1.3 Diels-Alder Reactions of 5-Substituted Cyclopentadienes 6

1.4 Models to Predict π-Facial Selectivity in the Diels-Alder Reaction 8

1.4.1 Orbital distortions 8

1.4.2 Electrostatic model 10

1.4.3 Paquette model 11

1.4.4 Torsional strain 12

1.4.5 Anh model 13

1.4.6 Hyperconjugative stabilization 14

1.5 Research Objectives 16

Chapter 1 References 18

Chapter 2 The Development of a Chiral Ketene Equivalent: Results and Discussion 21

2.1 Introduction 21

2.2 Preparation and Reactivity of Oxathiolane **26** 23

2.2.1 Synthesis of ester **26** 23

2.2.2 Diels-Alder reactions of ester **26** 27

2.2.3 Attempted preparation of diester **36** 30

2.3 Preparation and Reactivity of Vinyl Sulfoxide **46** 35

2.3.1 Vinyl sulfoxides in Diels-Alder reactions 35
2.3.2 Preparation of sulfoxide **46** 39
2.3.3 Thermal Diels-Alder cycloadditions of sulfoxide **46** 40
2.3.4 Thermal Diels-Alder cycloadditions of sulfoxide **56** 43
2.4 Rationalization of Observed π-Facial Selectivity 46
2.4.1 Filled orbital replusion 46
2.4.2 Electrostatic replusion 47
2.4.3 Transition state stabilization by hyperconjugation 54
2.5 Lewis Acid-Catalyzed Diels-Alder Reaction of Sulfoxide **46** 57
2.6 Synthesis of 2-Norbornenone **77** 61
2.7 Preparation of Optically Active 2-Norbornenone (+)-**77** 67
2.8 Conclusions 71
Chapter 2 References 73
Chapter 3 π-Selectivity Models for the Addition of Nucleophiles to Carbonyl Groups 76
3.1 Introduction 76
3.2 Cram Open Chain Model 81
3.3 Cram Chelate Model 83
3.4 Cornforth Dipolar Model 84
3.5 Karabatsos Model 84
3.6 Felkin Model 86
3.6.1 Acyclic ketones 86
3.6.2 Cyclic ketones 88
3.7 Steric Approach Control and Product Development Control 91
3.8 Carbonyl LUMO Extension 92
3.9 Felkin-Anh Model 92
3.9.1 Acyclic ketones 94

3.9.2 Cyclic ketones 97
3.10 Wigfield Model 98
3.11 Cieplak Hyperconjugative Model 99
3.12 Electrostatic Potential Model 102
3.13 Research Objectives 104
Chapter 3 References 106
Chapter 4 π-Facial Selectivity of Cyclic Ketones Containing Adjacent Heteroatoms: Results and Discussion 109
4.1 Introduction 109
4.2 Preparation of Cyclohexanone **97** 112
4.3 Nucleophilic Additions to Cyclohexanone **97** 113
4.3.1 Conformational considerations 113
4.3.2 Reactions of cyclohexanone **97** with Grignard and reducing agents 115
4.4 Cyclopentanone Systems 120
4.4.1 Preparation of cyclopentanone **108** 122
4.4.2 Carbon nucleophile addition to cyclopentanone **108** 124
4.4.3 Hydride additions 126
4.4.4 Preparation of napthalene **114** 128
4.4.5 Carbon nucleophile additions 130
4.4.6 Relative stereochemistry of the major diastereomer from Grignard addition to cyclopentanone **108** 133
4.4.7 Hydride additions 136
4.5 Factors that Influence π-Facial Selectivity of Ketones **108** and **114** 139
4.5.1 Steric interactions 139
4.5.2 Chelation control 140
4.5.3 Nucleophile approach angle 145
4.5.4 Hyperconjugative transition state stabilization 149

4.5.5 Electrostatic potential 153
4.6 Spiro-tetrahydrofuran and -tetrahydrothiophene Systems 154
4.6.1 Preparation of tetrahydrofuran **129** and tetrahydrothiophene **133** 155
4.6.2 π-Facial selectivity of tetrahydrofuran **129** 158
4.6.3 π-Facial selectivity of tetrahydrothiophene **133** 161
4.6.4 Sulfur ylides 162
4.7 Conclusions 165
Chapter 4 References 168
Experimental 172
Appendix 232

Schemes

2.1	Oxathiolane dienophiles as ketene equivalents	22
2.2	Synthesis of ester **26**	24
2.3	Wittig reaction of anhydride **27** and ylide **28**	25
2.4	Attempted Diels-Alder reactions of ester **26**	27
2.5	Attempted Wittig reaction of oxathiolane **25**	30
2.6	Attempted sunthesis of ylide **35**	32
2.7	Synthesis of ylide **35**	32
2.8	Attempted synthesis of diester **36**	33
2.9	Formation of disulfide **42**	34
2.10	Diels-Alder reaction of vinyl sulfoxide **47**	36
2.11	Oxidation of oxathiolane **26**	39
2.12	Diels-Alder reaction of sulfoxide **46** with cyclopentadiene	40
2.13	Diels-Alder reaction of sulfoxide **56** with cyclopentadiene	44
2.14	Diels-Alder reaction of thiirene **64**	47
2.15	Removal of sulfoxide group to give norbornenone **75**	61
2.16	Conversion of sulfoxide **51** to norbornenone **75**	63
2.17	Deoxygenation of sulfoxide **51**	63
2.18	Conversion of oxathiolane **74** to norbornenones **75** and **76**	65
2.19	Preparation of chiral sulfoxide (+)-**46**	69
2.20	Diene approach *syn* to the sulfur lone pair	70
2.21	Preparation of optically active 2-norbornenone (+)-**77**	71
4.1	Eliel's stereoselective Grignard reaction	110
4.2	Conjugative addition of Grignard reagents to cyclohexanone **90**	111
4.3	Synthesis of cyclohexanone **97**	112
4.4	Alternate synthesis of **97**	113

4.5 Attempted synthesis of 1,2-cyclopentadione 123

4.6 Synthesis of cyclopentanone **108** 123

4.7 Synthesis of napthalene **114** 128

4.8 Synthesis of epoxyalcohol **127** 156

4.9 Synthesis of tetrahydrofuran **129** 157

4.10 Synthesis of tetrahydrothiophene **133** 157

4.11 Sulfur ylide addition to ketone **129** 163

Figures

1.1	The Diels-Alder cycloaddition	1
1.2	Four possible cycloadducts from the Diels-Alder reaction	2
1.3	Two classes of dienes used in diastereoselectivity studies	4
1.4	Heteroatom influence on π-facial selectivity	4
1.5	Contrasteric Diels-Alder reactions	5
1.6	Related dienes that display high π-facial selectivity	7
1.7	Diene orbital distortions	8
1.8	Electrostatic interactions that influence π-facial selectivity	10
1.9	Paquette orbital tilting model	11
1.10	Reduction of torsional strain favours *endo* approach	13
1.11	Transition state stabilization by heteroatom lone pair	13
1.12	Hyperconjugative stabilization of a σ* orbital	14
1.13	Cieplak model	15
1.14	High π-facial selectivity is observed with 2,5-dimethylthiophene oxide	16
1.15	Oxathiolane acetals as π-facial selectivity control elements in Diels-Alder reactions	17
2.1	Dienophile effects on π-facial selectivity	21
2.2	Proposed mechanism for Z-configuration	26
2.3	Donor-acceptor dienophiles	28
2.4	Comparison of the LUMO energy of ethylene and acrolein	31
2.5	Disulfide **42** formation	34
2.6	Proposed cycloaddition of sulfoxide **46**	35
2.7	Diene approach *syn* to lone pair	37
2.8	Calculated preferred conformation of sulfoxide **49**	38
2.9	ORTEP structure of cycloadduct **51**	41

2.10 Diene approaches *syn* to sulfide lone pair 43

2.11 Filled orbital replusion gives *anti* approach 46

2.12 Electrostatic potential surfaces of sulfoxides **64** and **66** 48

2.13 Electrostatic potential surfaces of substituted cyclopentadienes 49

2.14 Electrostatic potential surface of sulfoxide **46** 51

2.15 AM1 structure of sulfoxide **46** 52

2.16 Electrostatic potential surface of sulfoxide **56** 53

2.17 Cieplak and electrostatic model predictions 54

2.18 Orbital symmetry of the Diels-Alder reaction 55

2.19 Sulfur lone pair orbital overlap 56

2.20 Secondary orbital interactions 57

2.21 The affect of Lewis acid on dienophile LUMO 58

2.22 Selected ^{1}H NMR signals of sulfoxide **51** and sulfide **73** 64

2.23 Optically active sulfoxide dienophiles 68

3.1 Two possible approaches of a nucleophile to a carbonyl group 76

3.2 The formation of diastereomeric products upon nucleophilic addition to chiral ketones 77

3.3 Cram's rule 78

3.4 The preferential axial attack of $NaBH_4$ on 4-*tert*-butylcyclohexanone 79

3.5 Cram's rule predicts preferential formation of diastereomer **A** 81

3.6 Important rotamers for Cram's rule 81

3.7 Nucleophilic attack over the least hindered π-face 82

3.8 The effect of increasing R group bulk on π-facial selectivity 83

3.9 Cram chelate model 83

3.10 Polar substituents become the **L** group in the Cornforth model 84

3.11 Important rotamers in the Karabatsos model 85

3.12 Felkin model transition state rotamers 87

3.13	Transition states in the Felkin model for cyclic ketones	89
3.14	Torsional strain during axial and equatorial nucleophilic attack	89
3.15	Product Development Control interactions	91
3.16	Steric Approach Control interactions	92
3.17	Carbonyl LUMO extension	93
3.18	Non-perpendicular attack as a result of orbital interactions	94
3.19	Two possible approaches of a nucleophile along the Bürgi-Dunitz trajectory	96
3.20	Interaction of carbonyl LUMO with adjacent σ^* orbital	96
3.21	Ring flattening favours axial approach	97
3.22	Transition states for $NaBH_4$ reduction of unhindered and hindered cyclohexanones	98
3.23	Cieplak model for axial and equatorial nucleophilic attack	100
3.24	The Cieplak model as applied to 5-substituted 2-adamantanones	101
3.25	Substrates used in electrostatic potential studies	103
3.26	Computer-generated electrostatic potential surfaces	103
3.27	Heteroatom-containing substrates used in π-facial selectivity studies	105
4.1	Heteroatom control of carbonyl addition reactions	110
4.2	Grignard addition *via* Cram chelate	111
4.3	Ground state chair conformer energies of **97**	113
4.4	Axial and equatorial conformer energies	114
4.5	Space-filling models of **97**	117
4.6	Torsional strain from nucleophilic attack	118
4.7	Hyperconjugative stabilization of the forming nucleophile-carbon bond	118
4.8	Grignard addition according to Cram chelate model	119
4.9	Cyclopentanedione monoacetals used in π-facial selectivity study	121
4.10	Optimized structure of cyclopentanone **108**	121

4.11 ORTEP structure of 1-napthylurethane derivative **112** 127

4.12 Optimized structure of napthalene **114** 128

4.13 ORTEP structure of napthalene **114** 130

4.14 ORTEP structure of diastereomer **115** 132

4.15 ^{1}H NMR spectra of oxathiolane methylene region 134

4.16 ORTEP structure of diastereomer **118** 137

4.17 Summary of nucleophilic additions to cyclopentanone **108** and napthalene **114** 138

4.18 Space-filling models of cyclopentanone **108** and napthalene **114** 139

4.19 Expected π-facial selectivity according to Cram chelate model 141

4.20 Lanthanide reversal of diastereoselectivity 143

4.21 Bulky Lewis acids promote axial attack 144

4.22 Substituted adamantanones as probes for electronic effects 146

4.23 Optimized structure of 5-azoadamantanone *N*-oxide 146

4.24 Differences in steric interactions for *syn* and *anti* attack 147

4.25 Cieplak model 149

4.26 Expected π-facial selectivity based on the Cieplak model 150

4.27 Electrostatic potential surface of napthalene **114** 153

4.28 Does removal of heteroatom change π-facial selectivity? 154

4.29 Conjugate addition follows the Cieplak model 155

4.30 π-Facial control with tetrahydrofuran substituent 155

4.31 Comparison of the ^{1}H NMR spectra of the diastereomers from the reduction of ketone **129** 159

4.32 Comparison of the ^{1}H NMR signals of alcohols **134**, **109b**, and **116** 160

4.33 Electrostatic potential surfaces of ketones **129** and **133** 162

4.34 Sulfur ylide addition to ketones **129**, **108**, and **114** 164

Tables

1.1	π-Facial Selectivity of 5-Substituted Pentamethylcyclopentadienes	6
2.1	Comparison of Dienophile Bond Orders and LUMO Energy	29
2.2	π-Facial Selectivity of Chiral Vinyl Sulfoxide **48**	37
2.3	Selected ^{1}H NMR Chemical Shift Values of Adducts **51** to **54**	42
2.4	Selected ^{1}H NMR Chemical Shift Values of Adducts **57** to **60**	45
2.5	$ZnCl_2$-Catalyzed Diels-Alder Reactions of Sulfoxide **46**	59
2.6	Lewis Acid-Catalyzed Diels-Alder Reactions of Sulfoxide **46**	60
2.7	Calculated LUMO Energy (AM1) for BCl_3-Complexed Sulfoxide **46**	61
2.8	Unsuccessful Conditions for Oxathiolane Sulfoxide **51** Cleavage	62
2.9	Sulfoxide **51** Reduction Conditions	64
2.10	Decarboxylation of Norbornenones **75** and **76**	67
3.1	π-Facial Selectivity in Cyclohexanone Reductions	90
4.1	Reaction of Cyclohexanone **97** with Grignard and Reducing Agents	115
4.2	Reaction of Cyclopentanone **108** with Methyllithium and Grignard Reagents	124
4.3	Reaction of Cyclopentanone **108** with Reducing Agents	126
4.4	Reaction of Napthalene **114** with Methyllithium and Grignard Reagents	131
4.5	Reaction of Napthalene **114** with Reducing Agents	136
4.6	π-Facial Selectivity of Oxathiolane Cyclopentanones	150
4.7	Nucleophilic Additions to Tetrahydrofuran **129**	158
4.8	Nucleophilic Additions to Tetrahydrothiophene **133**	161

Dedicated to my family and friends with love and gratitude

CHAPTER 1

π-Facial Selectivity in Diels-Alder Cycloadditions

1.1 Introduction

The role of stereoelectronic effects in controlling diastereoselectivity in various reactions has continued to be the subject of a considerable amount of research.[1] Although steric interactions are thought to be a major factor in determining the stereoselectivity in many organic transformations, it has been less clear to what degree stereoelectronic factors influence diastereoselectivity. The Diels-Alder cycloaddition (Figure 1.1) has been investigated in this regard, as it is an extremely useful reaction with a large number of diastereoselective examples reported in the literature.[2] The stereochemistry produced at the termini of the new σ bonds is a result of diene and dienophile characteristics, such as the presense of a chiral centre, and the topography (cycloaddition to give *endo* or *exo* products) of the cyclization. The rationalization of the diastereoselectivity in many of these cases can not rely on steric or frontier orbital arguments alone and therefore, a number of models have been proposed to rationalize the observed diastereoselectivity in Diels-Alder cycloadditions.

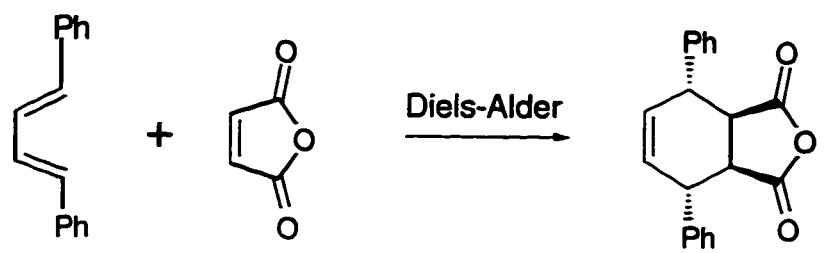

1 2 3

Figure 1.1 The Diels-Alder cycloaddition

The Diels-Alder reaction is capable of producing four adducts depending on the orientation of the interaction between diene and dienophile. As an example, the four possible modes of dienophile attack on pentamethylcyclopentadiene **4** are shown below (Figure 1.2). The term *syn* refers to the product that results from the dienophile approaching the plane of the diene closest to the C5 substituent while *anti* refers to approach opposite to the C5 substituent.

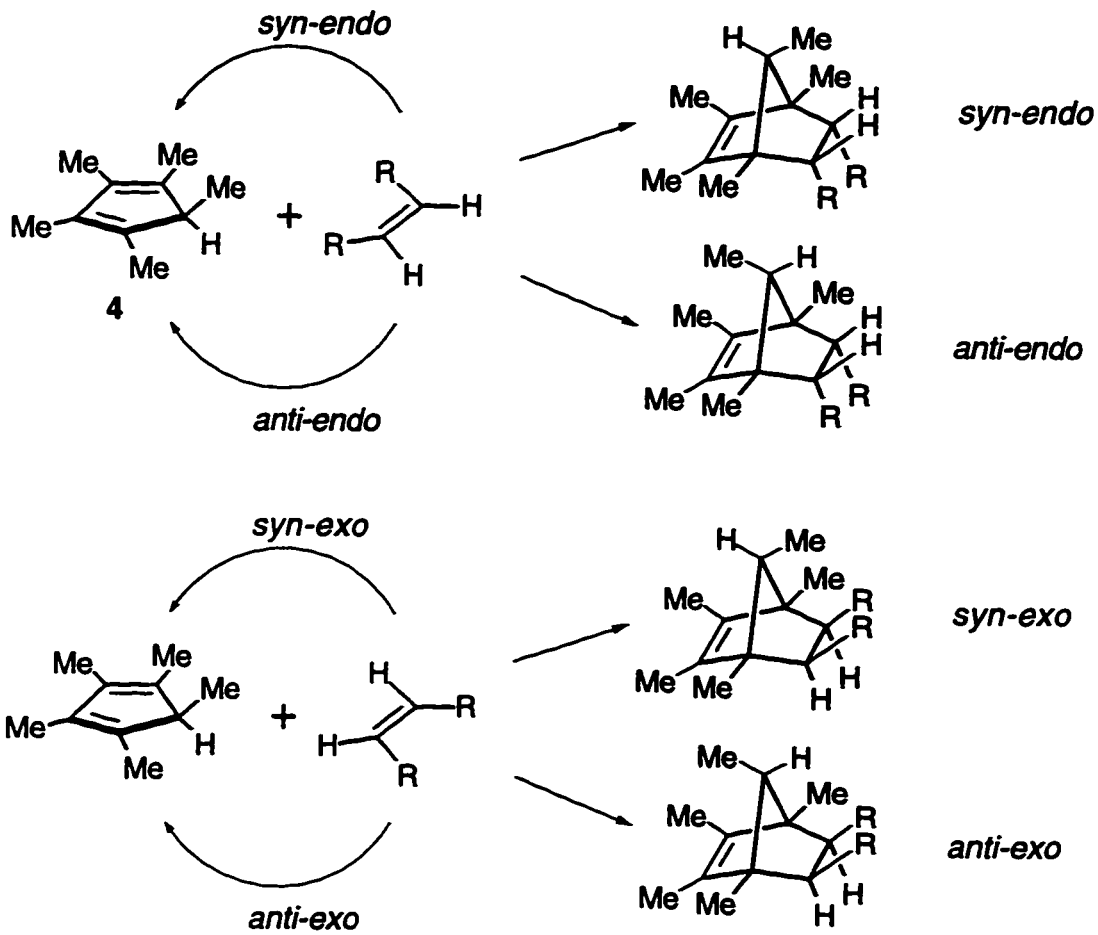

Figure 1.2 Four possible cycloadducts from the Diels-Alder reaction

In practice, reactive dienophiles such as maleic anhydride or *N*-phenylmaleimide give only the two *endo* cycloadducts.[3] However, cycloadditions involving less reactive dienophiles (methyl acrylate or butenone, for example), which

would presumably have weaker *endo*-directing secondary orbital interactions, may produce the *anti-exo* product as well. The *syn-exo* adducts are disfavoured for steric reasons and are usually not observed.[4]

If one is able to control the *syn-anti* selectivity in the example above, or in those circumstances where at least one of the reactants (diene or dienophile) posesses two different π-faces, the number of asymmetric centres being simultaneously introduced is capable of growing to five or more. The *syn* / *anti* selectivity possible with Diels-Alder cycloaddition reactions is referred to as π-facial selectivity, as it arises from steric and / or electronic differences between the faces of the π system on one (or both) of the reactants.

A common approach for obtaining π-facial selectivity in intermolecular cases is to link the diene or dienophile to a chiral auxiliary. Ideally, the auxiliary blocks one face of the diene or dienophile, a face selective cycloaddition takes place, the auxiliary is removed, and one obtains an adduct enriched in one enantiomer. An alternative approach involves the incorporation of a stereogenic centre within the diene or dienophile, usually at an allylic position. In these cases, the products of the cycloaddition reaction are now diastereomers as the stereogenic centre is not removed, but is built into the product.

1.2 Previous Studies

A number of reports in the literature have demonstrated that an allylic heteroatom substituent on either the diene or dienophile can greatly influence diastereofacial selectivity in intermolecular Diels-Alder reactions.[5] The majority of these reports have focussed on the diene partner of the cycloaddition and fall into

two classes: 5-substituted 1,3-cyclopentadienes **5** and chiral acyclic 1,3-dienes **6**, carrying an allylic oxygen or nitrogen substituent (Figure 1.3).

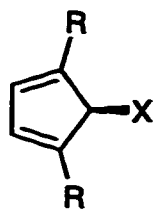

5

X = OH, OMe, OAc, Cl, Br, I, $SiMe_3$, NH_2, NHAc, SMe, SOMe, SO_2Me

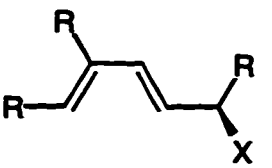

6

X = OR, NHCOOR

Figure 1.3 Two classes of dienes used in diastereoselectivity studies

Early studies undertaken in this laboratory[5g,h] and by other groups[6] have established that incorporation of a single substituent, particularly a heteroatom, in the allylic position of some cyclopentadienes, exerts a stereodirecting influence in Diels-Alder cycloadditions. This can result in very high π-facial selectivity, often in a contrasteric manner, as illustrated below (Figure 1.4).

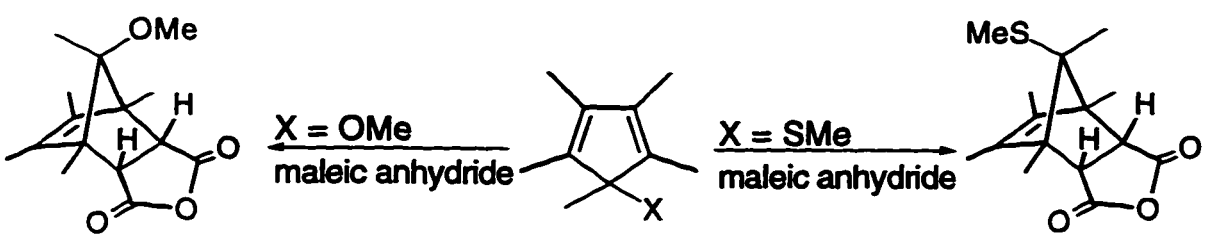

7 **8**

Figure 1.4 Heteroatom influence on π-facial selectivity

Heteroatom-directed π–facial diastereoselection is not a newly observed phenomenon. In 1955, Woodward and co-workers reported[7] that the reaction of 5-

acetoxycyclopentadiene (**9**) with ethylene resulted in a single adduct (**10**, Figure 1.5) The related diene **11**, gave similar results when treated with methyl acrylate, as reported by Jones in 1980.[8]

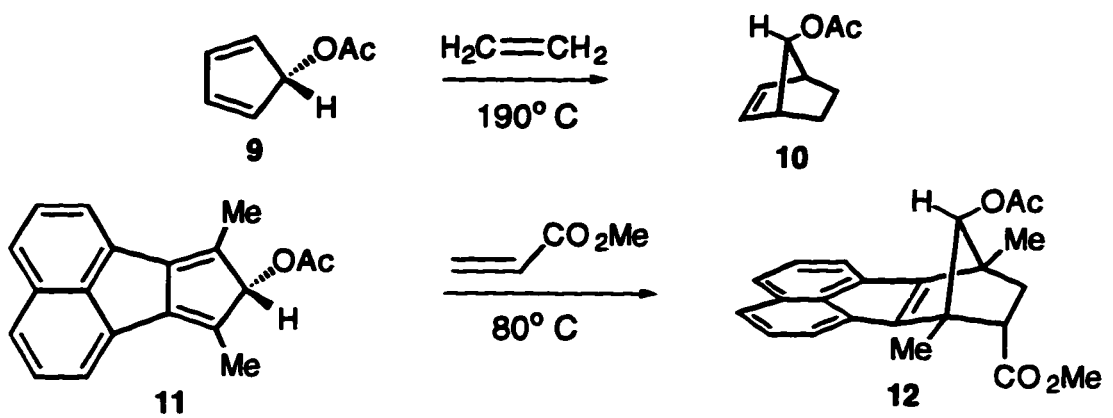

Figure 1.5 Contrasteric Diels-Alder reactions

The origin of the π-facial diastereoselectivity observed in Diels-Alder reactions of C-5 heteroatom-substituted cyclopentadienes is still the subject of lively debate.[9] Experimental and theoretical studies on a wide range of substrates has resulted in the identification of various factors thought to be responsible for the observed diastereoselectivity. These include steric effects, complexation between diene and dienophile,[4a] secondary orbital interactions,[10] polarizability of the reactants,[6c] electrostatic interactions,[4l,m] orbital mixing,[11] and transition state stabilization by hyperconjugation.[12]

1.3 Diels-Alder Reactions of 5-Substituted Cyclopentadienes

The results of an investigation[5g] from this laboratory regarding the π-facial selectivity displayed by 5-substituted 1,2,3,4,5-pentamethylcylopentadienes after reaction with maleic anhydride at room temperature are shown in Table 1.1.

Table 1.1 π-Facial selectivity of 5-Substituted Pentamethylcyclopentadienes

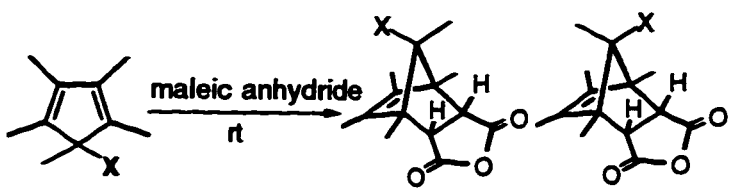

anti *syn*

entry	X	% *anti*	% *syn*
a	Cl	0	100
b	OH	0	100
c	OMe	0	100
d	NHAc	0	100
e	SH[a]	45	55
f	SMe	90	10
g	SCH_2Ph	90	10
h	SPh	97	3
i	SOMe	100	0
j	SO_2Me	100	0

[a] NPM adduct

The preference for the formation of a single or major cycloadduct with cyclopentadienes containing a chlorine, oxygen, nitrogen or sulfur substituent in the 5-position is clearly evident, as is the reversal in π-facial selectivity encountered with the sulfur substituents. While only a slight preference for the *syn* adduct was observed with the parent thiol (SH, entry e), other sulfur-containing functional groups such as SPh and SOMe (entries h and i) as well as dienes carrying Si[13] or Se[5e]

groups (not shown) produced the *anti* adducts as the major or exclusive product. The *anti* addition products that are formed preferentially with cyclopentadienes containing a heteroatom substituent may simply be a result of the steric effect exerted by these groups. It is the factors responsible for the unusual contrasteric *syn* addition, observed with oxygen, chlorine or nitrogen substituents, that are not yet understood. Other related compounds that display high π-facial diastereoselectivity to give the *syn* cycloadducts are shown below (Figure 1.6).[5b,8,14]

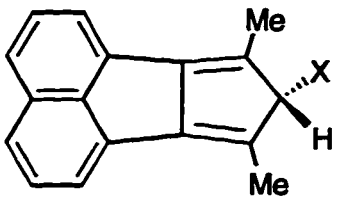

11

X = OH or OAc

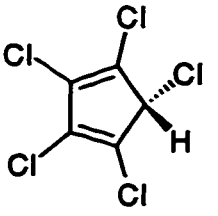

13

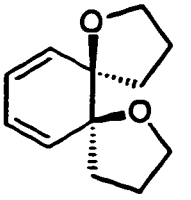

14

Figure 1.6 Related dienes that display high π-facial selectivity

The cycloadducts derived from **11** arise by exclusive attack from the direction *syn* to the oxygen functionality. The addition of dienophiles to **13** similarily proceedes with high preference for *syn* adducts. Interestingly, diastereoselectivity is dienophile-dependant with diene **14**, as maleic anhydride gave the *syn* cycloadduct while *N*-methyltriazolinedione produced the *anti* cycloadduct.

1.4 Models to Predict π-Facial Selectivity in the Diels-Alder Reaction

A number of models have been advanced to explain the origin of the contrasteric *syn* selectivity displayed by some of the cyclopentadiene systems described above.

1.4.1 Orbital distortion

There are two types of orbital distortions[11] of the diene π bond system, orbital extension and orbital tilting, that may be used to rationalize the contrasteric mode of cycloaddition involving heteroatom-substituted cyclopentadienes. Both types of distortions result in an increase in the orbital overlap between the diene and the dienophile, as illustrated below (Figure 1.7, for clarity only the terminal orbital lobes of the diene are shown).

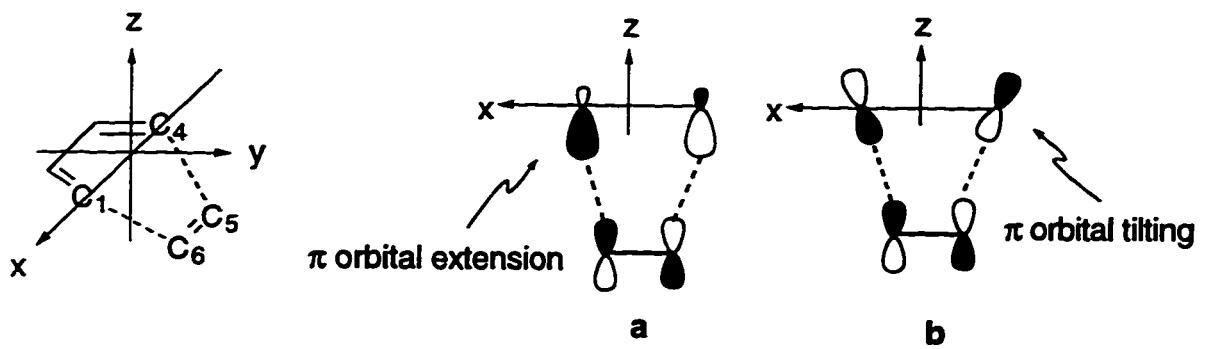

Figure 1.7 Diene orbital distortions

The distortion of the type depicted in Figure 1.7a involves an increase in the coefficients of the diene HOMO, the result of which will favour approach of a dienophile towards the diene face displaying these larger coefficients as this results in greater orbital overlap. The preference of C5 chloro-substituted cyclopentadienes

to produce this extension that resulted in the *syn* adduct was discussed by Fukui in terms of such a nonsymmetrical extension of the HOMO of the diene in the direction of the chlorine substituent. This extension is thought to arise from the orbital mixing between the diene HOMO π orbitals and the σ orbitals of the cyclopentadiene carbon skeleton. The orbital mixing is attributed to a perturbation of the diene HOMO caused by interaction with the nonbonding orbitals of the heteroatom substituent.

The second type of distortion, π orbital tilting, (Figure 1.7b) also distinguishes one π-face from the other with respect to the ability to obtain maximum orbital overlap between the reactants. The effectiveness of this distortion in influencing π-facial selectivity relies on the basis that the distance between the sp^2 terminal carbons of a conjugated diene is greater than the distance between the sp^2 carbons of a typical dienophile. It follows that increased overlap will occur between the reacting centres on the face of the diene when the orbital lobes of the diene are tilted towards each other (Figure 1.7b). Semi-emperical calculations by Yonezawa[15] and co-workers have shown that the HOMO of 5-chlorocyclopentadiene is biased as described in Figure 1.7b towards the chlorine atom. This tilting promotes addition from the *syn* face, as the dienophile enjoys greater overlap with the addends of the diene when approaching from this face of the diene.

Unfortunately, the orbital distortion models are difficult to apply when discussing the observed reversal of diastereoselectivity with Diels-Alder reactions of 5-S, -Si or -Se substituted cyclopentadienes. In a conceptionally difficult explanation, Fukui's orbital mixing concept was applied by Inagaki.[5e,f] Inagaki argued that the direction of the orbital rotation is determined by the relative energies of the diene HOMO and the nonbonding orbital of the heteroatom substituent. The higher the energy of the nonbonding orbital, the greater the propensity to give *anti* addition. A reversal was observed, as the sulfur, silicon and selenium atom lone pair

electrons were higher in energy compared to, for example, oxygen or chlorine atom lone pair electrons.

1.4.2 Electrostatic model

On the basis of calculations examining the electrostatic and polarization potentials of dienes and dienophiles, along with the electron density of their reacting surfaces, Hehre[5l,m] concluded that electrostatic interactions govern π-facial selectivity in Diels-Alder cycloadditions to a large extent. A "normal-type" Diels-Alder cycloaddition is believed to occur through the orbital interaction between the diene HOMO and the dienophile LUMO. In the electrostatic model, the diene is considered nucleophilic as it reacts through its HOMO, a filled orbital. Similarly, the dienophile is considered electrophilic as it reacts through its vacant LUMO. π-Facial selectivity then arises from the nucleophilic diene approaching the dienophile π-face that has the smaller electron density in order to minimize the unfavourable electrostatic replusion between the diene and dienophile. In an analogous manner, the electrophilic dienophile will prefer to approach the more electron-rich π-face of the diene, as this provides the more favourable electrostatic interaction. This is illustrated below (Figure 1.8) for a substituted cyclopentadiene where the arrow represents the approach of the dienophile.

X = electron donating ----> *syn* adduct
X = electron withdrawing ----> *anti* adduct

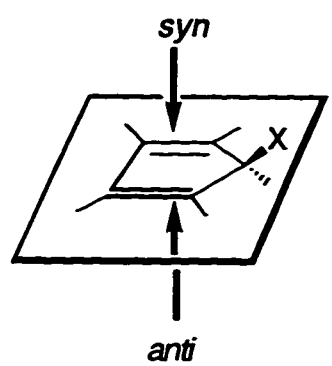

Figure 1.8 Electrostatic interactions that influence π-facial selectivity

The electrostatic bias is provided by the lone pairs on the heteroatom substituent, rendering that face of the diene more electron-rich, however this explanation can not account for the reversal in π-facial selectivity described above. Thus, steric arguments are envoked by Hehre to account for the failures of the electrostatic model.

1.4.3 Paquette model

π-Facial selectivity in Diels-Alder reactions is not restricted to those dienes containing heteroatom substituents. Isodicyclopentadiene (**15**) undergoes Diels-Alder cycloadditions with a variety of dienophiles primarily from the *endo* (bottom) face.[16] This π-facial diastereoselectivity observed in the Diels-Alder reaction of isodicyclopentadiene and many related systems has been explored extensively by Paquette.[16d,e] A phenomenon similar to orbital tilting was proposed and attributed to, interactions between the p orbitals of the carbon framework and the π orbitals of the diene moiety (Figure 1.9).

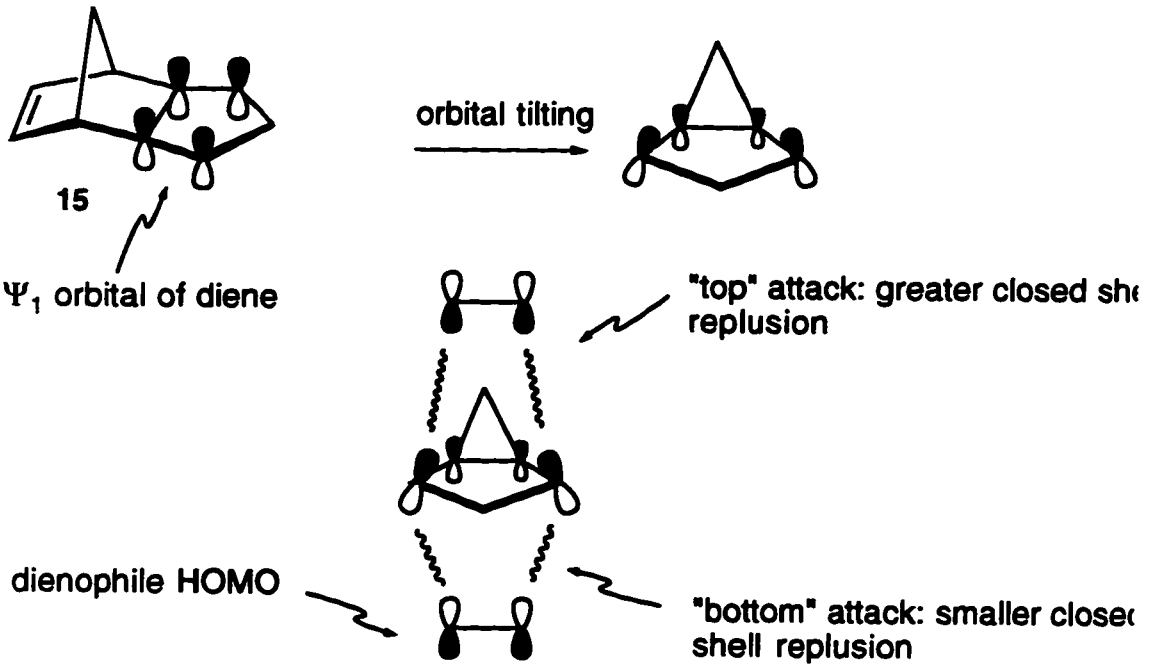

Figure 1.9 Paquette's orbital tilting model

In the Paquette model, the norbornene skeleton causes the mixing of σ and π orbitals such that the lowest energy π orbital (Ψ_1) of the diene tilts its terminal p lobes inward on top and outward on bottom. A dienophile then approaches from the bottom to avoid closed-shell replusion between the dienophile π HOMO and the tilted Ψ_1 orbital of the diene. Thus, attack from the top face is disfavoured as the two lobes are closer together, whereas less replusion is experiened during bottom attack as the lobes are further apart.

Although substituent effects on diene **15** produced diastereoselectivities that could be explained by these arguments, variations in the selectivity with different dienophiles could not be explained.

1.4.4 Torsional strain

Many explanations of the π-facial selectivity observed in Diels-Alder cycloadditions have emphasized the ground state properties of the substrate as being responsible for the π-facial diastereoselection. Alternate analyses involve consideration of the factors which may contribute to stabilizing one diastereomeric transition state over the other.

Both torsional and steric interactions were cited by Brown[17] and Houk[18] as the factors responsible for the preferred bottom attack by dienophiles on isodicyclopentadiene. This conclusion was based on calculations that indicated that the transition state for bottom attack is more stable due to the reduced torsional strain between the bridgehead C-H bonds and the C=C bond of the diene (Figure 1.10).

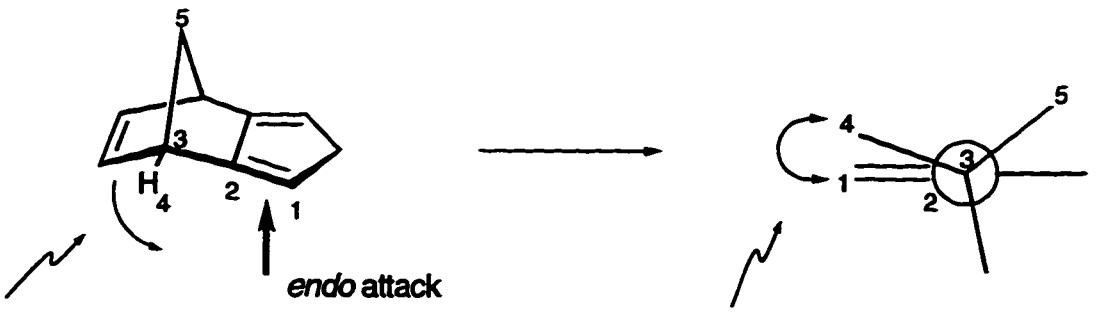

Figure 1.10 Reduction of torsional strain favours *endo* approach

This reduction in torsional strain is a manifestation of the bending of the norbornene portion of the molecule in the *endo* direction which occurs during bottom (*endo*) attack, according to Houk's calculations.

1.4.5 Anh model

Anh[10] called attention to the possibility that a non-bonded attraction between the heteroatom and the dienophile might serve as a stabilizing factor (Figure 1.11).

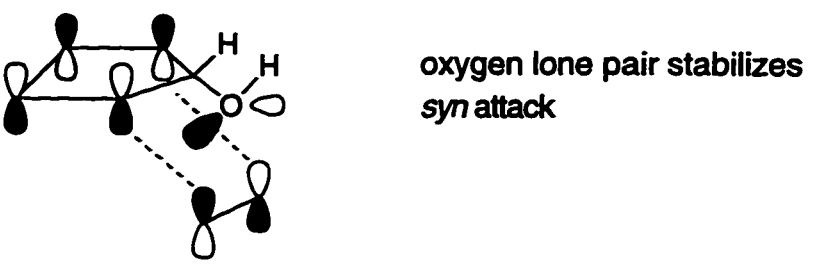

Figure 1.11 Transition state stabilization by heteroatom lone pair

This model, however, fails to predict the reversal observed with the S, Si and Se-substituted cyclopentadienes.

1.4.6 Hyperconjugative stabilization

To explain the diastereoselectivity shown in Table 1.1, the hyperconjugative σ-assistance model of Cieplak[12] was envoked by Fallis.[5g] The Cieplak model (this model is discussed in greater detail in Chapters 3 and 4) requires electron donation from an antiperiplanar σ bond into the σ* orbital of the forming bond (Figure 1.12) to achieve transition state stabilization.

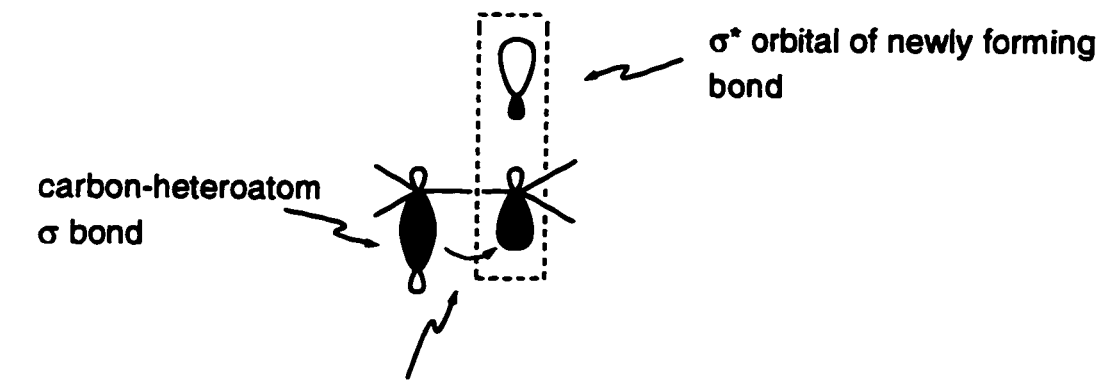

Figure 1.12 Hyperconjugative stabilization of a σ* orbital

The greatest stabilization occurs upon approach of the reagent *anti* to the best σ donating group (Figure 1.13) as this allows for maximum overlap between the adjacent σ and σ* orbitals. π-Facial selectivity is then determined by comparing the σ donating ability of the substituents adjacent to the reacting centres.

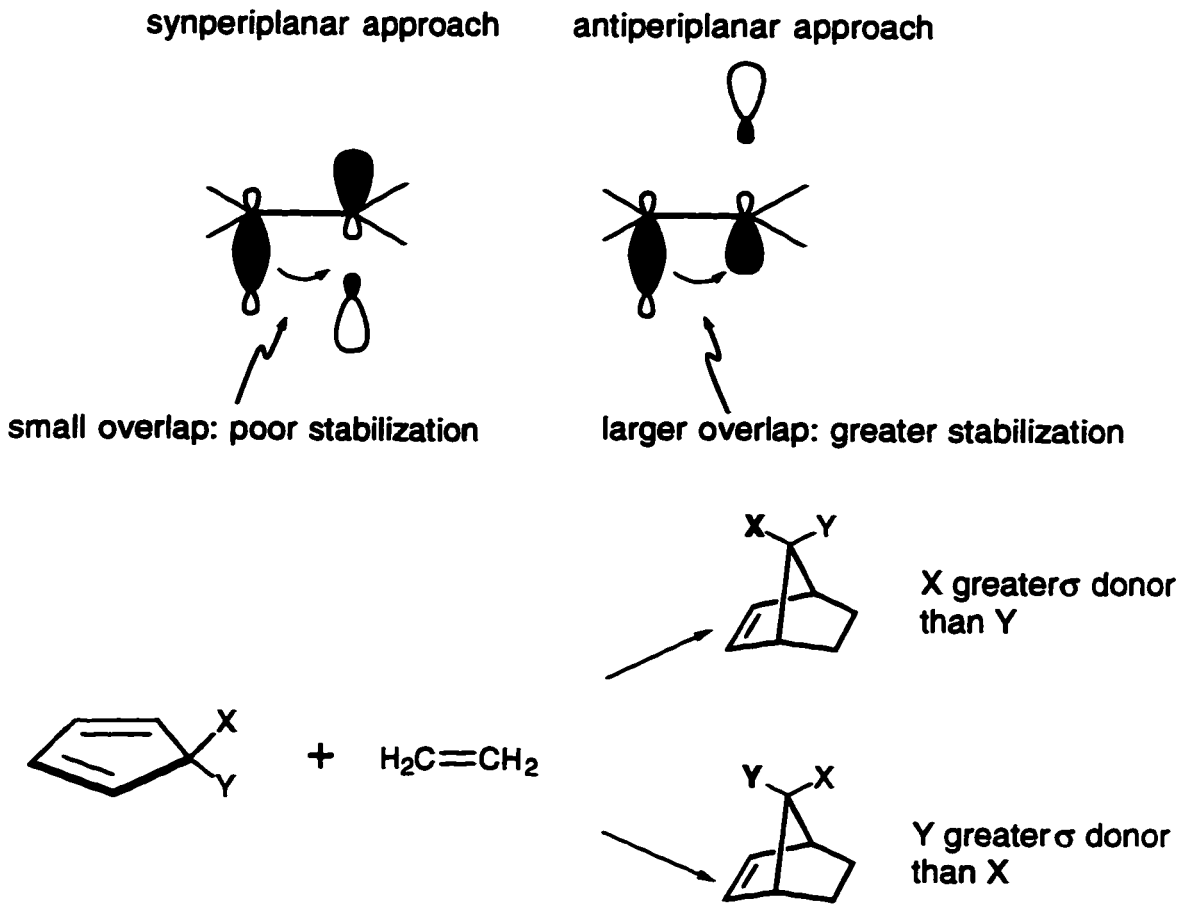

Figure 1.13 Cieplak model

The generally accepted[5g] order of increasing σ donor ability of various carbon-heteroatom bonds are:

$$\sigma_{CO} < \sigma_{CN} < \sigma_{CCl} < \sigma_{CC} < \sigma_{CH} < \sigma_{CS} < \sigma_{CSi}$$

If this order is correct, it explains the reversal of π-facial selectivity observed with C-5 substituted pentamethylcyclopentadiene upon replacing -Cl or -OH with -SPh or -SOMe. The lack of selectivity displayed by the parent thiol (-SH) however, remains an enigma in terms of the Cieplak model.

1.5 Research Objectives

In order to further explore the validity of applying the concept of Diels-Alder π-facial control by substituents with σ donating ability, a study was undertaken by this laboratory[5h] whereby 2,5-dimethylthiophene oxide (**16**, generated *in situ* from *m*-chloroperbenzoic acid oxidation of 2,5-dimethyl thiophene) was reacted with various dienophiles to give a single cycloadduct in all cases examined (Figure 1.14).

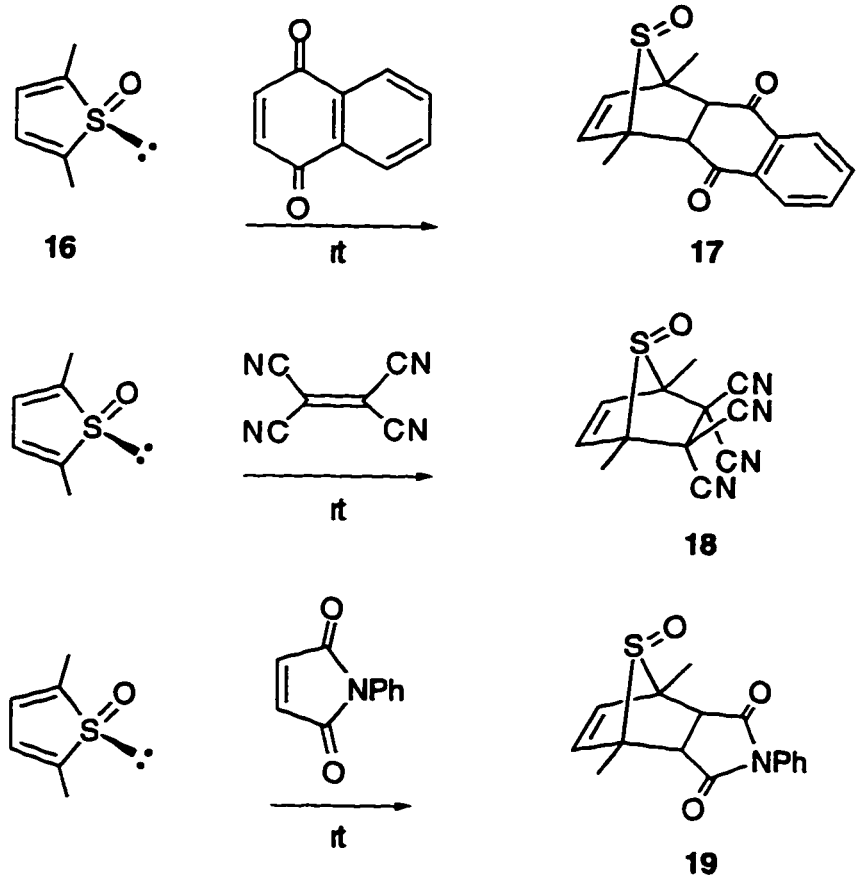

Figure 1.14 High π-facial selectivity is observed with 2,5-dimethylthiophene oxide

The only cycloadduct detected was a result of dienophile addition to give the *syn* (in relation to the oxygen of the thiophene oxide) product exclusively. The

superior σ donating ability of the sulfur lone pair compared to the S=O group was thought to be responsible for the observed selectivity.

The high π-facial selectivity observed with dimethylthiophene oxide **16** encouraged us to explore further the possibility of controlling facial selectivity with other heteroatom funtionalities. Oxathiolane acetals as control elements in radical reactions[19] were being developed concurrently by us and therefore, a study was initiated to investigate the effectiveness of oxathiolane acetals in controlling π-facial selectivity in Diels-Alder cycloadditions as outlined below (Figure 1.15). The results of these studies are described in the following chapter.

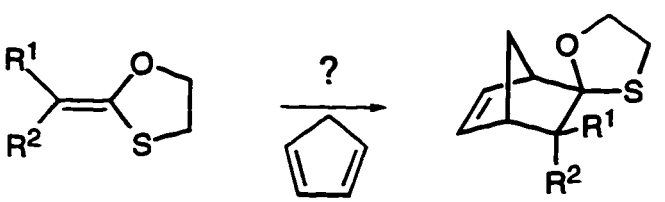

Figure 1.15 Oxathiolane acetals as π-facial selectivity control elements in Diels-Alder reactions

Chapter 1 References

1. a) Fallis, A. G.; Lu, Y.-F. In *Advances in Cycloaddition*; Curran, D. P., Ed.; JAI Press: Greenwich, CT, 1993; Vol. 3, pp 1-66. b) Li, H.; le Noble, W. J. *Recl. Trav. Chim. Pays-Bas* **1992**, *111*, 199.
2. Paquette, L. A. In *Asymmetric Synthesis*; Morrison, J. D., Ed.; Academic Press: New York, 1984, Vol. 3, Chapter 7.
3. Wasserman, A. *Diels-Alder Reactions*; Elsevier Publishing Co.: Amsterdam, 1965.
4. Desimoni, G.; Tacconi, G.; Barco, A.; Pollini, G. P. *Natural Product Synthesis Through Pericyclic Reactions*; ACS Monograph 180: American Chemical Society: Washington, D.C., 1983.
5. a) Adam, W.; Glaser, J.; Peters, K.; Prein, M. *J. Am. Chem. Soc.* **1995**, *117*, 9190. b) Paquette, L. A.; Branan, B. M.; Rogers, R. D.; Bond, A. H.; Lange, H.; Gleiter, R. *J. Am. Chem. Soc.* **1995**, *117*, 5992. c) Burry, L. C.; Bridson, J. N.; Burnell, D. J. *J. Org. Chem.* **1995**, *60*, 5931. d) Werstiuk, N. H.; Ma, J. *Can. J. Chem.* **1994**, *72*, 2493. e) Ishida, M.; Aoyama, T.; Beniya, Y.; Yamabe, S.; Kato, S.; Inagaki, S. *Bull. Chim. Soc. Jpn.* **1993**, *66*, 3430. f) Ishida, M.; Beniya, Y.; Inagaki, S.; Kato, S. *J. Am. Chem. Soc.* **1990**, *112*, 8980. g) Macaulay, J. B.; Fallis, A. G. *J. Am. Chem. Soc.* **1990**, *112*, 1136. h) Naperstkow, A. M.; Macaulay, J. B.; Newlands, M. J.; Fallis, A. G. *Tetrahedron Lett.* **1989**, *30*, 5077. i) Kaila, N.; Franck, R. W.; Dannenberg, J. J. *J. Org. Chem.* **1989**, *54*, 4206. j) Fisher, M. J.; Hehre, W. J.; Kahn, S. D.; Overman, L. E. *J. Am. Chem. Soc.* **1988**, *110*, 4625. k) Brown, F. K.; Houk, K. N.; Burnell, D. J.; Valenta, Z. *J. Org. Chem.* **1987**, *52*, 3050. l) Kahn, S. D.; Hehre, W. J. *J. Am. Chem. Soc.* **1987**, *109*, 663. m) Kahn, S. D.; Hehre, W. J. *Tetrahedron Lett.* **1986**, *27*, 6041. n) De Lucchi, O.; Lucchini, V.; Marchiro, C.; Valle, G.; Modena, G. *J. Org. Chem.* **1986**, *51*, 1457. o) Posner, G. H.; Harrison,

W. *J. Chem. Soc., Chem. Commun.* **1985**, 1786. p) Gree, R.; Kessabi, J.; Mosset, P.; Martelli, J.; Carrie, R. *Tetrahedron Lett.* **1984**, *25*, 3697.

6. a) McClinton, M. A.; Sik, V. *J. Chem. Soc., Perkin Trans. 1* **1992**, 1893. b) Breslow, R.; Hoffmann, J. M., Jr. *J. Am. Chem. Soc.* **1972**, *94*, 2110. c) Ishida, M.; Aoyama, T.; Kata, S. *Chem. Lett.* **1989**, 663. d) Fleming, I.; Micheal, J. P. *J. Chem. Soc., Chem. Commun.* **1978**, 245.
7. Winstein, S.; Shatavsky, M.; Norton, C.; Woodward, R. B. *J. Am. Chem. Soc.* **1955**, *77*, 4183.
8. Jones, D. W. *J. Chem. Soc., Chem. Commun.* **1980**, 739.
9. Coxon, J. M.; Fong, S. T.; McDonald, D. Q.; Steel, P. J. *Tetrahedron Lett.* **1993**, *34*, 163.
10. Anh, N. T. *Tetrahedron* **1973**, *29*, 3227.
11. Inagaki, S.; Fujimoto, H.; Fukui, K. *J. Am. Chem. Soc.* **1976**, *98*, 4054.
12. Cieplak, A. S. *J. Am. Chem. Soc.* **1981**, *103*, 4540.
13. a) Fleming, I.; Sarker, A. K.; Doyle, M. J.; Raithby, P. R. *J. Chem. Soc., Perkin Trans. 1* **1989**, 2023. b) Fleming, I.; Williams, R. V. *J. Chem. Soc., Perkin Trans 1* **1981**, 684.
14. Williamson, K. L.; Hsu, Y. L.; Lacko, R.; Young, C. H. *J. Am. Chem. Soc.* **1969**, *91*, 6129.
15. Kawamura, T.; Koyama, T.; Yonezawa, T. *J. Am. Chem. Soc.* **1973**, *95*, 3220.
16. a) Pinkerton, A. A.; Schwarzenbach, D.; Birbaum, J.-C.; Carrupt, P.-A.; Schwager, L.; Vogel, P. *Helv. Chim. Acta* **1984**, *67*, 1136. b) Avenati, M.; Vogel, P. *Helv. Chim. Acta* **1983**, *66*, 1279. c) Subramanyam, R.; Bartlett, P. D.; Iglesias, G. Y. M.; Watson, W. H.; Galloy, J. *J. Org. Chem.* **1982**, *47*, 4491. d) Gleiter, R.; Paquette, L. A. *Acc. Chem. Res.* **1983**, *16*, 328 and references therein. e) Paquette, L. A.; Carr, R. V. C.; Bohm, M. C.; Gleiter, R. *J. Am. Chem. Soc.* **1980**, *102*, 1186.

17. Brown, H. C.; Kawakami, J. H.; Liu, K.-T. *J. Am. Chem. Soc.* **1973**, *95*, 2209.

18. Brown, F. K.; Houk, K. N. *J. Am. Chem. Soc.* **1985**, *107*, 1971.

19. Yadav, V.; Fallis, A. G. *Can. J. Chem.* **1991**, *69*, 779.

Chapter 2

The Development of a Chiral Ketene Equivalent: Results and Discussion

2.1 Introduction

In contrast to the extensive literature on diene substituent effects on the π-facial selectivity of the Diels-Alder reaction, there has been less work reported on the extent the dienophile influences π-facial selectivity. A review by Paquette[1] in 1984 described the π-facial selectivity available with chiral acrylates, triazolinediones and carbohydrate derivatives, and emphasized the difficulties associated with distinguishing between the steric and electronic factors. More recently, a study by Franck[2] has shown that a reversal of π-facial selectivity occurs in the Diels-Alder reaction of diene **20** with *N*-phenylmaleimide (NPM), as compared to the same reaction using tetracyanoethylene, TCNE (Figure 2.1).

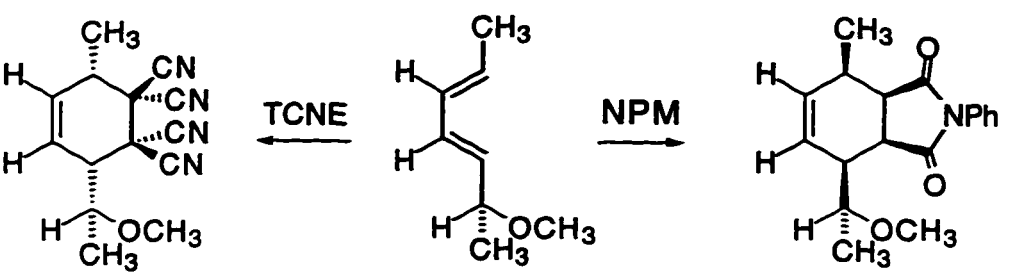

20

Figure 2.1 Dienophile effects on π-facial selectivity

The resultant π-facial selectivity in the above example is controlled "by some factor which still needs elucidation."[2] Interestingly, Foote[3] and Clennan[4] have

published results which show that *N*-phenyl-1,2,4-triazoline-3,5-dione, a dienophile used in many π-facial selectivity studies, reacts with activated dienes *via* non-Diels-Alder, multistep pathways.

Stimulated by our own interest in understanding and controlling the π-facial selectivity of Diels-Alder reactions, coupled with a concurrent study in these laboratories on the use of 1,3-oxathiolanes in radical reactions,[5] a study was initiated to determine the suitability of oxathiolane ketene equivalents in Diels-Alder cycloaddition reactions.[6] The proposed cyclization is outlined below (Scheme 2.1).

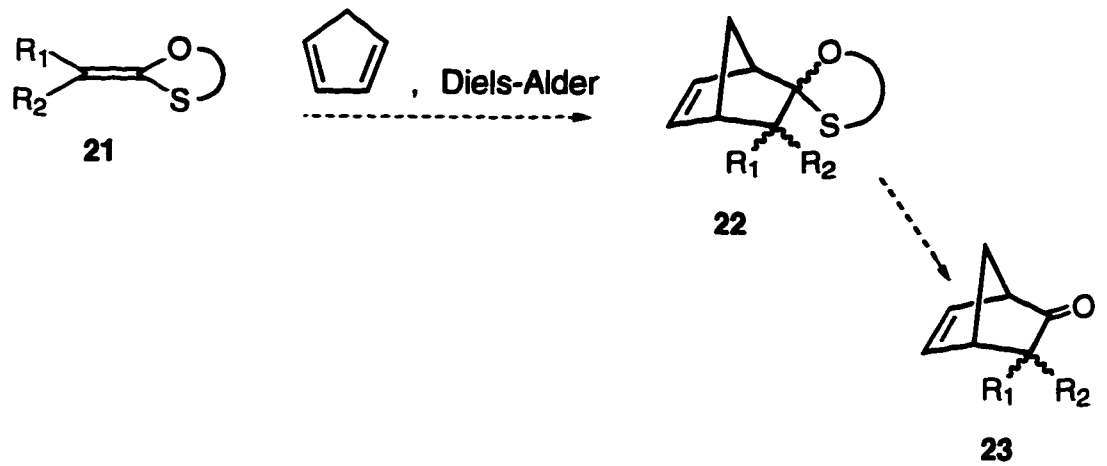

Scheme 2.1 Oxathiolane dienophiles as ketene equivalents

Compounds such as **22** were considered suitable targets, as the bicyclo[2.2.1]heptane skeleton of norbornenone **23** is widely distributed in Nature, and there is considerable interest in the preparation of molecules containing this ring system.[7]

For the purposes our study, oxathiolane-protected ketenes were chosen for a number of reasons:

•ketene equivalents such as **21** are required to avoid the preferred [2+2] cyclization that the parent ketenes undergo in the presence of dienes;[8]

• to determine whether the oxygen or sulfur atoms of an oxathiolane acetal would influence the dienophile π-face such that synthetically useful levels of π-facial selectivity result;

• there exists a variety of methods to remove the 1,3-oxathiolane group efficiently, allowing for the further elaboration of the Diels-Alder adduct using appropriate chemistry.

2.2 Preparation and Reactivity of Oxathiolane 26

2.2.1 Synthesis of ester 26

At the outset, it was of particular interest to determine if heteroatom substituents at the vinyl position of a dienophile (sulfur and oxygen, in this case) would produce a π-facial-directing effect similar to that observed with C5-substituted cyclopentadienes or 2,5-dimethylthiophene oxide. In this regard, the commercially available alcohol, 6-hydroxy-1,3-benzoxathiol-2-one (**24**), was considered to be a suitable starting material. Phenol **24** not only contains the requisite oxathiolane system, but a straightforward synthetic sequence would allow for its conversion to a suitable dienophile. It was also hoped that any cycloadducts using phenol **24** would be sufficiently crystalline for analysis by X-ray. The synthesis of ester **26** is outlined below (Scheme 2.2).

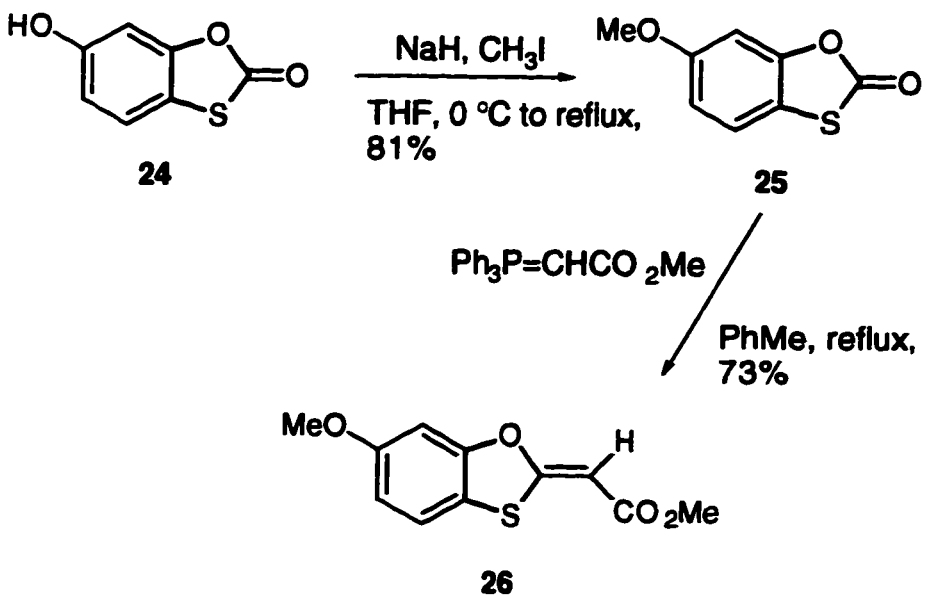

Scheme 2.2 Synthesis of ester 26

Conversion of alcohol **24** to its methyl ether **25** was accomplished by treatment of **24** with sodium hydride in tetrahydrofuran, and quenching the resultant salt with methyl iodide to afford ether **25** in 81% yield. A Wittig reaction between methyl ether **25** and the commercially available ylide, methyl (triphenylphosphoranylidene)acetate, gave the vinylic ester **26** in 73% yield. The resultant vinylic ester **26** was tentatively assigned the *Z* configuration, based on a proposed mechanism in a related study by Abell,[9] who demonstrated a reaction mechanism for cyclic anhydride **27** with stabilized ylides (Scheme 2.3).

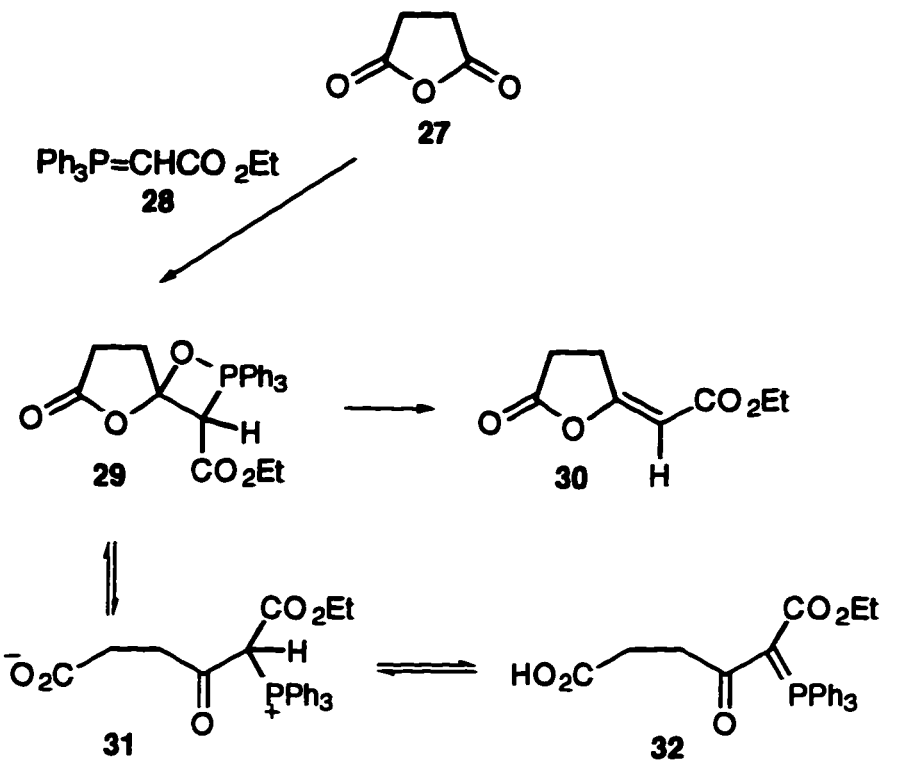

Scheme 2.3 Wittig reaction of anhydride 27 and ylide 28

In the Abell study, the reaction of ylide **28** with succinic anhydride (**27**) had been used previously for the preparation of acyl phosphorane **32**. It was postulated that oxaphosphetane **29** collapses to give lactone **30**, or alternatively, the phosphonium salt **31**. This was based on the fact that phophorane **32** had been isolated and shown to be a precursor to lactone **30**. The phosphonium salt **31** was not detected, but is thought to undergo a reversible rearrangement to the more stable lactone **30**. A proposed mechanism to account for the *Z* configuration, drawn by analogy with that of Abell, is shown below (Figure 2.2).

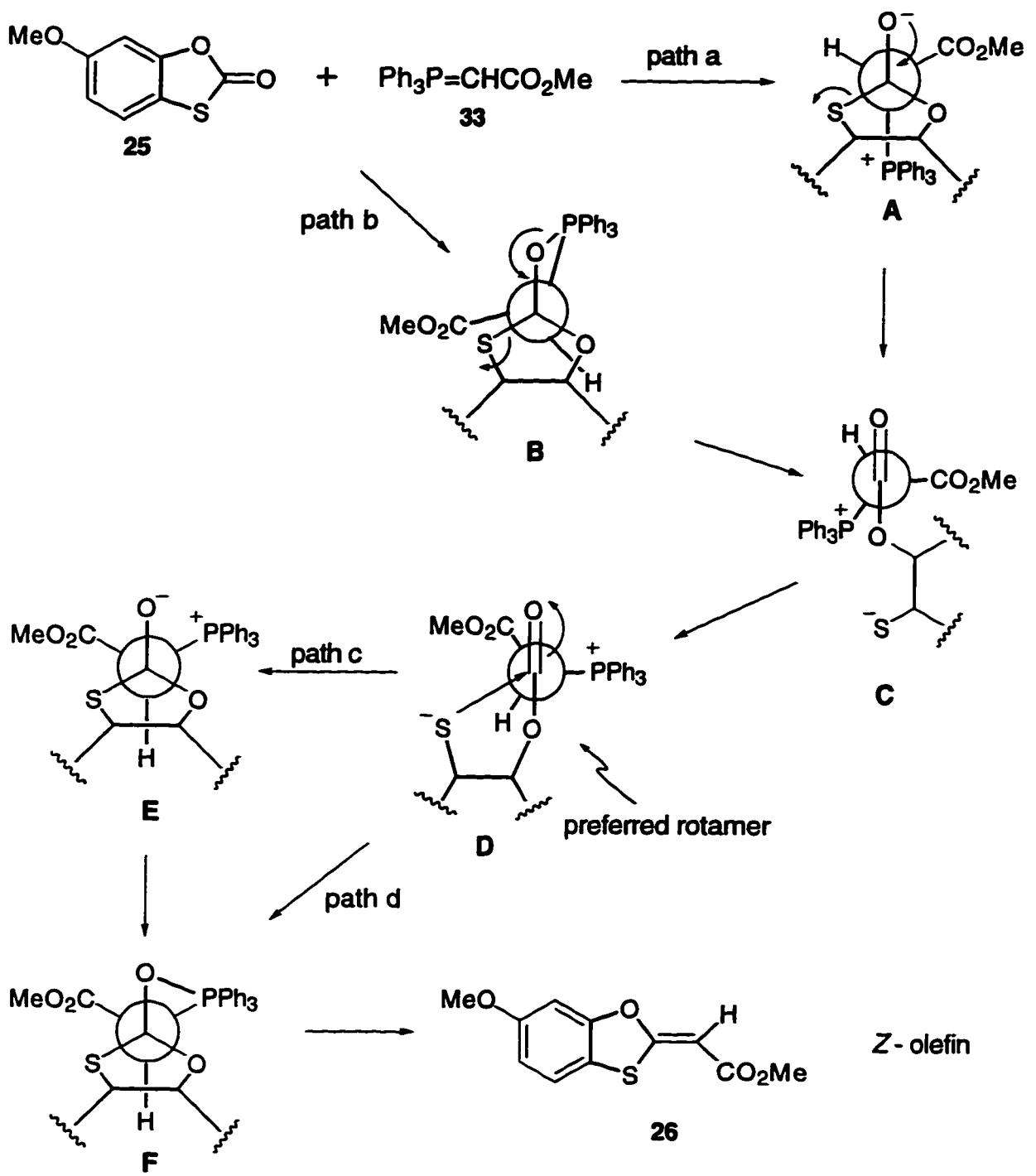

Figure 2.2 Proposed mechanism for *Z* configuration

The mechanism shown in Figure 2.2 above is based on the assumption that oxaphosphetane **B** may not immediately collapse to an alkene. After initial addition

of the ylide to the carbonyl group of **25**, phosphonium salt **C** may result by either collapse of the tetrahedral intermediate **A** and cleavage of the carbon-sulfur bond (path a), or oxaphosphetane **B** fragmentation (path b). Rotamer **D** represents the favoured rotamer (in Felkin-Anh terms), as nucleophilic attack *via* this rotamer involves nucleophilic attack opposite to the largest group (Ph_3P), on the side of the smallest group (H). Nucleophilic attack *via* rotamer **C** may be the sourse of the minor product (4%) isolated from the reaction mixture. Oxaphosphetane **F** may form as a result of the sulfide addition to the carbonyl group of **D** (path d), or *via* betaine **E** (path c) to give *Z*-olefin **26** after oxaphosphetane collapse.

2.2.2 Diels-Alder reactions of ester 26

With the ketene equivalent **26** in hand, the Diels-Alder reaction with cyclopentadiene was attempted under both uncatalyzed and Lewis acid-catalyzed[10] conditions (Scheme 2.4).

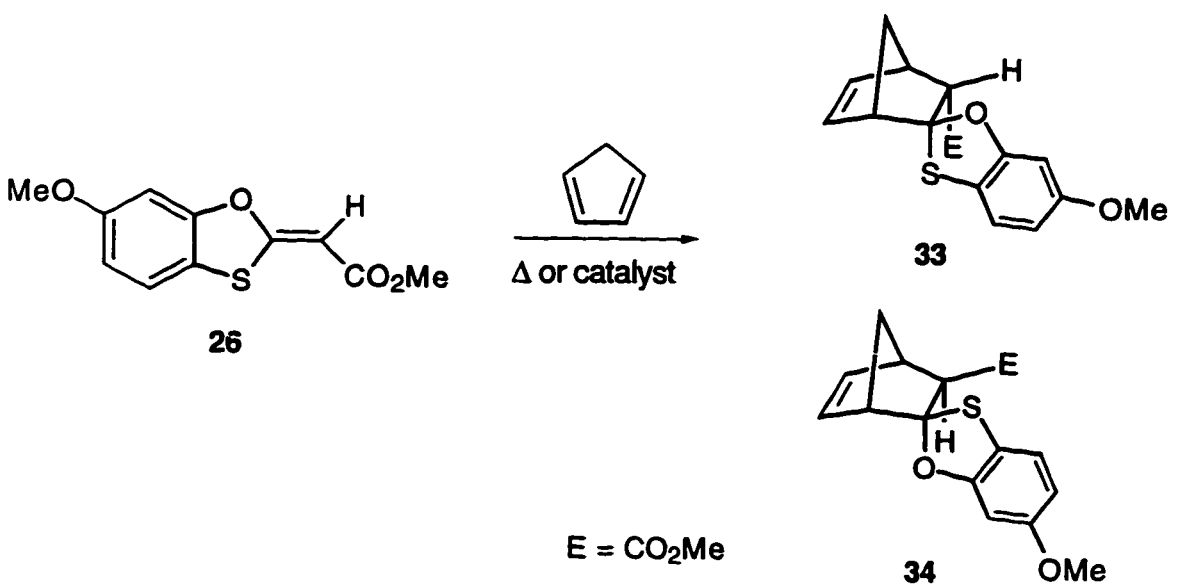

Scheme 2.4 Attempted Diels-Alder reactions of ester 26

The cyclization was attempted initially at refluxing benzene temperature, with no sucess. Attempted cyclizations at higher temperatures (*m*-xylene, bp 138 °C) or by the addition of Lewis acids (BF_3, $AlCl_3$, $TiCl_4$, $ZnCl_2$) were similarly unsuccessful, and resulted in recovered starting material along with unidentifiable material presumably from decomposition of starting material or polymerization of the diene.

This lack of reactivity displayed by oxathiolane **26** most likely arises from its donor-acceptor[11] electronic character. The two canonical structures that result with an alkene containing geminal electron-donating and -accepting substituents are shown below (Figure 2.3).

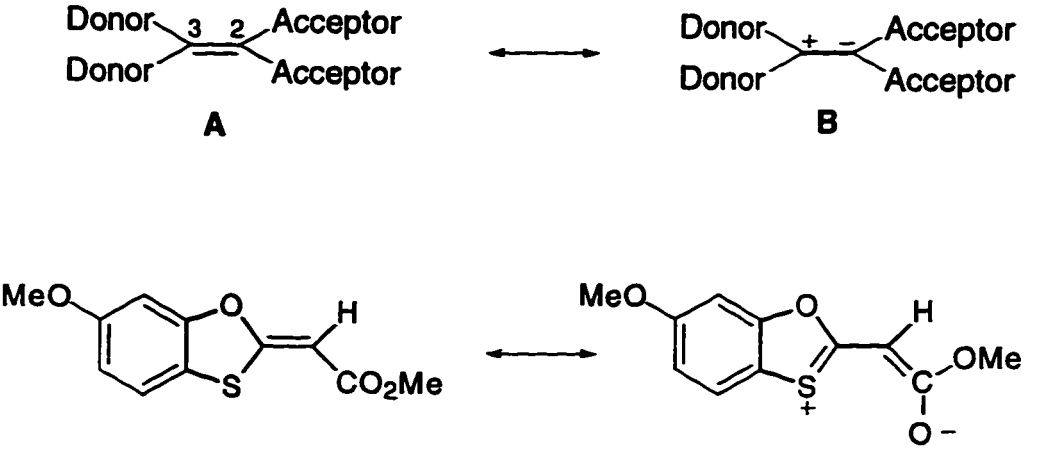

Figure 2.3 Donor-acceptor dienophiles

The arrangement shown in Figure 2.3 results in a marked decrease in the barrier to rotation of the central carbon-carbon double bond compared to "normal" ethylenes, as demonstrated by Kleinpeter[11] in an ^{13}C NMR study. The Kleinpeter study exploited the ^{13}C NMR chemical shift differences of the two olefinic carbon atoms as a measure of the double-bond polarization. Their study showed that electron-withdrawing substituents, that stabilize canonical structure B (Figure 2.3), shift the C2 ^{13}C NMR signal to lower field, whereas the of C3 signal is shifted to

higher field. This implied that the influence of donor-acceptor groups on the electron density along the carbon-carbon double bond should also be reflected by a decrease in bond order.

To investigate the possibility of a link between bond order and the poor reactivity of sulfide **26**, the carbon-carbon bond order and LUMO energies for a number of dienophiles were calculated using semi-empirical methods (AM1).[12] The results are presented below (Table 2.1).

Table 2.1 Comparison of Dienophile Bond Orders and LUMO energy

entry	dienophile	bond order (C=C)	LUMO (eV)
a	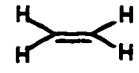	2.00	1.438
b		1.93	-0.137
c	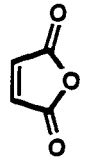	1.91	-1.621
d	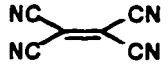	1.74	-2.524
e	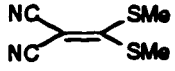	1.61	-1.110
f	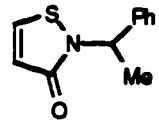	1.76	-0.209
g	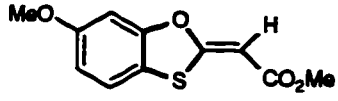	1.70	-0.466

Inspection of Table 2.1 reveals that oxathiolane **26** (entry g) indeed possesses a lower bond order compared with non-donor-acceptor dienes (entries a through d). A relatively low bond order, however, does not necessarily equate with low reactivity, as evident by the bond order of 1.74 for the very reactive dienophile, tetracyanoethylene (entry d). The low-lying LUMO of tetracyanoethylene is believed to be responsible for its high reactivity.[13] Using this criterion, oxathiolane **26** is expected to be be more reactive than acrolein (entry b), but this is contrary to the experimental observations.[6] The thiazolinone (entry f) system exhibits a low bond order, characteristic of a donor-acceptor double bond, and this has been shown to be unreactive towards cyclopentadiene.[14] The combination of low bond order *and* a relatively high LUMO may be responsible for the lack of reactivity of oxathiolane **26** and other donor-acceptor alkenes.

2.2.3 Attempted preparation of diester 36

The next line of investigation involved conversion of ester **26** into a more reactive dienophile by replacement of the vinylic hydrogen atom with a second electron-withdrawing group (Scheme 2.5).

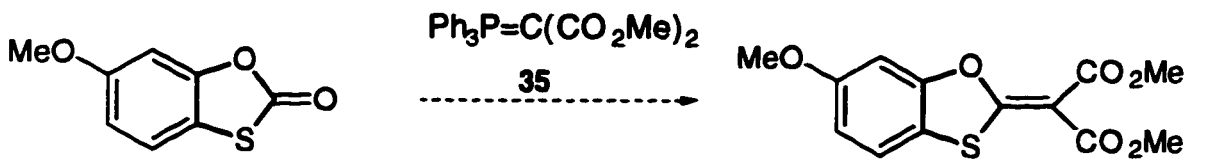

25 **36**

Scheme 2.5 Attempted Wittig reaction of oxathiolane 25

It is well known that electron-withdrawing substituents on the dienophile increase the rate of Diels-Alder cycloaddition reactions.[15] For example, cyclopentadiene reacts with ethene at very high pressure and temperature to give a

74% yield of norbomene.[16] In contrast, acrolein reacts at room temperature in 95% yield. This dramatic rate increase is attributed to a lowering of the acrolein LUMO energy by the electron-withdrawing effect of the carbonyl group (entries a and b, Table 2.1), as depicted (Figure 2.4).

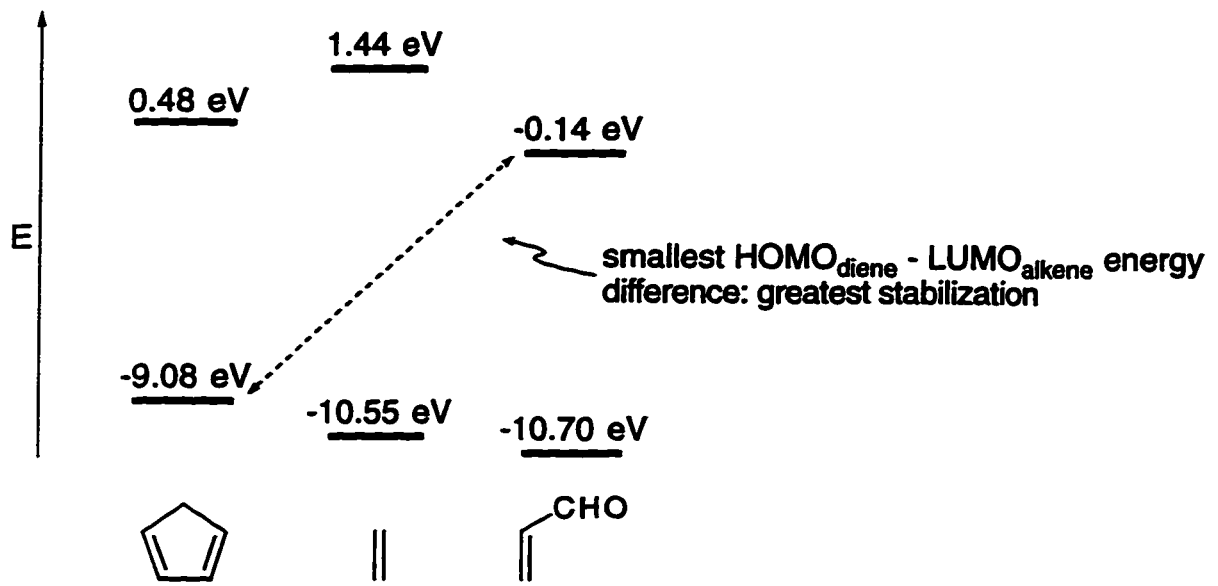

Figure 2.4 Comparison of the LUMO energy of ethylene and acrolein

With the closing of the HOMO$_{diene}$-LUMO$_{alkene}$ energy gap, the two reacting orbitals become more similar in energy. A basic postulate of perturbation molecular orbital theory is that interactions are strongest between orbitals that are close in energy[13] and therefore, the transition state stabilization arising from the interaction of the HOMO and LUMO orbitals becomes greater the closer in energy these two orbitals become.

The preparation of the required ylide **35** was attempted by two routes: the first is shown below (Scheme 2.6).

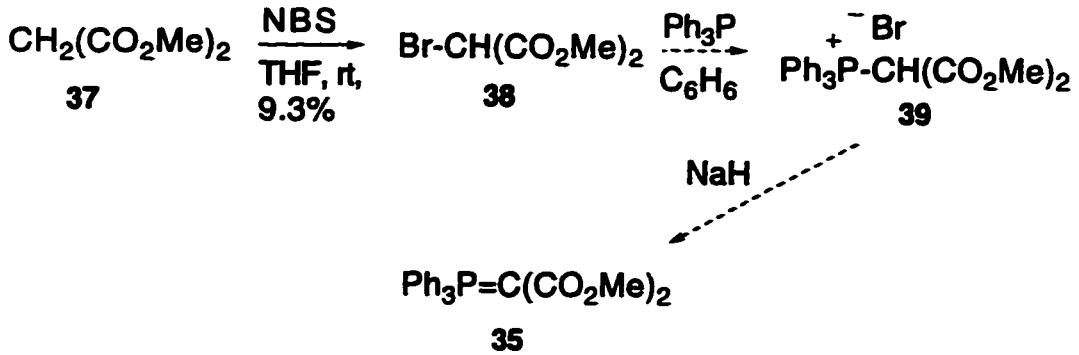

Scheme 2.6 Attempted synthesis of ylide 35

Treatment of dimethyl malonate (**37**) with *N*-bromosuccinimide[17] and a catalytic amount of *p*-toluenesulfonic acid in tetrahydrofuran at room temperature gave a low yield of bromide **38**. The remainder of the reaction mixture was composed of dibrominated material and starting diester. The reaction was performed on a sufficiently large scale (1 mole), however, and a reasonable amount of the desired bromide **38** was obtained (20 g) upon fractional distillation. Unfortunately, formation of the Wittig salt **39**, and subsequent deprotonation to form ylide **35**, proved problematic and therefore the synthesis was modified by treatment of diester **37** with triphenylphosphine / bromine,[18] which produced a reasonable yield (36%) of ylide **35** (Scheme 2.7).

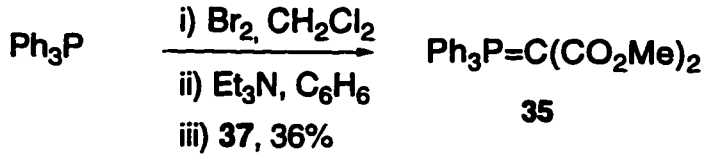

Scheme 2.7 Synthesis of ylide 35

With ylide **35** in hand, the Wittig reaction with oxathiolane **26** was attempted. No product was observed under conditions employing *m*-xylene or 1,2-

dichlorobenzene at reflux temperature. These results were not altogether surprising, given the highly stabilized nature of ylide **35**. It is known that stabilized ylides may react slowly or not at all with ketones.[19] Nucleophilic attack of the ylide **35** on carbonyl compounds such as ketones or esters is also expected to be sluggish due to the reduced electrophilicity of the carbonyl group as compared to aldehydes. These two factors most likely account for the lack of success of the attempted Wittig reactions.

An alternative route to the desired diester **36** was explored as outlined below (Scheme 2.8).

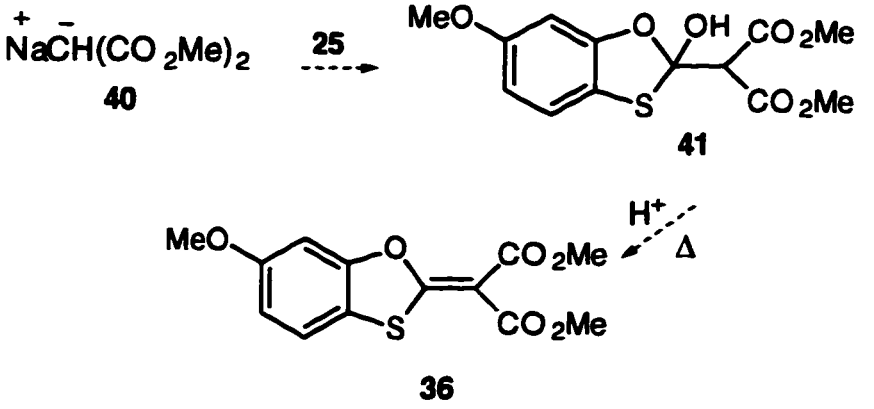

Scheme 2.8 Attempted synthesis of diester 36

It was hoped that treatment of malonate anion **40** with a solution of oxathiolane **25**, and subsequent dehydration of alcohol **41**, would generate diester **36**. Thus, dimethyl malonate was treated with sodium amide, followed by addition of a tetrahydrofuran solution of oxathiolane **25**. Unfortunately, analysis of the major product by ^{1}H / ^{13}C NMR and GC-MS indicated it to be the disulfide **42** (Scheme 2.9).

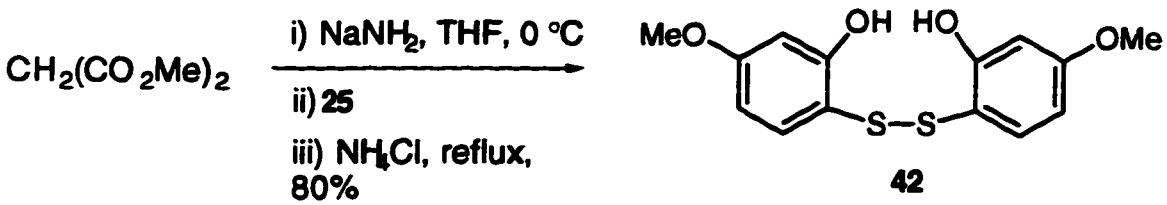

Scheme 2.9 Formation of disulfide 42

A number of conditions were explored which only gave varying amounts of disulfide **42** (up to 80%). A possible mechanism for its formation is shown below (Figure 2.5).

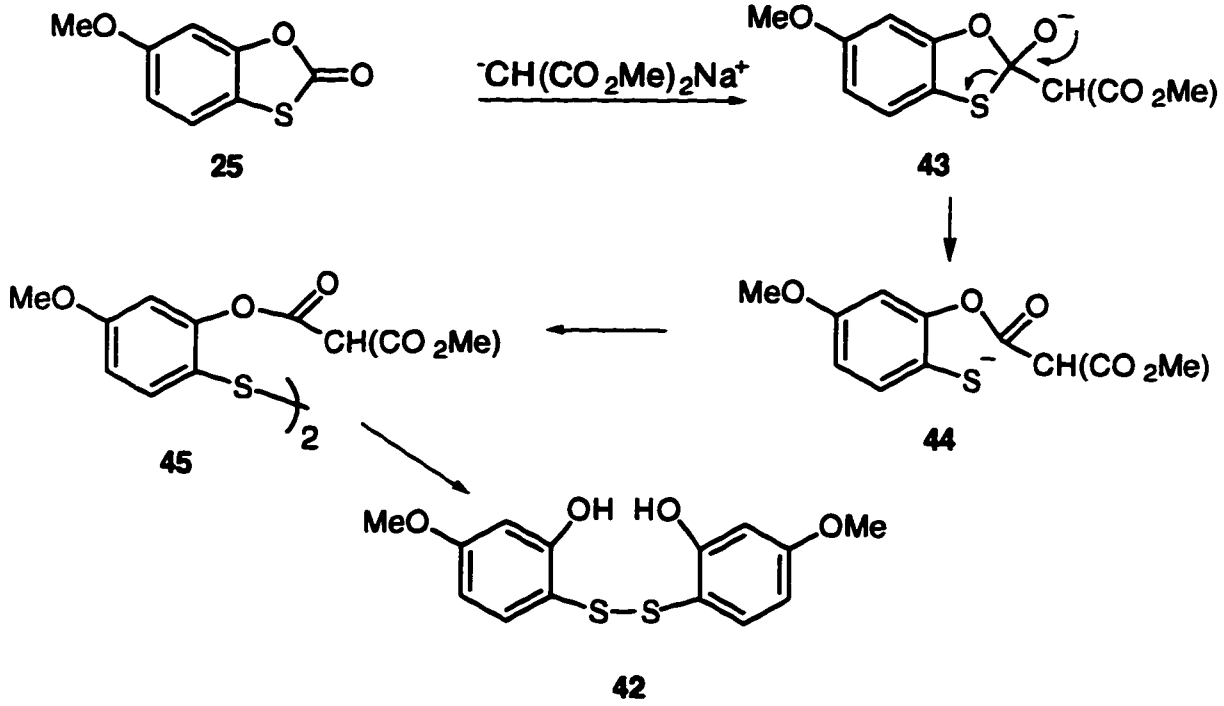

Figure 2.5 Disulfide 42 formation

The addition of dimethylmalonate anion to **25** leads to tetrahedral intermediate **43**, that may collapse with concomitant breakage of the carbon-sulfur bond to give sulfide **44**. Air oxidations of sulfides are known[20] to produce thiyl

radical species that couple, thereby producing dimer **45**. Hydrolysis of dimer **45** gives the recovered disulfide **42**.

2.3 Preparation and Reactivity of Vinyl Sulfoxide 46

2.3.1 Vinyl sulfoxides in Diels-Alder reactions

The lack of reactivity of dienophile **26** and the difficulty in preparing diester **36** was disappointing in that it prevented a direct comparison of the effect of oxygen versus sulfur in Diels-Alder π-facial selectivity. Efforts were therefore focussed on a preparation of sulfoxide **46**, based on reports that vinyl sulfoxides are reasonable dienophiles, particularly if substituted with an additional electron-withdrawing group (Figure 2.6).[21]

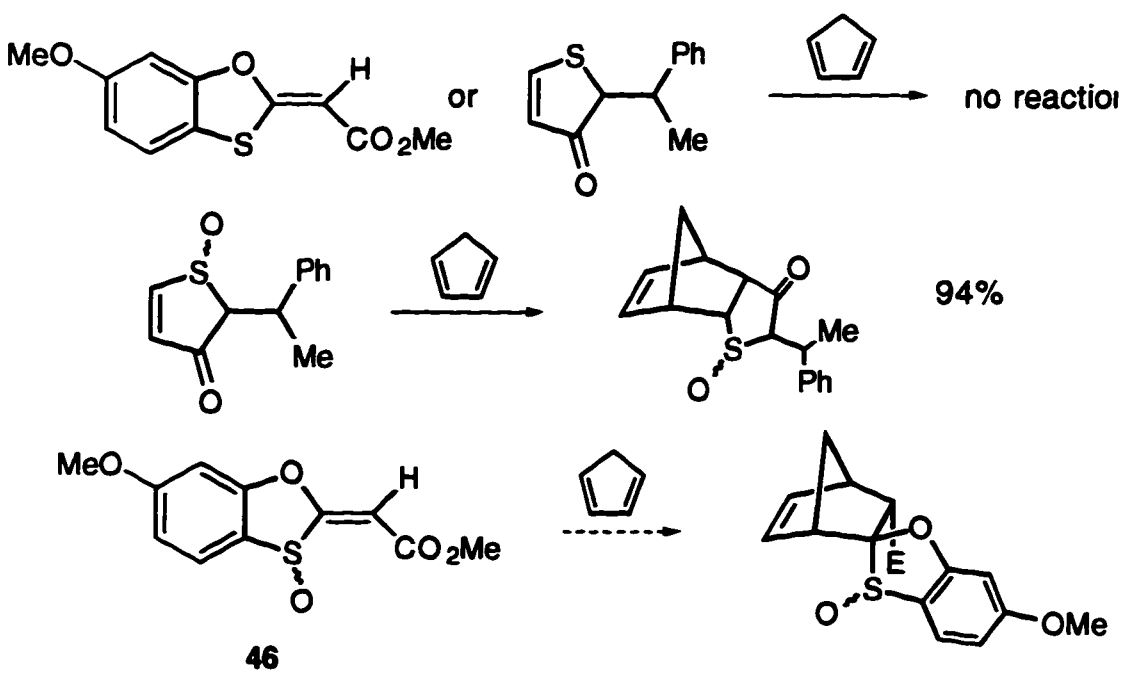

46

Figure 2.6 Proposed cycloaddition of sulfoxide 46

One of the first investigations of the stereochemical outcome of the Diels-Alder reaction using chiral alkenyl sulfoxides was published by Maignon and Raphael,[21a] describing the cycloaddition between (R)-*p*-tolyl sulfoxide (**47**) with cyclopentadiene (Scheme 2.10).

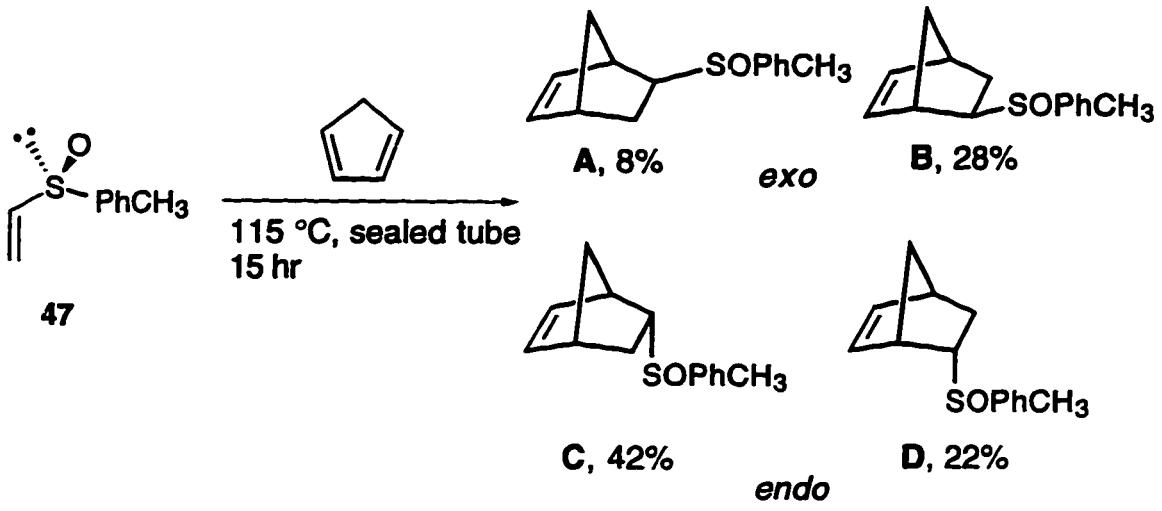

Scheme 2.10 Diels-Alder reaction of vinyl sulfoxide 47

With respect to the selectivity provided by sulfoxide **47**, the results were disappointing, as the *endo*:*exo* ratio (**C+D** : **A+B**) was less than 2 : 1 and the π-facial selectivity for the *endo* and *exo* adducts was 1.9:1 and 3.5:1, respectively. The incorporation of an ester group within sulfoxide **47** resulted in an acrylate that proved to be a superior reagent with respect to both reactivity and π-facial selectivity[22] when treated with cyclopentadiene (Table 2.2).

Table 2.2 π-Facial Selectivity of Chiral Vinyl Sulfoxide 48

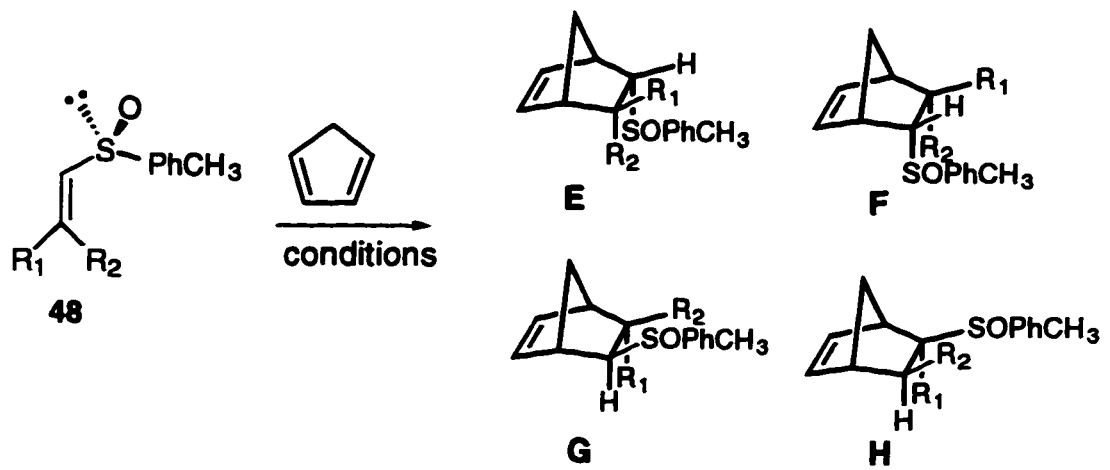

dienophile	conditions	% endo E	F	% exo G	H
R_1=H, R_2=CO_2Me	toluene, 4 °C, 60 h	93	0	7	0
R_1=Me, R_2=CO_2Me	sealed tube, 90 °C, 3 h	63	2	35	0

The predominance of *endo* diastereomer **E** was explained by a smaller steric interaction between the diene and the lone pair of electrons on sulfur, as compared with the phenyl ring of the tolyl group and cyclopentadiene (Figure 2.7).

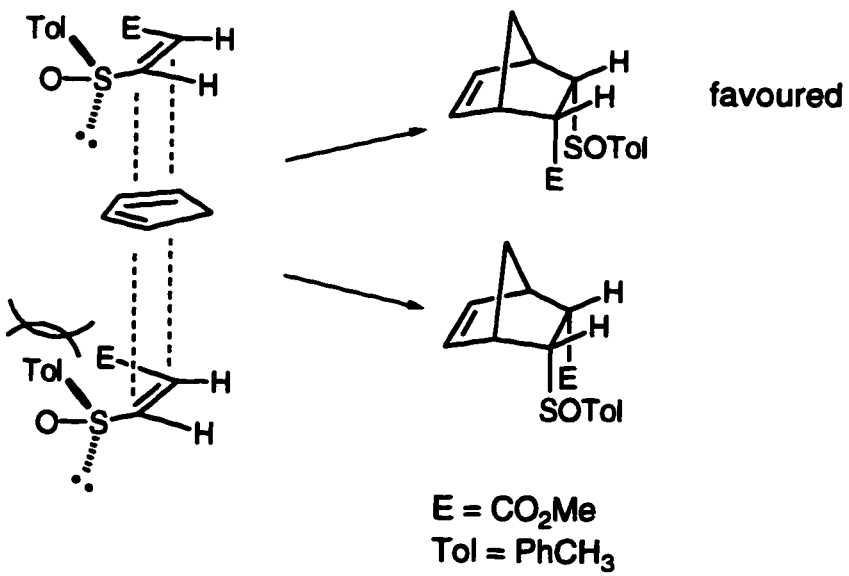

Figure 2.7 Diene approach *syn* to lone pair

This rationalization is valid only if the S=O and C=C bonds are in an s-*trans* conformation. The opposite results are predicted if the dienophile adopts an s-*cis* conformation

When the electrostatic potential model is applied to the above example, the same facial selectivity is predicted, but based on diene approach *anti* to the sulfur atom lone pair. This is attributed to the lone pair rendering that face of the dienophile relatively electron-rich. The opposite face containing the tolyl group is considered relatively electron-poor. The π-facial selectivity arises from the preference for a "nucleophilic" diene to avoid the electron-rich face of the dienophile, even at the expense of encountering a sterically bulky substituent such as the toluene group. This rationalization is valid only, however, if the S=O and C=C bonds assume an s-*cis* conformation, and was based on calculations by Hehre that this is indeed the preferred conformation of such sulfoxides.[23] Unfortunately, these calculations were carried out on cyclopentenone **49**, a considerably different molecule than the sulfoxides described above (Figure 2.8).

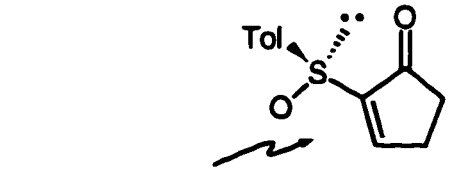

49

Figure 2.8 Calculated preferred conformation of sulfoxide 49

The conformation adopted by cyclopentenone **49** may be a result of dipole-dipole replusion between the sulfoxide bond and the cyclopentanone carbonyl group. The question of which conformation the C=C and S=O groups adopt in simple vinyl sulfoxides remains unanswered and emphasizes the widely differing explanations

found in the literature with repect to factors controlling π-facial selectivity, even for a relatively simple case as that described above. This uncertainty does not arise in cyclic sulfoxide **46**. The sulfur lone pair and the sulfoxide bond are fixed above or below the molecular plane of sulfoxide **46** and therefore, this sulfoxide would appear to be a suitable dienophile to investigate the factors responsible for π-facial selectivity in the Diels-Alder reaction.

2.3.2 Preparation of sulfoxide 46

The preparation of sulfoxide **46** was carried out by oxidation of sulfide **26** with *m*-chloroperbenzoic acid in dichloromethane as outlined in Scheme 2.11. A small excess of *m*-chloroperbenzoic acid and relatively short reaction times at 0 °C limited the amount of over-oxidized product (sulfone **50**) and resulted in reproducible yields of the racemic sulfoxide **46** of approximately 60%.

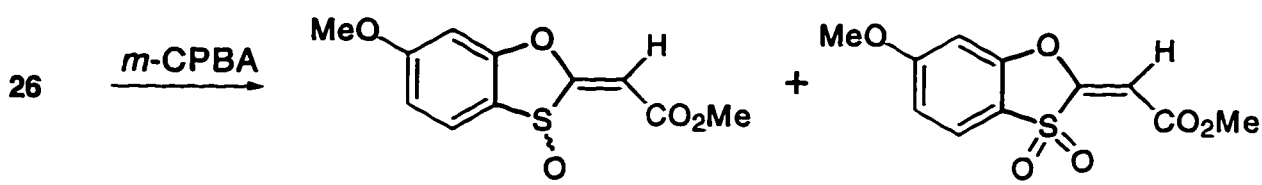

	46	**50**
2 eq. *m*-CPBA CH_2Cl_2, -24 °C to rt, 60 min	47%	11%
1.25 eq. *m*-CPBA CH_2Cl_2, 0 °C, 25 min	62%	4%

Scheme 2.11 Oxidation of oxathiolane 26

2.3.3 Thermal Diels-Alder cycloadditions of sulfoxide 46

The cycloaddition reaction of sulfoxide **46** with cyclopentadiene was attempted initially at room temperature in *m*-xylene. No reaction was observed at this temperature. By performing the reaction at refluxing *m*-xylene temperature, all starting material was consumed after 15 hours. Chromatographic separation on silica gel of the resultant cycloadducts revealed that the reaction proceeded in excellent yield (98%). A disappointing level of both *endo*:*exo* and π-facial selectivity resulted, however, as all four possible norbornenes **51** to **54** were recovered (Scheme 2.12).

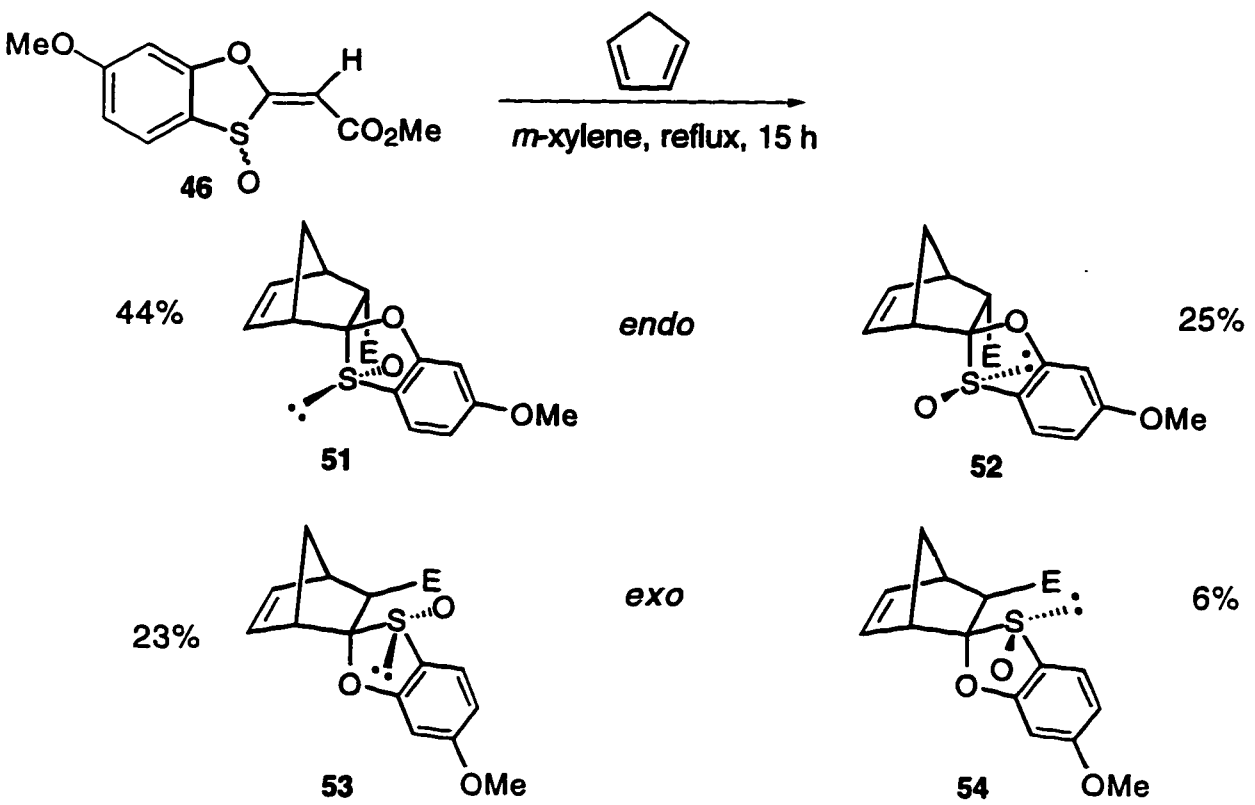

Scheme 2.12 Diels-Alder reaction of sulfoxide 46 with cyclopentadiene

The relative stereochemistry of the products shown in Scheme 2.12 were based on a single crystal X-ray structure analysis of major adduct **51** and ^{1}H / ^{13}C NMR analysis. The *cis* relationship between the ester group and the sulfur atom was evident from the X-ray structure, confirming the assignment of the double bond generated from the previous Wittig reaction (Figure 2.9).

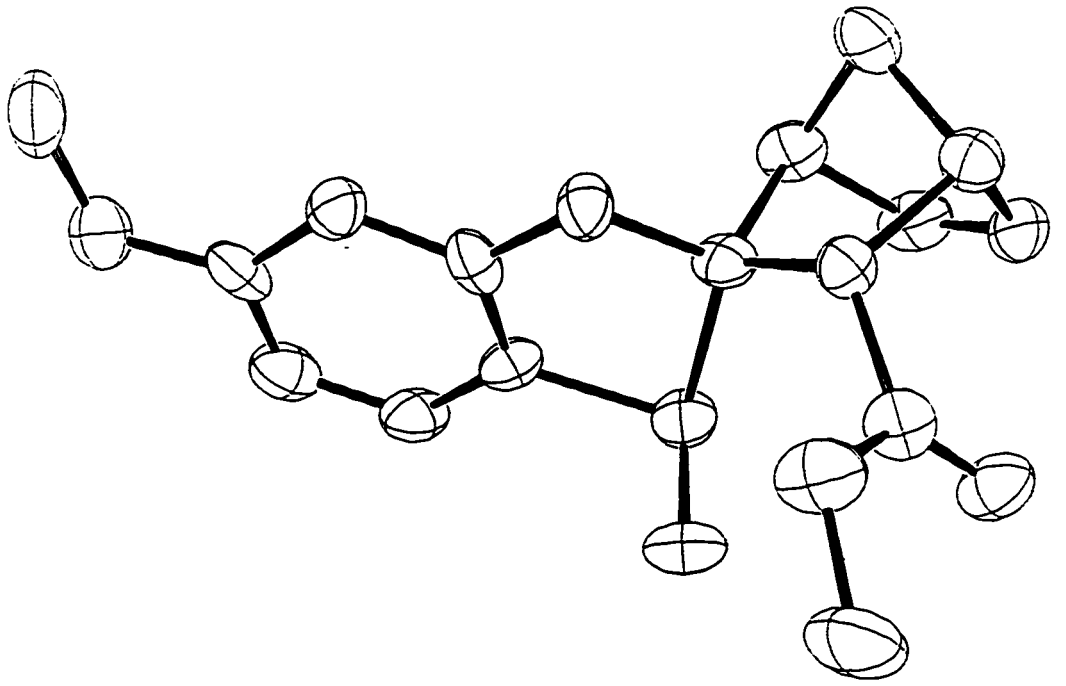

Figure 2.9 ORTEP structure of cycloadduct 51

The assignment of the ^{1}H NMR signals of cycloadduct **51** required ^{1}H ^{1}H COSY NMR experiments. The relevant ^{1}H chemical shift values are shown below (Table 2.3).

Table 2.3 Selected ^1H Chemical Shift Values of Adducts 51to 54

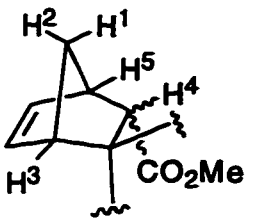

	chemical shift (δ ppm)				
adduct	H-1	H-2	H-3	H-4	H-5
51	1.97	1.82	2.52	3.56	3.22
52	2.01	1.87	3.37	3.17	3.26
53	2.68	1.76	2.58	2.84	3.17
54	2.10	1.84	3.67	2.51	3.35

The bridgehead hydrogen atoms of **51** (H3 and H5) were assigned first, based on the presence of cross-peaks in the COSY spectrum that indicated coupling with vinylic hydrogen atoms. These hydrogen atoms were further distinguished by virtue of H5 coupling with an additional three non-vinylic hydrogen atoms while only two additional hydrogen atoms were coupled to H3. Hydrogen atom H4 was coupled to a single hydrogen atom (H5) and was easily assigned from the COSY spectrum. The discrimination of the methylene hydrogens of the bridge was based on literature precedent: norbornenes typically display a larger chemical shift for the hydrogen *syn* to the double bond.[24] The identification of the remaining adducts was based primarily on a comparison of the ^1H chemical shifts with those of cycloadduct **51**. The lower chemical shift values for *endo* hydrogen atoms compared to *exo* hydrogen atoms, typical of norbornene systems, was also consistant with the stereochemical assignments shown in Scheme 2.12.[24]

The π-facial selectivity was low for both the *endo* and the *exo* adducts (*endo*, 1.7:1; *exo*, 3.5:1) with approach of the diene *syn* to the sulfur lone pair being favoured in both cases, as illustrated below (Figure 2.10).

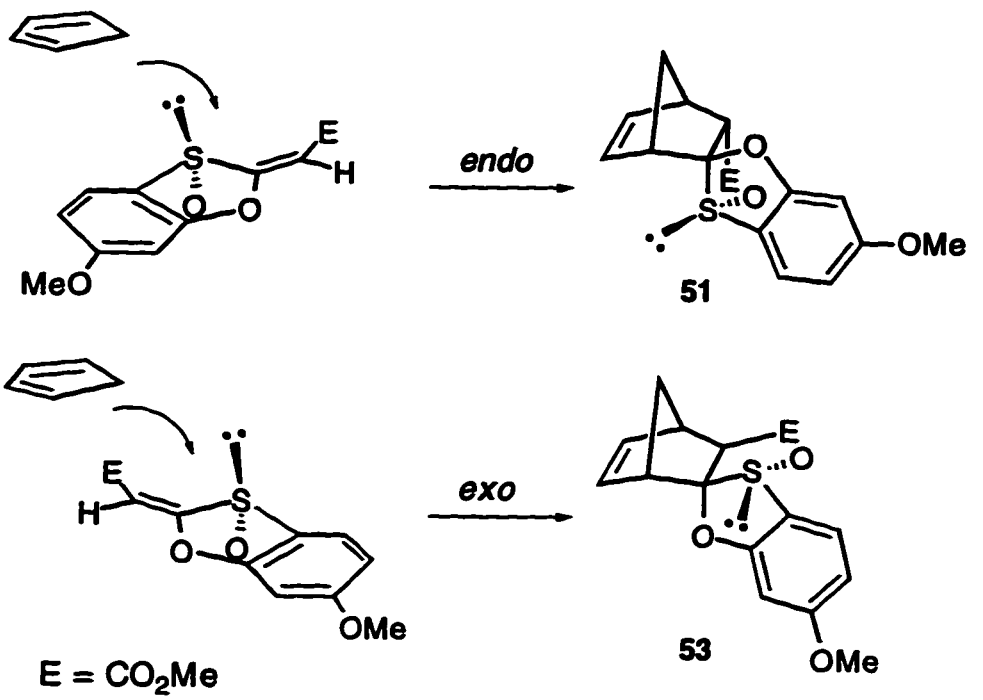

Figure 2.10 Diene approaches *syn* to sulfur lone pair

2.3.4 Thermal Diels-Alder cycloaddition of sulfoxide 56

In an effort to determine if alkene configuration was a factor leading to the low *endo:exo* and π-facial selectivity observed, the cycloaddition reaction was repeated with sulfoxide **56** (Scheme 2.13). This sulfoxide was obtained by *m*-chloroperbenzoic acid oxidation (48% yield) of the *E*-sulfoxide **55**, the minor product of the Wittig reaction performed earlier (Scheme 2.2).

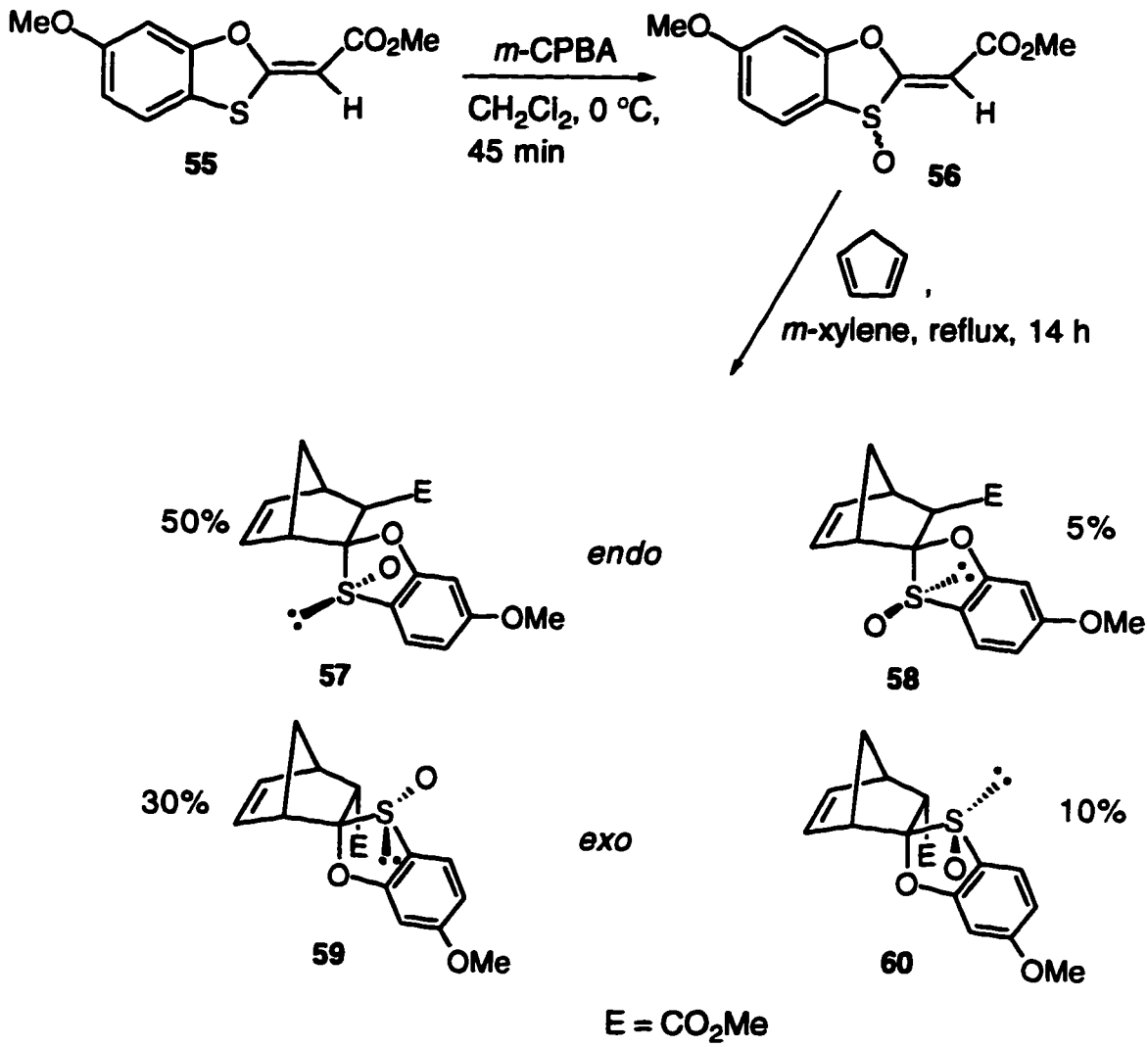

Scheme 2.13 Diels-Alder reaction of sulfoxide 56 with cyclopentadiene

As in the case of sulfoxide **46**, the reaction of sulfoxide **56** with cyclopentadiene required elevated temperatures and no conclusions regarding the effect of reaction temperature on the *endo*:*exo* selectivity could be made. The reaction at refluxing *m*-xylene temperature resulted in an excellent yield (95%) of cycloadduct, however, all four possible diastereomers were present in the reaction mixture. The cycloadducts were separable by silica gel chromatography and the yields refer to isolated compounds. Unfortunately, a crystal suitable for X-ray

analysis could not be obtained and therefore, the identification of the cycloadducts was based on ^{1}H NMR COSY spectroscopy (Table 2.4).

Table 2.4 Selected ^{1}H Chemical Shift Values of Adducts 57 to 60

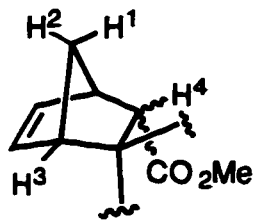

	chemical shift (δ ppm)			
adduct	H-1	H-2	H-3	H-4
57	2.48	2.00	2.67	3.49
58	2.40	1.97	3.42	2.83
59	1.76	1.76	2.96	4.12
60	1.79	1.76	3.75	3.42

Hydrogen atom H3 displayed characteristic chemical shift changes in the cycloadducts depending on the proximity of the sulfoxide oxygen. When this oxygen atom is *syn* to H3, as in cycloadduct **58**, a downfield shift is observed. As before, the *endo* hydrogen atom displayed a lower chemical shift, compared to the *exo* hydrogen atom (H4).

The π-facial selectivity in both the *endo* and *exo* adducts of *E*-sulfoxide **56** was considerably better (10:1 for *exo* addition; 3:1 for *endo* , with the preferred approach of the diene *syn* to the sulfur lone pair in both cases) than *Z*-sulfoxide **46**.

2.4 Rationalization of Observed π-Facial Selectivity

2.4.1 Filled orbital replusion

Both the preferred *endo* and *exo* modes of cycloaddition with sulfoxide **46** were a consequence of the diene approach *syn* to the sulfur lone pair. This may reflect the greater steric demand imposed by the oxygen atom of the sulfoxide compared with the lone pair. This situation is similar to that described earlier (Figure 2.6) wherein the greater steric bulk of a toluene group, compared to a lone pair, was believed responsible for the high observed π-facial selectivity of chiral vinyl sulfoxides when reacted with cyclopentadiene. The relatively low π-facial selectivity of sulfoxide **46** however suggests that other factors compete with this steric influence. A possible candidate is a filled orbital repulsion between the cyclopentadiene HOMO and the sulfur lone pair, favouring dienophile approach *syn* to the sulfoxide oxygen atom. A similar orbital repulsion has been cited[25] as the cause of the π-facial selectivity observed with diene **61** (Figure 2.11).

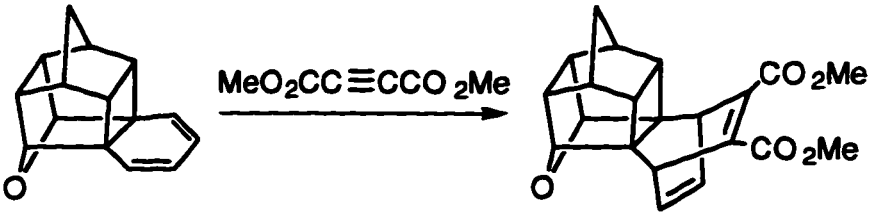

61 **62**

Figure 2.11 Filled orbital repulsion gives *anti* approach

In the example above, the ether oxygen lone pair interacts unfavourably with the π bond of the acetylene dienophile, forcing it to approach in an *anti* fashion. Unfortunately, sulfoxide **46** contains lone pairs on both the sulfur atom, as well as

the sulfoxide oxygen atom, making any π-facial selectivity predictions on the basis of filled orbital repulsion difficult.[26]

2.4.2 Electrostatic potential

Electrostatic repulsion has been implicated in the observed π-facial selectivity of dienophiles such as thiirene **64** (Scheme 2.14).

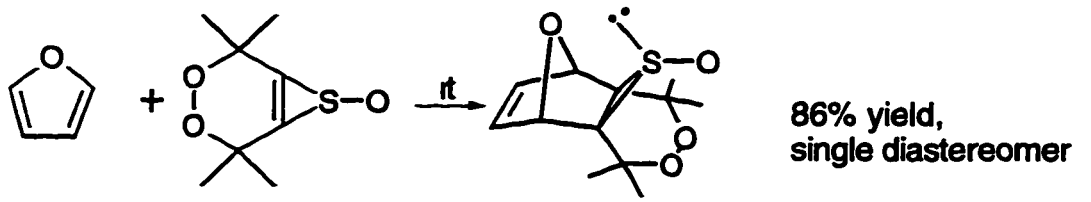

63 **64** **65**

Scheme 2.14 Diels-Alder reaction of thiirene 64

The question arises as to which group is more electron-rich, the sulfoxide group or the sulfur lone pair, in compounds such as thiirene **64** or sulfoxide 46. A study by Hehre concluded[27] that the sulfoxide group was more electron-rich than the sulfur lone pair. This was based on the high π-facial selectivity that resulted from the cycloaddition reaction of thiirene **64** with furan (**63**) and from *ab initio* calculations to generate the dienophile electrostatic potential surface. Thus, exclusive addition of furan *anti* to the sulfoxide oxygen of **64** ("the more electron-rich face," according to Hehre), is interpreted in terms of electrostatic replusion that directs the nucleophilic diene to the relatively electron-poor face containing the sulfur lone pair.

To determine whether electrostatic potentials could be used to predict the π-facial selectivity of Diels-Alder cycloaddition reactions without resorting to high level *ab initio* calculations, semi-empirical calculations (AM1) were performed to generate electrostatic potential surfaces for thiirene **64** and the related diene, 2,5-

dimethylthiophene *S*-oxide **66**. The graphical results of these calculations are shown below with the respective Diels-Alder adduct that each sulfoxide forms exclusively (Figure 2.12).

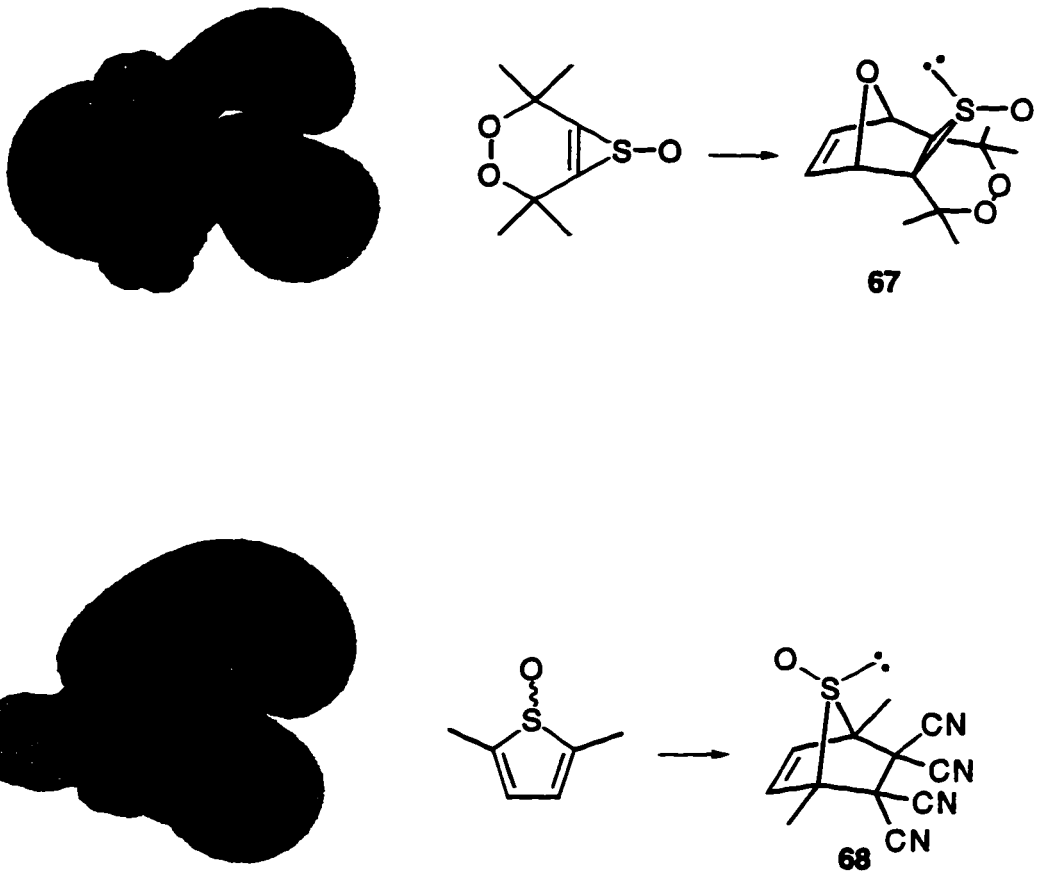

67

68

Figure 2.12 Electrostatic potential surfaces of sulfoxides 64 and 66

The blue areas of Figure 2.12 represent regions of negative potential (electron-rich areas) and the red areas represent relatively electron-poor areas. In both cases, the electrostatic surfaces that are generated indicate that the face of the π system containing the sulfoxide bond is more electron-rich than the face of the molecule with the sulfur lone pair. Thus, in the case of thiirene **64**, a nucleophilic

diene should approach the relatively electron-poor face of the dienophile to give adduct **67**. Diels-Alder adduct **67** is the exclusive product, as determined experimentally. In an analogous fashion, an electrophilic dienophile (TCNE in this case) prefers approach to the more electron-rich face of the diene thiophene S-oxide **66**, in accordance with experimental results.

These results prompted us to re-investigate various substituted dienes, used previously in this laboratory, to determine whether electrostatic potentials may also predict correctly the π-facial selectivity in these cases. The observed π-facial selectivity for these dienes was originally attributed to an hyperconjugative stabilization (Cieplak model) of the reaction transition state by the σ bond of the substituent at the 5-position.[28] The results of the electrostatic potential calculations are shown below (Figure 2.13).

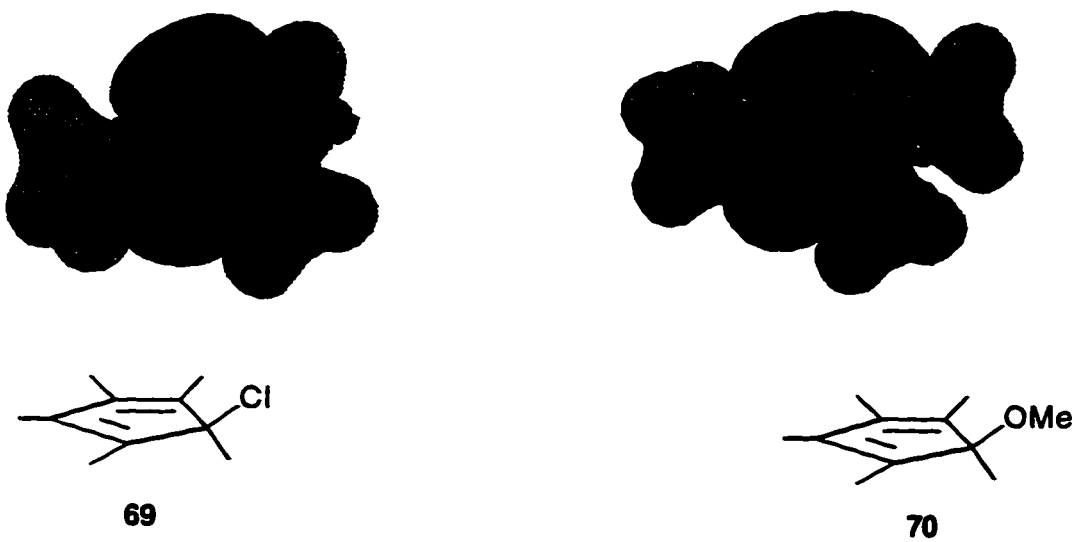

69 **70**

Figure 2.13 Electrostatic potential surfaces of substituted cyclopentadienes

72 71

Figure 2.13 cont. Electrostatic potential surfaces of substituted cyclopentadienes

The electrostatic potential surfaces generated for cyclopentadienes with a chlorine (69) or methoxy substituent (**70**) at the 5-position both display a larger electron-rich area on the face of the molecule containing the heteroatom substituent. Thus, the resultant π-facial selectivity is in accord with the electrostatic model, in that the cycloadducts formed are a result of the electrophilic dienophile approach *syn* to the relatively electron-rich face of the diene. It is noteworthy that the electrostatic model also correctly predicts lower π-facial selectivity of thiol **71**, contrary to the Cieplak model. The electrostatic potential surface of thiol **71** has a more symmetrical distribution of negative electrostatic potential and is predicted to have lower π-facial selectivity, as observed. Thioether **72** also has a similar electrostatic potential surface as thiol **71**, yet displays much higher π-facial selectivity. The failure of the electrostatic model in this case may be due to the steric effect of the thioether group.

In the Diels-Alder cycloaddition reaction of oxathiolane sulfoxide **46** with cyclopentadiene (Scheme 2.12), both steric and electrostatic interactions should direct approach of the diene *syn* to the sulfur lone pair. Thus, a high π-facial selectivity was expected but not observed. The electrostatic potential for sulfoxide **46** was calculated in an effort to account for this lack of selectivity (Figure 2.14).

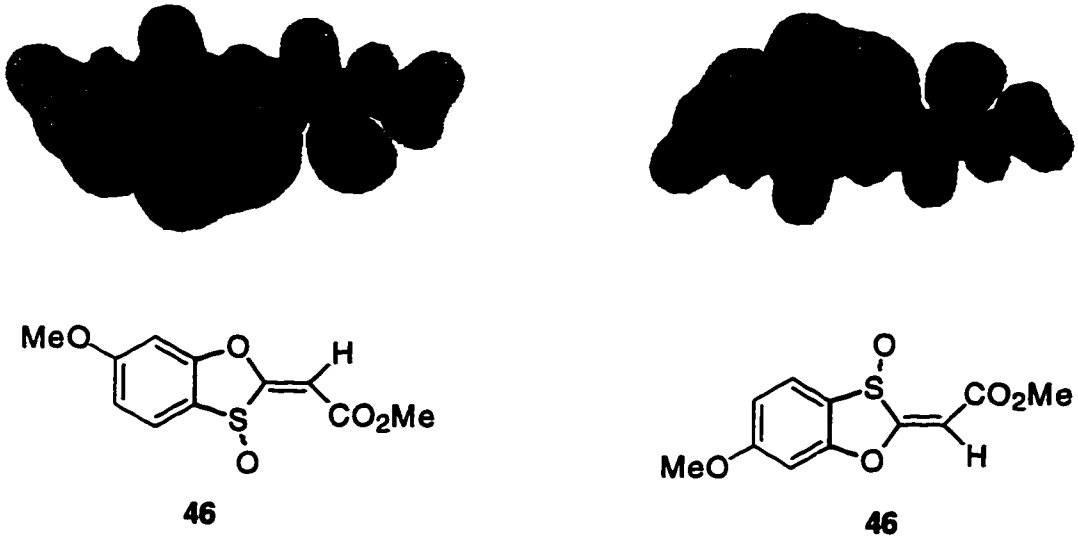

Figure 2.14 Electrostatic potential surfaces of sulfoxide 46

The electrostatic potential surface of sulfoxide **46** shown in Figure 2.14 accounts for the low π-facial selectivity of the molecule in cycloaddition reactions: both surfaces are similar and no discrimination is expected by an approaching diene. The question of why sulfoxide **46** has similar electrostatic potential surfaces on both π-faces of the molecule, while the related thiirene **64** displays very different electrostatic potential surfaces (and higher selectivity: only a single adduct is formed when reacted with furan), may be answered by inspection of the AM1-optimized structure of sulfoxide **46** (Figure 2.15).

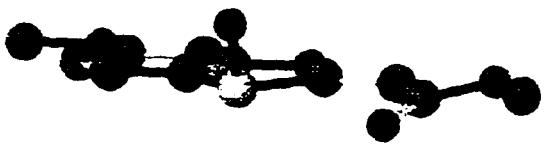

Figure 2.15 AM1 structure of sulfoxide 46

The ester carbonyl group of sulfoxide **46** is bent out of the plane of the molecule (as defined by the aromatic and oxathiolane ring) by approximately 18° in the direction of the sulfur lone pair in the AM1-optimized structure. This bending may be due to unfavourable dipole-dipole interactions between the carbonyl double bond and the S-O bond of the sulfoxide group. The AM1 optimization was repeated with a starting geometry in which the carbonyl was bent towards the sulfoxide S-O bond and resulted in the same minimized structure shown in Figure 2.15. With the carbonyl group out of the plane of the molecule, the combination of the sulfur lone pair and the carbonyl double bond to the electrostatic potential on that face of the molecule may be balanced by that of the sulfoxide group, rendering both faces of the molecule electrostatically similar. Thus, the molecular geometry can account for the low observed π-facial selectivity.

As described earlier, the *E* isomer **56** resulted in better π-facial selectivity in both *endo* and *exo* modes of addition. In order to determine whether electrostatic potential was responsible for the higher π-facial selectivity observed with sulfoxide **56** the electrostatic potential was calculated from the AM1-optimized geometry (Figure 2.16).

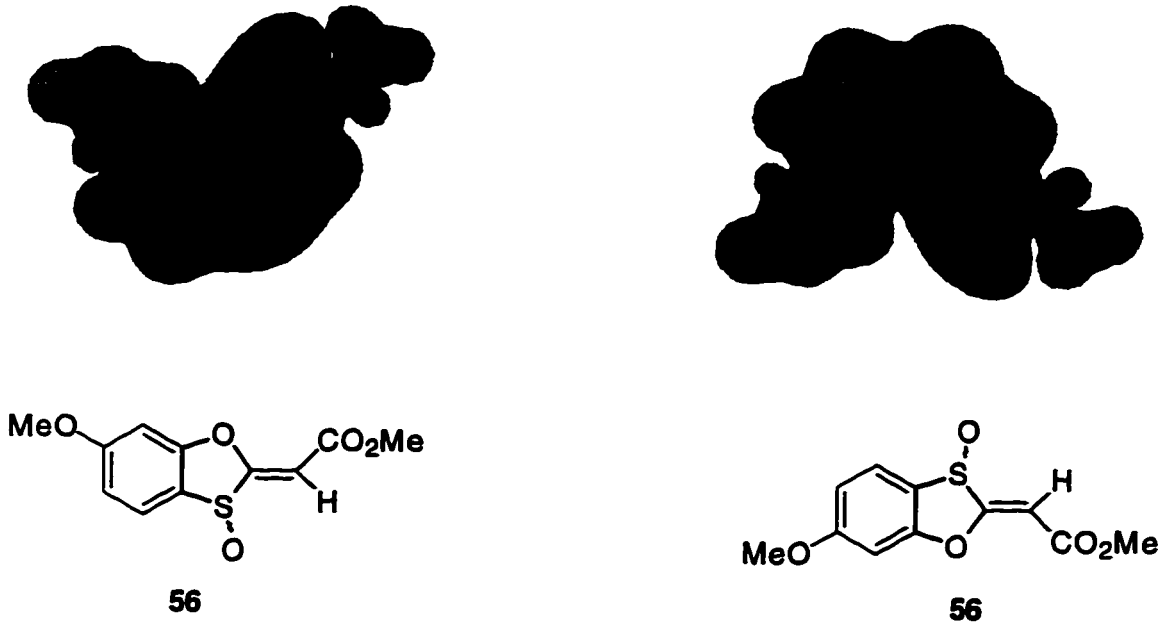

Figure 2.16 Electrostatic potential surfaces of sulfoxide 56

In the AM1-optimized structure of sulfoxide **56**, the ester carbonyl group is 3.5° out of the plane of the molecule, in the direction of the sulfur lone pair face of the molecule. Thus, a smaller contribution by the ester carbonyl group to the electrostatic potential on this face of the molecule is expected. The electrostatic potential between the two π faces is caused primarily by the sulfur lone pair and the sulfoxide oxygen atom, in a manner similar to thiirene **64** to give an electrostatic potential surface that displays a greater difference between the two π faces. The electrostatic potential surfaces for both faces of the molecule shown in Figure 2.16 indicate that the sulfoxide-containing face of the molecule to be relatively electron-rich as compared to the face containing the sulfur lone pair. This difference in the electrostatic potential between the two π-faces of sulfoxide **56** should result in greater π-facial selectivity, and this is reflected in the experimental results.

2.4.3 Transition state stabilization by hyperconjugation

In the event that a Cieplak-type of transition state stabilization is operative and competes with an electrostatic effect, a low π-facial selectivity may be expected in the cycloaddition reaction of oxathiolane sulfoxide **46** with cyclopentadiene. This is a consequence of the directing effect of the sulfur lone pair (best σ-donor) promoting diene approach *syn* to the sulfur oxygen, opposite that to predicted by the electrostatic potential model. The relevant factors in the case of the *endo* adducts, are summarized below (Figure 2.17).

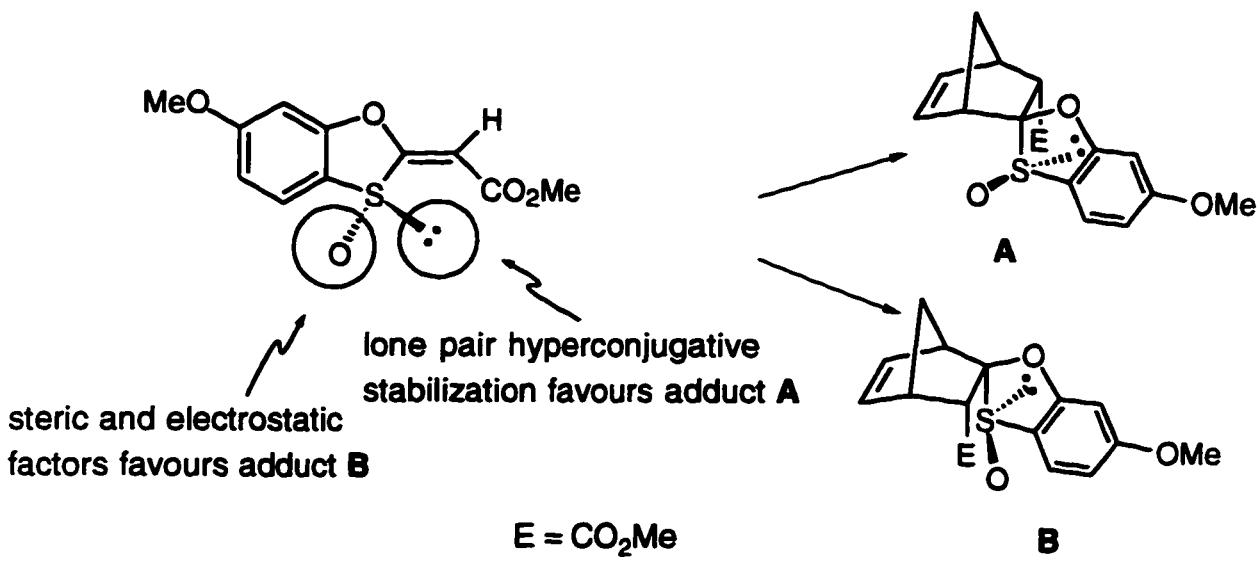

Figure 2.17 Cieplak and electrostatic model predictions

The lone pair on the sulfur atom of a sulfoxide group is considered to be a better σ-donor of electron density than the sulfur-oxygen σ-bond, as the lone pair electrons are not involved in bonding with another atom. According to the Cieplak model, the diene approaches the π-face of the molecule *anti* to the best σ donor that provides stabilization of the developing carbon-carbon bonds. The results of the thermal Diels-Alder reaction of oxathiolane sulfoxide **46** (and isomer **56**) are,

however, contrary to the Cieplak model. The cycloadduct formed preferentially in *endo* and *exo* modes of addition for both sulfoxides was a result of the diene approach *syn* to the sulfur lone pair, despite the fact that the sulfur lone pair should exert the same effect in either mode of addition.

The anti-Cieplak behavior of sulfoxide **46** may be a consequence of the orbital symmetry requirements of the Diels-Alder reaction. According to frontier molecular orbital theory, the important interactions between reacting molecules in the Diels-Alder reaction are the HOMO of one reactant and the LUMO of the other reactant.[13] The basis for concentrating attention on these two orbitals is that they will usually be closest in energy of the interacting orbitals, and this interaction is favourable since it involves one filled (HOMO) and one empty (LUMO) orbital. A basic postulate of perturbation molecular orbital theory is that interactions are strongest between orbitals that are close in energy. Thus, the majority of Diels-Alder reactions involve interactions between the dienophile LUMO and the diene HOMO, as this arrangement represents the smallest energy difference between the frontier molecular orbitals (Figure 2.18A).

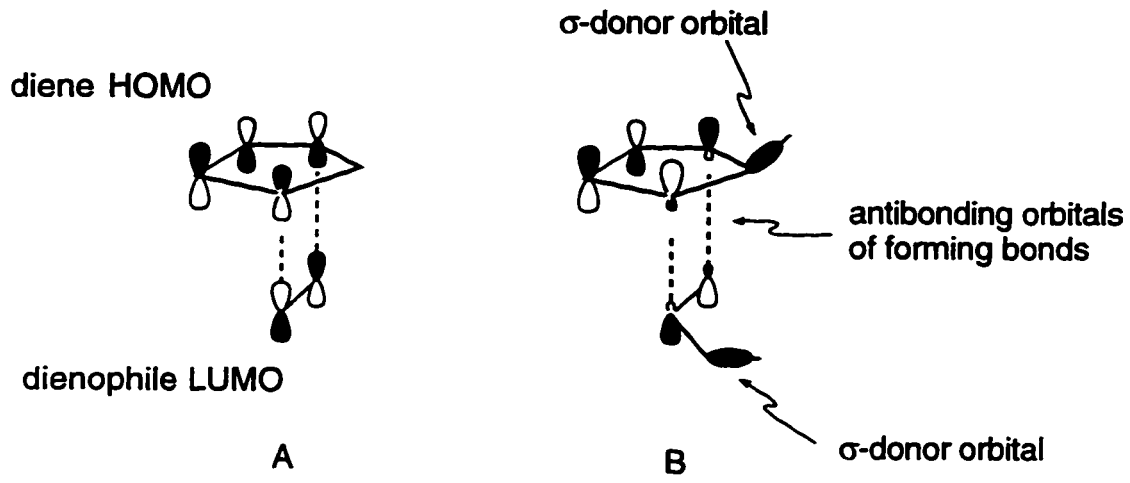

Figure 2.18 Orbital symmetry of the Diels-Alder reaction

The HOMO of cyclopentadiene and the LUMO of ethylene are shown in Figure 2.18A. The HOMO of cyclopentadiene contains a single node, as does the LUMO of ethylene, resulting in the terminal lobes of both π systems being opposite in sign and antisymmetric. Thus, the Diels-Alder reaction shown in Figure 2.18A follows the Woodward-Hoffmann rules and is termed a symmetry-allowed reaction. The antibonding orbitals of the forming carbon-carbon bonds are also shown in Figure 2.18B along with a σ-donor orbital on both the diene and the dienophile. These carbon-carbon antibonding orbitals are the orbitals that interact with the σ-donor orbital in the Cieplak model. The orbital symmetry of the dienophile and diene is antisymmetric and therefore, the incipient antibonding orbitals must also reflect this symmetry. By definition, however, a σ-donor is a symmetrical orbital and will only interact with an orbital of similar symmetry. Therefore, no hyperconjugative stabilization should be expected from σ-donation by either diene or dienophile in these types of Diels-Alder reactions.[29]

The thiirene *S*-oxide **64** described previously is an ideal dienophile to test the Cieplak model, as the sulfur lone pair bisects the alkene π-system. This should allow for maximum interaction (neglecting orbital symmetry) with the antibonding orbitals of the forming carbon-carbon bonds compared with oxathiolane sulfoxide **46** (Figure 2.19).

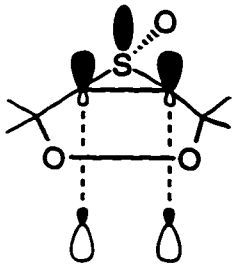

64

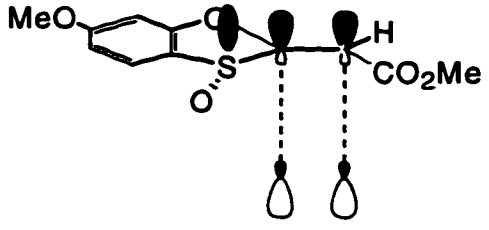

46

Figure 2.19 Sulfur lone pair orbital overlap

The sole adduct of the reaction of thiirene *S*-oxide **64** with furan (Scheme 2.14) is the adduct from approach of the diene *syn* to the lone pair on the sulfur atom, contrary to the Cieplak model. The σ donor group of sulfoxide **46** is not as ideally positioned to donate electron density into the forming carbon-carbon bonds as thiirene **64** and may not contribute, in the Cieplak sense, to the π-facial selectivity. Finally, the Cieplak model does not predict any differences in π-facial selectivity based on whether the reaction procedes *via* an *endo* or an *exo* mode of cycloaddition. This is also contrary to the experimental results for sulfoxides **46** and **56**. The fact that the major cycloadducts are all anti-Cieplak suggests that hyperconjugative stabilization is not a factor in determining the π-facial selectivity of these cycloaddition reactions.

2.5 Lewis Acid-Catalyzed Diels-Alder Reactions of Sulfoxide 46

The poor *endo:exo* ratio that resulted from the reaction of sulfoxide **46** with cyclopentadiene was the first issue to be addressed in order to improve the synthetic utility of such dienophiles. Dienophiles that contain alkenes conjugated with ester groups usually give high *endo:exo* ratios, due to the favourable secondary orbital interactions between the carbonyl LUMO and the diene HOMO (Figure 2.20).

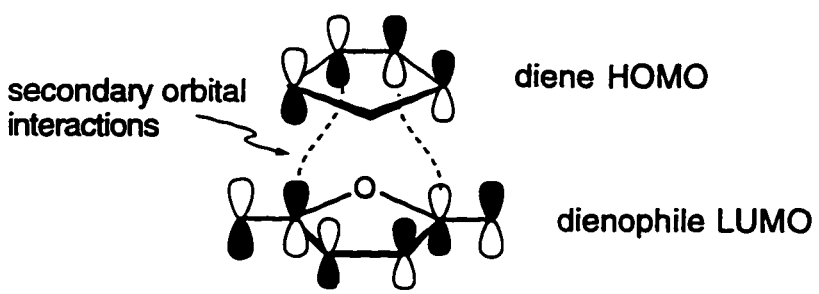

Figure 2.20 Secondary orbital interactions

Another method of obtaining greater *endo:exo* selectivity is by the use of Lewis acids.[30] A temperature effect is also observed with the use of Lewis acids, with many cases sucessfully performed at low temperature. These features of Lewis acid-catalyzed Diels-Alder reactions may be explained by the effect the Lewis acid has on the LUMO of the dienophile (Figure 2.21).

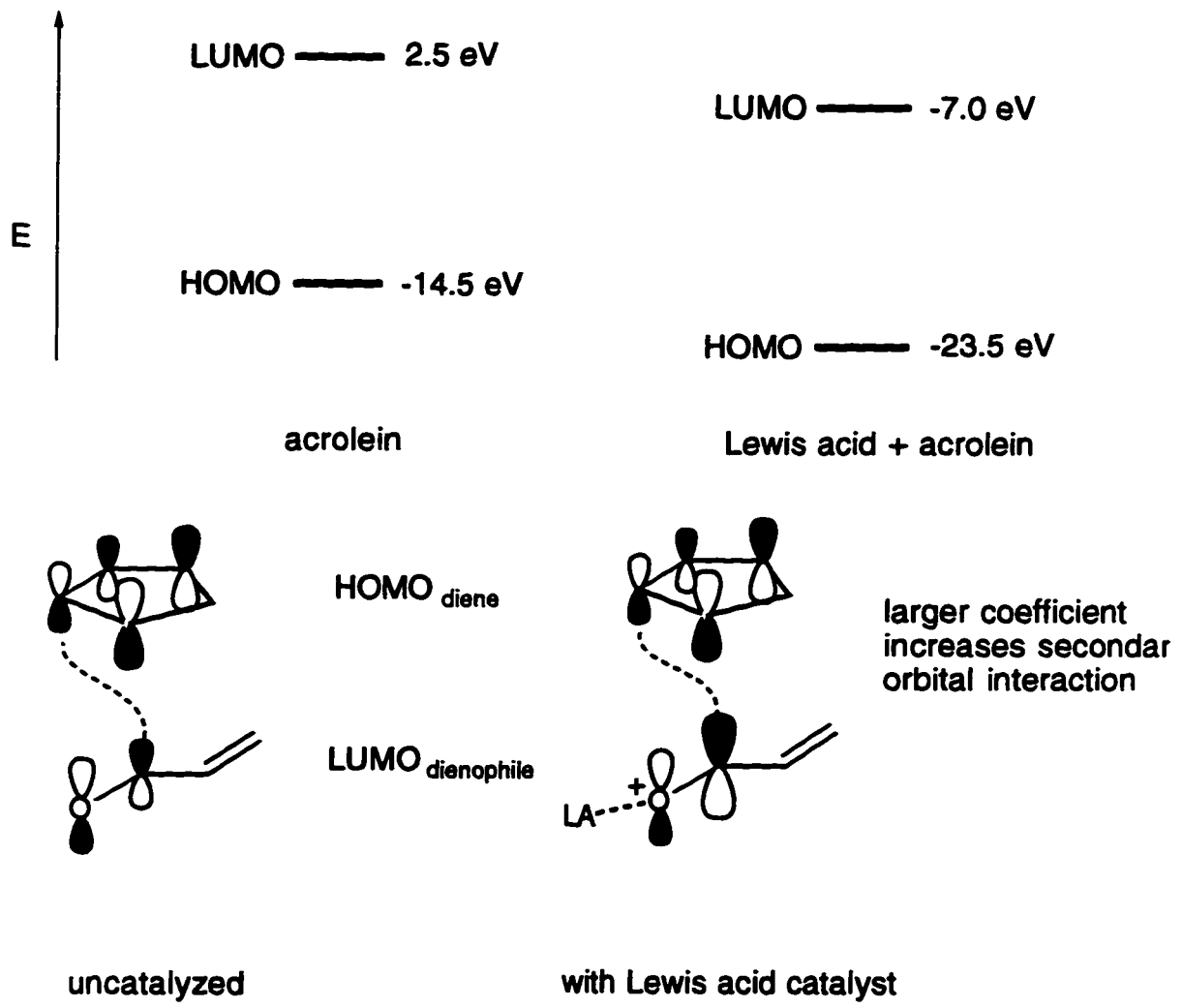

Figure 2.21 The effect of Lewis acid on dienophile LUMO

Upon addition of a Lewis acid, the donor-acceptor interaction between the dienophile and catalyst lowers the energy of both the HOMO and LUMO of the

dienophile . As a consequence, the $HOMO_{diene}$-$LUMO_{dienophile}$ energy separation decreases and a increased stabilization of the transition state results, allowing the reaction to proceed at lower temperatures. The greater *endo* selectivity is a result of a increased polarization of the dienophile carbonyl bond upon addition of a Lewis acid. This polarization leads to a larger coefficient at the carbonyl carbon of the LUMO and makes the secondary orbital interaction greater than in the uncatalyzed case.

Several conditions were investigated to induce cycloaddition of sulfoxide **46** with cyclopentadiene at low temperature using Lewis acids. The reactivity of sulfoxide **46** was increased by the use of $ZnCl_2$ (no reaction was observed at -78 °C) with a modest *endo:exo* selectivity (Table 2.5), but complete π-facial selectivity occurred.

Table 2.5 $ZnCl_2$ Catalyzed Diels-Alder Reactions of Sulfoxide 46

entry	conditions[a]	% yield	*endo* : *exo*
a	rt, C_6H_6, 18 h	98	2.6 : 1
b	0 °C, CH_2Cl_2, 38 h	97	3.1 : 1
c	-78 °C to rt, CH_2Cl_2, 14 h	94	3.1 : 1
d	-78 °C, CH_2Cl_2, 5 h	NR	

[a] all reactions were carried out with 1.1 equiv. $ZnCl_2$ and 2 equiv. cyclopentadiene

Only a single *endo* and *exo* adduct were produced (**51** and **53**, respectively), based on ^1H NMR analysis of the two isolated products from the reaction mixture. Thus, cyclopentadiene approached exclusively *syn* to the sulfur lone pair under Lewis acid-catalyzed conditions. These results were encouraging, but conditions were still required that also gave high *endo:exo* selectivity. The *endo:exo* selectivity improved marginally upon cooling the mixure to -78 °C and allowing to warm slowly to room temperature.

Several other Lewis acids were surveyed, all resulting in varying degrees of *endo:exo* selectivity and high π-facial selectivity (in all cases, only adducts **51** and **53** were detected by GC-MS). Treatment of sulfoxide **46** with boron trichloride in dichloromethane at -78 °C afforded a single diastereomer, norbornene **51**.[31] The results are summarized below (Table 2.6).

Table 2.6 Lewis Acid Catalyzed Diels-Alder Reactions of Sulfoxide 46

entry	conditions		*endo* : *exo*
a	$SnCl_2$, CH_2Cl_2, rt, 12 h	90%	2.2 : 1
b	Et_2Al-$TiCl_4$, -78 °C to rt, 5 h	87%	2.5 : 1
c	Et_2Al-$TiCl_4$, -78 °C, CH_2Cl_2, 24 h	NR	
d	BCl_3, -78 °C, CH_2Cl_2, 5 h	88%	10 : 0

An analysis of the boron trichloride-catalyzed reaction mixture by GC-MS, ^1H and ^{13}C NMR spectroscopy, indicated norbornene **51** as the only cycloadduct produced, arising from an *endo* transition state with complete π-facial control *syn* to the sulfur lone pair.

The increased reactivity and π-facial selectivity of the Lewis acid catalyzed cycloaddition reactions may be rationalized based on the ester carbonyl oxygen or sulfoxide oxygen complexing with the Lewis acid. This complexation lowers the LUMO energy (along with the HOMO) of the sulfoxide as described earlier. Calculations (AM1) were carried out to determine if a significant lowering of the LUMO energy occured preferentially, based on the site of Lewis acid complexation. The results show a lowering of the LUMO energy of sulfoxide **46** occurs by complexation by either sulfoxide oxygen or ester oxygen (Table 2.7).

Table 2.7 Calculated LUMO Energy (AM1) for BCl_3-Complexed Sulfoxide 46

	LUMO energy
sulfoxide (no Lewis acid)	- 0.7056 eV
carbonyl-BCl_3 complex	- 1.4505 eV
sulfoxide-BCl_3 complex	- 1.6368 eV

The complexation of boron trichloride to the sulfoxide group not only provides the greater lowering of LUMO energy, but would also be expected to block any approaching diene from that face of the molecule more effectively than compared with the ester carbonyl-Lewis acid complex. These electronic and steric factors are most likely responsible for the high *endo:exo* and π-facial selectivity of sulfoxide **46**.

2.6 Synthesis of 2-norbornenone 77

Having established the conditions required to effect efficient cycloaddition of dienophile **46** with cyclopentadiene in good yield with high *endo:exo* and π-facial selectivity, attention was focused on a means to remove the aromatic sulfoxide and ester moiety to afford 2-norbornenone **77**. A brief survey of the literature revealed no examples of the transformation of a sulfoxide such as **51** directly to norbornenone **75** (Scheme 2.15).

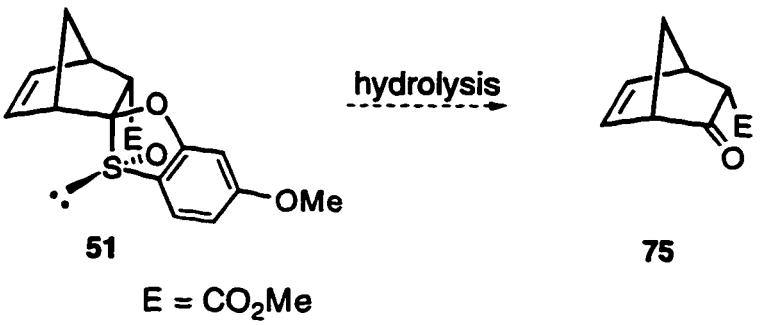

51 **75**

E = CO_2Me

Scheme 2.15 Removal of sulfoxide group to give norbornenone 75

Standard methods[32] for the transformation of 1,3-oxathiolanes to ketones were investigated, together with various conditions (Table 2.8) normally used for the cleavage of 1,3-dithianes and 1,3-dithiolanes, as many of these conditions are also applicable to 1,3-oxathiolanes. Unfortunately, these experiments only resulted in recovered starting material along with varying amounts of polymeric material that were not characterized.

Table 2.8 Unsuccessful Conditions for Oxathiolane Sulfoxide 51 Cleavage

entry	conditions
a	HgCl, AcOH, reflux, 10 h
b	HCl, AcOH, reflux, 4 h
c	$CuCl_2$, CuO, acetone, reflux, 13 h
d	*p*-$MeC_6H_4SO_2N(Cl)Na$, aq. MeOH, reflux, 6 h
e	$AgNO_3$, EtOH, reflux, 5 h
f	TFA, THF, H_2O, reflux, 2 h
g	$Tl(NO_3)_3$, MeOH, reflux, 5 h
h	$Ce(NH_4)_2(NO_3)_6$, aq. CH_3CN, reflux, 4 h

The difficulty in converting sulfoxide **51** directly to 2-norbornenone **75**, though not unexpected, forced the implementation of a two step sequence comprised of a reduction step followed by a hydrolysis step (Scheme 2.16).

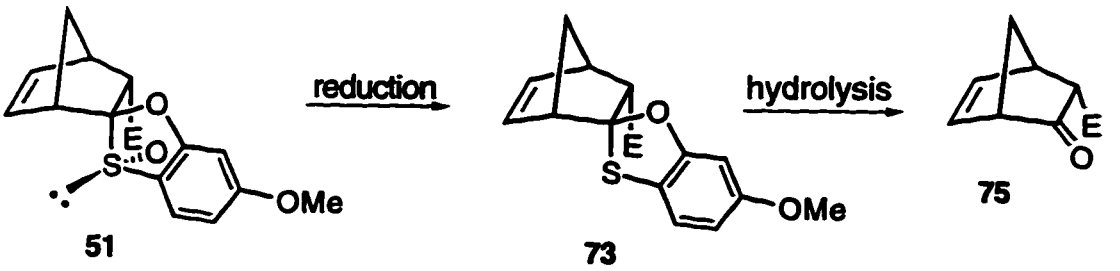

Scheme 2.16 Conversion of sulfoxide 51 to norbornenone 75

The first step was performed by treatment of sulfoxide **51** with triphenylphosphine in dichloromethane with a catalytic amount of iodine.[33] The white solid that was isolated thwarted all attempts to form X-ray suitable crystals, however, HRMS, ^{1}H / ^{13}C NMR and combustion data was consistant for oxathiolane **73** (Scheme 2.17).

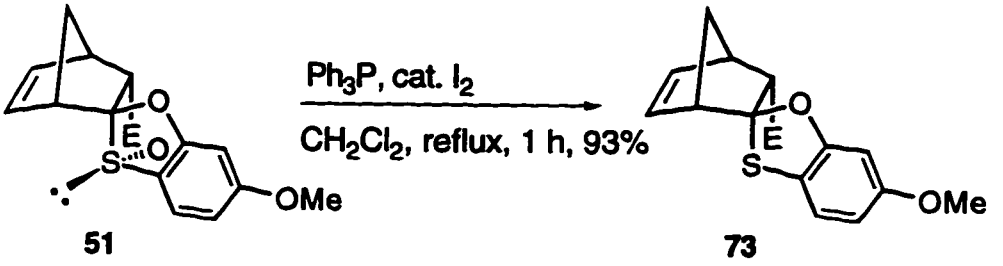

Scheme 2.17 Deoxygenation of sulfoxide 51

Analysis of the product by HRMS confirmed the loss of 16 amu as compared to sulfoxide **51** Further, the ^{1}H NMR signals for the hydrogen atoms attached to the carbon atoms proximate to the former sulfoxide group, displayed the greatest change in chemical shifts while all others remained relatively constant (Figure 2.22).

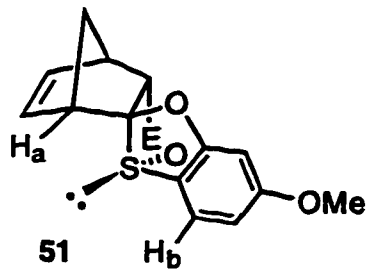

H_a: 2.52 ppm
H_b: 7.66 ppm

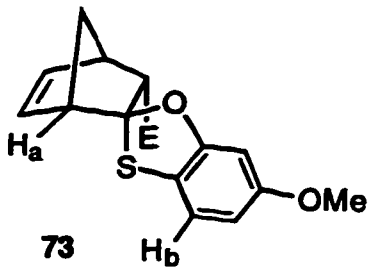

H_a: 3.25 ppm
H_b: 6.92 ppm

E = CO_2Me

Figure 2.22 Selected ^1H NMR signals of sulfoxide 51 and sulfide 73

The presence of a double bond in norbornene **51** was initially a matter of concern regarding the possibility of a competing iodolactonization reaction. Fortunately, the high isolated yield (93%) of sulfide **73** confirmed that this particular complication did not arise under these particular conditions. All conditions investigated to effect the reduction of sulfoxide **51** resulted in high yields of sulfide **73** (Table 2.9).

Table 2.9 Sulfoxide 51 Reduction Conditions

entry	conditions	yield
a	NaI, $POCl_3$, CH_3CN, DMF, rt, 5 h	85%
b	Ph_3P, cat. I_2, CH_2Cl_2, 40 °C, 21 h	93%
c	$C_6H_5P(O)Cl_2$, py, CH_2Cl_2, 10 °C, 45 min	96%

The method of choice eventually became that reported by Kagan[34] (Table 2.9, entry c). The use of phenyl dichlorophosphate gave yields comparable to the

triphenylphosphine / iodine method, but required much shorter reaction times (45 min vs. 21 h).

The conversion of oxathiolane **73** to norbornenone **75** followed the method of Emerson and Wynberg,[35] whereby oxathiolane **73** was treated with sodium *N*-chloro-*p*-toluenesulfonamide (Chloramine-T) in methanol at room temperature (Scheme 2.18).

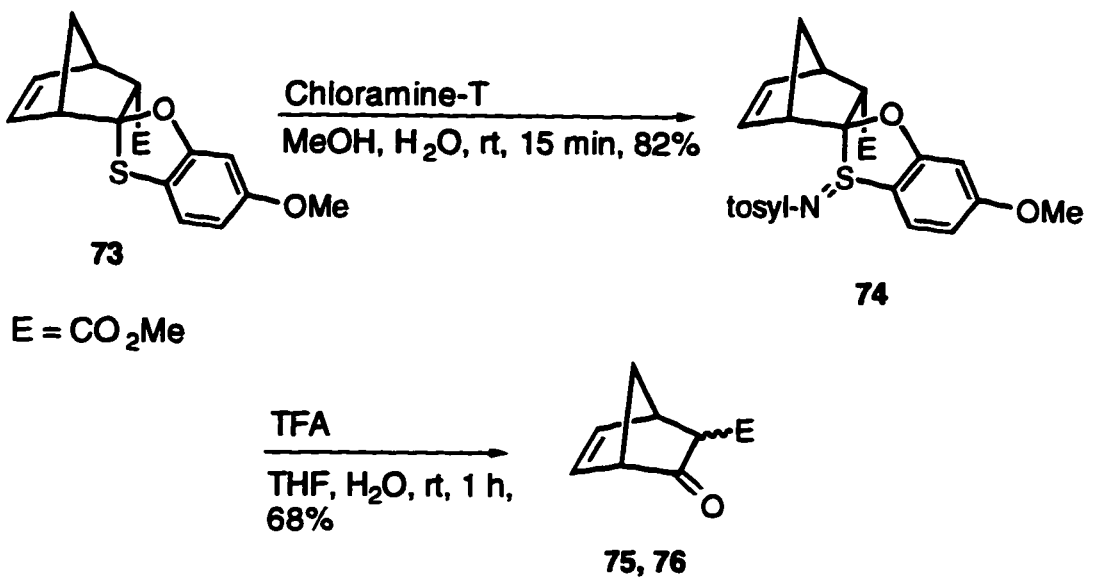

Scheme 2.18 Conversion of oxathiolane 73 to norbornenones 75 and 76

Following purification by chromatography on silica gel, ^{1}H / ^{13}C NMR and HRMS analyses gave data consistent for the sulfinylimine **74** (82% yield) shown above. The isolation of this stable, crystalline compound was unexpected in light of the reported[35] instability of sulfinylimine compounds. Initial attempts to hydrolyse sulfinylimine **74** were carried out with trifluoroacetic acid in aqueous tetrahydrofuran at room temperature. A modest yield (68%) of a mixture of norbornenones **75** and **76**, epimeric at C3 with an *endo:exo* ratio of 3:1, was obtained. The separation of the norbornenones by silica gel chromatography was not sucessful and therefore,

the *endo:exo* ratio was determined by integration of the ^1H NMR signals of the hydrogen atom adjacent to the carbomethoxy group. The structure of the epimers followed from a comparison of NMR data with the known literature[36] values for these compounds and experimental values from HRMS and elemental analyses, consistant for these compounds. If the crude sulfinylimine **74** is employed, a "one-pot" operation is possible that results in improved yields (81% over two steps), and the same amount of epimerization.

In an attempt to reduce the epimerization, the hydrolysis was repeated using acetic acid in tetrahydrofuran / water at room temperature. In this instance, the yield was improved dramatically (95%), although at the expense of increased C3 epimerization (*endo:exo*, 1.5:1) due to an increase in the required reaction time. The epimerization did not represent a significant problem, as the ester group at C3 was to be removed eventually.

In this regard, the final step of the synthesis was the removal of the ester group from norbornenone **75**. Compounds such as norbornenone **75** are known to be sensitive to ring cleavage by classical saponification conditions (treatment with alkoxides or hydroxides) and thus, other conditions were employed to avoid this cleavage (Table 2.10).

Table 2.10 Decarboxylation of Norbornenone 75 and 76

75, 76 77

entry	conditions	outcome
a	BCl_3, CH_2Cl_2, 40 °C, 1h	decomposition
b	TFA, THF/H_2O, reflux, 1 h	decomposition
c	LiI, DMF, H_2O, reflux, 1 h	~ 30% yield
d	TMSCl, NaI, THF/H_2O, reflux, 2 h	~ 60% yield

The method described by Olah[37] (Table 2.10, entry d) involves *in situ* generation of TMSI, and produced the highest yields (~60%) of 2-norbornenone **77**. The use of Lewis acids such as boron trichloride or protic acids resulted in the formation of polymeric material. In order to avoid large losses of product during purification, solvent must be distilled off carefully at atmospheric pressure, followed by bulb-to-bulb distillation at 110-125 °C (25 torr). For maximum product recovery, the literature[7b] recommends preparatory GC or spinning-band distillation. The identity of the product was confirmed by comparison of NMR data of **77** with literature values.[24b]

2.7 Preparation of Optically Active 2-Norbornenone (+)-77

The current interest in the synthesis of enantiomerically pure Diels-Alder cycloadducts has led to the design of chiral ketene equivalents,[38] a number of which are based on alkenyl sufoxides (Figure 2.23).

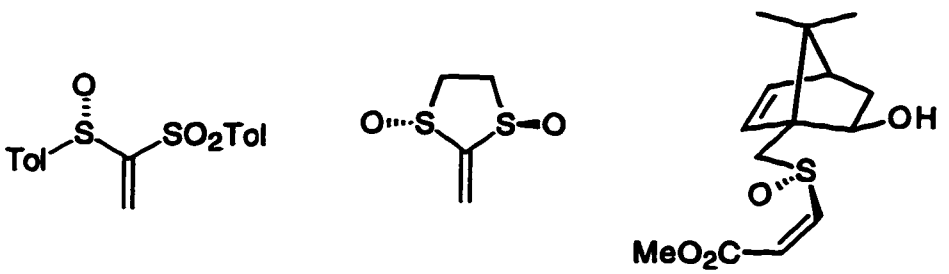

Figure 2.23 Optically active sulfoxide dienophiles

In order to increase the synthetic utility of the ketene equivalent **46**, the preparation of the optically active sulfoxide **(+)-46** was investigated. The oxidation was attempted initially by employment of the standard Sharpless conditions[39] [Ti(O-*i*-Pr)$_4$/diethyl tartrate/*t*-BuOOH (1:1:2 in CH_2Cl_2, -20 °C)] but this method proved ineffective, as only starting material was recovered. The addition of one mole of water (the Kagan modification[40]) improved the yield considerably (45% yield, 80% ee). The enantiomeric excess in this and subsequent experiments was determined by ^{1}H NMR spectroscopy (500 MHz) by the additon of chiral shift reagent Eu-(+)-(hpc)$_3$ to the NMR sample.[41] In the case of sulfoxide **(+)-46**, both the methyl ester and methyl ether singlets split sufficiently to be measured; the ee reported are based on the integration of these signals.

The alkyl portion of the oxidizer usually has little effect on the enantiomeric excess or yield in the classical Sharpless epoxidation (*ie* replacing *t*-BuOOH with cumene hydroperoxide) but can lead to dramatic improvements in enantiomeric excesses of sulfur oxidation reactions.[42] The combination of cumene hydroperoxide and diisopropyl-(L)-tartrate resulted in the best chemical yield and ee (74% yield, ≥99% ee after recrystallization from MeOH). The use of diisopropyl tartrate reportedly causes problems during work-up of asymmetric epoxidations (work-up difficulties can be avoided by purification of the product as described below), but nevertheless was effective here and improved the ee of the oxidation of sulfide **26** by

7% when compared with diethyl-(L)-tartrate. The conditions used are shown below (Scheme 2.19).

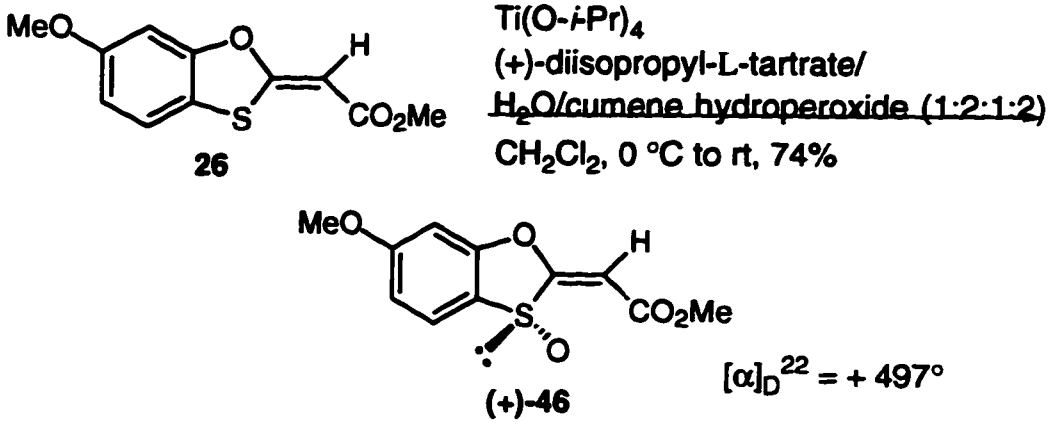

Scheme 2.19 Preparation of chiral sulfoxide (+)-46

The assignment of the absolute stereochemistry of **(+)-46** was not possible until the subsequent transformation to the known norbornenone (*vide infra*). The avoidance of a typical work-up, and the purification of the diisopropyl tartrate and titanium isopropoxide are both crucial to the success of the reaction. Preliminary reactions that employed reagents without purification resulted in both low ee and low yields. The reaction mixture was poured directly onto a silica gel column without work-up and purified by gradient elution (100% dichloromethane to 100% ether). The resultant white solid was recrystallized from methanol to afford the optically active sulfoxide **(+)-46** in 74% yield ($[\alpha]_D^{22}$ = + 497°, c = 2.8, $CHCl_3$).

The steps neccessary for the synthesis of optically active 2-norbornenone **77** from optically active sulfoxide **(+)-46** paralleled those used with the racemic sulfoxide. The boron trichloride-catalyzed Diels-Alder reaction was repeated with optically active sulfoxide **(+)-46** and cyclopentadiene. The yield of norbornene **(+)-51** after purification was 86%; the reaction is apparently quite sensitive to the purity of the boron trichloride reagent, as earlier experiments with older stock resulted in

lower (ca. 15%) yields. The optically active sulfoxide **(+)-51** resisted all attempts at crystallization, unlike the racemic sulfoxide, and thus prevented X-ray analysis. The ^{1}H and ^{13}C NMR specta of **(+)-51** were comparable to cycloadduct **51** indicating that the cycloaddition had occured exclusively in an *endo* fashion with complete π-facial selectivity (Scheme 2.20).

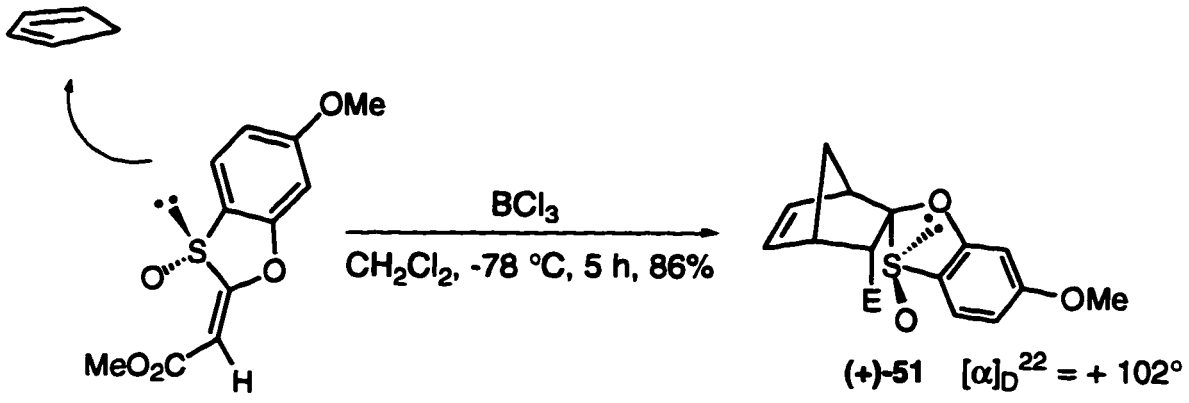

Scheme 2.20 Diene approach *syn* to the sulfur lone pair

Reduction of sulfoxide **(+)-51** to sulfide **(+)-73** with phenyl dichlorophosphate afforded a high yield of a colourless oil in 89% yield ($[\alpha]_D^{22}$ = +77°, c = 2.0, $CHCl_3$). Spectral characteristics of this compound matched that of the racemic sulfide **73**. The sulfide was next converted into the norbornenone esters **75** and **76**, without isolation of the intermediate sulfinyimine, by treatment of sulfide **(+)-73** with Chloramine-T, followed by acetic acid to afford esters **75** and **76** in 78% yield. The degree of epimerization of the resultant thick oil was similar to that observed with the racemic sulfide as determined by ^{1}H NMR.

Removal of the methyl ester functionality from esters **75** and **76** was accomplished by treatment with *in situ*-generated TMSI (Scheme 2.21). The yield of 2-norbornenone **(+)-77** was 63% after purification by bulb-to-bulb distillation, and the sign of the optical rotation[38a] ($[\alpha]_D^{22}$ = +893 °, c = 1.9, $CHCl_3$) allowed for the

determination of the absolute stereochemistry of the Diels-Alder adduct to be assigned as shown in Scheme 2.20.

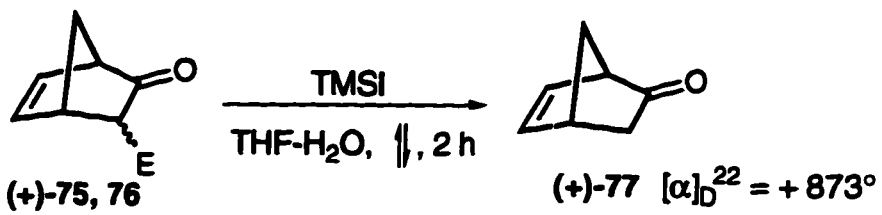

(+)-75, 76 (+)-77 $[\alpha]_D^{22} = +873°$

E = CO_2Me

Scheme 2.21 Preparation of optically active 2-norbornenone (+)-77

2.8 Conclusions

The π-facial selectivity in the Diels-Alder reaction between cyclopentadiene and the vinyl sulfoxides prepared was modest to good under thermal conditions depending on the geometry of the groups at the terminus of the alkene portion of the molecule. The *endo:exo* selectivity, however, was poor irrespective of the double bond geometry. Upon addition of Lewis acid catalysts, the π-facial selectivity increases dramatically, with complete *endo* selectivity and π-facial control with the use of boron trichloride at -78 °C in dichloromethane. All of the Lewis acid-catalyzed cases studied resulted in the major cycloadducts forming from diene approach *syn* to the dienophile sulfur lone pair. This *syn* addition was also the preferred approach taken by the diene in the thermal Diels-Alder reactions investigated. The stereochemical outcome of the Diels-Alder reactions may be rationalized by consideration of the electrostatic differences between the two π-faces of the dienophile. The electrostatic model correlated well with the selectivities observed and also served to explain the π-facial selectivity displayed by substituted

cyclopentadienes and related systems. The high π-facial selectivity of the Lewis acid catalyzed cycloaddition reactions are likely a combination of electrostatic and steric effects. Complexation onto the sulfoxide oxygen by the Lewis acid effectively blocks one face of the molecule. Exclusive approach by cyclopentadiene *syn* to the sulfur lone pair is the result. A re-examination of the substituted cyclopentadienes and thiophene oxides studied earlier in these laboratories by semi-empirical methods revealed that the electrostatic model correctly predicted the observed selectivity in most cases. It should be noted that the electrostatic potential surfaces generated are based on ground state structures and may not reflect the transition state electrostatic potential. They do, however, have useful predictive power with respect to π-facial selectivity in the Diels-Alder reactions examined.

The observed π-facial selectivity in the prepared vinyl sulfoxides **46** and **56** was opposite to that predicted on the basis of hyperconjugative stabilization of the transition state. The failure of the Cieplak model in these cases, in conjunction with orbital symmetry considerations for the normal-type Diels-Alder reaction in general, make it unnecessary as well as inappropriate to invoke the Cieplak model in Diels-Alder reactions.

The vinyl sulfoxide **46** was demonstrated to be a suitable ketene equivalent which underwent cycloaddition with cyclopentadiene with complete π-facial control in the presence of Lewis acid with moderate *endo:exo* selectivity and thus allowed for the preparation of racemic 2-norbornenone **77**. The current interest in the synthesis of enantiomerically pure compounds prompted the synthesis of optically pure ketene equivalent **(+)-46** by use of the Kagan modification of the Sharpless conditions on sulfide **26**. This allowed for the synthesis of the optically active 2-norbonenone **(+)-77** by following the procedures developed for the racemic sulfoxide. The 2-norbonenone **77** and its keto-ester precursors **75** and **76** may find use in the field of natural product synthesis.

Chapter 2 References

1. Paquette, L. A. In *Asymmetric Synthesis*, Vol. 3, Part B; Morrison, J. D., Ed.; Academic Press, Inc.: New York, 1984, p. 455.
2. Tripathy, R.; Franck, R. W.; Onan, K. D. *J. Am. Chem. Soc.* **1988**, *110*, 3257.
3. Jensen, F.; Foote, C. S. *J. Am. Chem. Soc.* **1987**, *109*, 6376.
4. Clennan, E. L.; Earlywine, A. D. *J. Am. Chem. Soc.* **1987**, *109*, 7104.
5. Yadav, V.; Fallis, A. G. *Can. J. Chem.* **1991**, *69*, 779.
6. Martynow, J.; Dimitroff, M.; Fallis, A. G. *Tetrahedron Lett.* **1993**, *34*, 8201.
7. a) Corey, E. J.; Loh, T.-P. *Tetrahedron Lett.* **1993**, *34*, 3979. b) Corey, E. J.; Loh, T.-P. *J. Am. Chem. Soc.* **1991**, *113*, 8966.
8. Woodward, R. B.; Hoffmann, R. *Angew. Chem., Int. Ed. Eng.* **1969**, *8*, 781.
9. Abell, A. D.; Morris, K. B.; Litten, J. C. *J. Org. Chem.* **1990**, *55*, 5217.
10. Yates, P.; Eaton, P. *J. Am. Chem. Soc.* **1960**, *82*, 4436.
11. Fischer, G.; Rudorf, W.-D.; Kleinpeter, E. *Magn. Reson. Chem.* **1991**, *29*, 212.
12. Dewar, M. J. S.; Zoebisch, E. G.; Healy, E. F.; Stewart, J. J. P. *J. Am. Chem. Soc.* **1985**, *107*, 3902.
13. Fleming, I. *Frontier Orbitals and Organic Chemical Reactions*; Wiley: New York, 1976.
14. Waldner, A. *Tetrahedron Lett.* **1989**, *30*, 3061.
15. Fringuelli, F.; Taticchi, A. *Dienes in the Diels-Alder Reaction*; John Wiley & Sons, Inc.: New York, 1990, p. 23.
16. Smith, M. B. *Organic Synthesis*; McGraw-Hill, Inc.: New York, 1994, p. 1115.
17. Reed, S. F., Jr. *J. Org. Chem.* **1965**, *30*, 2195.
18. Cooks, J. C.; Ward, R. S.; Williams, D. H.; Shaw, M. A.; Tebby, J. C. *Tetrahedron* **1968**, *24*, 3289.

19. March, J. *Advanced Organic Chemistry*, 4th Edition; John Wiley & Sons, Inc.: New York, 1992, p. 957.

20. Wallace, T. J.; Schriesheim, A.; Bartok, W. *J. Org. Chem.* **1963**, *28*, 1311.

21. a) Maignon, C.; Raphael, R. A. *Tetrahedron* **1983**, *39*, 3245. b) Arai, Y.; Kuwayama, S.; Takeuchi, Y.; Koizumi, T. *Synth. Commun.* **1986**, *16*, 233. c) Maignon, C.; Belkasmioui, F. *Tetrahedron Lett.* **1988**, *29*, 2823.

22. Maignon, C.; Guessous, A.; Rouessac, F. *Tetrahedron Lett.* **1984**, *25*, 1727.

23. Fisher, M. J.; Hehre, W. J.; Kahn, S. D.; Overman, L. E. *J. Am. Chem. Soc.* **1988**, *110*, 4625.

24. a) Emerson, D. W.; Wynberg, H. *Tetrahedron Lett.* **1971**, 3445. b) Paquette, L. A.; Doecke, C. W.; Kearney, F. R.; Drake, A. F.; Mason, S. F. *J. Am. Chem. Soc.* **1980**, *102*, 7228.

25. Coxon, J. M.; Fong, S. T.; McDonald, D. Q.; Steet, P. J. *Tetrahedron Lett.* **1993**, *34*, 163.

26. McCarrick, M. A.; Wu, Y.-D.; Houk, K. N. *J. Am. Chem. Soc.* **1992**, *114*, 1499.

27. a) Posner, G. H.; Mallamo, J. P; Hulce, M.; Frye, J. *J. Am. Chem. Soc.* **1982**, *104*, 4180. b) Kahn, S. D.; Hehre, W. J. *Tetrahedron Lett.* **1986**, *27*, 6041.

28. a) Macaulay, J. B.; Fallis, A. G. *J. Am. Chem. Soc.* **1990**, *112*, 1136. b) Cieplak, A. S. *J. Am. Chem. Soc.* **1981**, *103*, 4540.

29. The Ψ_3 orbital of the diene and the dienophile HOMO have the correct symmetry for σ donation to occur, however the energy gap between these two orbitals is greater than that for the "normal" Diels-Alder reaction. Thus, the reaction is not expected to dominated by the interaction of these two orbitals.

30. a) Houk, K. N.; Strozier, R. W. *J. Am. Chem. Soc.* 1973, *95*, 4094. b) Alston, P. V.; Ottenbrite, R. M. *J. Org. Chem.* **1975**, *40*, 1111.

31. Earlier experiments with BCl_3 catalysis at longer reaction times (14 h) resulted in the production of the deoxygenated compound **26** in 14% yield along with the Diels-Alder cycloadduct **51** (63%).

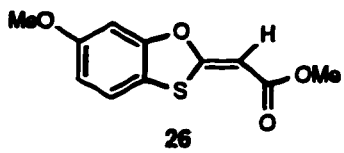

26

32. Greene, T. W.; Wuts, P. G. M. *Protective Groups in Organic Synthesis*, 2nd Edition; John Wiley & Sons, Inc.: New York, 1991.

33. Olah, G. A.; Gupta, B. G. B.; Narang, S. C. *J. Org. Chem.* **1978**, *43*, 4503.

34. Ronan, B.; Kagan, H. B. *Tetra. Asymm.* **1991**, *2*, 75.

35. Emerson, D. W.; Wynberg, H. *Tetrahedron Lett.* **1971**, 3445.

36. Chamberlain, P.; Rooney, A. E. *Tetrahedron Lett.* **1979**, 383.

37. a) Olah, G. A.; Hussain, A.; Singh, B. P.; Mehrota, A. K. *J. Org. Chem.* **1983**, *48*, 3667. b) Jung, M. E.; Lyster, M. A. *J. Am. Chem. Soc.* **1977**, *99*, 968.

38. a) Aggarwal, V. K.; Drabowicz, J.; Grainger, R. S.; Gultekin, Z.; Lightowler, M.; Spargo, P. L. *J. Org. Chem.* **1995**, *60*, 4962. b) Ranganathan, S.; Ranganathan, D.; Mehrotra, A. K. *Synthesis* **1977**, 289.

39. Sharpless, K. B.; Katsuki, K. *J. Am. Chem. Soc.* **1980**, *102*, 5974.

40. a) Pitchen, P.; Dunach, E.; Deshmukh, M. N.; Kagan, H. B. *J. Am. Chem. Soc.* **1984**, *106*, 8188. b) Pitchen, P.; Kagan, H. B. *Tetrahedron Lett.* **1984**, *25*, 1049.

41. Whitesides, G. M.; Lewis, D. W. *J. Am. Chem. Soc.* **1970**, *92*, 6979.

42. Zhao, S. H.; Kagan, H. B. *Tetrahedron* **1987**, *43*, 5135.

CHAPTER 3

π-Facial Selectivity Models for the Addition of Nucleophiles to Carbonyl Groups

3.1 Introduction

The addition of a nucleophile to a carbonyl group is one of the most important reactions in organic synthesis. Reactions of carbonyl compounds with nucleophiles such as Grignard reagents or organolithium compounds are an important method of increasing molecular complexity, and are widely used carbon-carbon bond-forming methods. The hydride-mediated reduction of carbonyl groups can also be described in terms of a nucleophilic addition of a hydride ion to an electrophilic carbon centre and therefore, are closely related to carbon-carbon bond-forming reactions that involve a carbon nucleophile addition to a carbonyl group. In regards to the direction of nucleophile approach, the planar geometry of the π-bond of a ketone or aldehyde group makes available two faces with which a nucleophile can attack (Figure 3.1).

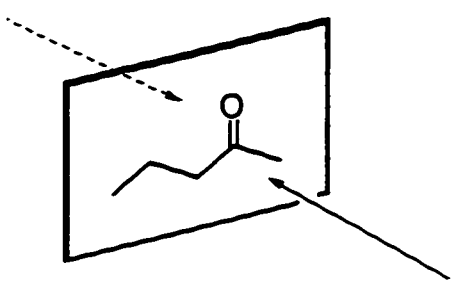

Figure 3.1 Two possible approaches of a nucleophile to a carbonyl group

The prediction and control over which carbonyl π face a particular nucleophile will attack holds considerable importance and has commanded a great deal of experimental and theoretical attention.[1] The preferential attack of a nucleophile on one face of the carbonyl group is usually referred to as π-facial selectivity and many theories have been proposed to account for the experimental observations concerning nucleophilic attack onto carbonyl groups, especially ketones.

Nucleophilic addition to carbonyl groups present in chiral molecules commonly displays π-facial selectivity. The trigonal centre in these molecules displays diastereotopic faces towards an attacking nucleophile (Figure 3.2).

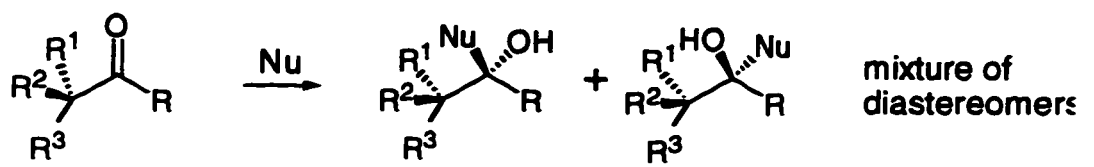

Nu = *e.g.* Grignard or hydride reagent

Figure 3.2 The formation of diastereomeric products upon nucleophilic addition to chiral ketones

Although the necessary requirement for a diastereoselective addition to a carbonyl group is that its faces should be diastereotopic (or alternatively, one can use a chiral nucleophile), a significant degree of selectivity is generally achieved only when the stereogenic centre is close or adjacent to the carbonyl group, or if some interaction can be established (e.g. chelation) between the carbonyl group and a distant stereogenic centre.

The first successful model that predicted the π-facial selectivity in acyclic carbonyl-containing compounds was introduced as "Cram's rule", published by Cram and Elhafez in 1952.[2] Cram's rule is illustrated below (Figure 3.3) for the addition of

an organometallic reagent or reducing agent (Met = metallic portion of the reagent, Nu = H or alkyl group).

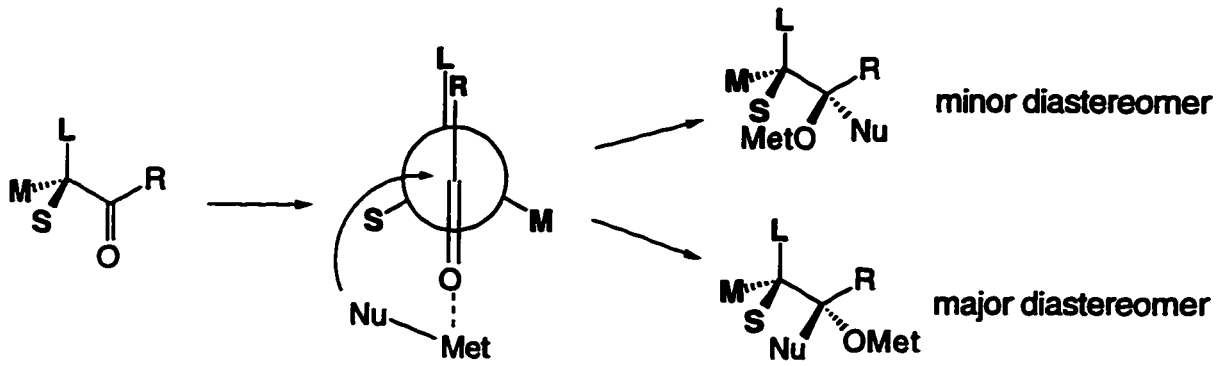

Figure 3.3 Cram's rule

Substituents attached to the chiral centre were classified as being small (**S**), medium (**M**), and large (**L**), and it was assumed that due to complexation with the metallic portion of the reagent, the carbonyl group provided considerable steric bulk. The resultant more stable rotamer had the C=O bond *anti* to the **L** group in order to minimize steric strain. Preferred attack to the face containing the small substituent follows from this model, and this was observed experimentally for a large number of reactions.

This purely steric model to explain the π-facial selectivity of nucleophilic additions to carbonyl compounds worked well in acyclic systems where **L**, **M**, and **S** were assigned to electronically similar groups of varying sizes. However, the Cram model failed in substrates in which the sizes of the substituents attached to the chiral centre varied only slightly or where an electronegative substituent was present. Another discrepancy in the Cram model was the observation that small nucleophiles preferred to attack conformationally-locked cyclohexanones at, what would appear

to be, the more sterically demanding axial position by approaching the carbonyl group from the axial direction (Figure 3.4).[3]

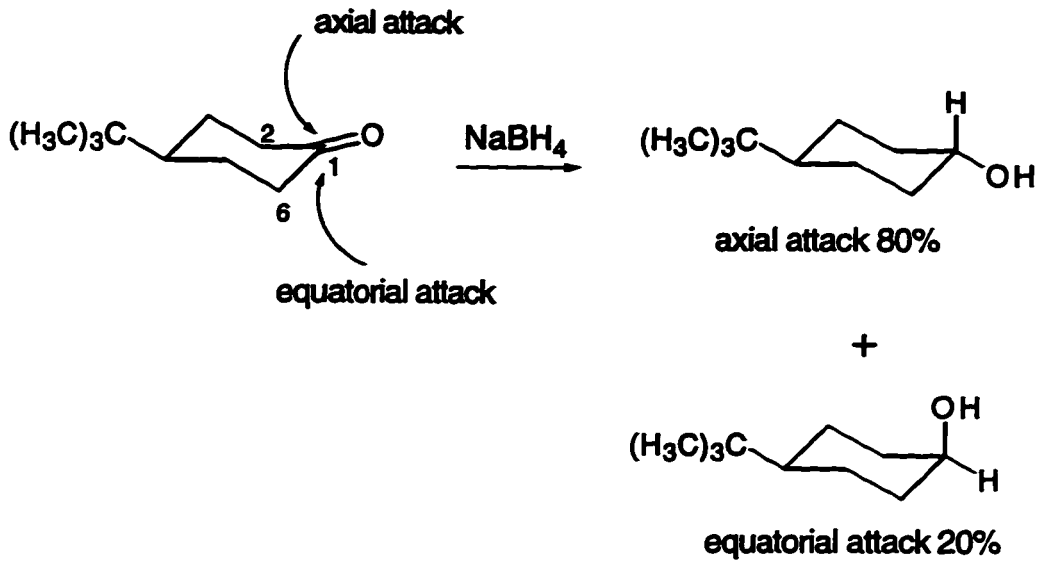

Figure 3.4 The preferred axial attack of $NaBH_4$ onto 4-*tert*-butylcyclohexanone

These exceptions prompted the proposal of several different transition state models to account for the π-facial selectivity differences in the addition and reduction reactions of acyclic ketones and conformationally-locked cyclohexanones. These models are listed below (principal authors in parentheses) and involve a number of different factors thought to influence the approach of the nucleophile to one π-face over the other:

- steric strain and chelation (Cram, Cornforth, Karabatsos);
- torsional strain (Felkin, Anh);
- product development control (Dauben);
- carbonyl LUMO extension (Klein, Anh);
- transition state stability (Wigfield);

• transition state stabilization by hyperconjugation (Cieplak).

• electrostatic potential (Hehre, Kahn)

This plethora of models have resulted from attempts to explain any particular reaction by its proposed transition state model. However, any exceptions to any one model could be explained by one or more competing models. Unfortunately, a substrate of interest could be applied to more than one model with conflicting stereochemical results being predicted. Indeed, the debate continues regarding the origin of preferential axial attack by small nucleophiles onto cyclohexanones.

Though many models for π-facial selectivity have been developed since Cram's original transition state model, few have withstood detailed scrutiny. It is generally accepted, however, that torsional strain and transition state stabilization, along with steric interactions, all play a role in the stereochemical outcome of many addition reactions to carbonyl groups. A number of assumptions are nevertheless required for the success of these models. These include assumptions in regards to:

• the location of transition states (early or late) along the reaction coordinate

• the electron-withdrawing or -donating ability of both substrate and nucleophile;

• the size of the functional groups in both substrate and nucleophile;

• trajectories of the attacking reagent;

• the degree of pyramidalization of the sp^2 carbonyl carbon atom.

It is therefore not surprising that early attempts to rationalize π-facial selectivity on steric / conformational grounds ignored any stereoelectronic effect, which is now thought to be important. Though early transition state models for π-facial selectivity have been superseded by more sophisticated models, they serve as

a useful starting point to understand the models that are invoked today. In the following sections, the various models that have been proposed to rationalize the origin of π-facial selectivity in acyclic and cyclic ketones are described.

3.2 Cram Open Chain Model

The reaction of hydrides and Grignard reagents with simple acyclic ketones (Figure 3.5: **L**, **M**, **S** = large, medium, and small-sized alkyl groups, respectively) are known to lead predominantly to diastereomer **A**.

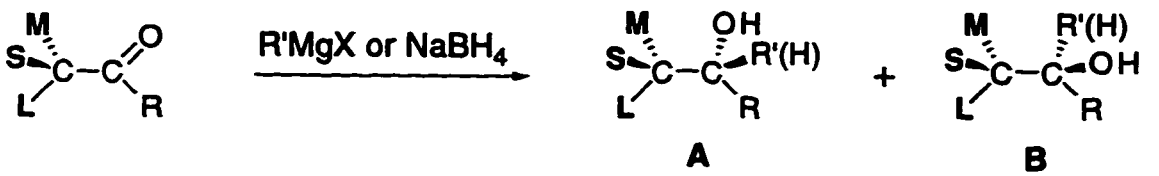

Figure 3.5 Cram's rule predicts preferred formation of diastereomer A

Cram suggested a model for the observed diastereoselectivity (Cram's open-chain model, or simply Cram's rule).[2] This model invokes an early, reactant-like transition state in which the nucleophile (Nu) approaches perpendicular to the carbonyl group (Figure 3.6).

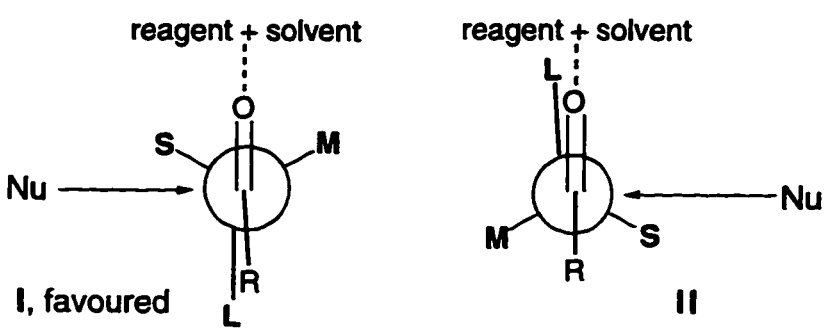

Figure 3.6 Important rotamers for Cram's rule

Of the rotamers shown above (Figure 3.6), rotamer **I** is preferred over rotamer **II** as **I** only involves steric strain between **L** and R, rather than between L and the supposedly bulkier reagent-complexed and solvated carbonyl oxygen as may occur in rotamer **II**. The nucleophile attacks the less sterically hindered face, past the smallest substituent **S** (rotamer **I**) to give the alcohol shown as the major diastereomer (Figure 3.7).

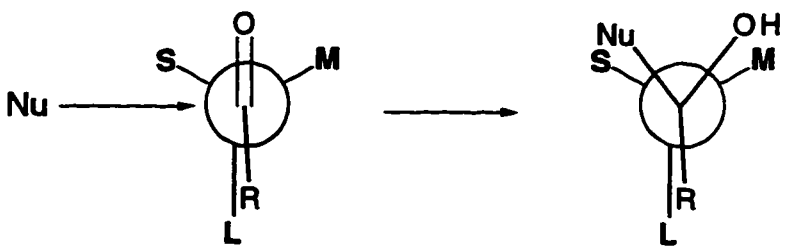

Figure 3.7 Nucleophilic attack over the least hindered π-face

The results of the lithium aluminum hydride reduction of ketone **78** are shown below (Figure 3.8)[4]. By increasing the steric bulk of the achiral group R adjacent to the carbonyl group of ketone **78**, an increasingly large proportion of alcohol **79** resulted. The Cram model, however, predicts that the selectivity of this reduction would be adversely effected by increasing the size of the R group. Inspection of rotamer **I** (Figure 3.6) suggests that an increase in the size of R would force the **L** group out of its eclipsed conformation with R and a lowered π-facial selectivity would be expected. The anti-Cram results shown below (Figure 3.8) suggest that when R is large, the R---L replusive interaction predominates over the L---C=O···reagent interaction.

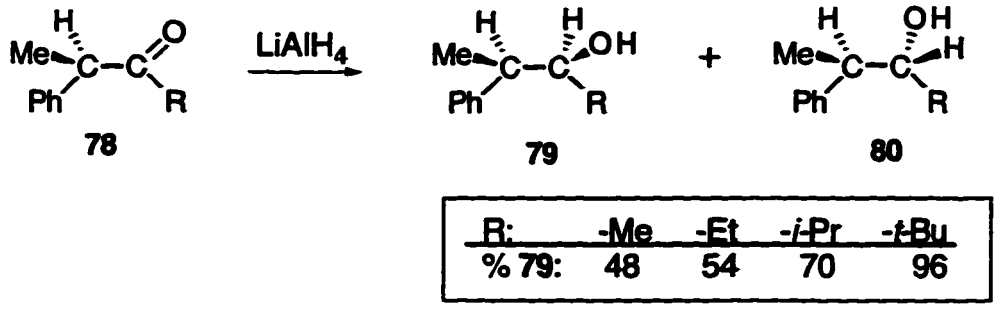

Figure 3.8 The effect of increasing R group bulk on π-facial selecivity

3.3 Cram Chelate Model

Replacement of one of the **L**, **M**, or **S** substituents by an oxygen, sulfur, or nitrogen atom allows the metal of a hydride or organometallic reagent to chelate with both the heteroatom and the carbonyl oxygen. This leads to a cyclic structure that, in effect, locks this portion of the molecule into a single rotamer. A prediction of the diastereoselectivity that arises from this conformational fix is based on the Cram chelate model (Figure 3.9).[5] Nucleophilic attack of hydride occurs from the least hindered face; the Cram chelate model correctly predicts the alcohol shown as the major diastereomer.

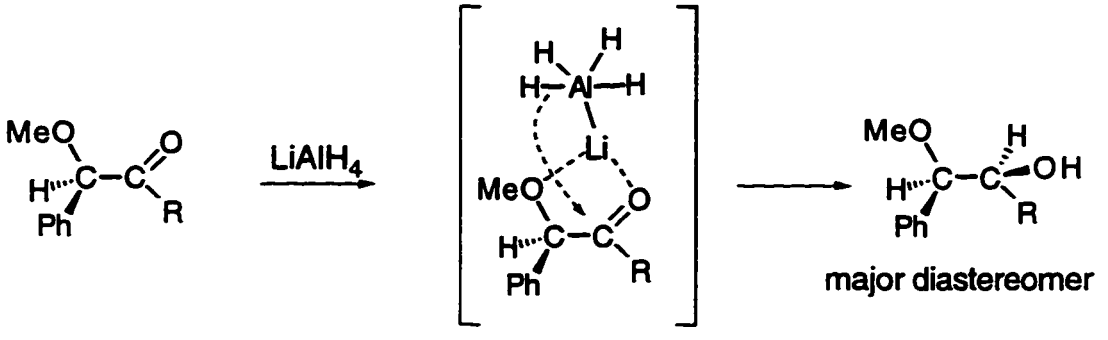

Figure 3.9 Cram chelate model

3.4 Cornforth Dipolar Model

A modification of Cram's model was proposed by Cornforth,[6] in order to accommodate those cases where one of the **L**, **M**, or **S** substituents is replaced by a polar group such as a halogen atom. Neither Cram's open-chain, nor chelate models, predict correctly the diastereoselectivity found for nucleophilic additions to α-haloketones. In the Cornforth model, the halogen atom plays the role of the **L** substituent regardless of its size. Cornforth suggested that the lone pairs of both the halogen atom and the carbonyl oxygen would adopt an *anti* conformation in order to minimize dipolar interactions (Figure 3.10). As an example, reduction of α-chloroketone **81** with lithium aluminum hydride resulted in a 3 : 1 mixture of alcohols **82** and **83**, with the major product being predicted by the Cornforth model.[6]

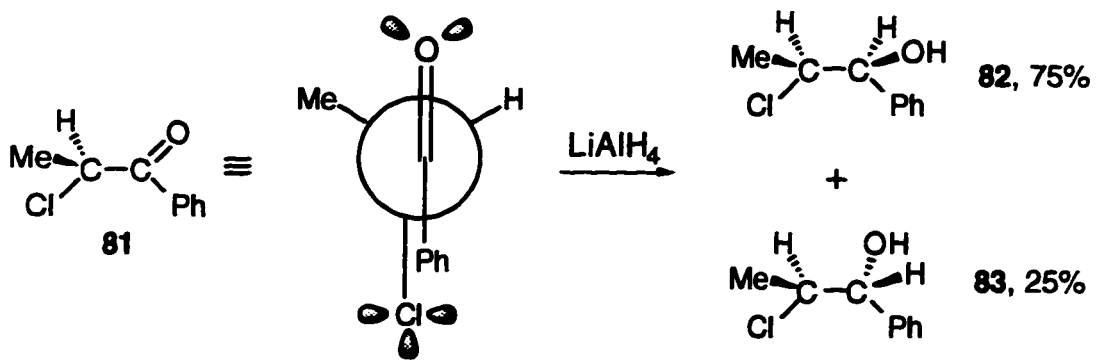

Figure 3.10 Polar substituents become the L group in the Cornforth model

3.5 Karabatsos Model

In an attempt to extend the Cram model, Karabatsos[7] suggested an alternative approach to the problem, still based on ground state rotamers. It

contrasted with the Cram model, however, with respect to the rotamers considered important. The basis of the Karabatsos model is based on evidence that indicates that the preferred rotamer about an sp^3-sp^2 bond (*e.g.* in propene or acetaldehyde) is such that one of the ligands at the sp^3 centre is eclipsed with the double bond[8] and therefore, a similar rotamer should also be preferred in acyclic ketones. Nucleophilic attack then occurs closest to the **S** group. The three rotamers meeting the first criterion are shown below (Figure 3.11). Rotamers **B** and **C** were considered the most important as these featured the nucleophile approaching the carbonyl group on the same side as the **S** ligand.

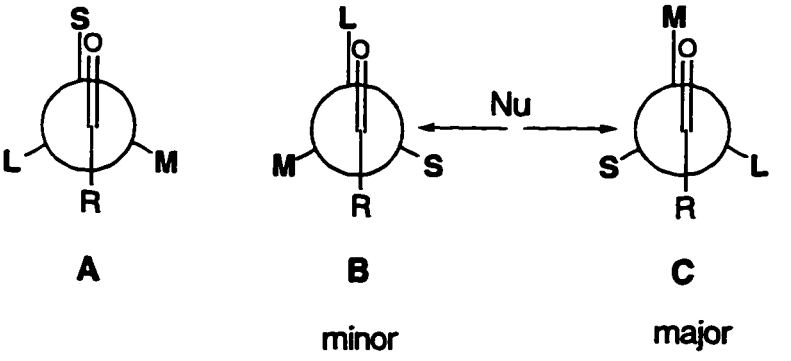

Figure 3.11 Important rotamers in the Karabatsos model

The destabilizing O-**L** and O-**M** interactions in rotamers **B** and **C**, respectively, control the diastereoselectivity of the addition reaction, where rotamer **C** is preferred on the basis in that it involves smaller (O-**M** vs. O-**L**) substituent-carbonyl group interactions.

3.6 Felkin Model

Felkin and co-workers[9] were the first to direct attention to the reaction transition state of nucleophile additions to carbonyl groups, and also attempted to rationalize both acyclic and cyclic ketone π-facial selectivity through a common concept. Neither the Cram nor Karabatsos models could account for the effect of varying the size of the R group on the selectivity observed in the reduction of acyclic ketones. Similarily, both models failed to predict the major diastereomer from the reduction of cyclohexanone using $NaBH_4$ or other small hydride reagents, as illustrated earlier (Figure 3.4).

The Felkin model was originally developed to account for the observed diastereoselectivities when both acyclic and cyclic ketones were treated with lithium aluminum hydride or Grignard reagents, and was based on the following four premises:

- the transition states in these reactions are reactant-like (occur early along the reaction coordinate);
- torsional strain between partially formed bonds in the transition state must be considered even when the degree of bonding is quite low;
- important steric interactions involve the incoming nucleophile and the R substituent of the ketone;
- polar effects stabilize those transition states where the distance between the nucleophile and an electronegative group is the greatest.

3.6.1 Acyclic ketones[9a]

The Felkin model contrasts to both the Cram and Karabatsos models by its emphasis on the importance of minimizing torsional strain in the transition state and

the relationship between the **L** group and the incoming nucleophile. It does, however, retain the perpendicular attack by the nucleophile on the carbonyl group.

Torsional Strain:

Torsional strain is the increase in energy of a compound arising when adjacent bonds become more eclipsed, causing increased repulsion between the overlapping filled molecular orbitals.[10] Torsional strain in the Felkin transition state occurs between the partially formed carbon-nucleophile bond and the C-**L**, C-**M**, or C-**S** bonds on the adjacent carbon atom. The requirement of the Felkin model that the approach of the nucleophile should be both perpendicular to the carbonyl group alongside the **S** group and staggered between the C-**L**, C-**M**, or C-**S** bonds (minimizing torsional strain) can only be fulfilled by transition state rotamers of the type shown below (Figure 3.12).

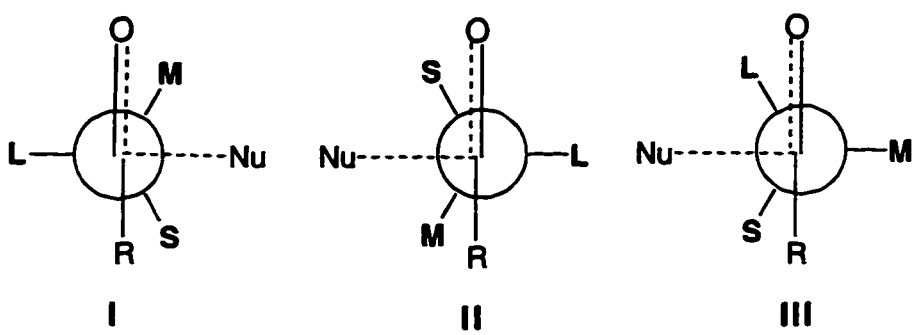

Figure 3.12 Felkin model transition state rotamers

Nucleophile approach:

The Felkin model also differs with the Cram and Karabatsos models in that the bulkiest ligand (**L**) is antiperiplanar to the incoming nucleophile. Therefore, transition state **III** (Figure 3.12) is not considered important in the Felkin model. Also, the metal / solvent-coordinated carbonyl oxygen is not considered to be a

bulky substituent, as in the Cram model. The dominant interaction is no longer between the carbonyl oxygen and the substituents, but now involves the incoming nucleophile, the **L**, **M**, and **S** substituents, and the R susbstituent. The major diastereomer thus results from rotamer **I** (Figure 3.12) as it experiences the smaller R-**S** interaction, in comparison to rotamer **II** which suffers from a larger R-**M** interaction.

The diastereoselectivity of reactions that follow the Felkin model are expected to increase when either **L** or Nu is made bulkier as this increases the steric interactions in **III** (relative to **I**, Figure 3.12) and also as R is made bulkier as this increases the steric strain between **M** and R in **II**. *Ab initio* calculations by Anh and Eisenstein for the approach of hydride ion to 2-chloro- and 2-methylpropanal established that transition state **I** in Figure 3.12 represented an energy minimum,[11a] while those proposed by Cram and Karabatsos were all of higher energy. Calculations by Anh also indicated that in the favoured transition state the incoming nucleophile is antiperiplanar to one of the groups attached to the asymmetric centre. The magnitude of this antiperiplanar effect followed the order Cl > CH_3 > H.[12]

3.6.2 Cyclic ketones

To account for the diastereoselectivity observed in the reduction of cyclohexanones, Felkin again cited torsional strain and steric strain as the major factors that influenced the stereochemical outcome of the reduction.[9b] Whereas the acyclic model led to a transition state rotamer that minimized both torsional and steric strain, the cyclohexanone case resulted in two transition states suffering some degree of both types of strain (Figure 3.13). Therefore, the outcome of the reaction was determined by the relative magnitudes of torsional strain in transition state **I** and the steric strain in **II**.

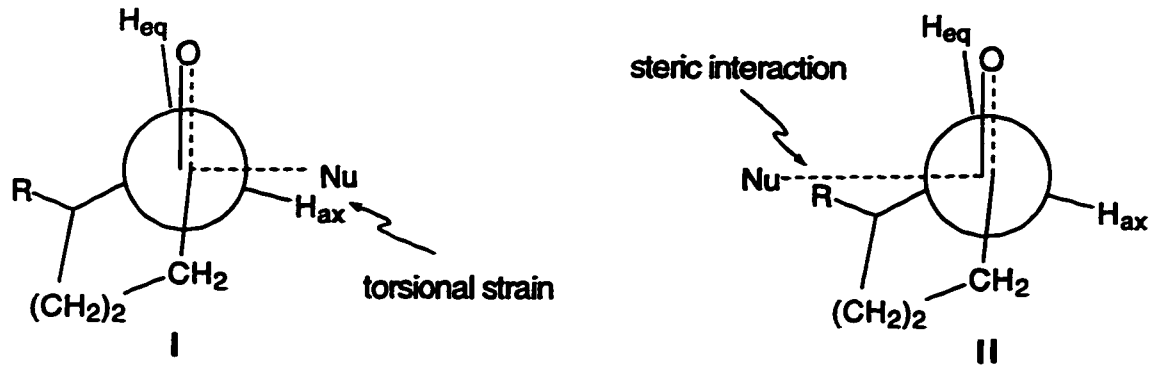

Figure 3.13 Transition states in the Felkin model for cyclic ketones

The preferred axial attack by small nucleophiles onto unhindered cyclohexanones was explained in terms of the torsional strain that arises when the developing carbon-oxygen single bond passed through an eclipsed conformation with the equatorial C2-H and C6-H bonds during equatorial attack (Figure 3.14).

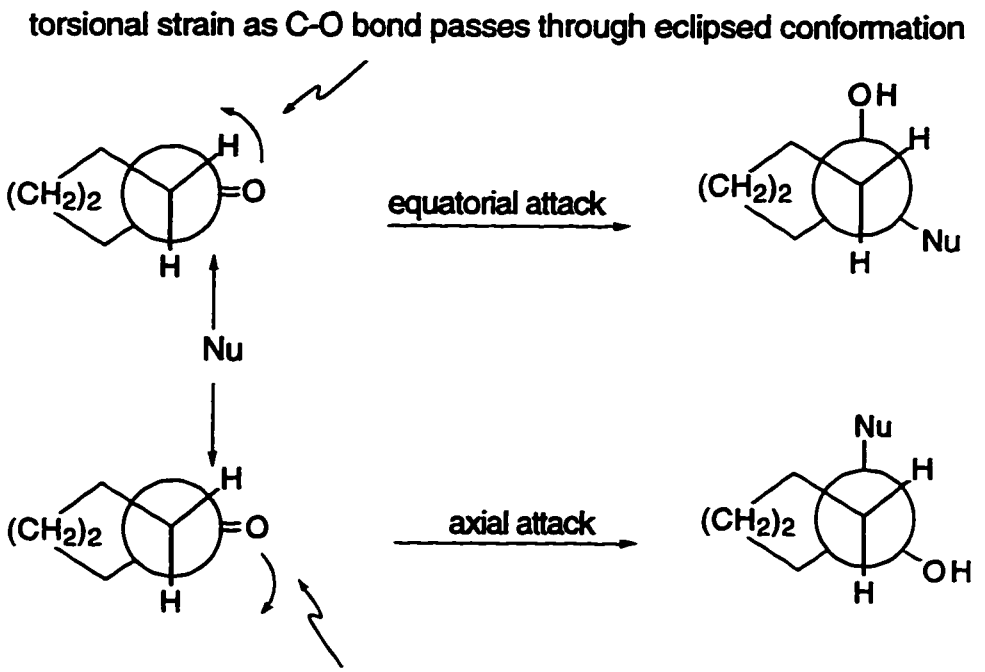

Figure 3.14 Torsional strain during axial and equatorial nucleophilic attack

Ab initio calculations[13] and X-ray studies[14] indicated that the carbonyl group in cyclohexanones is bent downwards with respect to the C2-C1-C6 plane and is almost eclipsed with the equatorial C2-H and C6-H bonds. This torsional strain is increased upon equatorial attack as the developing carbon-oxygen bond must move through a fully eclipsed arrangement, but it is decreased when the nucleophile attacks from the axial direction.

In addition to the structure of the ketone, it was found that the nature of the reducing agent also affected the stereochemistry of hydride reductions. The results of a series of reduction reactions of cyclic ketones employing reducing agents of varying bulk are presented below (Table 3.1).[15]

Table 3.1 π-Facial Selectivity in Cyclohexanone Reductions

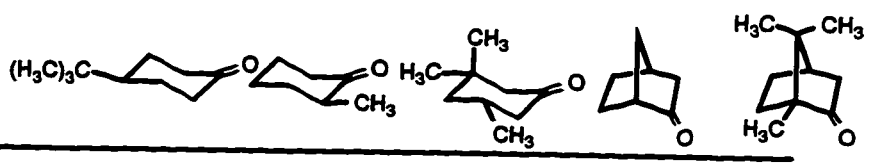

		% attack				
entry	reducing agent	axial	axial	axial	endo	exo
a	$NaBH_4$	80	75	42	14	14
b	$LiAlH_4$	92	76	17	11	8
c	$LiAl(t\text{-}OBu)_3H$	91	31	0	2	1
d	$Li(CH_3CH_2CHCH_3)_3BH$	7	2	0.2	0.4	0.4
e	$Li((CH_3)_2CHCHCH_3)_3BH$	<1	<1	0	<1	---

When both the nucleophile and R are small, the steric strain in transition state II (Figure 3.13) will be smaller than the torsional strain in transition state I and a greater proportion of the alcohol from axial attack resulted as observed in Table 1 for $LiAlH_4$ and $NaBH_4$. An increase in the steric bulk of R led to increased steric strain in

transition state **II** (Figure 3.13) and resulted in preference for equatorial attack. This trend is reflected above (Table 3.1).

The Felkin model assumes that torsional strain is independent of the "effective bulk" of the reagent. That is, an increase in the size of the reagent leaves the torsional strain in **I** (Figure 3.13) essentially unchanged. Thus, with bulky hydride reagents such as lithium tri-*sec*-butylborohydride and lithium trisamylborohydride, steric strain is the dominant factor and nucleophilic attack is equatorial (Table 3.1, entries d and e).

3.7 Steric Approach Control and Product Development Control

Prior to the studies by Felkin, an explanation for the preference of nucleophilies for axial attack on conformationally rigid, sterically unhindered cyclohexanones was proposed by Dauben[3] and became known as "product development control". This phenomenon was believed to involve a late, or product-like, transition state (Figure 3.15).

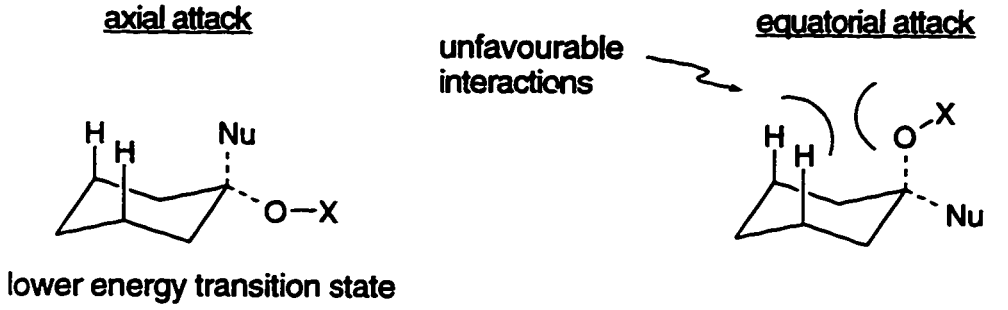

Figure 3.15 Product Development Control interactions

In the case of hindered ketones (Figure 3.16), unfavourable steric interactions were considered to favour equatorial attack and became known as "steric approach control" caused by an early or reactant-like transition state.

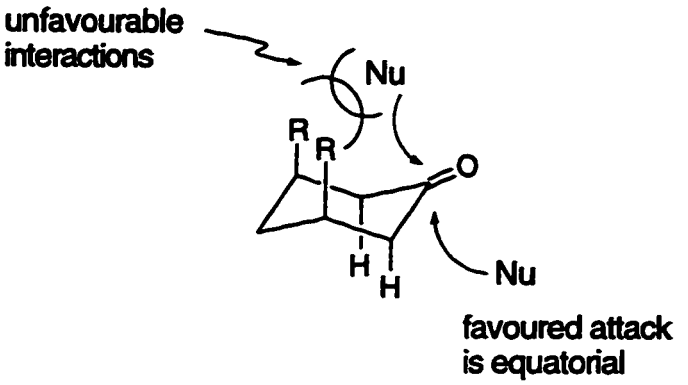

Figure 3.16 Steric Approach Control interactions

3.8 Carbonyl LUMO Extension

An entirely different rationalization for the predominance of axial attack was put forward by Klein[16] and was similar to earlier theoretical work by Anh.[17] Its importance stemmed from being the first model to consider that the LUMO of the carbonyl group could be facially dissymmetric and could influence π-facial selectivity. In this model, the π and π^* orbitals of the carbonyl group are aligned to interact with the σ and σ^* bonds between C2–C3 and between C5–C6 (Figure 3.17).

interaction between C-Cσ and C=O π* orbitals

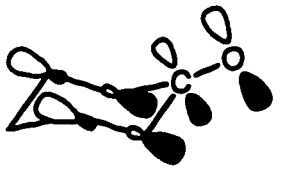

interaction between C-Cσ* and C=O π orbitals

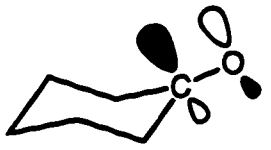

combination of both interactions resu in larger coefficients on axial side of C=O π* orbital

Figure 3.17 Carbonyl LUMO extension

The most stabilizing interactions are between the C-C σ orbitals and the carbonyl π* orbital, and between the carbonyl π and C–C σ* orbitals, as these interactions each involve one filled and one empty orbital.

The carbonyl π* orbital becomes distorted such that it will have its largest coefficients on one face of the molecule so as to maximize overlap with the filled C–C σ orbitals. Similarily, the interaction of the carbonyl π orbital with the C–C σ* orbital effectively decreases the orbital coefficients at the C and O atoms of the carbonyl HOMO. The combination of these two interactions distorts the carbonyl LUMO such that the larger coefficients are on the axial side of the carbonyl group. A nucleophile will then prefer axial attack as the larger LUMO coefficients on the axial side provide better overlap with the nucleophile HOMO.

3.9 Felkin-Anh Model

3.9.1 Acyclic ketones

This model arose from the series of *ab initio* calculations undertaken by Anh and Eisenstein in 1976 to determine if the limited number of conformers utilized in the Felkin model was a valid assumption.[11b]

An important contribution by Anh was the introduction of the principle of optimal intermolecular overlap. This principle was based on the results of crystallographic studies of several aminoketones by Bürgi, Dunitz and Shefter.[18] Their study concluded that the angle made by the nitrogen atom with the carbonyl group was always greater than 90°. The average angle for a series of different aminoketones was 107° and this was taken to represent the trajectory taken by a nucleophile (in this case, the nitrogen lone pair) as it approaches a carbonyl group and has become known as the Bürgi-Dunitz trajectory. The cause for non-perpendicular attack was also illustrated by Anh, by consideration of the carbonyl HOMO and LUMO interactions with the HOMO of a nucleophile (Figure 3.18).

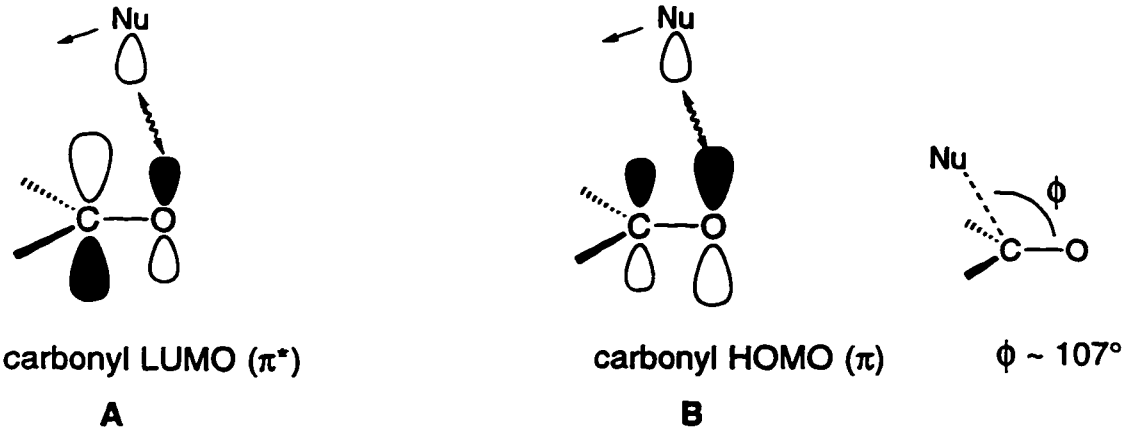

carbonyl LUMO (π^*) carbonyl HOMO (π) $\phi \sim 107°$

A **B**

Figure 3.18 Non-perpendicular attack as a result of orbital interactions

Both interactions (Nu-π^*_{CO} and Nu-π_{CO}) shown above serve to induce an increase of the Nu---C=O angle ϕ. The interaction between the HOMO of the nucleophile with the π^*_{CO} orbital (Figure 3.18, **A**) is a two-electron stabilizing interaction[19] that is maximized by lateral displacement of the nucleophile towards the carbon atom. This displacement is also facilitated by the out-of-phase overlap between the nucleophile HOMO and the orbital on the oxygen atom from the carbonyl LUMO.

A similar result is produced from the interaction between the π_{CO} orbital and the HOMO of the nucleophile (Figure 3.18, **B**). This is a four-electron destabilizing interaction that is minimized by the smallest possible overlap. In the carbonyl HOMO, the orbital coefficient on oxygen is larger than that on carbon, so in order to minimize this interaction, the nucleophile is again displaced towards the carbon atom. The theoretical studies conducted by Anh have been combined with the model proposed by Felkin and has become known as the Felkin-Anh model.

The Felkin-Ahn model incorporates the understanding that a nucleophile attacks a carbonyl group along a Bürgi-Dunitz trajectory. This implies, in addition to the R-**S** and R-**M** interactions shown in rotomers **A** and **B** (Figure 3.19), that the steric interaction of the nucleophile with the **S** and **M** groups is also encountered. Thus, in rotomer **A** both the steric interactions of the R group and that of the nucleophile are minimized and a predominance of one diastereomer can be rationalized.

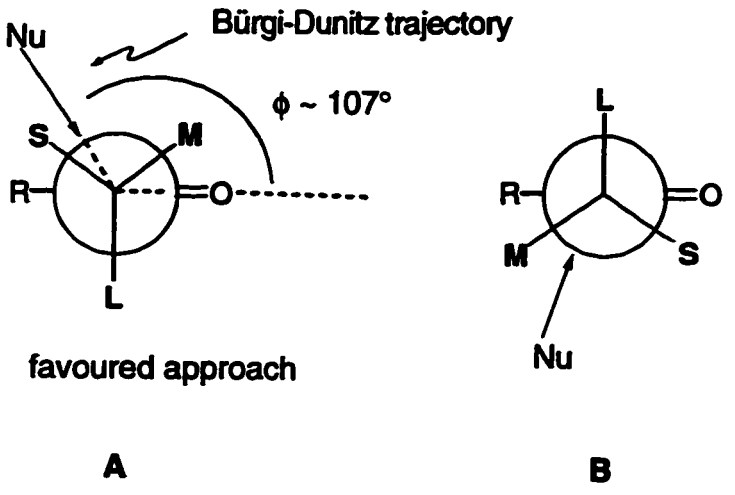

Figure 3.19 Two possible approaches of a nucleophile along the Bürgi-Dunitz trajectory

A second feature of the Felkin-Anh model is the interaction of the carbonyl π^* orbital with the **L** group σ^* orbital. This orbital interaction lowers the energy of the carbonyl LUMO and in turn reduces the energy difference between the carbonyl LUMO and the nucleophile HOMO (Figure 3.20).[20]

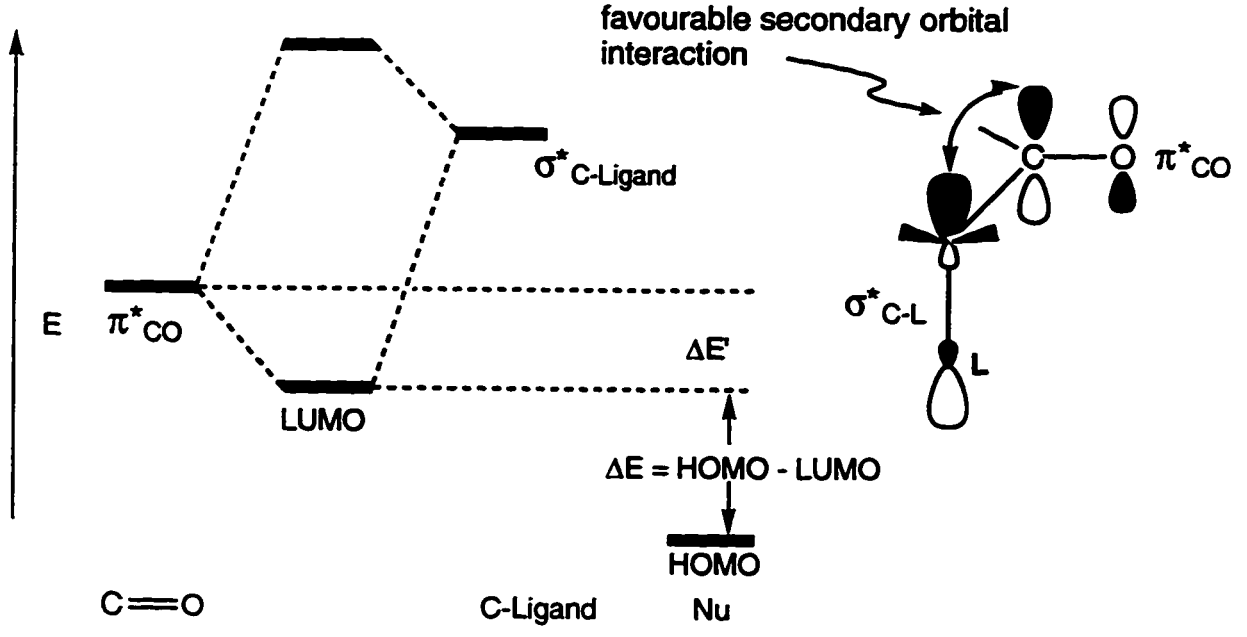

Figure 3.20 Interaction of the carbonyl LUMO with adjacent σ^* orbital

The smaller the gap in energy of the π^*_{CO} with an adjacent σ^* orbital, the greater the lowering ($\Delta E'$) of the carbonyl LUMO. This situation leads to the HOMO-LUMO energy separation becoming smaller and thus, the reaction becomes more favourable. The major diastereomer will result from nucleophilic attack opposite to the substituent with the lowest-lying σ^* orbital.

3.9.2 Cyclic ketones

To account for the preferred axial approach of nucleophiles to cyclohexanones, the Felkin-Anh model assumes (as in the Klein model) a degree of flattening of the carbonyl portion of the cyclohexanone ring. Axial approach leads to a more stabilized transition state by better overlap with the axial C2-H and C6-H σ^* orbitals as compared with equatorial C2-H and C6-H σ^* orbitals (Figure 3.21).

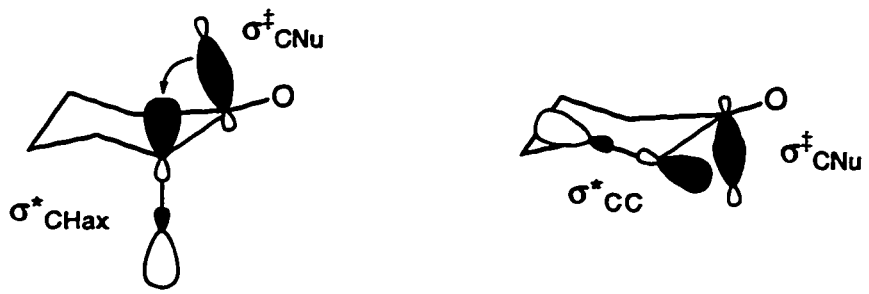

orbital alignment allows for effective overlap

poor overlap

Figure 3.21 Ring flattening favours axial approach

Torsional strain is also considered: axial attack is favoured over equatorial attack by torsional strain factors as increased torsional strain would arise between the C2-H/C6-H bonds and the nucleophile in a equatorial attack.

3.10 Wigfield model

This model was put forward to interpret the observed selectivities with the $NaBH_4$ and $LiAlH_4$ reduction of cyclohexanones. It distinguishes between those reactions that proceed *via* reactant-like transition states and those that involve product-like transition states. The Wigfield model[1c] is unique in that it requires $NaBH_4$ reduction to involve product-like transition states. One should recall that the majority of transition state models require reactant-like transition states to correctly predict the stereochemistry of such reduction reactions. The product-like transition state of the Wigfield model is based on thermodynamic data[21] suggesting that reductions by $NaBH_4$ are far less exothermic than previously thought. The rationalization for the stereochemistry of such reductions based on product-like transition states is shown below (Figure 3.22).

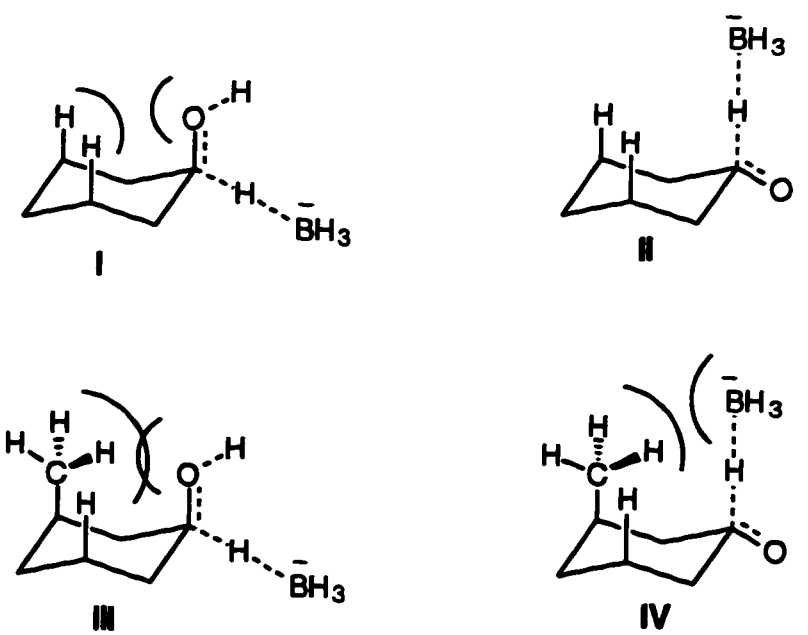

Figure 3.22 Transition states for $NaBH_4$ reduction of unhindered and hindered ketones

The Wigfield product-like transition state involves sp^3 hybridization of the carbonyl carbon atom, with attack by hydride at such an angle so as to produce a tetrahedral geometry at that centre. The preference of transition state **II** (Figure 3.22) over transition state **I** follows as a consequence of the steric interaction between the forming axial hydroxyl group and the axial C3 and C5 hydrogen atoms. Such an interaction is absent in **II**. However, in the case of hindered ketones (Figure 3.22, **III** and **IV**), transition state **IV** is destabilized with respect to **III** due to the steric interaction between the axial methyl group and the remainder of the borohydride reagent; an interaction that is neglected in other models.

Reductions that employ $LiAlH_4$ as reagent are believed to take place with a reactant-like transition state, as in other models. Steric approach control is cited by Wigfield as the controlling factor for the selectivity from the reduction of hindered cyclohexanones, together with "some other non-steric factor which provides an intrinsic preference for axial attack" for the case of unhindered cyclohexanones.

3.11 Cieplak Hyperconjugative Model

The Cieplak model[22], introduced in 1981, arose from arguments raised by Cieplak with the Felkin-Anh model. The Felkin-Anh model requires a flattening of the cyclohexanone ring, which must be preserved in the transition state so that axial attack would be preferred over equatorial attack. This was felt, by Cieplak, to be a weakness of the Felkin-Anh model and argued that even a distant interaction of a nucleophile would produce a pyramidalization of the planar carbonyl carbon atom. This effect, along with the calculated deviation[13] of the cyclohexanone O-C1-C2-H_{eq} dihedral angle of 3.3° (the angle in crystal structures[14] ranges from 2.5° to 12.7°), led to the conclusion that these effects would not prevent the optimization of orbital

interactions during the transition state. Therefore, according to Cieplak, transition state stabilization for equatorial attack by interaction with C2-C3 and C5-C6 σ^* orbitals can not be disregarded on the grounds that axial attack provided better antiperiplanarity. If one neglected the difference in antiperiplanarity, Cieplak argued, the Felkin-Anh model actually predicts equatorial attack of unhindered cyclohexanones since the energy of a $\sigma^*_{C\text{-}C}$ orbital is less than a $\sigma^*_{C\text{-}H}$ orbital.[22a]

The Cieplak model is, in a sense, the opposite of the Felkin-Anh model: the transition state is now stabilized by σ-bond electron donation into the orbital associated with the newly-forming bond, $\sigma^{*\ddagger}$ (Figure 3.23).

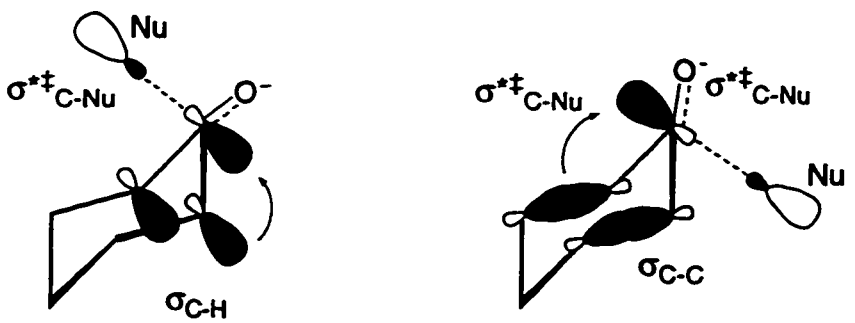

Figure 3.23 Cieplak model for axial and equatorial nucleophilic attack

During nucleophilic axial attack of a cyclohexanone carbonyl group, the developing vacant $\sigma^{*\ddagger}$ orbital interacts with the filled orbitals of the C2-H and C6-H σ-bonds. Similarily, during equatorial attack, the $\sigma^{*\ddagger}$ orbital is stabilized by interaction with the filled orbitals of the C2-C3 and C5-C6 σ-bonds. The resultant stereochemistry of nucleophilic addition to cyclohexanones therefore arises from a combination of two effects: i) steric hindrance that favours equatorial attack and ii) electron donation from the neighbouring $\sigma_{C\text{-}C}$ or $\sigma_{C\text{-}H}$ bonds into the $\sigma^{*\ddagger}$ orbital of the developing bond. In sterically unhindered ketones, the Cieplak model predicts axial attack based on the Baker-Nathan effect,[23] which states that C-H σ-bonds are better electron donors than C-C σ-bonds. Thus, axial attack is preferred since the

stabilization from electron delocalization of σ_{C-H} bonds into the $\sigma^{*\ddagger}$ orbital is greater than the stabilization arising from the corresponding interaction with σ_{C-C} bonds, which occurs during equatorial attack.

The question of whether C-C or C-H bonds are better electron donors has not yet been answered. Calculations by a number of researchers give contradictory results. Results from gas-phase experiments[24] support the idea that C-C bonds are better electron donors but results from condensed phase experiments[23] suggest that C-H bonds are better σ donors.

5-Substituted 2-adamantanones (**I** and **II**, Figure 3.24) are substrates in which the Cieplak model has been used successfully to predict the π-facial selectivity of nucleophilic additions.[25] The relevant orbital interactions for nucleophile approach *syn* and *anti* to a 5-substituent are shown below (Figure 3.24).

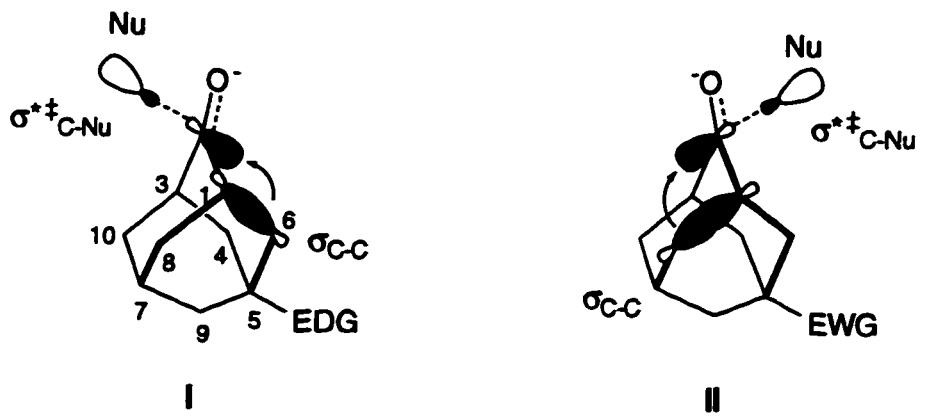

Figure 3.24 The Cieplak model as applied 5-substituted 2-adamantanones

The apparent symmetry of 2-adamantanones makes this ketone an ideal substrate to investigate electronic effects on transition state stabilization, as both faces on the carbonyl group are little effected by the bulk of the substituent at the 5-position. The question of whether C-C or C-H bonds are better electron donors

becomes a non-issue when one considers such adamantanones, as all four antiperiplanar bonds are C-C bonds, identical except for the substituent at C5.

When an electron-withdrawing group is present (transition state **II**), the Cieplak model predicts that nucleophilic attack will occur *syn* to the electron-withdrawing substituent. The electron-withdrawing group renders the C3-C10 and C1-C8 bonds more electron rich compared to the C3-C4 and C1-C6 bonds. Therefore, the nucleophile approaches antiperiplanar to the best electron-donating σ-bonds to give the *syn* alcohol. Conversely, when an electron-donating group is present (Figure 3.24, transition state **I**) C1-C6 and C3-C4 are now comparatively electron-rich σ-bonds, and the nucleophile thus approaches to give the *anti* alcohol. The π-facial selectivity observed in the reduction of many 5-substituted 2-adamantanones has been interpreted in terms of the Cieplak model.[26]

3.12 Electrostatic Potential Model

Electrostatic interactions[27] between the substrate and reagent have recently been cited as factors that have been used to rationalize reactivity and selectivity in Diels-Alder cycloadditions,[28] Cope rearrangements,[29] and nucleophilic additions to carbonyl compounds.[30] The electrostatic model involves the computer generation of a three dimensional surface and allows for the prediction of whether a reagent will prefer to approach one face of a molecule based on which face presents the most favourable electrostatic interaction. The model has until recently only been applied to predict π-facial selectivity, and has become more popular with the development of computational algorithms and the availability of low-cost / high-power workstations.

Substituted norbornenones such as **84** and **85** and 5-substituted adamantanones (Figure 3.25) have been used extensively in electrostatic potential

studies. These molecules possess little or no geometrical distortions about their carbonyl groups and therefore, steric or torsional effects are not important factors for the stereoselectivity in these compounds.

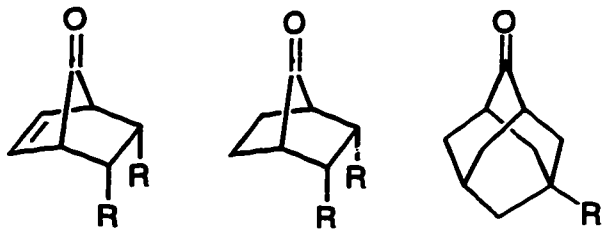

84 85 86

R = electron-withdrawing or -donating group

Figure 3.25 Substrates used in electrostatic potential studies

The calculation of the electrostatic potential surface of a molecule involves the placement of a test charge around the calculated electronic density surface of the molecule to generate a surface that is colour-coded to represent areas of negative or positive electrostatic potential as illustrated below (Figure 3.26).

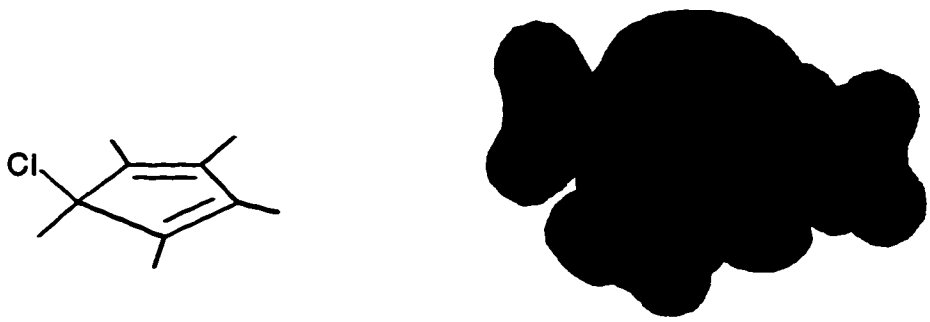

Figure 3.26 Computer-generated electrostatic potential surfaces

Throughout this discussion, the blue region represents an area of high electron density and attraction for a positive charge (negative potential). Similarly, the red regions are areas of lower electron density and represent regions that are susceptible for attack by a negative charge (positive potential).

It must be noted that the electrostatic potential surfaces give only qualitative information on the expected π-facial selectivity for a nucleophilic addition reaction. However, this method has been used sucessfully to interpret π-facial selectivities in systems where other models have failed (see Chapter 2.4). The electrostatic model has also been used extensively by Hehre and Kahn as an alternative to the frontier orbital explanations that rationalize changes in reactivity and stereoselectivty when electron-donating or -withdrawing groups are placed adjacent to π-systems (*e.g.* Micheal additions).[30] Both types of explanations are likely related as changes in orbital energies may lead to changes in electron densities and thus electrostatic potentials as well.

3.13 Research Objectives

As part of our continuing interest in the use of heteroatoms as control elements in synthesis,[31] the following chapter describes the preparation and the π-facial selectivity of sterically unbiased cyclopentanone derivatives such as ketones **114**, **108** and **129** that contain heteroatom substituents adjacent to the carbonyl group (Figure 3.27).

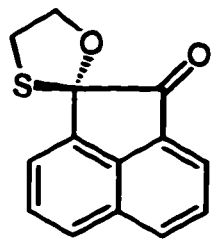

114

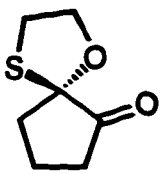

108

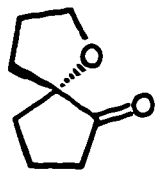

129

Figure 3.27 Heteroatom containing substrates employed in π-facial selectivity studies

Ideally, the spiro ketones shown in Figure 3.27 above will present an incoming nucleophile with a sterically unbiased carbonyl group and allow for the evaluation of stereoelectronic factors that may influence the approach of a nucleophile. The study of the mixed O, S acetals (oxathiolanes) also avoids the question of C-H versus C-C σ-donating ability, as the competition is now between C-C vs. C-O and C-S bonds, of which there is general agreement on σ-donor ability. In addition, regardless of the factors responsible for the π-facial selectivity (if any) of these oxathiolane ketones, high levels of selectivity would make these types of systems useful in the synthesis of more highly functionalized ketones.

Chapter 3 References

1. a) Li, H.; le Noble, W. J. *Recl. Trav. Chim. Pay-Bas* **1992**, *111*, 199. b) Frenking, G.; Köhler, K. F.; Reetz, M. T. *Tetrahedron* **1991**, *47*, 8991. c) Wigfield, D. C. *Tetrahedron* **1979**, *35*, 449.
2. Cram, D. J.; Elhafez, F. A. *J. Am. Chem. Soc.* **1952**, *74*, 5828.
3. Dauben, W. G.; Fonken, G. J.; Noyce, D. S. *J. Am. Chem. Soc.* **1956**, *78*, 2579.
4. Morrison, J. D.; Mosher, H. S. *Asymmetric Organic Reactions*; American Chemical Society: Washington, D.C., 1976, *pp* 100-108.
5. Cram, D. J.; Wilson, D. R. *J. Am. Chem. Soc.* **1963**, *85*, 1245.
6. Cornforth, J. W.; Cornforth, R. H.; Mathew, K. K. *J. Chem. Soc.* **1959**, 112.
7. Karabatsos, G. J. *J. Am. Chem. Soc.* **1967**, *89*, 1367.
8. a) Karabatsos, G. J.; Hsi, N. *J. Am. Chem. Soc.* **1965**, *87*, 2864. b) It is interesting to note that a recent study, Chounan, Y.; Ebata, T.; Yamamoto, Y. *J. Am. Chem. Soc.* **1995**, *117*, 3167., concluded that the most stable ground state rotamer of 2-phenylpropanal in the gas phase is **A** in which the carbonyl group bisects the angle defined by the C-CH_3 and C-H bonds:

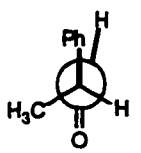

A

Rotamer **A** is the rotamer considered important in the Cram model.
9. a) Chérest, M.; Felkin, H.; Prudent, N. *Tetrahedron Lett.* **1968**, 2199. b) Chérest, M.; Felkin, H. *Tetrahedron Lett.* **1968**, 2205.
10. Carey, F. A.; Sundberg, R. J. *Advanced Organic Chemistry, 3rd edition*; Plenum Press: New York, 1990.
11. Anh, N. T.; Eisenstein, O. *Nouv. J. Chim.* **1977**, *1*, 61. b) Anh, N. T.; Eisenstein, O. *Tetrahedron Lett.* **1976**, 155.

12. Anh, N. T. *Top. Curr. Chem.* **1980**, *88*, 145.

13. Allinger, N. L.; Tribble, M. T.; Miller, M. A. *Tetrahedron* **1972**, *28*, 1173.

14. Lectard, A.; Lichanot, A.; Metras, F.; Gaultier, J.; Hauw, C. *J. Mol. Struct.* **1976**, *34*, 113.

15. a) Ashby, E. C.; Laemmle, J. T. *Chem. Rev.* **1975**, *75*, 521. b) ref. 2

16. a) Klein, J. *Tetrahedron* **1974**, *30*, 3349. b) Klein, J. *Tetrahedron Lett.* **1973**, 4307.

17. Anh, N. T.; Eisenstein, O.; Lefour, J.-M.; Trân Huu Dâu, M.-E. *J. Am. Chem. Soc.* **1973**, *95*, 6146.

18. Bürgi, H. B.; Dunitz, J. D.; Shefter, E. *J. Am. Chem. Soc.* **1973**, *95*, 5065. The aminoketones studied were: methadone, cryptopine, clivorine, retusamine, *N*-brosylmitomycin A.

19. Fleming, I. *Frontier Molecular Orbitals and Chemical Reactions*; Wiley: New York, 1976.

20. Coxon, J. M.; Houk, K. N.; Luibrand, R. T. *J. Org. Chem.* **1995**, *60*, 418.

21. a) Hammond, G. S. *J. Am. Chem. Soc.* **1955**, *77*, 334. b) Wipke, W. T.; Gund, P. *J. Am. Chem. Soc.* **1976**, *98*, 8107.

22. a) Cieplak, A. S. *J. Am. Chem. Soc.* **1981**, *103*, 4540. b) Cieplak, A. S.; Tait, B. D.; Johnson, C. R. *J. Am. Chem. Soc.* **1989**, *111*, 8447. c) Wiberg, K. B.; Cieplak, A. S. *J. Am. Chem. Soc.* **1992**, *114*, 9226.

23. a) Cooney, B. T.; Happer, D. A. R. *Aust. J. Chem.* **1987**, *40*, 1537. b) Edlund, U. *Org. Magn. Res.* **1978**, *11*, 516.

24. a) Perkins, P. G.; Stewart, J. J. P. *J. Chem. Soc., Faraday Trans. 2* **1982**, *78*, 285. b) Radom, L.; Pople, J. A.; Buss, V.; Schleyer, P. v. R. *J. Am. Chem. Soc.* **1970**, *92*, 6380.

25. a) Hahn, J. M.; le Noble, W. J. *J. Am. Chem. Soc.* **1992**, *114*, 1916. b) Cheung, C. K.; Tseng, L. T.; Lin, M.-H.; Srivastava, S.; le Noble, W. J. *J. Am. Chem. Soc.* **1987**, *109*, 1598. c) ref. 20a

26. refs. 1a and 22b

27. Wu, Y.-D.; Li, Y.; Na, J.; Houk, K. N. *J. Org. Chem.* **1993**, *58*, 4625.

28. Chao, T. M.; Baker, J.; Hehre, W. J.; Kahn, S. D. *Pure Appl. Chem.* **1991**, *63*, 283.

29. Kahn, S. D.; Hehre, W. J. *J. Org. Chem.* **1988**, *53*, 301.

30. a) Wu, Y.-D.; Tucker, J. A.; Houk, K. N. *J. Am. Chem. Soc.* **1991**, *113*, 5018. b) Kahn, S. D.; Hehre, W. J. *J. Am. Chem. Soc.* **1986**, *108*, 7399. c) Kahn, S. D.; Dobbs, K. D.; Hehre, W. J. *J. Am. Chem. Soc.* **1988**, *110*, 4602. d) Sjoberg, P.; Ploitzer, P. *J. Phys. Chem.* **1990**, *94*, 3959.

31. a) Yadav, V.; Fallis, A. G. *Can. J. Chem.* **1991**, *69*, 779. b) Martynov, J.; Dimitroff, M.; Fallis, A. G. *Tetrahedron Lett.* **1993**, *34*, 8201.

Chapter 4

π-Facial Selectivity of Cyclic Ketones Containing Adjacent Heteroatoms: Results and Discussion

4.1 Introduction

It has been nearly twenty years since the publication of Wigfield's review on the stereochemistry and mechanism of hydride reductions of cyclohexanones.[1] This highly-cited review concluded with the statement: "... it is no longer justified to expect that one global explanation of stereoselectivity covering reductions with all the common reducing agents will be found. Such a search or expectation is almost certainly futile." An explanation to account for all the π-facial selectivity shown by cyclohexanones and other ketones in reduction reactions (and other nucleophilic additions) may not be found, although the amount of theoretical and experimental work in this area indicates that many researchers disagree with the notion that the search is a futile one. The π-facial selecivity observed from the addition of hydride and organometallic reagents to carbonyl compounds continues to be a topic of immense current interest[2] as the search for ever-increasing generality and selectivity continues. These investigations have improved our understanding in many instances, although a truly general theory may not be feasible.

An understanding of the origin of π-facial selectivity is of importance in organic synthesis and has resulted in the proposal of many different models for the prediction of the major diastereomer from the addition of nucleophilies to ketones, as described in Chapter 3. This chapter will emphasize the applicability of some of these models in the determination of the predominant factors responsible for π-facial

selectivity in cyclic ketones that contain one or two heteroatoms (sulfur or oxygen) adjacent to the carbonyl group that undergoes nucleophilic attack. More specifically, the use of oxathiolane acetals and their simpler analogues as control elements in carbonyl addition reactions (Figure 4.1), and the level of π-facial selectivity that may be achieved, is described.

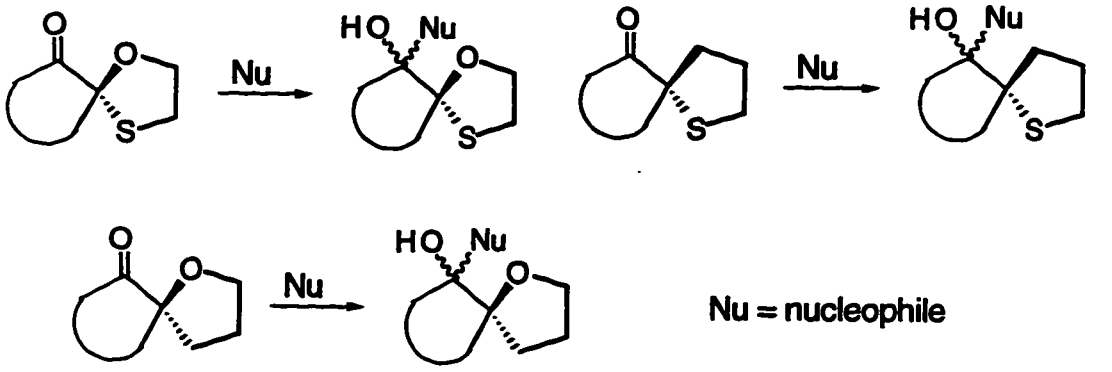

Figure 4.1 Heteroatom control of carbonyl addition reactions

Previous work by Eliel[3] with acyclic ketones had demonstrated a highly stereoselective synthesis of oxathiane alcohols **89** (Scheme 4.1) in two steps.

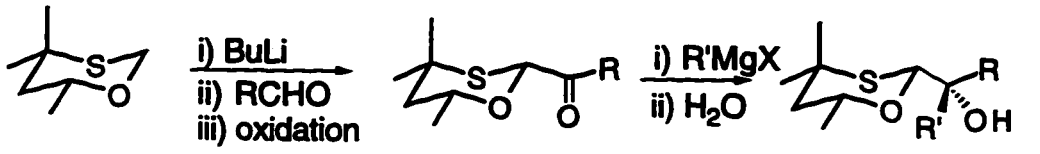

Scheme 4.1 Eliel's stereoselective Grignard reaction

An electrophilic substitution with the conformationally-locked 1,3-oxathiane **87** led to equatorial-substituted ketone **88** after oxidation. The second step was the Grignard reagent addition to ketone **88** to give the tertiary alcohol **89**. The

stereoselectivity of the first step is a consequence of the greater stability of the equatorial 1,3-oxathiane-2-carbanion over the axial anion,[4] and the second step stereoselectivity is attributed to the formation of a Cram[5] chelate as shown below (Figure 4.2).

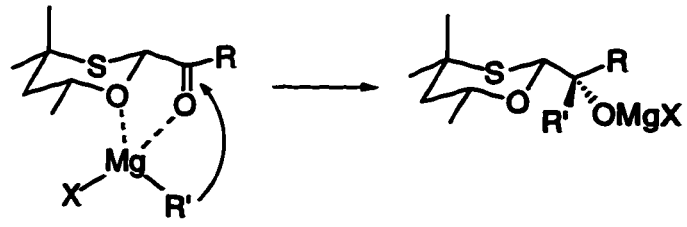

Figure 4.2 Grignard addition *via* Cram chelate

A recent example of the use of oxathiolane acetals as control elements in conjugate additions was reported by Takei.[6] Addition occured predominantly *syn* to the C-O σ bond at the γ carbon of enone **90**. This is in contrast to the reported[7] preference of cuprates to generally add to enones possessing a γ-oxygen atom in a manner that results in an addition *anti* to the C-O σ bond.

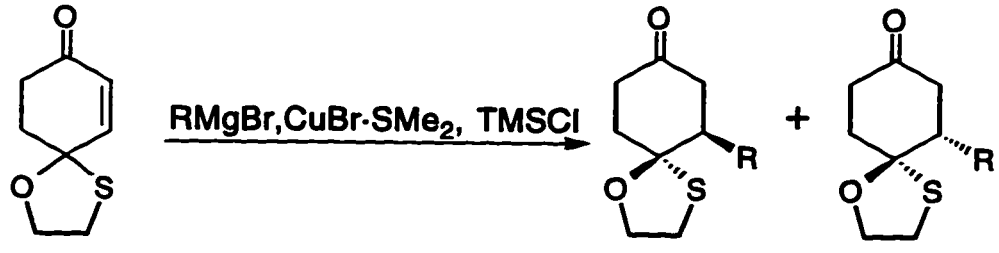

90 **91** **92**

R = Me:	97%	3%
R = Ph:	96%	4%
R = *i*-Pr:	87%	13%

Scheme 4.2 Conjugate addition of Grignard reagents to cyclohexenone 90

High selectivity was reported when various cuprates were reacted with enone **90** (Scheme 4.2) but no explanation for the diastereoselectivity was given.

4.2 Preparation of Cyclohexanone 97

Our initial studies employed cyclohexanone **97**, prepared from the commercially available 1,2-cyclohexanedione (**94**) and 2-mercaptoethanol (**95**) in the presence of a catalytic amount of *p*-toluenesulfonic acid in benzene with azeotropic removal of water (Scheme 4.3).

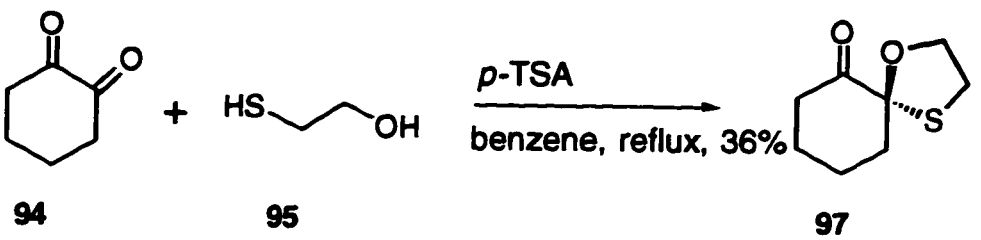

94 **95** **97**

Scheme 4.3 Synthesis of cyclohexanone 97

The treatment of diketone **94** with 2-mercaptoethanol (**95**) was carried out under various conditions in an effort to increase the yield of ketone **97**. The use of boron trifluoride, zinc chloride or pyridinium *p*-toluenesulfonate, with and without azeotropic removal of water, resulted in very low yields of the desired product. Analysis of the crude reaction mixtures by GC-MS indicated the presence of compounds with masses that correspond to compounds arising from the addition of two or three molecules of 2-mercaptoethanol to diketone **94**.

An alternate synthesis based on first preparing the acetal[8] **96**, followed by introduction of the carbonyl group (Scheme 4.4) also resulted in low yields[9] and therefore, the method described in Scheme 4.3 was employed.

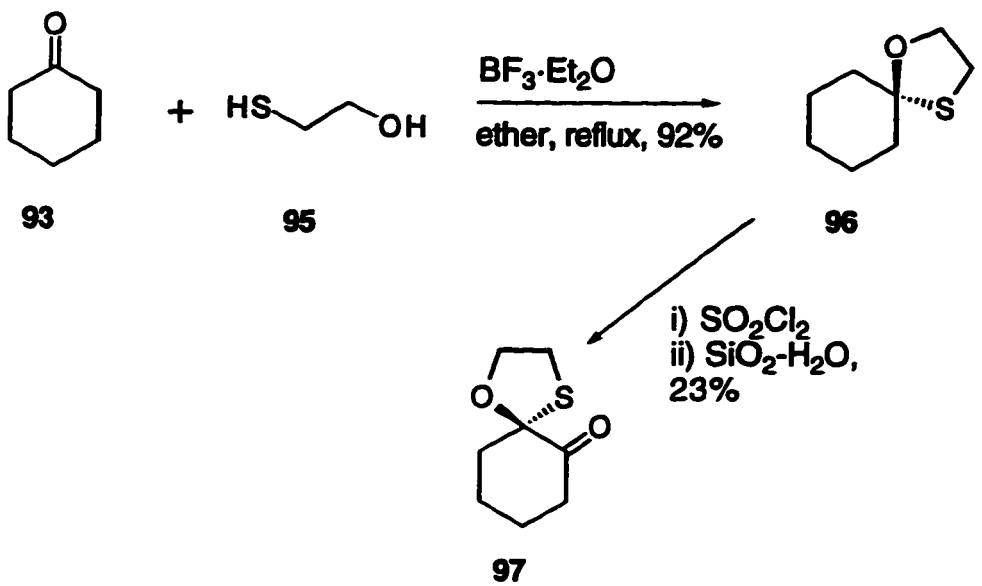

Scheme 4.4 Alternate synthesis of 97

4.3 Nucleophilic Additions to Cyclohexanone 97

4.3.1 Conformational considerations

Predictions of the relative stereochemistry of the major diastereomer that may be formed from nucleophilic additions to cyclohexanone **97** is complicated by the possibilty of the interconversion of the two chair forms of the molecule (assuming the energy of activation is roughly similar to substituted cyclohexanes). The results of calculations (MM2[10] and AM1[11]) on the ground state energy of these conformers of cyclohexanone **97** are shown in Figure 4.3.

97a **97b**

Figure 4.3 Ground state chair conformer energies of 97

Based on this ground state energy difference between the two conformers shown above, an approximately 4-to-1 ratio favouring conformer **97b** may be expected. As a comparison, the conformational free energy difference between the equatorial and axial conformers of 4-*tert*-butylcyclohexane is approximately 5 kcal/mol.[12]

Although the Van der Waals radii for oxygen and sulfur atoms are 1.52 and 1.80 Å respectively,[13] the difference between the carbon-oxygen[14] bond length (1.43 Å) and carbon-sulfur[14] bond length (1.81 Å) may account for the small energy difference between the two conformers of cyclohexanone **97** with respect to the 1,3-diaxial interactions between the heteroatom and the axial hydrogens. The conformational energy difference is comparable to the calculated conformational free energy difference between the axial and equatorial conformers of the monosubstituted cyclohexanes **98** and **99** and cyclohexanones **100** and **101** (Figure 4.4).

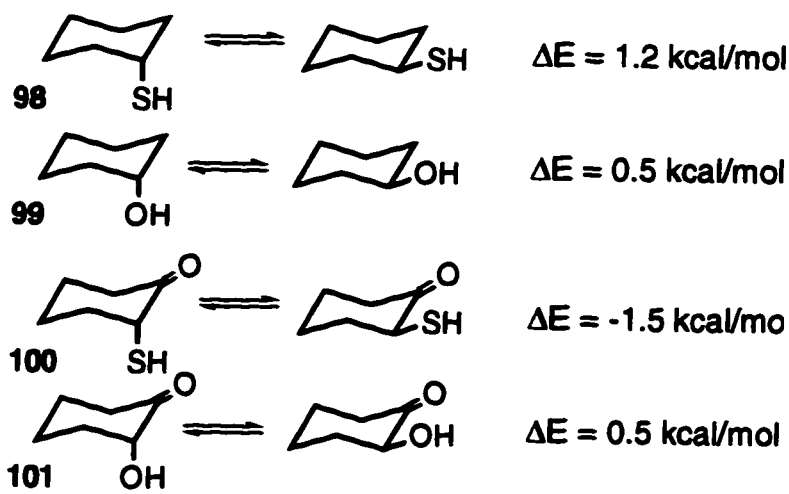

Figure 4.4 Axial and equatorial conformer energies

4.3.2 Reaction of cyclohexanone 97 with Grignard and reducing agents

The diastereomeric excess that resulted from the treatment of ketone **97** with various organometallic and reducing agents are shown below (Table 4.1). For comparison, the diastereoselectivity for the same reaction using 4-*tert*-butylcyclohexanone[15] are given in parentheses.

Table 4.1 Reaction of Cyclohexanone 97 with Grignard and Reducing Agents

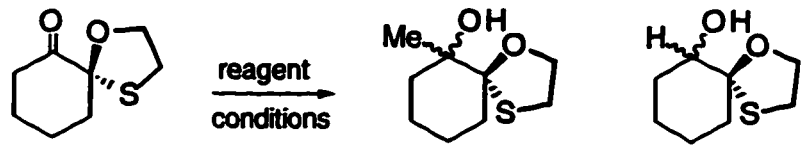

97 102 103

entry	reagent[a]	conditions	% yield[b]	% de[c, d]
a	CH_3Li	ether, 0 °C	76	100
b	MeMgBr	ether, 0 °C	79	69
c	MeMgCl	ether, 0 °C	78	78
d	$NaBH_4$	MeOH, 22 °C	93	50 (60)
e	$LiBH_4$	THF, 0 °C	91	64
f	$LiAlH_4$	ether, 0 °C	83	79 (84)
g	$Al(i\text{-}Bu)_2H$	THF, -78 °C	89	81
h	$LiAl(t\text{-}OBu)_3H$	ether, 0 °C	86	79 (82)
i	$LiB(CHMeEt)_3H$	THF, 0 °C	65	83 (86)
j	SmI_2, *i*-PrOH	THF, 22 °C	no reaction	----

[a] all reactions were performed with approximately 1.1 equivalent of reagent except SmI_2 (10 mol %). [b] combined yield of diastereomers. [c] Determined by GC-MS. [d] results in parentheses refer to reaction with 4-*tert*-butylcyclohexanone.

The diastereomeric excess shown in Table 4.1 were calculated by the integration of GC-MS signals of the crude reaction mixture, and the yields were determined by the amount of alcohol recovered after silica gel chromatography.

Separation of the diastereomers by column chromatography was not possible and therefore, the yield refers to a mixture of both diastereomers. Moderate diastereoselectivity was observed with methylmagnesium bromide and chloride and good diastereoselectivity was displayed by all of the reducing agents except sodium borohydride (entry d). A variation of the Meerwein-Ponndorf-Verley reduction[16], which involves the use of samarium diiodide (entry j) as catalyst, failed to reduce the substrate.

A single diastereomer was detected from the reaction with methyllithium. In order to obtain a crystalline derivative for X-ray analysis, the alcohol produced from the methyllithium addition reaction was treated with 1-napthylisocyanate and again with 3,5-dinitrobenzyl chloride. Unfortunately, the alcohol proved to be unreactive in both cases. The relative stereochemistry of the major diastereomer was unknown in the methyl addition and hydride addition reactions, although both series of reactions resulted in the preferential formation of one diastereomer, as based on the GC-MS retention times and the ^{13}C NMR spectrum of the mixture containing both diastereomers. The ^{1}H NMR signals overlapped considerably and assignment to any single diastereomer was not possible.

The preferred formation of the same diastereomer, irrespective of the type of reducing agent used, is contrary to the behavior of 4-*tert*-butylcyclohexanone, which displays a reversal in the major diastereomer produced when treated with lithium tri-*sec*-butylborohydride[15c] (L-Selectride®) when compared to, for example, sodium borohydride. Thus, the oxathiolane group of cyclohexanone **97** apparently overrides the steric approach control that is believed to be operative with reactions between cyclohexanones and bulky reducing agents.[17] Another possible explanation is that *all* of the reducing agents employed approach the cyclohexanone carbonyl group by steric approach control, however this is contrary to the behavior exhibited by small reducing agents with 4-*tert*-butylcyclohexanone. The use of less bulky reducing

agents such as lithium aluminum hydride and sodium borohydride gave diastereomeric excesses that were comparable to that obtained with 4-*tert*-butylcyclohexanone.

The space-filling models of the AM1-optimized structures of the two chair conformations of cyclohexanone **97** are shown below (Figure 4.5).

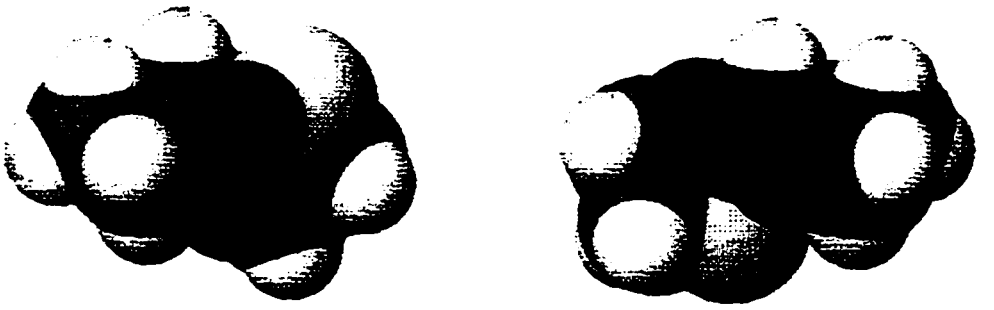

Figure 4.5 Space-filling models of 97

Inspection of the above models suggests that the axially disposed heteroatom presents a more hindered approach to the incoming nucleophile and therefore, some π-facial selectivity would be expected from cyclohexanone **97** on steric arguments alone, as both conformers are expected to be present in unequal amounts. Approach of the nucleophile alongside the equatorial heteroatom also avoids the torsional strain[18] that would be expected if the nucleophile approached *syn* to the axial heteroatom (Figure 4.6). Thus, steric arguments alone predict some π-facial selectivity in nucleophilic additions to cyclohexanone **97**, in accordance with the experimental results.

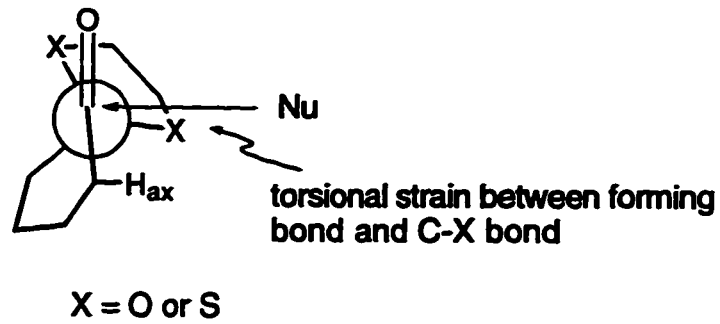

Figure 4.6 Torsional strain from nucleophilic attack

In terms of the Cieplak[19] model, both conformers contain orbitals suitably arranged to participate in hyperconjugative transition-state stabilization. As illustrated below (Figure 4.7), both chair conformers of cyclohexanone **97** should result in the preferred formation of the same diastereomeric alcohol **102** or **103**.

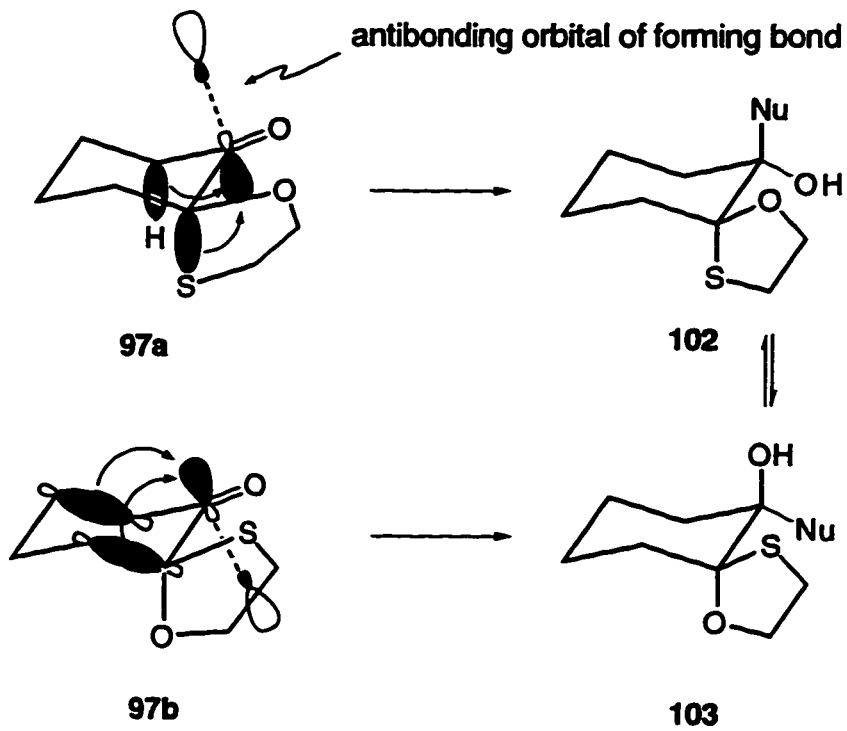

Figure 4.7 Hyperconjugative stabilization of the forming nucleophile-carbon bond

Chair conformer **97a** predominantly leads to alcohol **102** due to the combined σ-donation from the carbon-sulfur and axial carbon-hydrogen bonds into the antibonding orbital of the forming bond. This approach provides greater hyperconjugative stabilization as compared to the stabilization that is provided by the two α,β carbon-carbon bonds when an equatorial approach is taken. Alcohol **103** should also predominate in nucleophilic attack on chair conformer **97b**. In this situation, the equatorial approach of the nucleophile is stabilized to a greater extent than the axial approach by the greater σ donation provided by the two α,β carbon-carbon bonds over that of the axial carbon-hydrogen and carbon-oxygen bonds. Therefore, the Cieplak model as applied to cyclohexanone **97** predicts that the same diastereomer is produced regardless of the nucleophile. This is consistant with the results shown in Table 4.1, as there was no reversal of the major diastereomer produced throughout the series of reagents employed.

A Cram chelate model may also be operative in some of the organometallic and reduction reactions explored with cyclohexanone **97**. The possibility of chair conformer interconversion again makes prediction difficult as illustrated below (Figure 4.8).

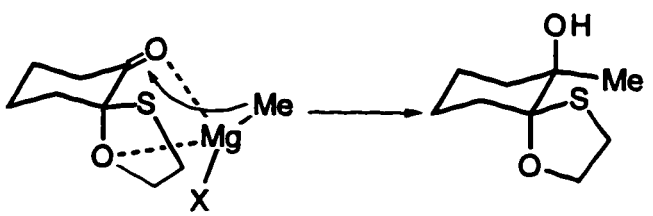

97b

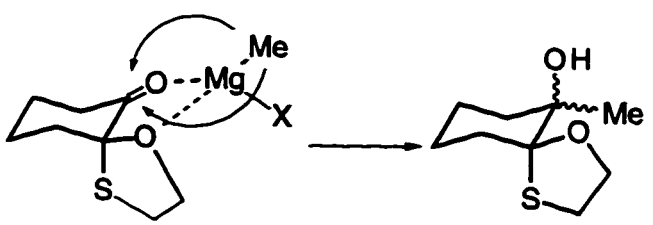

97a

Figure 4.8 Grignard addition according to Cram chelate model

Based on Hard-Soft acid-base theory,[14] chelation by lithium or magnesium is believed to occur preferentially with the two oxygen atoms of cyclohexanone **97**, rather than between the sulfur and carbonyl (or oxathiolane) oxygen atoms.[3] The diastereomer produced preferentially depends on the conformer of the cyclohexanone. Chelate structure **97b** may be expected to produce the axial alcohol to a greater extent, due to the organometallic reagent occupying a position below the carbonyl group, thus delivering the methyl nucleophile to the equatorial position. Chelate structure **97a** is expected to be less selective than structure **97b** due to the roughly equal steric environments that the methyl nucleophile encounters.

The chelate model can therefore account for the predominance of one diastereomer in the nucleophilic addition reactions to cyclohexanone **97**. The greater π-facial selectivity observed with methyllithium compared to methylmagnesium bromide and chloride (both are considered as possessing greater chelating ability) in these reactions however, indicates factors other than chelation may be involved.

X.4 Cyclopentanone Systems

During the course of experiments with cyclohexanone **97** it was evident that this molecule was not the ideal substrate, due to the absence of a preferred conformation for the molecule, and also because of the sterically biased environment around the carbonyl group, irrespective of conformation. The use of an oxathiolane acetal in any cyclic ketone cannot present a completely unbiased environment around the carbonyl group due to the difference in size between the sulfur atom and the oxygen atom and the difference in bond lengths between the carbon-oxygen and carbon-sulfur bond. Thus, a flatter cyclic ketone would posses less steric bias.

Cyclopentanone **108** and napthalene **114** were thus prepared and investigated (Figure 4.9).

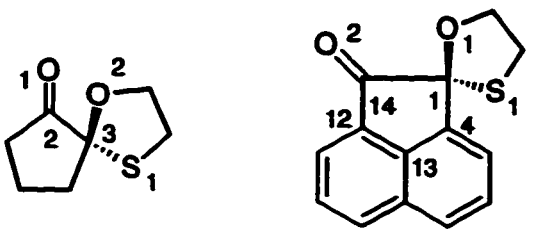

108 **114**

Figure 4.9 Cyclopentanedione acetals used in π-facial selectivity study

Ideally, the carbonyl group of the cyclopentanone moiety of oxathiolanes **108** and **114** would now bisect the oxathiolane group to reduce the steric difference between the two π-faces of the molecule, as seen by an incoming nucleophile. To determine whether this was the case, geometry optimization calculations were carried out on cyclopentanone **108** using semi-emperical (AM1) and *ab initio* (6-31G*)[21] basis sets. The AM1-optimized structure along with the relevant bond angle data, as determined by both methods are shown below (Figure 4.10).

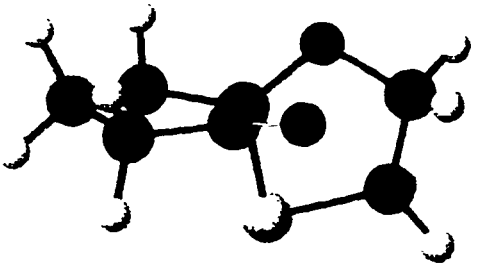

	dihedral angles (°)	
	AM1	6-31G*
O1-C2-C3-O2	46.1	32.2
O1-C2-C3-S1	73.5	86.2

Figure 4.10 Optimized structure of cyclopentanone 108

The calculated carbon-sulfur and carbon-oxygen dihedral angles of cyclopentanone **108** resemble the axial and equatorial bonds of cyclohexanone **97**, respectively. The dihedral angle between the carbonyl double bond and the carbon-sulfur bond of cyclopentanone **108** is approximately 86°; the dihedral angle between the carbonyl bond and the carbon-oxygen bond is calculated to be approximately 32°. Thus, the change from the cyclohexanone system **97** to the cyclopentanone system **108** apparently does not improve the steric imbalance between cyclopentanone **108** two π-faces. The flatness of the cyclopentanone ring, however, reduces the steric effect that this portion of the molecule will exert on an incoming nucleophile. Any π-facial selectivity observed may now be a consequence of the oxathiolane ring rather than the carbon skeleton of the remainder of the molecule. The environment about the carbonyl group of cyclopentanone **108** would therefore be expected to result in high π-facial selectivity with respect to both the steric model and the Cieplak model, as both models predict the same preferred approach of a nucleophile: nucleophile attack *anti* to the sulfur atom represents the least sterically demanding approach for an incoming nucleophile, and only the carbon-sulfur bond is suitably aligned to provide hyperconjugative stabilization during attack *anti* to the sulfur atom.

4.4.1 Preparation of cyclopentanone 108

The preparation of cyclopentanone **108** was first attempted by the treatment of oxathiolane **105** with sulfuryl chloride.[9] This reaction, which gave poor results with the cyclohexanone system, did not produce any of the desired cyclopentanone **108**. Attempted oxidation of cyclopentanone (**104**) with selenium dioxide[21] also failed (Scheme 4.5).

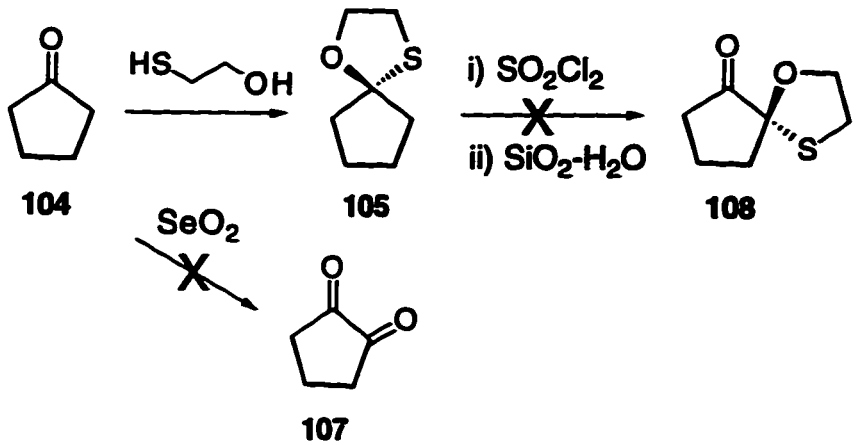

Scheme 4.5 Attempted syntheses of 1,2-cyclopentanedione

The synthesis of cyclopentanone **108** required the implementation of a three-step sequence (Scheme 4.6).

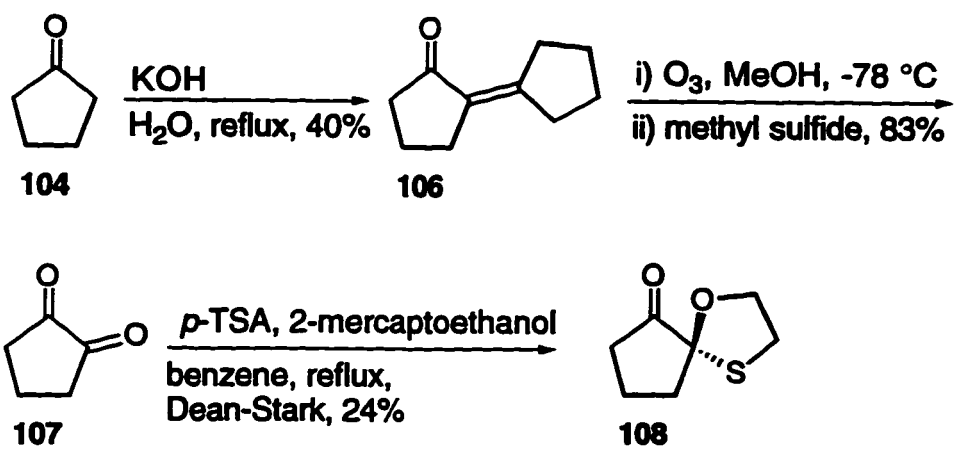

Scheme 4.6 Synthesis of cyclopentanone 108

The base-catalyzed self-condensation of cyclopentanone (**104**) resulted in a modest yield of α,β-unsaturated ketone **106**, followed by treatment of this molecule with ozone[22] to afford diketone **107** in a yield of 33% for the two steps. The highest yield (24%) for the formation of cyclopentanone **108** was achieved with the use of a catalytic (10 mol%) amount of *p*-toluenesufonic acid in benzene at reflux temperature. All attempts to improve the yield by variation of the temperature (toluene or *m*-xylene at reflux), the amount of *p*-toluenesulfonic acid, or the use of

boron trifluoride, zinc chloride or pyridinium *p*-toluenesulfonate resulted in low yields (~10%) of cyclopentanone **108**.

The increase in torsional strain[23] that accompanies the conversion of the sp^2 carbonyl carbon atom of diketone **107** to an sp^3 carbon is probably not a factor responsible for the low yield, as the same reaction with 1,2-cyclohexanedione (acetalization in this case *reduces* torsional strain) gave comparable yields of the monoacetal product. The low yield is most probably due to the formation of diacetals similar to that observed with the acetalization of 1,2-cyclohexanedione.

4.4.2 Carbon nucleophile addition to cyclopentanone 108

The diastereoselectivity of the addition of carbon nucleophiles to cyclopentanone **108** are shown in Table 4.2.

Table 4.2 Reaction of Cyclopentanone 108 with Methyllithium and Grignard Reagents

108 **109**

entry	reagent[a]	conditions	% yield[b]	% de[c]
a	CH_3Li	ether, 0 °C	79	82
b	CH_3Li	THF, 0 °C	82	75
c	MeMgBr	ether, 0 °C	90	67
d	MeMgBr	THF, 0 °C	89	71
e	MeMgBr	THF, -78 °C	43	41
f	MeMgCl	ether, 0 °C	66	56
g	MeMgI	ether, 0 °C	88	73

[a] all reactions were performed with approximately 1.1 equivalent of reagent.
[b] combined yield of isolated diastereomers. [c] Determined by GC-MS.

The determination of the relative stereochemistry of the resultant tertiary alcohols was not possible. The diastereomers were separable by silica gel chromatography, although the derivatization of the alcohols to crystalline products failed. The major diastereomer produced by the treatment of cyclopentanone **108** with methyllithium was unreactive towards 3,5-dinitrobenzoyl chloride. Reaction with 1-napthyl isocyanate also failed: the result of both of these experiments was the recovery of starting material. The unreactive nature of the alcohol towards these reagents may be a result of the sterically congested nature about the tertiary alcohol centre. The use of NOESY NMR techniques also failed to establish the relative stereochemistry of either diastereomer.

The π-facial selectivity of cyclopentanone **108** towards organolithium and Grignard reagents was generally higher than that of cyclohexanone **97**. A notable exception was the much lower π-facial selectivity that resulted with the use of methyllithium. The use of methyllithium nonetheless resulted in higher π-facial selectivity as compared with the Grignard reagents.

4.4.3 Hydride additions

The results of various hydride additions to cyclopentanone **108** are shown below (Table 4.3).

Table 4.3 Reaction of Cyclopentanone 108 with Reducing Agents

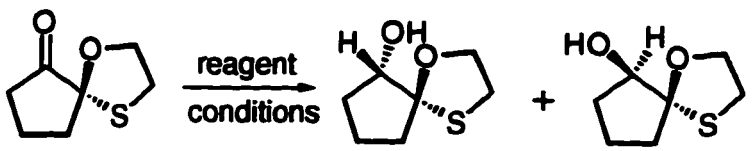

108 **110** **111**

entry	reagent[a]	conditions	% yield[b]	% **110** : % **111**[c]
a	$NaBH_4$	MeOH, 22 °C	80	67 : 33
b	$LiBH_4$	THF, 0 °C	89	83 : 17
c	$LiAlH_4$	ether, 0 °C	84	75 : 25
d	Al(*i*-Bu)$_2$H	THF, -78 °C	74	16 : 84
e	Al(*i*-Bu)$_2$H	ether, -78 °C	69	9 : 91
f	Al(*i*-Bu)$_2$H	CH_2Cl_2, -78 °C	72	11 : 89
g	LiAl(*t*-OBu)$_3$H	ether, 0 °C	75	87 : 13
h	LiB(CHMeEt)$_3$H	THF, 0 °C	65	59 : 41
i	NaAl(MeOEtO)$_2$H$_2$	ether, 0 °C	77	96 : 4
j	SmI_2, *i*-PrOH	THF, 22 °C	no reaction	

[a] all reactions were performed with approximately 1.1 equivalent of reagent.
[b] combined yield of isolated diastereomers. [c] Determined by GC-MS.

Diastereomers **110** and **111** were separable by silica gel chromatography, and their relative stereochemistry was determined by single crystal X-ray analysis of the major diastereomer produced from the reaction of cyclopentanone **108** and sodium bis(methoxyethoxy)aluminum hydride (entry i). The crystalline derivative was prepared by the treatment of alcohol **110** with 1-napthyl isocyanate. The resultant 1-napthylurethane **112** was recrystallized from carbon tetrachloride to afford a suitable crystal, the X-ray structure of which is shown below (Figure 4.11).

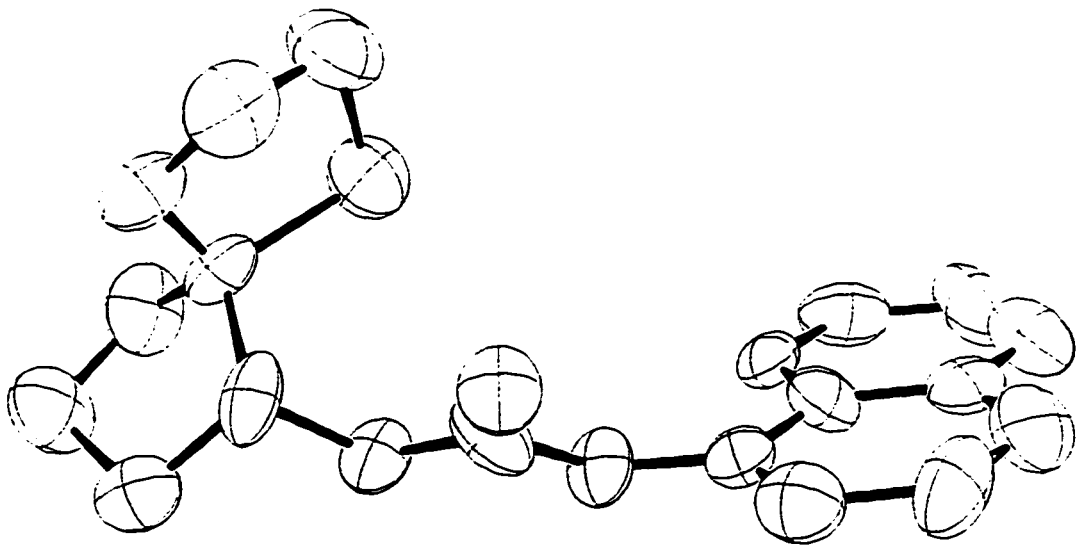

Figure 4.11 ORTEP structure of 1-napthylurethane derivative 112

The X-ray structure indicated that the relative stereochemistry of the major diastereomer from all hydride addition reactions shown in Table 4.3 (except diisobutylaluminum hydride), features the oxathiolane oxygen atom and the hydroxyl oxygen atom in an *anti* relationship. The use of diisobutylaluminum hydride resulted in the preferred formation of the opposite diastereomer in high diastereomeric excess in a number of different solvents (entries d, e, and f). The highest levels of diastereomeric excess were obtained with the use of sodium bis(methoxyethoxy)aluminum hydride and diisobutylaluminum hydride in ether at -78 °C. It is noteworthy that the opposite diastereomers are produced under these two conditions, and this allows for the control of the π-facial selectivity of cyclopentanone **108** by simply choosing the appropriate reagent. A comparison of the results shown in Table 4.3 with those for cyclohexanone **97** under similar conditions (Table 4.2), shows a slight lowering of the level of π-facial selectivity with cyclopentanone **108** but still at synthetically useful levels. Unfortunately, no general trend emerged from this series of experiments. Bulky reducing agents such as L-Selectride®, that might be expected to diplay high π-facial selectivity, resulted in lower π-facial selectivity, as

did less bulky reagents such as sodium borohydride, in comparison with cyclohexanone **97**.

4.4.4 Preparation of napthalene 114

The commercial availability of acenapthene quinone (**113**) allowed for the preparation of its monoacetal **114** by treatment of the diketone with 2-mercaptoethanol in the presence of *p*-toluenesulfonic acid (Scheme 4.7).

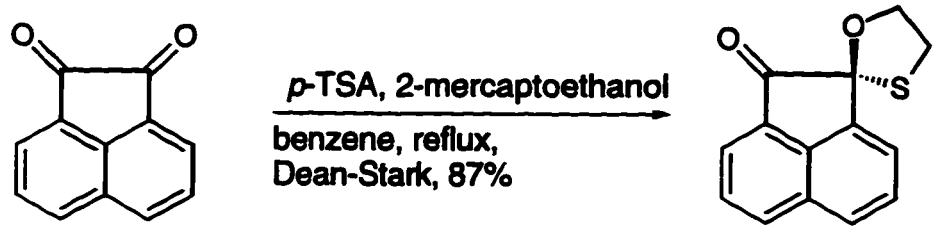

113 **114**

Scheme 4.7 Synthesis of napthalene 114

Geometry optimization calculations were carried out by both semi-emperical (AM1) and *ab initio* (6-31G*) methods and the results are shown below (Figure 4.12 and 4.13).

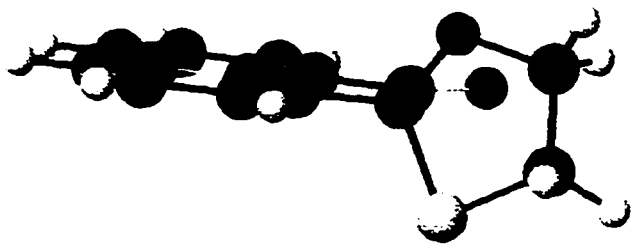

Figure 4.12 Optimized structure of napthalene 114

The results of these calculations suggest that napthalene **114** has a number of features that make this molecule more suitable than cyclopentanone **108** for determining if any purely stereoelectronic factors brought about by the presence of the oxathiolane ring, are responsible for π-facial selectivity:

- the calculated dihedral angles indicate that the oxathiolane group is roughly bisected by the carbonyl group: the S1-C1-C2-O2 dihedral angle is ~64° and the O1-C1-C2-O2 dihedral angle is ~54°.
- the relatively flat aromatic portion of napthalene **114** should allow for the stereoelectronic differences between the two π-faces of the molecule, if any, to exert a greater influence as compared with cyclohexanone **97** and cyclopentanone **108**;
- whereas cyclopentanone **108** has only one of the carbon-heteroatom bonds of the oxathiolane aligned suitably to interact with the newly forming bond, both the carbon-oxygen and carbon-sulfur bond of napthalene **114** have roughly similar dihedral angles with the carbonyl group, though not at optimal angles for hyperconjugative stabilization. Thus, if hyperconjugation is important in determining π-facial selectivity, lower π-facial selectivity is expected with napthalene **114** when compared to cyclopentanone **108**.

A single crystal X-ray analysis of napthalene **114** (Figure 4.13) was obtained later and thus allowed a direct comparison of the calculated bond angles of napthalene **114** to be compared to the values obtained from the X-ray analysis.

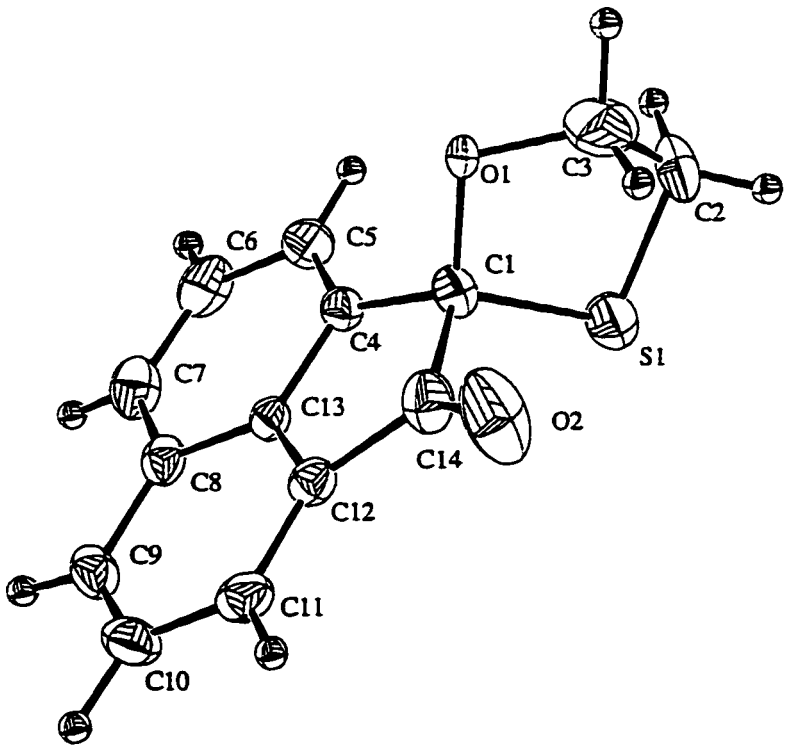

	dihedral angles (°)		
	AM1	6-31G*	X-ray
O1-C2-C3-O4	52.2	53.9	49.3
O1-C2-C3-S5	67.6	64.3	68.8
O1-C2-C3-C6	172.0	173.8	171.6
O1-C2-C8-C9	173.2	174.5	173.3
C8-C2-C3-C6	5.7	4.2	3.5

Figure 4.13 ORTEP structure of napthalene 114

4.4.5 Carbon nucleophile additions

The results of a series of Grignard and methyllithium additions onto napthalene **114** are shown in Table 4.4.

Table 4.4 Reaction of Napthalene 114 with Methyllithium and Grignard Reagents

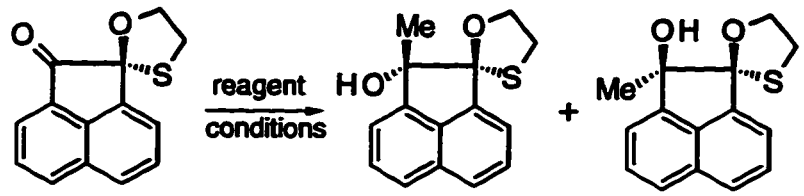

114 115 116

entry	reagent[a]	conditions	% yield[b]	% 115 : % 116[c]
a	CH_3Li	ether, 0 °C	83	98 : 2
b	CH_3Li	THF, 0 °C	89	97 : 3
c	$ZnCl_2$; CH_3Li	ether, -78 °C	91	78 : 22
d	MAD[d]; CH_3Li	toluene, -78 °C	87	87 : 13
e	MAD[e]; CH_3Li	toluene, -78 °C	79	77 : 23
f	$C_3H_7C{\equiv}CLi$	THF, 0 °C	no reaction	-----
g	MeMgCl	ether, 0 °C	80	78 : 22
h	MeMgBr	ether, 0 °C	85	76 : 24
i	MeMgI	ether, 0 °C	82	84 : 16
j	$ZnCl_2$; MeMgBr	ether, 0 °C	86	63 : 37
k	MeMgBr / $CeCl_3$	THF, 0 °C	94	77 : 23
l	MeMgBr / $YbCl_3$	THF, -78 °C	89	72 : 28
m	PhMgCl	ether, 0 °C	no reaction	-----
n	PhMgCl	ether, 22 °C	no reaction	-----

[a] all reactions were performed with approximately 1.1 equivalent of reagent. [b] combined yield of isolated diastereomers. [c] Determined by GC-MS. [d] MAD: methylaluminum bis(2,6-di-*t*-butyl-4-methylphenoxide). [e] 2 equivalents of MAD used.

The diastereomeric alcohols **115** and **116** were separable by silica gel chromatography and resulted in the isolation of a colourless oil and a white solid. The major product isolated from the reaction of napthalene **114** with methyllithium (entry a) was recrystallized from benzene and subjected to X-ray analysis (Figure 4.14). The X-ray structure confirmed the addition of a methyl group to the carbonyl

group of napthalene **114** and allowed for the determination of the relative stereochemistry of the resultant alcohol.

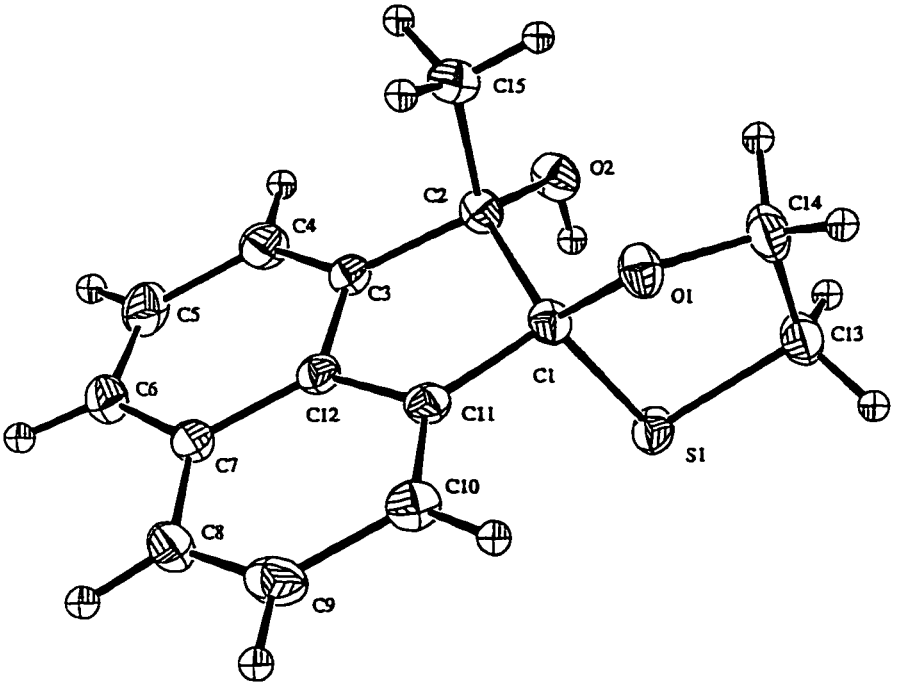

Figure 4.14 ORTEP structure of diastereomer 115

The relative stereochemistry of the major and minor diastereomers produced in the reactions shown in Table 4.4 were assigned by a comparison of the GC-MS retention time of the alcohol from which the relative stereochemistry was established by X-ray analysis, to the GC-MS retention times of the products in the reaction mixture. All of the results from Table 4.4 indicate that the predominant diastereomer formed (alcohol **115**) was a result of the addition of the methyl group *anti* to the carbon-sulfur bond.

The addition of zinc chloride to the reaction mixture prior to addition of organolithium or Grignard reagent (entries c and j) resulted in a lowered π-facial selectivity when compared with the same reactions without added zinc chloride (entries a and h). The addition of sp- and sp^2-type carbanions to napthalene **114**

was unsuccessful (entries f, m and n) and resulted in the recovery of starting material. The cause of the unreactivity of napthalene **114** towards these reagents is unknown. These particular reactions were repeated, with deuterium oxide added after the addition of the organolithium or Grignard reagent to determine if deprotonation, instead of nucleophilic addition, had occurred. The recovered starting material in each case showed no signs (by GC-MS or ^{1}H NMR) of deuterium incorporation.

The bulky aluminum reagent, methylaluminum bis(2,6-di-*tert*-butyl-4-methylphenoxide[24] (MAD), was added to the reaction mixture prior to addition of methyllithium (entries d and e) and lowered the π-facial selectivity of the reaction in comparison with methyllithium alone. Preparation of the cerium[25] or ytterbium[26] reagent followed by addition to napthalene **114** also led to a lower π-facial selectivity, as compared to that observed with methylmagnesium bromide alone.

4.4.6 Relative stereochemistry of the major diastereomer from Grignard addition to cyclopentanone 108

As discussed earlier, the relative stereochemistry of the major diastereomer produced by Grignard or organolithium addition to cyclopentanone **108** was not determined. Based on the known relative stereochemistry of alcohol **115** (from Grignard addition to napthalene **114**), along with its ^{1}H NMR spectrum suggests, however, that the major diastereomer from Grignard addition to cylopentanone **108** was also a result of carbon nucleophile addition *anti* to the carbon-sulfur bond. The ^{1}H NMR spectrum in the region of the two methylene groups belonging to the oxathiolane ring of cyclopentanone **108**, napthalene **114**, and the two diastereomers produced after methylmagnesium bromide addition to each ketone are shown below (Figures 4.15).

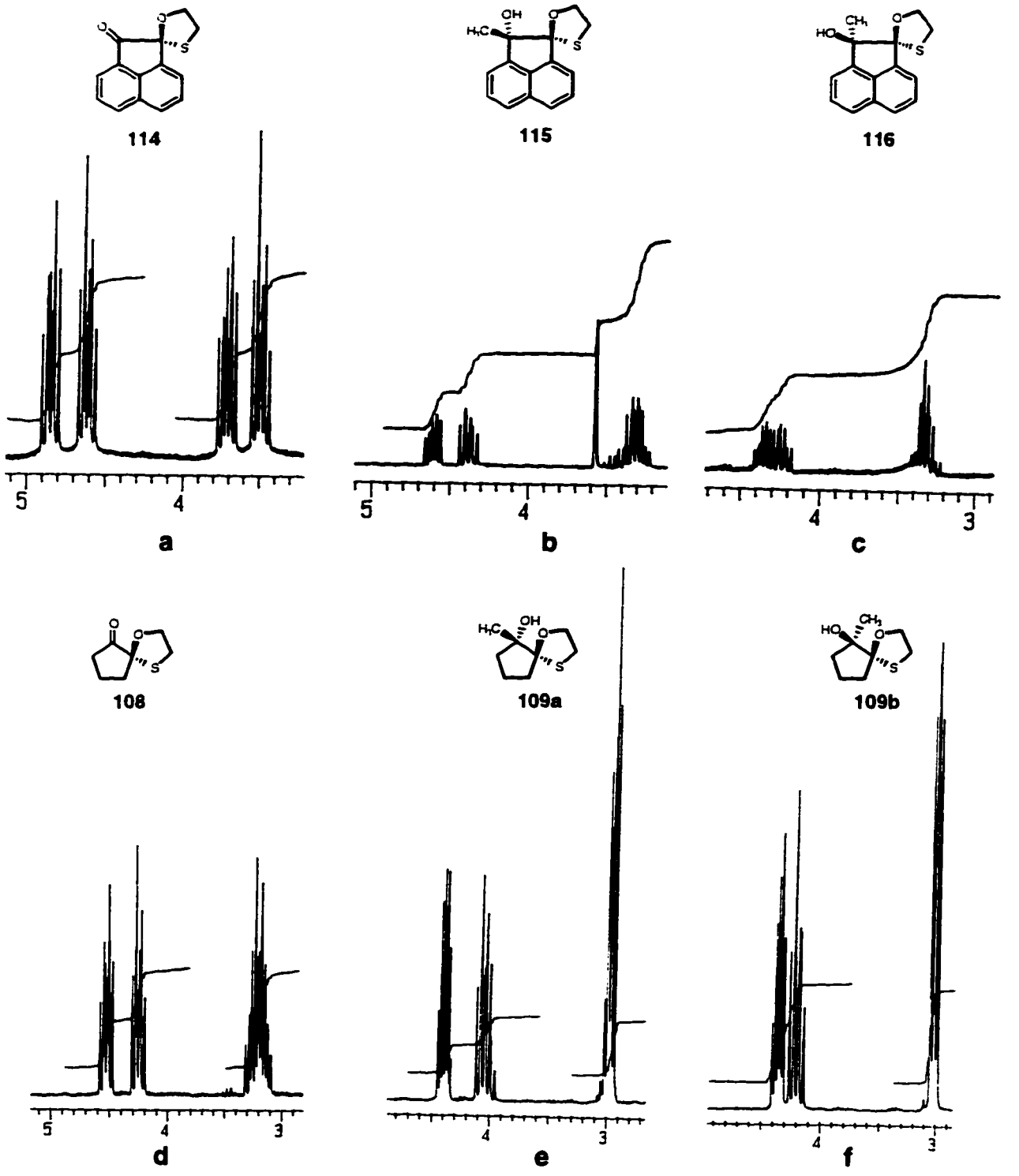

Figure 4.15 ^{1}H NMR spectra of oxathiolane methylene region

A comparison of the chemical shift changes between the two diastereomers and their respective starting ketones reveal subtle, but consistant, changes that infer the relative stereochemistry of cyclopentanol **109**. Upon Grignard addition to napthalene **114**, a small upfield shift of approximately 0.3 ppm for both methylene multiplets is observed (the methylene group adjacent to the oxathiolane oxygen is centred at 4.75 ppm; the methylene group adjacent to the sulfur atom is centred at 3.60 ppm in napthalene **114**, Figure 4.15a) in the spectrum for both the major (Figure 4.15b) and minor (Figure 4.15c) diastereomers. Another change is the signals due to the diastereotopic protons of the methylene group adjacent to the sulfur atom shifting towards each other in the spectrum of the major diastereomer (Figure 4.15b) The minor diastereomer is characterized by a similar change in the signals due to the methylene group adjacent to the oxygen atom (Figure 4.15c). These same changes are observed with the major and minor diastereomers formed after Grignard addition to cyclopentanone **108** (Figures 4.15e and 4.15f, respectively), and suggests that the relative stereochemistry of diastereomers **109a** and **109b** is the same as its napthalene counterparts.

4.4.7 Hydride additions

The outcome of the reaction of various reducing agents with napthalene **114** are shown in Table 4.5.

Table 4.5 Reaction of Napthalene 114 with Reducing Agents

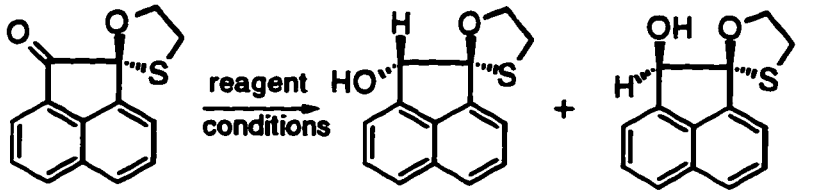

114 **117** **118**

entry	reagent[a]	conditions	% yield[b]	% **117** : % **118**[c]
a	$NaBH_4$	MeOH, 22 °C	77	24 : 76
b	$LiBH_4$	THF, 0 °C	86	31 : 69
c	$Zn(BH_4)_2$	ether, 0 °C	63	50 : 50
d	$Zn(BH_4)_2$	THF:ether[d], 0 °C	67	48 : 52
e	$LiAlH_4$	ether, 0 °C	82	29 : 71
f	$Al(i\text{-}Bu)_2H$	THF, -78 °C	86	83 : 17
g	$Al(i\text{-}Bu)_2H$	ether, -78 °C	75	88 : 12
h	$Al(i\text{-}Bu)_2H$	CH_2Cl_2, -78 °C	79	81 : 19
i	$LiAl(t\text{-}OBu)_3H$	ether, 0 °C	69	11 : 89
j	$LiB(CHMeEt)_3H$	THF, 0 °C	80	26 : 74
k	$NaAl(MeOEtO)_2H_2$	ether, 0 °C	81	9 : 91

[a] all reactions were performed with approximately 1.1 equivalent of reagent. [b] combined yield of isolated diastereomers. [c] Determined by GC-MS. [d] 1:1 ratio.

The resultant diastereomeric alcohols **117** and **118** were separable by silica gel chromatography. The X-ray structure of the major diastereomer produced from the reduction of napthalene **114** by sodium borohydride is shown below (Figure 4.16).

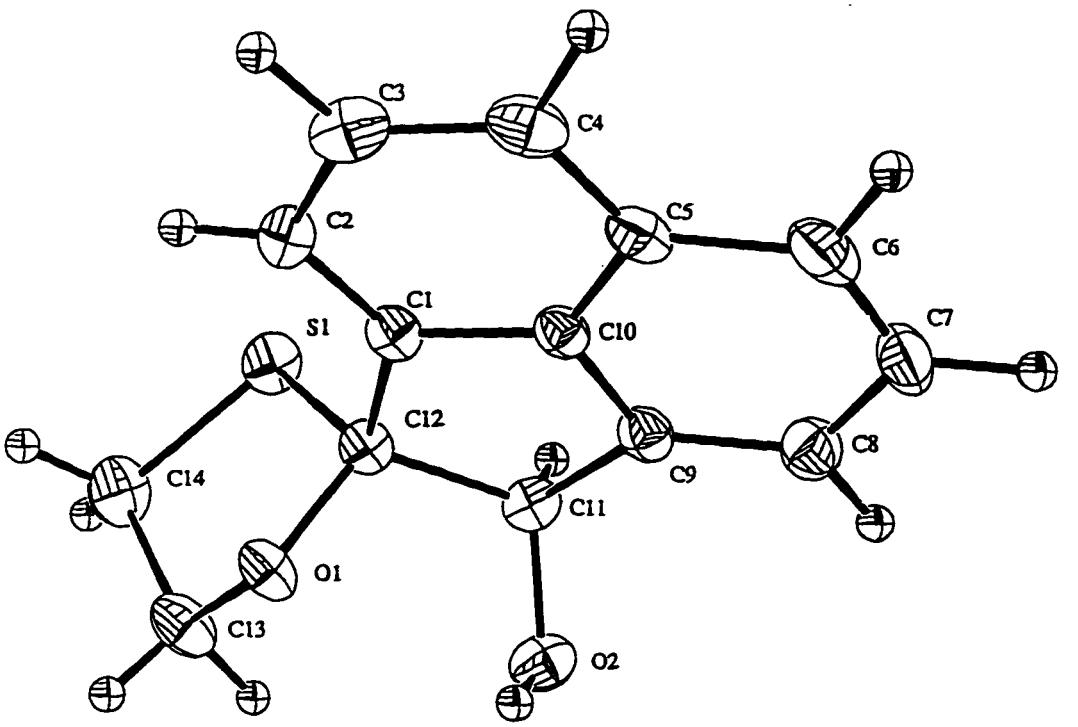

Figure 4.16 ORTEP structure of diastereomer 118

The X-ray structure of alcohol **118** allowed for the assignment of the relative stereochemistry of the minor and major diastereomers produced by each reagent. Reductions with zinc borohydride (entries c and d) resulted in the formation of equal amounts of diastereomeric alcohols. The remainder of the reducing agents employed (except diisobutylaluminum hydride, entries f, g and h) led to the predominant formation of alcohol **118** when reacted with napthalene **114**. Thus, the behavior displayed by diisobutylaluminum hydride in these reactions was similar to the reduction reactions of cyclopentanone **108**, in that a reversal in π-facial selectivity was observed with this reagent. The predominant diastereomer in the case of napthalene **114** reductions is a result of hydride addition *syn* to the carbon-sulfur bond: there is a complete reversal of the π-facial selectivity observed in the reduction reactions of cyclopentanone **108** compared with napthalene **114**. In the case of cyclopentanone **108**, both carbon nucleophile and hydride addition reactions (except diisobutylaluminum hydride) arose from addition of the nucleophile *anti* to

the carbon-sulfur bond, while with napthalene **114** only diisobutylaluminum hydride added with the same facial selectivity as the carbon nucleophiles employed. The results are summarized below (Figure 4.17), where only the major diastereomer for each type of reaction is shown.

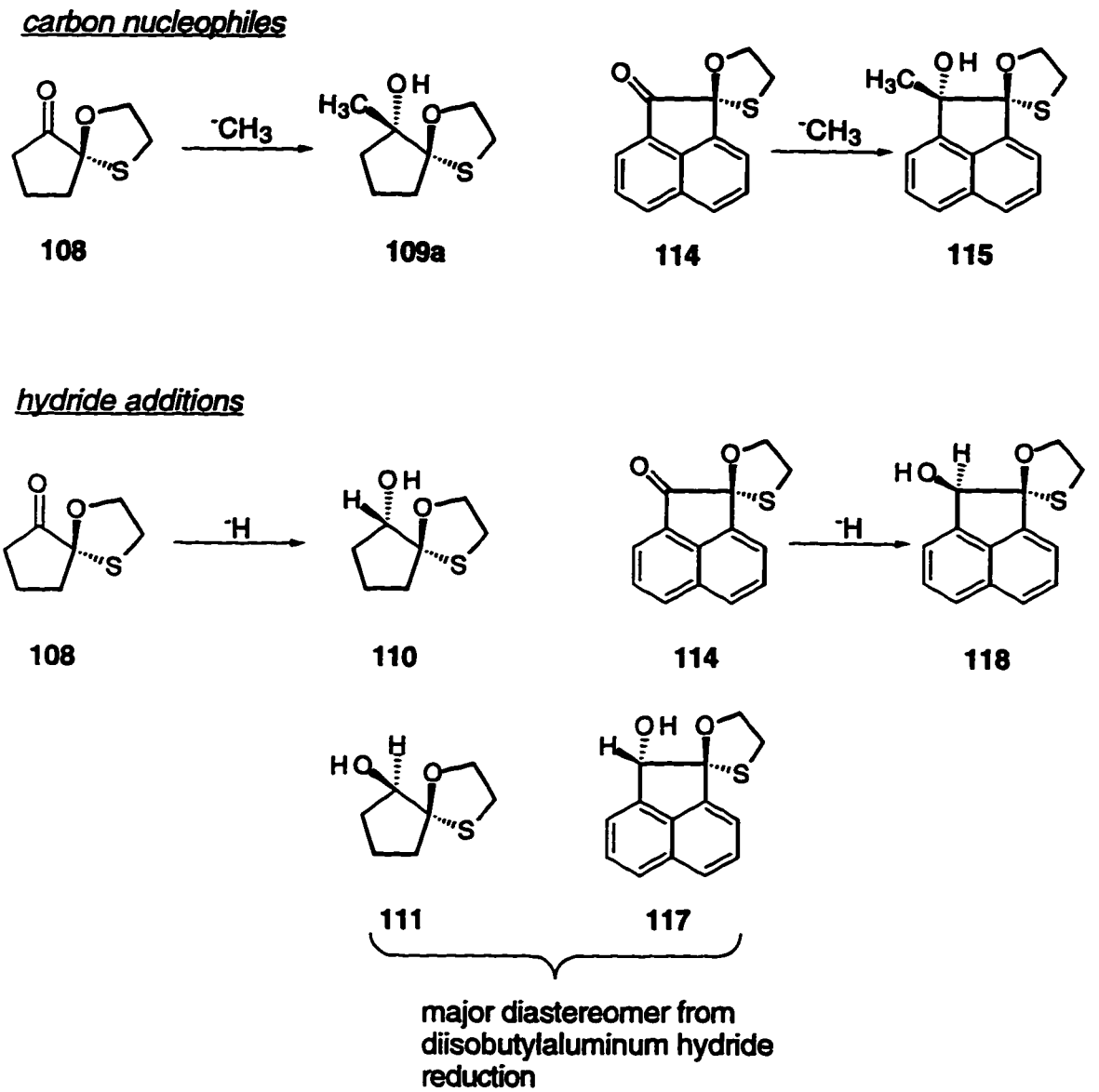

Figure 4.17 Summary of carbon and hydride additions to cyclopentanone 108 and napthalene 114

4.5 Factors that Influence π-Facial Selectivity of Ketones 108 and 114

4.5.1 Steric Interactions

The optimized (AM1) space-filling models of cyclopentanone **108** and napthalene **114** are shown below (Figure 4.18). Nucleophilic approach to the carbonyl group of these substrates from the direction *anti* to the carbon-sulfur bond represents a sterically less demanding approach that should lead to the preferential formation of alcohols **109a** and **115** from cyclopentanone **108** and napthalene **114**, respectively.

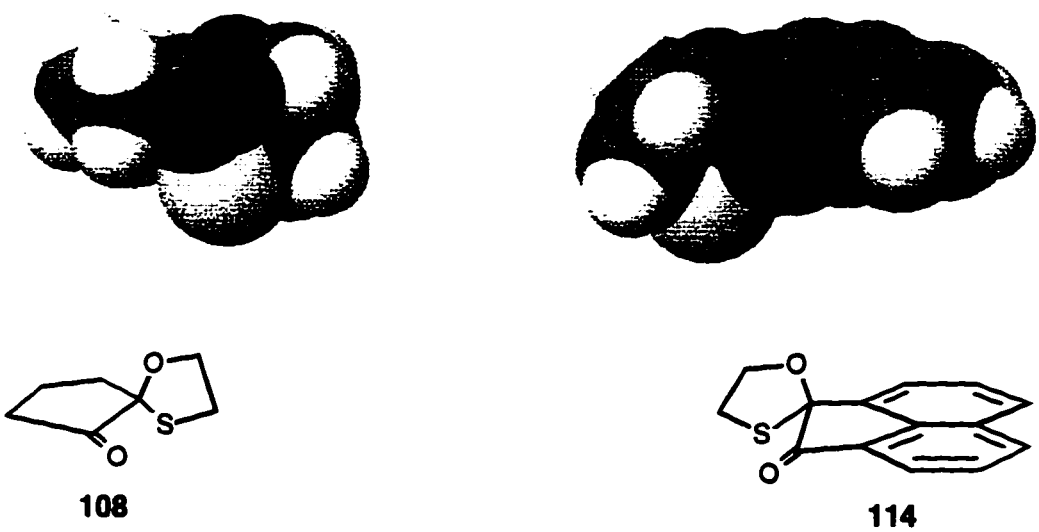

Figure 4.18 Space-filling models of cyclopentanone 108 and napthalene 114

All of the organometallic reagents reacted with ketone **108** and **114** such that approach to the carbonyl group was *anti* to the carbon-sulfur bond, the least sterically demanding approach. The majority of reducing agents approached the carbonyl group of napthalene **114** *syn* to the carbon-sulfur bond, opposite to that

predicted on steric factors alone. In contrast, the majority of reduction reactions of cyclopentanone **108** followed the least sterically demanding approach and resulted in the preferred formation of alcohol **110**. The steric bulk of the reducing agent employed did not affect the π-facial selectivity as in the case of 4-*tert*-butylcyclohexanone. The smaller reducing agents produced selectivities comparable to the larger reducing agents in reactions with cyclopentanone **108**, but with no reversal observed. The bulkier reducing agents provided marginally greater selectivity in the reduction of napthalene **114**, as compared with the smaller reducing agents employed.

The carbonyl group of napthalene **114** bisects the adjacent oxathiolane group more evenly as compared to cyclopentanone **108** to present a sterically less biased π-face. Thus, higher π-facial selectivity might be expected with cyclopentanone **108**, as compared with napthalene **114**. This is not observed experimentally with methyllithium, and the Grignard reagents used result in similar diastereomeric excesses for both ketones. Reduction reactions displayed no trends as approximately one half of the reagents resulted in higher π-facial selectivity with cyclopentanone **108**, as compared with napthalene **114**.

4.5.2 Chelation control

The presence of heteroatoms adjacent to the carbonyl group of cyclopentanone **108** and napthalene **114** allow for the possibilty of coordination or chelation with the metallic portion of the reagent with a heteroatom and the carbonyl oxygen atom. The chelation of magnesium by the two oxygen atoms of oxathiane **88** was considered to be the primary factor responsible for the high stereoselectivity in the Grignard reaction of oxathiane **88** (Figure 4.2).

The major diastereomer from the reaction shown in Figure 4.2 was formed in accordance with the Cram chelate model in which the nucleophile attacks the least

hindered face of the carbonyl. The two alcohols that are expected to form preferentially from ketones **108** and **114**, after addition of Grignard reagent and formation of a Cram chelate, are shown below (Figure 4.19).

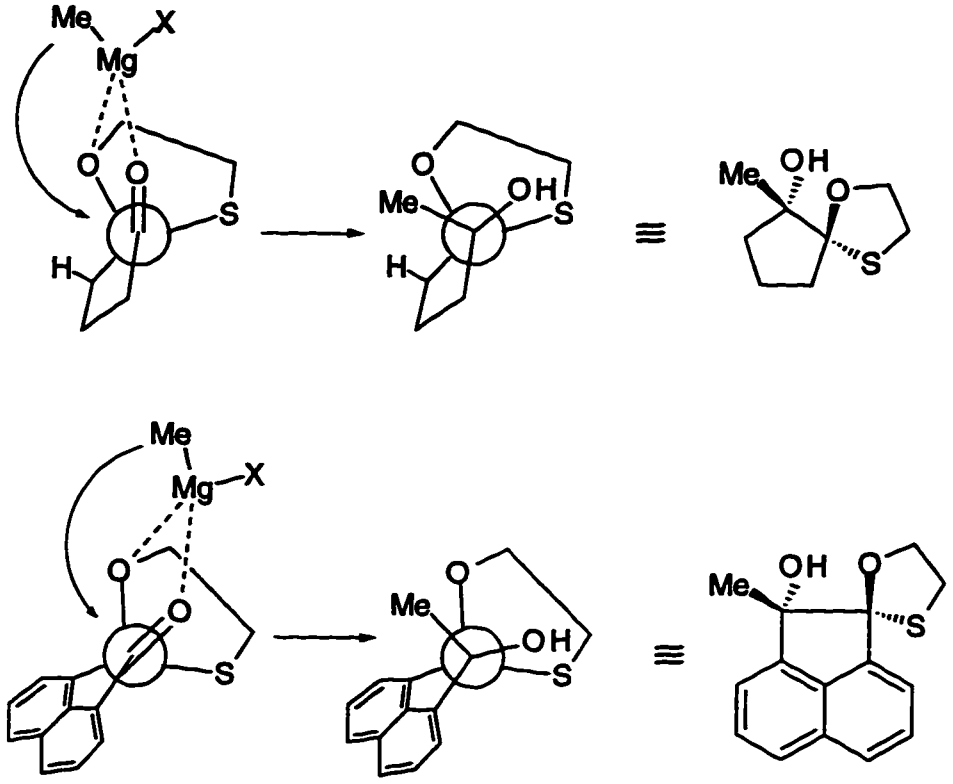

Figure 4.19 Expected π-facial selectivity according to Cram chelate model

In both cases, nucleophilic attack is expected to occur *anti* to the sulfur atom, as this avoids approach alongside the relatively bulky sulfur atom. Attack *anti* to the sulfur atom is predominant with napthalene **114**, however two observations from the reaction of Grignard reagents with cyclopentanone **108** are inconsistant with the chelate model. Firstly, the effect of changing the reaction solvent from ether to tetrahydrofuran resulted in a increase in the π-facial selectivity of the reaction (Table 4.2, entries c and d). Tetrahydrofuran is a more highly-coordinating solvent than

ether[3] and should interfere with the chelation of the Grignard reagent to the oxygen atoms of cyclopentanone **108**, lowering the diastereoselectivity of the reaction. Secondly, the effect of lowering the temperature (Table 4.2, entries d and e) results in a lower observed diastereoselectivity along with a concomitant lowering of the yield of the reaction. A lowering of the reaction temperature in a reaction that proceedes *via* a Cram chelate would not be expected to result in a decrease in diastereoselectivity, as the chelate model is favoured, for entropic reasons, at lower temperatures.

The nature of the halide atom in Grignard reagents may also influence a reagent's chelating ability and hence, affect the level of diastereoselectivity of reactions that form a Cram chelate. Methylmagnesium chloride exists as a halogen-bridged dimer whereas methylmagnesium bromide and iodide exist as equilibrating monomeric and oligomeric species.[27] Thus, chelation to cyclopentanone **108** or napthalene **114** with methylmagnesium chloride may be lower, when compared with its bromine or iodide counterparts, and result in lower diastereoselectivity. This trend is observed with cyclopentanone **108** (Table 4.2, entries c, e and f) but not with napthalene **114** (Table 4.4, entries g, h and i).

The influence of lathanides on the π-facial selectivity of Grignard additions to napthalene **114** was explored based on the reported reversal in diastereoselectivity with the use of cerium-[25] or ytterbium-Grignards[26] on oxathiane substrates (Figure 4.20).

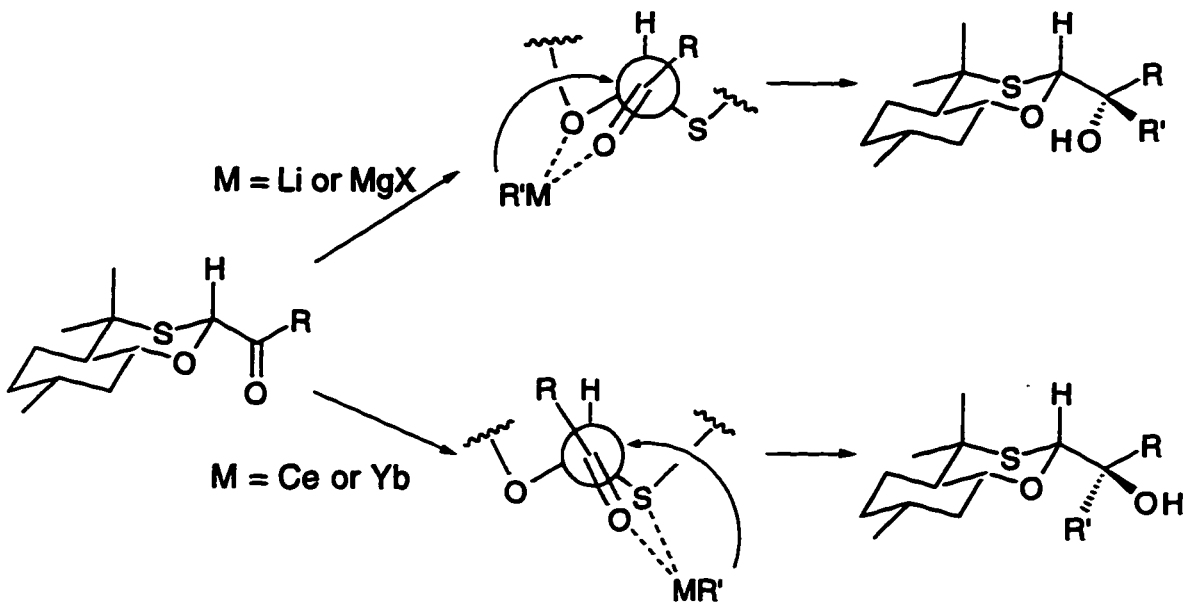

Figure 4.20 Lanthanide reversal of diastereoselectivity

The results shown above are attributed to the preferred formation of a cerium chelate, after reaction with a Grignard reagent that has been pretreated with cerium trichloride. A similar reversal was also reported[24] with the ytterbium analogue. Napthalene **114** was treated with the cerium and ytterbium reagents, prepared from methylmagnesium bromide and the corresponding lanthanide trichloride, with very little change in the sense or level of diastereoselectivity compared to the Grignard reagents alone.

The pretreatment of the substrate with a bulky Lewis acid such as methylaluminum bis(2,6-di-*tert*-butyl-4-methylphenoxide (MAD) is an alternative approach that has been reported to reverse the diastereoselectivity of nucleophilic additions to conformationally-locked cyclohexanones to give the equatorial alcohols preferentially (Figure 4.21).

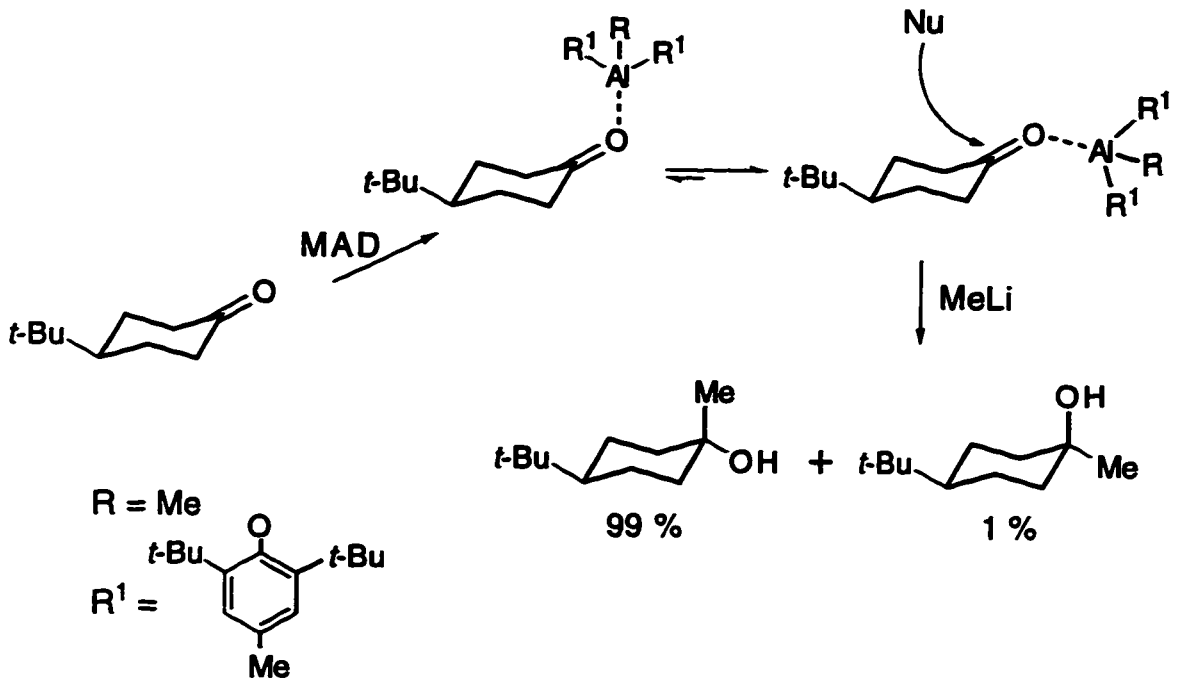

Figure 4.21 Bulky Lewis acids promote axial attack

The addition of a carbon (or hydride) nucleophile to the Lewis-acid complex in Figure 4.21 occurs from the axial direction preferentially. This is a consequence of the steric interaction of the Lewis acid with the 3,5-diaxial hydrogens being the dominant interaction, and places the Lewis acid in a position that effectively blocks the equatorial approach. Pretreatment of napthalene **114** with MAD, followed by methyllithium addition, resulted in a lowering of the π-facial selectivity of the reaction as compared to methyllithium alone (Table 4.4, entries d and e). This small drop in diastereoselectivity indicates that the complexed Lewis acid may occupy a position as to only partially block any approaching nucleophile. The addition of two equivalents of MAD, theoretically complexing both oxygens atoms of napthalene **114**, did not have any effect on the diastereoselectivity of the methyllithium addition reaction. This result suggests that the Lewis acid complexes in such a fashion as to

leave the steric environment about the carbonyl essentially unchanged, or that no complexation occured.

The greatest change in π-facial selectivity with napthalene **114** occured upon precomplexation with zinc chloride (Table 4.5, entries c and j). A 20 % increase in the product from addition of the nucleophile *syn* to the sulfur atom was observed when methyllithium was employed and a 13 % increase occurs with the use of methylmagnesium bromide. Thus, zinc chloride apparently blocks the nucleophile approach more effectively than MAD, but only to a relatively small extent.

4.5.3 Nucleophile approach angle

The steric effect associated with the trajectory taken by the incoming nucleophile onto the carbonyl π-system may also be a factor governing the outcome of π-facial selectivity in reactions with cyclopentanone **108** and napthalene **114**. The attack of a carbonyl group is in the plane made by the carbonyl π-bond as this provides maximum overlap between the nucleophile HOMO and the carbonyl LUMO.[28] As described in Chapter 4, a study of the X-ray structures of a series of aminoketones by Bürgi, Dunitz and co-workers led to the proposal that the optimal trajectory for nucleophilic attack on a carbonyl group is at angle of 107 ± 5° to the carbon - oxygen bond in the plane made by this bond (Figure 4.18, Chapter 3).

One particular class of compound that has been used extensively to study electronic effects[29] in diastereofacial selectivity are 5-substituted adamantanones such as amine **119** and *N*-oxide **120** (Figure 4.22).

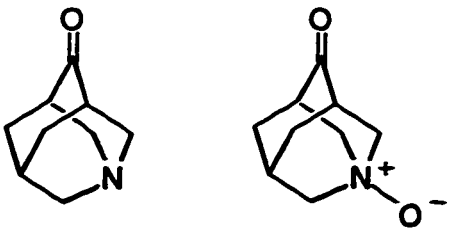

119 120

Figure 4.22 Substituted adamantanones as probes for electronic effects

Substituted adamantanones were extensively studied as it is believed that they are free of steric bias about the carbonyl group and any π-facial selectivity observed from nucleophilic addition arises from an electronic effect exerted by the substituent at the 5-position. Unfortunately, recently reported[30] MNDO/PM3 calculations on amine **119** are not in agreement with equally recent *ab initio* calculations (6-31G**).[31] The former calculations result in a symmetrical environment about the carbonyl group while the latter produces a structure that is distorted somewhat about the carbonyl group due to a slight puckering of the cyclohexane ring not containing the heteroatom substituent (Figure 4.23).

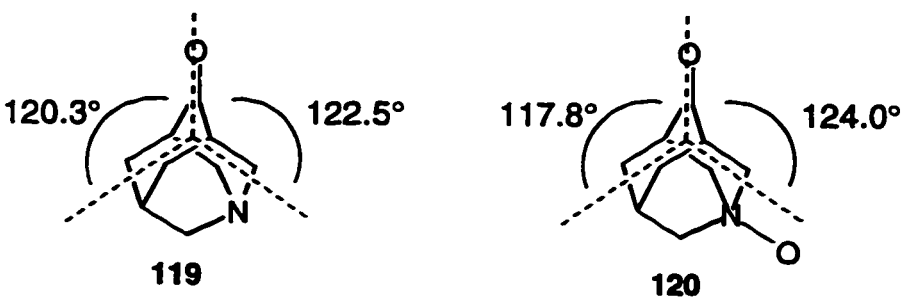

119 120

Figure 4.23 6-31G* optimized structures of adamantanones 119 and 120

This distortion effectively renders the nucleophile approach *syn* to the nitrogen atom less sterically demanding if the Bürgi-Dunitz trajectory is adopted and,

according to the authors of the study, can account for the observed π-facial selectivity with amine **119** and *N*-oxide **120** (Figure 4.24).

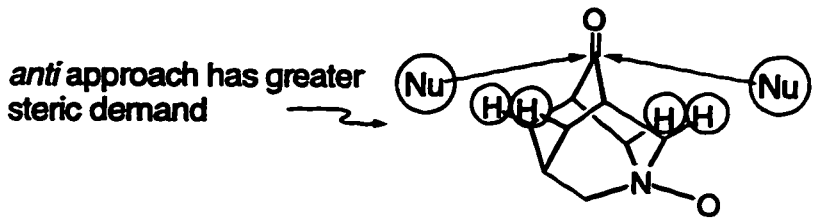

Figure 4.24 Differences in steric interactions for *syn* and *axial* attack

The semi-empirical study concluded that there was no steric bias in amine **119**, the observed π-facial selectivity could be explained in terms of the Cieplak model.

Nucleophilic additions to the symmetrical parent ketone, adamantanone, may also be expected to result in π-facial selectivity in the situation where the carbonyl carbon atom is pyramidalized[32], which slightly tilts the carbonyl group to one side. This tilting of the carbonyl sp^2 carbon atom is believed to arise from the angle strain in the C-C_{CO}-C bond of small and medium-sized cyclic ketones. In this situation, the incoming nucleophile would experience less steric interaction with the adamantanone skeleton and "axial" hydrogen atoms by attacking along the Bürgi-Dunitz trajectory opposite the direction of the carbonyl tilt: the same interactions as described in Figure 4.24 would also dictate which approach would be favoured by the nucleophile. The direction of carbonyl tilting would also be expected to effect the diastereoselectivity in the torsional strain model in a manner similar to that previously described for cyclohexanone systems: nucleophilic attack from the face of the molecule opposite to the direction of the carbonyl tilt should be favoured since the carbonyl C-O bond will not have to become fully eclipsed with the C_{CO}-C_α bond as the reaction progresses.

To determine the degree, if any, of pyramidalization of the carbonyl group in cyclopentanone **108** and napthalene **114**, calculations were performed using both semi-emperical and *ab initio* methods. The bond angle about the carbonyl sp^2 carbon atom was calculated (6-31G*) to be 112° in **108** and measured as 107° in **114** (from X-ray structure), but ideally should be 120°. To relieve some of this strain, the carbonyl carbon atom may assume a pyramidalized configuration, as based on several reports in the literature.[33] Both types of calculations indicate a small amount of tilting of the carbonyl group in the direction of the oxathiolane oxygen atom for both cyclopentanone **108** (1.7° [AM1], 2.5° [6-31G*]) and napthalene **114** (1.8° [AM1], 1.7° [6-31G*]). The direction of the tilt in both compounds **108** and **114** would tend to favour approach of a nucleophile *syn* to the sulfur atom, neglecting any steric bias about the carbonyl group. In the case of cyclopentanone **108**, the asymmetrical nature about the carbonyl group is significant and approach by a nucleophile is less demanding in an attack *anti* to the sulfur atom. The preference for all reagents tested to add *anti* to the sulfur atom may indicate that any effect that carbonyl tilting has on the π-facial selectivity of the addition reactions to cyclopentanone is small compared to other factors. The carbonyl group is similarly tilted towards the oxathiolane oxygen atom in napthalene **114**, but in this case the steric environment about the carbonyl group is more symmetrical, and a preference for hydride attack *syn*to the sulfur atom is observed. The degree of carbonyl tilting is, however, very small in ketones **108** and **114**, as well as the substituted adamantanones described eariler. The degee of uncertainty in the Bürgi-Dunitz angle is at least twice the amount of carbonyl tilting in these cases and it is unlikely that this plays a role in determining the approach of the nucleophile in any of these cases.

4.5.4 Hyperconjugative transition state stabilization

The stabilization of the transition state during nucleophilic addition to carbonyl groups remains controversial.[34] Despite this fact, Cieplak's model[19] has been cited as an important factor in a wide range of reaction types including Diels-Alder cycloadditions,[35] electrophilic additions,[36] conjugate addition,[37] cyclopropanations[38] and radical reactions.[39] An oxathiolane ring at the α carbon of a ketone contains carbon-oxygen and carbon-sulfur bonds adjacent to the carbonyl group and therefore, each bond can potentially participate in transition state stabilization as described in chapter 3. The Cieplak models requires the presence of a low-lying orbital, $\sigma^{*\ddagger}$, associated with the σ bond being formed in the reaction plus an adjacent bond to interact with $\sigma^{*\ddagger}$ and provide transition state stabilization (Figure 4.25).

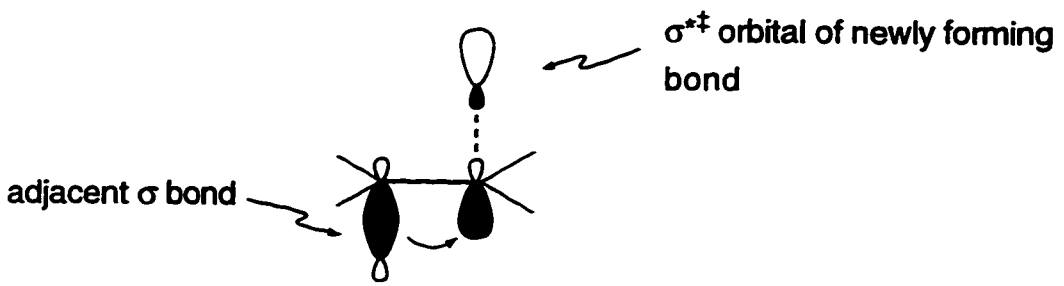

Figure 4.25 Cieplak model

According to frontier molecular orbital theory,[40] this two-electron stabilization resulting from the interaction of a filled molecular orbital with a vacant molecular orbital (in this case, $\sigma^{*\ddagger}$), is dependant on the energy separation between the two orbitals and the amount of orbital overlap. Thus, both of these factors should effect π-facial selectivity in a reaction that follows the Cieplak model. Fundamental to this model is the question of which bond adjacent to a carbonyl group is the better σ donor, as this determines the stereoselectivity of the reaction. Fortunately, there is general agreement that a carbon-sulfur bond is a better σ donor than a carbon-

oxygen bond.[41] The expected products from nucleophilic addition to cyclopentanone **108** and napthalene **114**, based on the Cieplak model, are shown below (Figure 4.26).

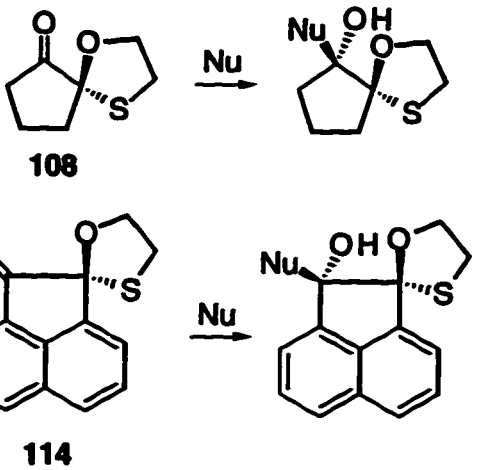

Figure 4.26 Expected π-facial selectivity based on the Cieplak model

Table 4.6 describes the resultant π-facial selectivity observed with cyclopentanone **108** and napthalene **114** after treatment with various reagents in terms of the Cieplak model.

Table 4.6 π-Facial Selectivity of Oxathiolane Cyclopentanones

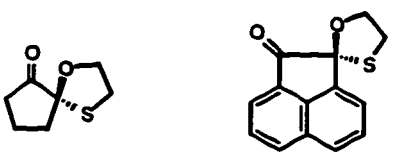

		108	selectivity	114
entry	reagent			
a	CH_3Li	Cieplak		Cieplak
b	MeMgBr	Cieplak		Cieplak
c	$NaBH_4$	Cieplak		anti-Cieplak
d	$LiBH_4$	Cieplak		anti-Cieplak
e	$LiAlH_4$	Cieplak		anti-Cieplak
f	$Al(i\text{-}Bu)_2H$	anti-Cieplak		Cieplak
h	$LiAl(t\text{-}OBu)_3H$	Cieplak		anti-Cieplak
i	$LiB(CHMeEt)_3H$	Cieplak		anti-Cieplak
j	$NaAl(MeOEtO)_2H$	Cieplak		anti-Cieplak

When treated with organometallic reagents, both ketones resulted in the preferrential formation of the diastereomer predicted by the Cieplak model. The greater dihedral angle between the carbon-sulfur bond and the carbonyl double bond in cyclopentanone **108** compared to napthalene **114** (86° and 64°, respectively) should provide superior antiperiplanarity with the forming carbon-carbon bond and lead to higher levels of π-facial selectivity. This is observed with the Grignard reagents, but not with methyllithium, suggesting that orbital overlap may not be a dominant factor. The higher levels of selectivity measured for both ketones upon treatment with methyllithium as compared to the Grignard reagents possibly reflects a difference in the ability of the metal ion to stabilize the developing charge on the carbonyl oxygen atom. According to the Cieplak model, the lone pair which develops on the carbonyl oxygen atom as the nucleophilic addition proceeds is also involved in an antiperiplanar interaction with the orbital of the forming bond. The result of delocalization of this lone pair into the $\sigma^{*\ddagger}$ orbital raises its energy (lowering selectivity) and therefore, high selectivity is believed to be dependent on the stabilization of this lone pair by the metal cation. The harder[42] lithium cation is expected to stabilize the developing lone pair to a greater extent than magnesium and a comparatively lower $\sigma^{*\ddagger}$ energy would expect to result in greater π-facial selectivity, as observed.

The diastereoselectivity of the reduction of cyclopentanone **108** followed the Cieplak model with all of the reducing agents employed, with the exception of diisobutylaluminum hydride (entry f). It is noteworthy that these results are reversed in the reduction reactions of napthalene **114**. These findings underscore the danger in basing π-facial selectivity prediction solely on the substrate structure. Although there are obvious structural differences between the two ketones, a complete reversal in reduction selectivity is surprising. The absense of a counterion may play

a role in the reversal of the π-facial selectivity, as this is observed for both ketones with diisobutylaluminum hydride.

It is evident from Table 4.6 that the Cieplak model fails in the case of napthalene **114**. As the steric environment about the carbonyl groups of both ketones would not suggest reversal in selectivity, this points to electronic differences between the two ketones as a factor for the change in selectivity. A necessary condition in the Cieplak model is that the $\sigma^{*\ddagger}$ orbital energy be lower than the π^* (carbonyl LUMO) energy. The $\sigma^{*\ddagger}$ energies for the reactions shown in Table 4.6 are unknown, however the carbonyl LUMO energies may be calculated. Using semi-emperical methods (AM1), the calculated LUMO energy for cyclopentanone **108** and napthalene **114** is 0.162 and -0.179 eV, respectively. The lower LUMO energy for napthalene **114** may be due to the conjugation of the carbonyl π bond with the π bonds of the aromatic framework of the molecule. Thus, if the $\sigma^{*\ddagger}$ energy for napthalene **114** during hydride reduction is higher than -0.179 eV, Cieplak-type stabilization may not be possible with this molecule. Unfortunately, it is not yet determined if the Cieplak-type behavior of napthalene **114** toward organometallic reagents is fortuitous, or that indeed the $\sigma^{*\ddagger}$ orbital energy is lower than the carbonyl LUMO energy.

If the Cieplak effect is inoperative in hydride addition to napthalene **114**, the cause of the selectivity reversal between the two ketones is unclear. The Felkin-Anh model predicts that reduction of napthalene **114** should be favoured to occur *anti* to the carbon-sulfur bond: the sulfur atom behaves as the **L** group, in the Felkin-Anh sense, by virtue of its lower-lying $\sigma^*_{C\text{-}S}$ orbital.[37] This is contrary to the π-facial selectivity observed.

4.5.5 Electrostatic potential

The use of electrostatic potential calculations as a tool for interpreting and predicting molecular behavior towards electrophiles is well established.[43] There is also an increasing number of reports in the literature regarding the use of electrostatic potential in determining the preferred sites and direction of nucleophilic attack.[44] Although the calculation of the electrostatic potential is unnecessary to determine the *site* of nucleophilic attack in ketones **108** and **114**, it was hoped that the calculated surfaces may reveal a preferred direction of attack. The electrostatic potential surfaces of cyclopentanone **108** and napthalene **114** were calculated and gave very similar results. The electrostatic potential surface for napthalene **114** is shown below (Figure 4.27).

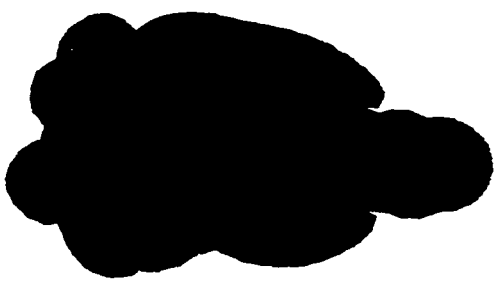

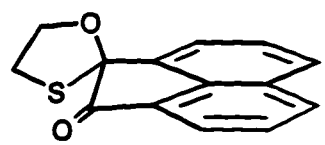

114

Figure 4.27 Electrostatic potential surface of napthalene **114**

The surface depicted was calculated from the AM1-optimized geometry and represent areas of positive (coloured red) and negative (coloured blue) electrostatic potential on the -1.25 kcal/mol surface of ketone **114** total electronic density function. The red areas represent sites most susceptible to nucleophilic attack. The suface in Figure 4.4 does not, however, reflect the π-facial selectivity observed with ketones **108** and **114**. Both surfaces contain roughly symmetrical areas of positive potential and are of little predictive value.

4.6 Spiro-tetrahydrofuran and -tetrahydrothiophene Systems

The π-facial selectivity for cyclopentanone systems with an adjacent oxathiolane ring, although displaying high selectivity, showed no broad trends. This is undoubtedly due to a number of factors that may be competing with, or reinforcing each other, to direct nucleophilic approach. Thus, it was of interest to determine the effect of removing a heteroatom (to give ketones **129** and **133**) on π-facial selectivity of nucleophilic addition.

129 **133**

Figure 4.28 Does removal of a heteroatom change π-facial selectivity?

An added advantage in the study of ketones **129** and **133** is that the issue of possible reagent complexation with either heteroatom, as with the oxathiolane systems, becomes irrelevant. With regard to the Cieplak model, ketones **129** and **133** are now predicted to display opposite π-facial selectivity, as carbon-carbon bonds are considered to posess greater σ-donating ability than carbon-oxygen bonds, but less donating ability than carbon-sulfur bonds.

There are some examples found in the literature that report high π-facial selectivty with ketones where hyperconjugation may be from a carbon-carbon or carbon-oxygen bond. A study by Meyers[38a] applied the Cieplak model in order to explain the stereochemical course of the reaction described below (Figure 4.29).

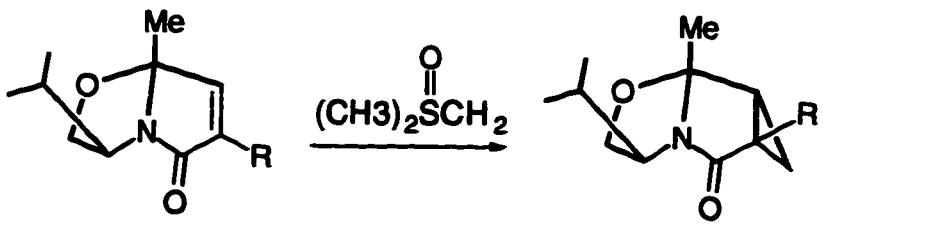

119, R = H, CO_2Me, Ph

120 (*endo* 96-99%)

Figure 4.29 Conjugate addition follows the Cieplak model

In another example,[45] conjugate addition was the major product from spirocyclic ether **121** after treatment with methylmagnesium bromide, and resulted in a single diastereomer **122** as a result from nucleophile approach *anti* to the carbon-carbon bond (Figure 4.30).

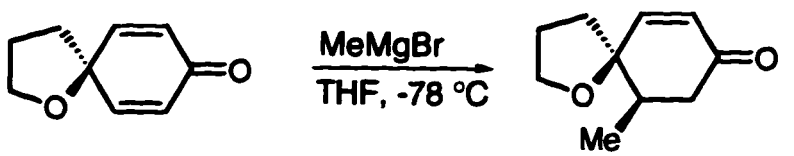

121 **122**

Figure 4.30 π-Facial control with tetrahydrofuran substituent

4.6.1 Preparation of tetrahydrofuran 129 and tetrahydrothiophene 133

The preparation of the desired ketone **129** required the synthesis of a key intermediate, epoxyalcohol **127** (Scheme 4.8). This intermediate not only allows for the preparation of ketone **129**, but ketone **133** may also be prepared from this compound.

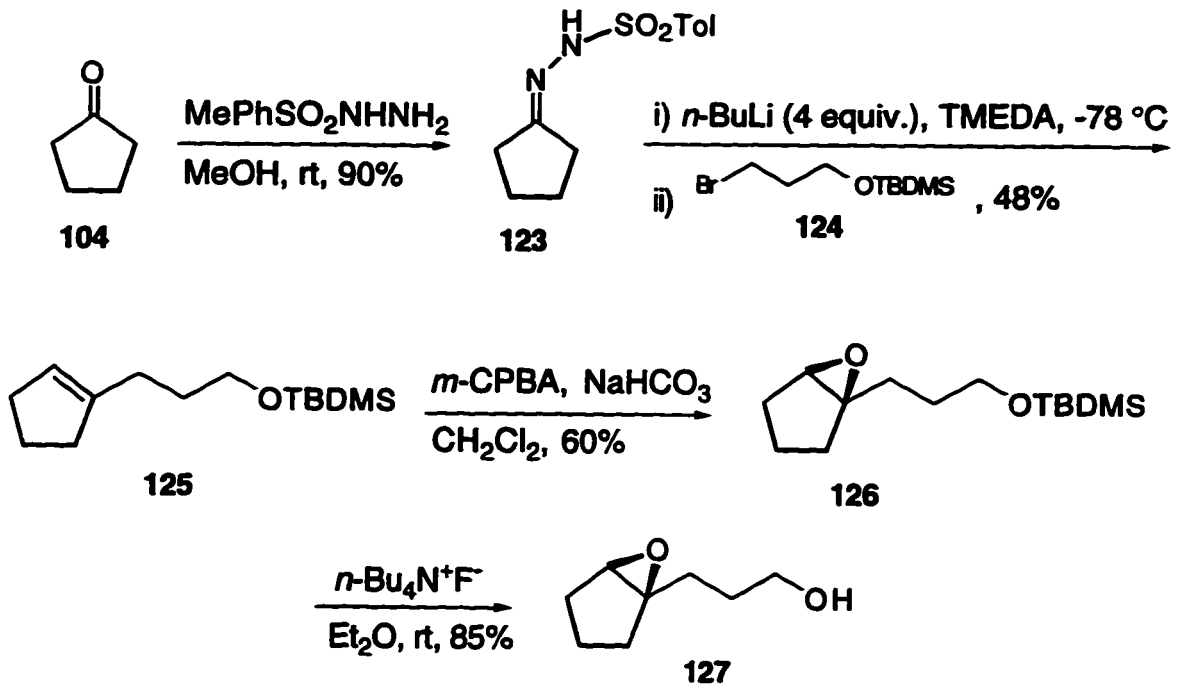

104 123 124 125 126 127

Scheme 4.8 Synthesis of epoxyalcohol 127

Cyclopentanone (**104**) was treated with *p*-toluenesulfonyl hydrazine to afford hydrazone **123** in 90% yield. A vinyl anion was next generated *in situ* by subjecting hydrazone **123** to Shapiro[46] conditions, followed by quenching with the protected bromoalcohol **124**[47] in 48% yield. Oxidation of the resultant cyclopentene **125** was accomplished with *m*-chloroperbenzoic acid to afford epoxide **126** in 60% yield. Removal of the silyl protecting group proceeded in 85% yield by treatment of epoxide **126** with tetrabutylammonium fluoride to give epoxyalcohol **127**.

A two-step sequence (Scheme 4.9), consisting of treatment of epoxyalcohol **127** with boron trifluoride etherate at low temperature (-78 °C), followed by oxidation[48] of the resultant spiro-tetrahydrofuran **128**, afforded the required ketone **129** (65%, two steps).[49]

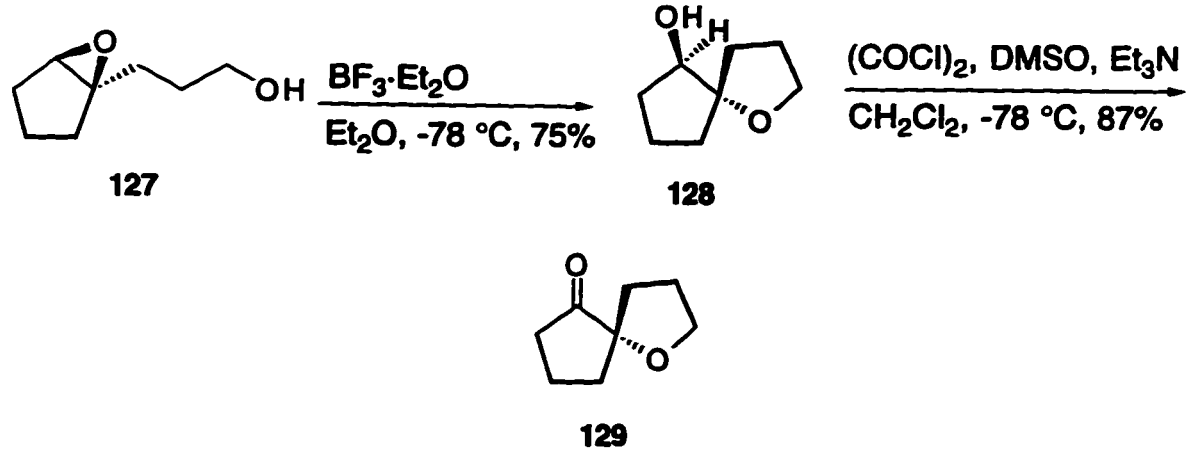

Scheme 4.9 Synthesis of tetrahydrofuran 129

The conversion of epoxyalcohol **127** to tetrahydrothiophene **133** was carried out by the three-step sequence outlined below (Scheme 4.10).

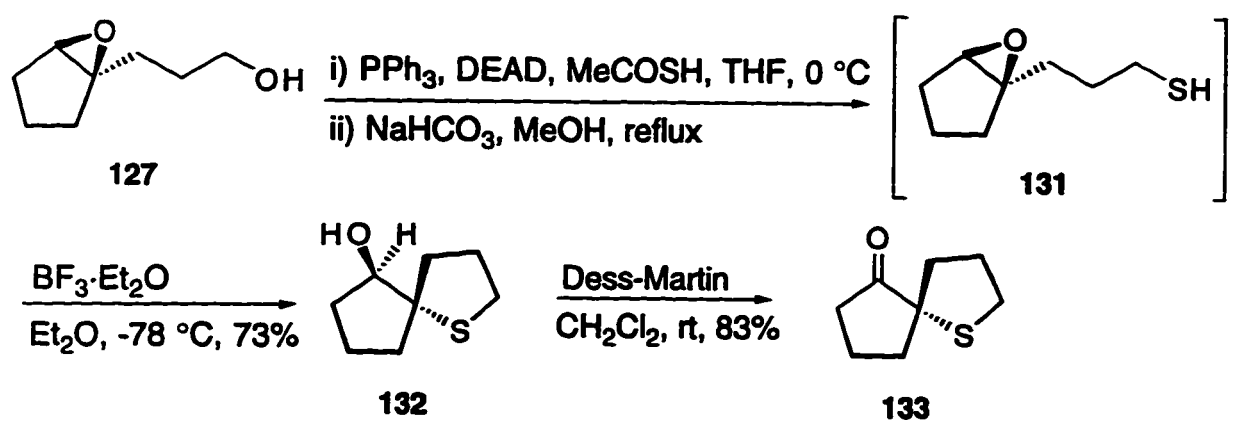

Scheme 4.10 Synthesis of tetrahydrothiophene 133

Treatment of epoxyalcohol **127** with thiolacetic acid in the presense of diethyl azodicarboxylate[50], followed by basic hydrolysis afforded epoxythiol **131**. The thiol was not isolated but converted directly to the tetrahydrothiophene **132** by *in vacuo*

removal of methanol and treatment with boron trifluoride etherate (73%, three steps). Oxidation[51] of alcohol **132** gave the required ketone **133** in 83% yield.

4.6.2 π-Facial selectivity of tetrahydrofuran 129

The resultant π-facial selectivity shown by tetrahydrofuran **129** after treatment with various reagents are summarized in Table 4.7.

Table 4.7 Nucleophilic Additions to Tetrahydrofuran 129

129 A B

entry	reagent	conditions	% yield	% A[a]	% B[a]
a	$NaBH_4$	MeOH, rt	89	94	6
b	$LiBH_4$	THF, rt	94	84	16
c	$Al(i\text{-}Bu)_2H$	CH_2Cl_2, -78 °C	92	80	20
d	$LiAlH_4$	Et_2O, 0 °C	84	86	14
e	$Zn(BH_4)_2$	Et_2O, rt	85	50	50
f	$Zn(BH_4)_2$	THF/Et_2O[b], -42 °C	52	52	48
g	CH_3Li	Et_2O, 0 °C	90	100	0
h	CH_3MgBr	Et_2O, 0 °C	93	100	0

[a] Determined by GC-MS

The relative stereochemistry assignments for the diastereomers are tentative, due to the fact that a solid derivative suitable for X-ray analysis of the secondary or tertiary alcohol was not possible to prepare. The relative stereochemistry of the diastereomeric secondary alcohols are based on a comparison with the ^1H NMR spectrum of the alcohols from the reduction of **129** and the compound formed from the treatment of epoxyalcohol **127** with boron trifluoride etherate (Figure 4.31).

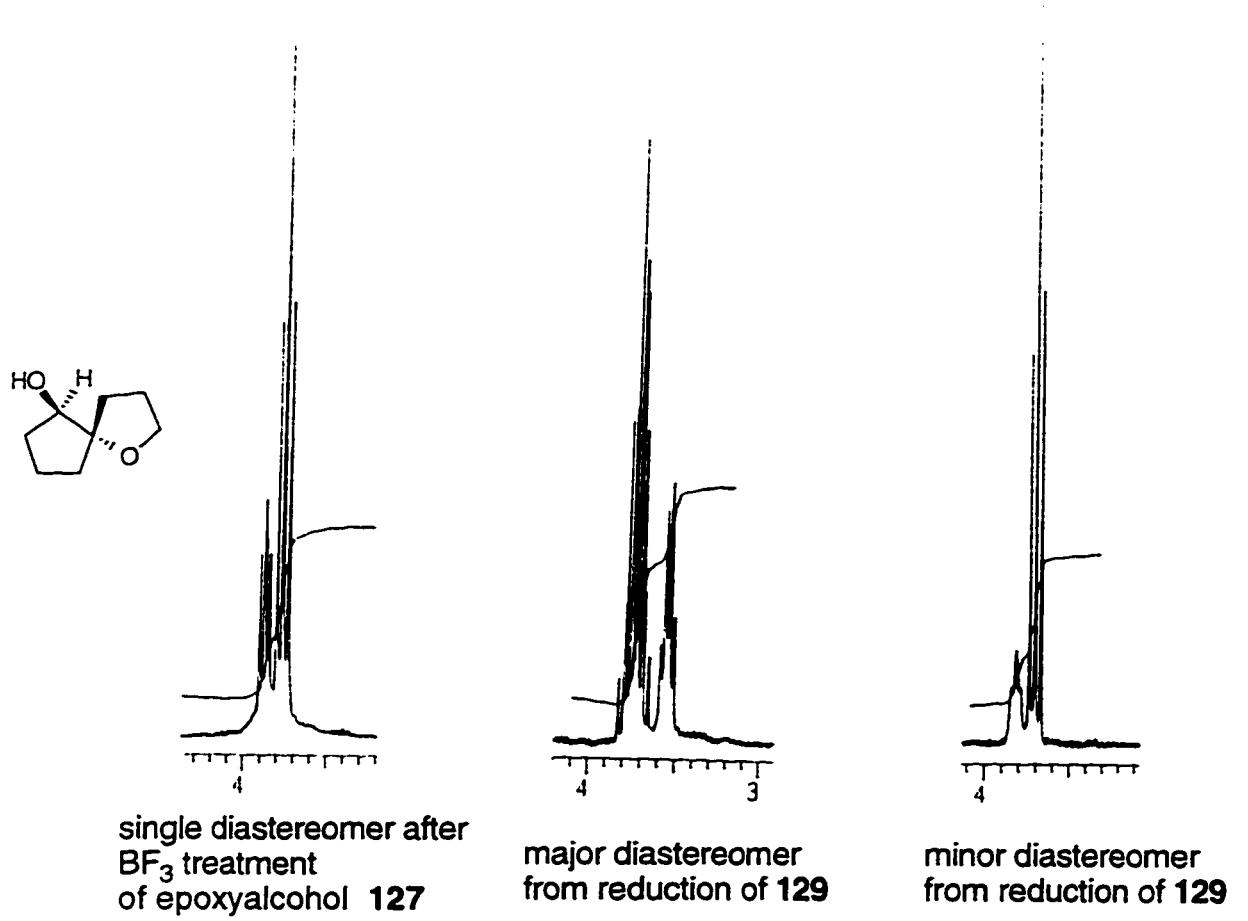

Figure 4.31 Comparison of the ^{1}H NMR spectra of the diastereomers from the reduction of ketone 129.

The signals shown in Figure 4.31 are due to the methylene hydrogens adjacent to the ether oxygen, as well as the hydrogen attached to the carbon bearing the hydroxyl group. The spectrum of the minor diastereomer from the reduction of ketone **129** matched that of the alcohol derived from epoxyalcohol **127**. The treatment of epoxyalcohol **127** with boron trifluoride etherate resulted in the formation of a single isomer, and most likely has its oxygen atoms in an *anti* arrangement as shown in Scheme 4.9. Based on the stereochemical assignments described above, all of the reducing agents examined added preferentially *syn* to the carbon-carbon bond of the tetrahydrofuran moiety, resulting in the anti-Cieplak product.

Reaction of ketone **129** with methyllithium and methylmagnesium bromide (entries g and h) each afforded a single diastereomer **134** with the same relative stereochemistry, based on a comparison of their ^{1}H and ^{13}C NMR spectra and GCMS retention times. The absence of a minor diastereomer from these reactions makes relative stereochemistry assignment difficult. The ^{1}H NMR signals of the diastereotopic hydrogen atoms of the methylene group adjacent to the ether oxygen of diastereomer **134** have very similar chemical shifts. This is also observed with the minor diastereomers formed from ketones **108** and **114**, and suggests that the addition of the methyl group to ketone **129** was also in an anti-Cieplak manner (Figure 4.32).

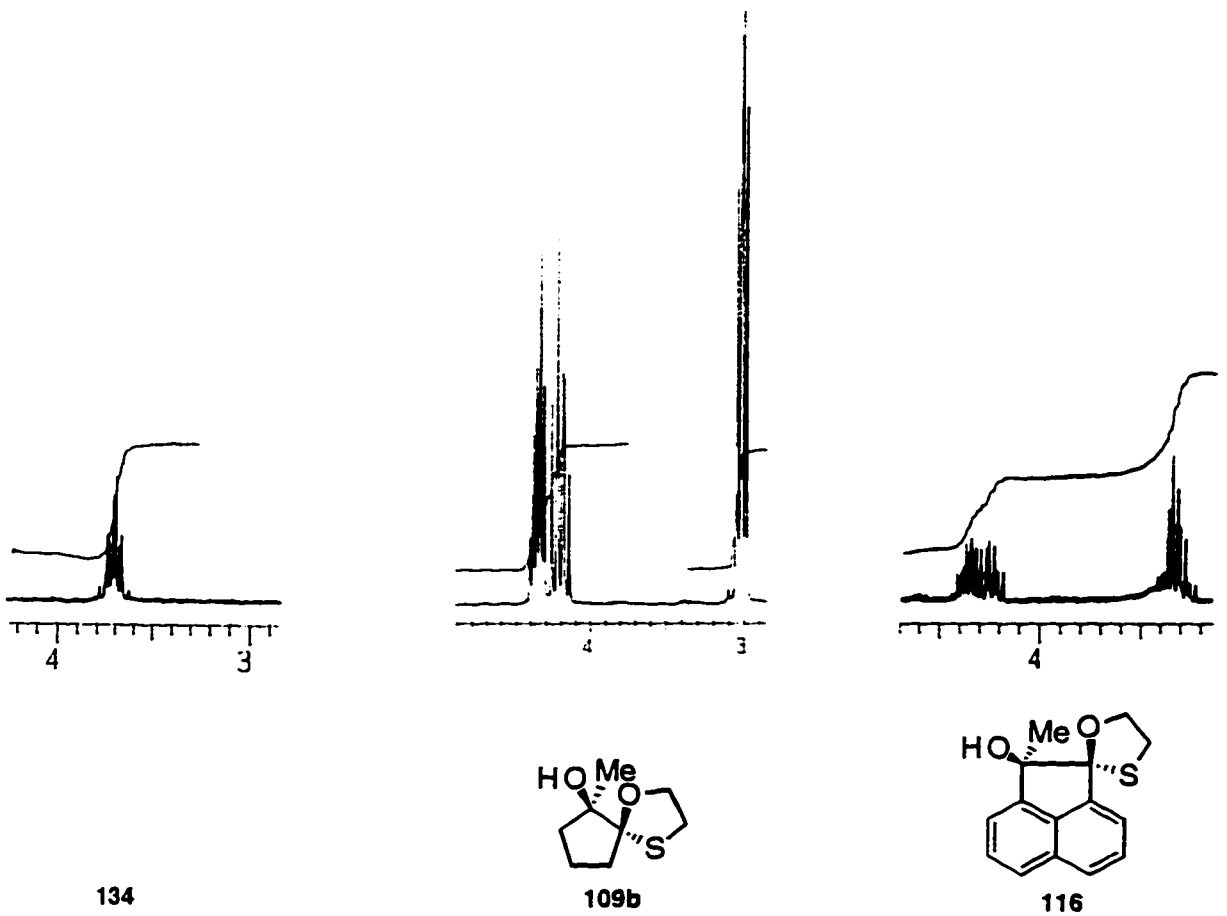

Figure 4.32 Comparison of ^{1}H NMR signals of alcohols 134, 109b and 116

4.6.3 π-Facial selectivity of tetrahydrothiophene 133

The reactions performed on ketone **129** were repeated with tetrahydrothiophene **133**. The results are summarized in Table 4.8.

Table 4.8 Nucleophilic Additions to Tetrahydrothiophene 133

133 **C** **D**

entry	reagent	conditions	yield	% C[a]	% D[a]
a	$NaBH_4$	MeOH, rt	89	89	11
b	$LiBH_4$	THF, rt	94	84	16
c	$Al(i\text{-}Bu)_2H$	CH_2Cl_2, -78 °C	81	95	5
d	$LiAlH_4$	Et_2O, 0 °C	81	100	0
e	$Zn(BH_4)_2$	Et_2O, rt	86	50	50
f	CH_3Li	Et_2O, 0 °C	87	100	0
g	CH_3MgBr	Et_2O, 0 °C	80	100	0

[a] Determined by GC-MS

The relative stereochemistry of alcohols **C** and **D** was again based on the same rationale as in the tetrahydrofuran case. As before, boron trifluoride etherate treatment of epoxythiol **131** produced a single diastereomer. This diastereomer had a relative stereochemistry that corresponded with the minor diastereomer formed upon reduction of tetrahydrothiophene **133**, based on a comparison of their ^1H NMR spectrum. The stereochemistry of the single diastereomer produced from organolithium or Grignard addition was tentatively assigned in the same manner as for tetrahydrofuran **129**, and indicated an *anti* relationship between the methyl group and the carbon-sulfur bond.

The selectivity of tetrahydrothiophene **133** followed the Cieplak model, although the fact that tetrahydrofuran **129** displayed anti-Cieplak selectivity suggests

that hyperconjugation is not the major factor in determining π-facial selectivity with ketones **129**.

Nucleophilic addition occured *anti* to the heteroatom for all the reagents examined with ketones **129** and **133** and may be a consequence of the attacking nucleophile simply avoiding the electron density associated with the lone pairs of the heteroatom. Based on AM1 calculations, the HOMO of ketones **129** and **133** are both associated with the heteroatom lone pairs and therefore, the four-electron destabilizing interaction between the ketone HOMO and a nucleophile HOMO may direct the nucleophile to approach the carbonyl π-face opposite to the heteroatom. This unfavourable interaction is also predicted by the electrostatic potential surfaces of ketones **129** and **133** (Figure 4.33).

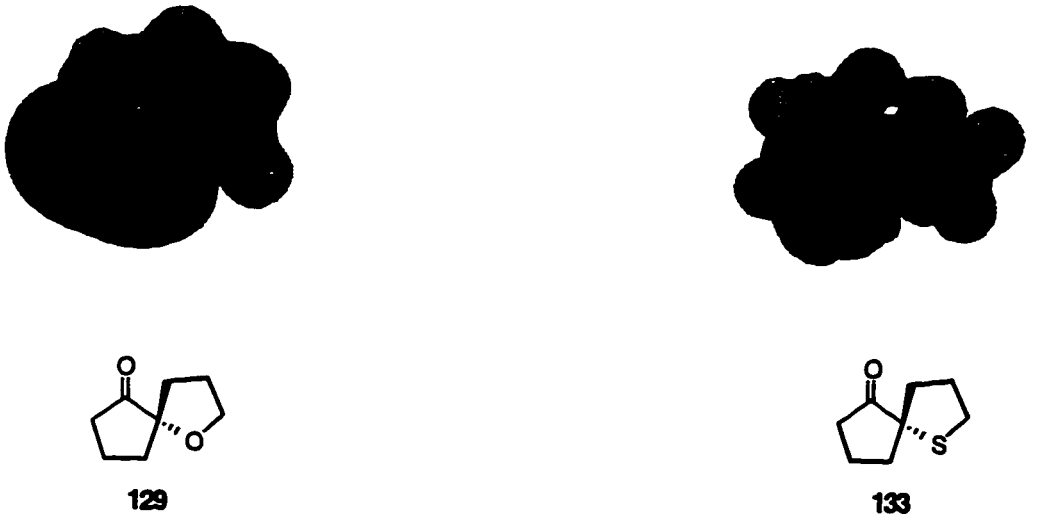

129 133

Figure 4.33 Electrostatic potential surfaces of ketones 129 and 133

4.6.4 Sulfur ylides

It is noteworthy that no reversal in π-facial selectivity is observed with ketones **129** and **133** after treatment with diisobutylaluminum hydride. The unusual behavior

of this reagent may be due to the lack of a metallic counterion. In this regard, dimethylsulfoxonium methylide was employed to determine if the absence of a metallic counterion effects π-facial selectivity. An attractive feature of the use of a methylide is the convenient determination of the resultant oxirane stereochemistry by conversion to the known tertiary alcohols (Scheme 4.11).

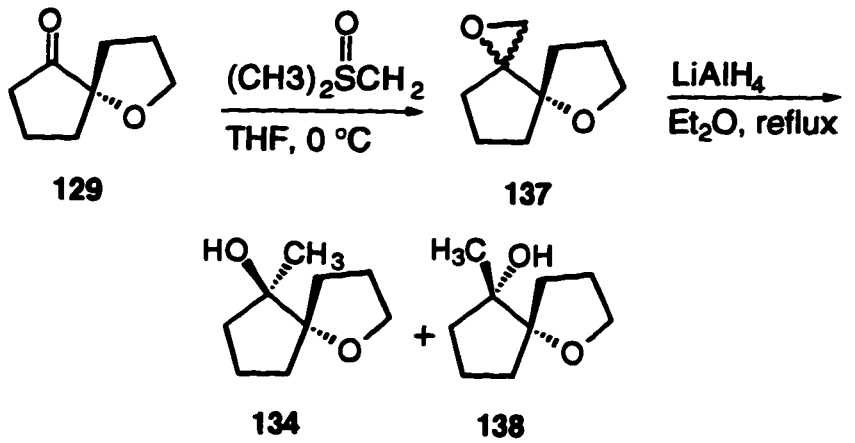

129 137 134 138

Scheme 4.11 Sulfur ylide addition to ketone 129

The oxiranes were prepared by treatment of ketones **129**, **108** and **114** with dimethylsulfoxonium methylide[52] in tetrahydrofuran at 0 °C. The resultant diastereomeric oxiranes were treated with lithium aluminum hydride in ether at reflux temperature to afford the corresponding tertiary alcohols. The results of these experiments are summarized below (Figure 4.34).

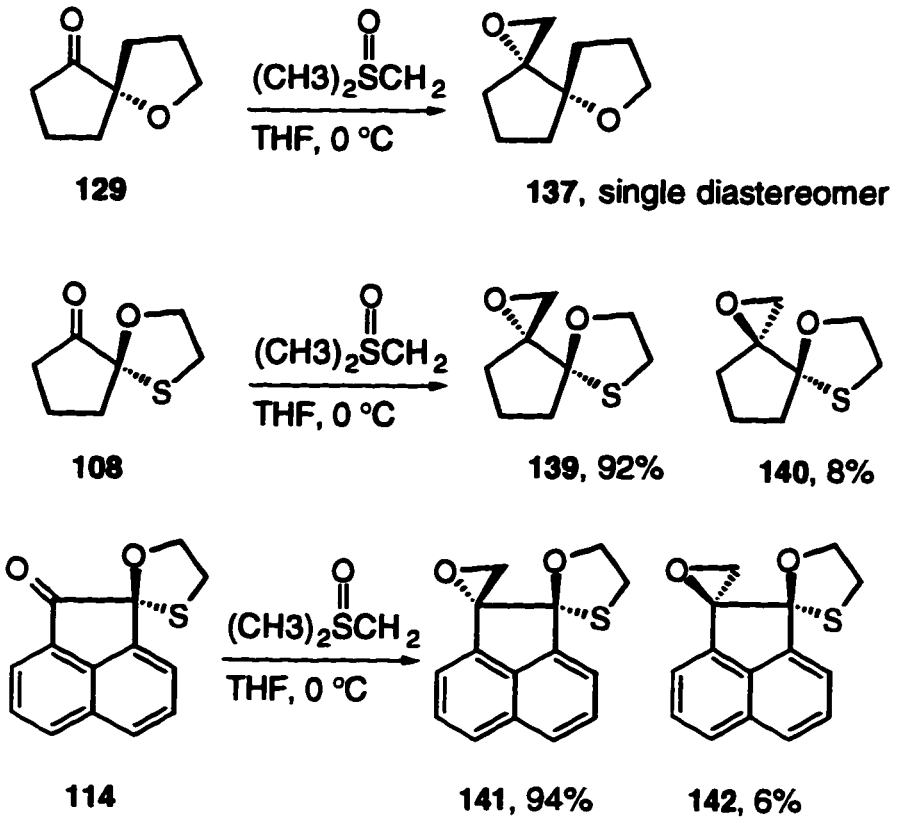

Figure 4.34 Sulfur ylide addition to ketones 129, 108 and 114

The percentages of the diastereomers were determined by GC-MS analysis of the crude reaction mixture after reduction of the oxiranes. There was no change in the π-facial selectivity of ketones **129**, **108** and **114** from reaction with the sulfur ylide as compared with the Grignard and organolithium reagents. Thus, the absense of a metal cation apparently does not effect the π-facial selectivity in the examples studied.

4.7 Conclusions

Some of the factors responsible for π-facial selectivity (*e.g.* sterics) in nucleophilic additions to carbonyl groups have long been understood. However, the electronic contribution made by substituents remains controversial. Indeed, it has been argued that the principle models used to predict π-facial selectivity are neither right nor wrong, but that the contribution that each makes varies from case to case.[17] This argument is most likely true, however the π-facial selectivity of the ketones examined was relatively independent of the reagent employed. The same major diastereomer resulted with either organometallic reagent tested, and the same diastereomer was produced preferentially with all the reducing agents examined (except for diisobutylaluminum hydride), despite the fact that a selection of sterically diverse reagents were used. This suggests that an electronic component responsible for directing the nucleophile is likely associated with the substrate. This does not preclude the possibility of the nucleophile playing a role in determining π-facial selectivity. The fact that different reagents give different levels of diastereomeric excess with the same substrate indicates that the reagent must also be considered. Unfortunately, no trends based on reagent characteristics, such as size of alkyl group, were observed. This severely limits any selectivity prediction based on type of reagent. This consistency unfortunately, was not observed when comparing the selectivity results between ketones subjected to reducing agents. Hydrides preferred to add to cyclopentanone **108** *anti* to the carbon-sulfur bond, while the reverse was true for napthalene **114**. There was also large differences in the behavior of tetrahydrofuran **129** and tetrahydrothiophene **133**. Replacement of the sulfur atom in cyclopentanone **108** with a carbon atom gave tetrahydrofuran **129**, to which all reagents examined added *anti* to the carbon-oxygen bond, in an anti-Cieplak fashion. The replacement of the ether oxygen atom of cyclopentanone **108**

to give the corresponding tetrahydrothiophene **133** continued to react with the reducing agents and organometallic reagents such that the Cieplak product was the major diastereomer.

The presence of a heteroatom in all the substrates studied complicates the interpretation of the results due to the possibility of complexation of the reagent by the heteroatom. The observed π-facial selectivity of tetrahydrofuran **129** and tetrahydrothiophene **133** suggests that complexation is not a major factor, as the resultant selectivity was *anti* to the ring heteroatom with all reagents, for both ketones. A complexed reagent may be expected to deliver the reagent *syn* to the heteroatom.

Possible reagent complexation notwithstanding, the oxathiolane group is an ideal group for testing the Cieplak model, due to the large differences in the σ donating ability between a carbon-sulfur bond and a carbon-oxygen bond. A criticism of the use of the Cieplak model in cyclohexanones is that the small difference in σ donating ability between carbon-carbon and carbon-hydrogen bonds is not expected to translate into large π-facial selectivity, as had been previously observed with cyclohexanones.[34] The failure of the Cieplak model to predict the major diastereomer in hydride reductions of napthalene **114** and tetrahydrofuran **129** suggests that hyperconjugative transition state stabilization from a σ bond into the $\sigma^{*\ddagger}$ orbital appears to be of minor importance in hydride reductions of these types of substrates. The Cieplak model may correctly predict the selectivity of nucleophilic addition to substrates containing carbon-carbon and carbon-hydrogen bonds, however, molecules that contain carbon-heteroatom bonds add a complexity that results in the failure of the Cieplak model in many of the examples presented. This is unfortunate, as many important molecules contain carbon-heteroatom bonds and a model that can predict selectivity, even if its basis is not fully understood, is useful.

Carbon nucleophiles preferred to add *anti* to the better σ donor in all cases except tetrahydrofuran **129** and thus, the Cieplak model seems to posses good predictive power with organometallic reagents. It would be of interest to determine whether the $\sigma^{*\ddagger}$ energy for these reactions varies greatly from that of the corresponding reduction reactions. The absence of a low-lying $\sigma^{*\ddagger}$ orbital may be the determining factor for some of the anti-Cieplak behavior observed.

The selectivity of tetrahydrofuran **129** is consistent with the electrostatic potential model, as removal of a heteroatom resulted in a sufficiently asymmetric electrostatic potential surface, and is apparently sufficient to dominate any transition state stabilization due to Cieplak hyperconjugation.

The prediction and rationalization of the outcome of reactions involving nucleophilic additions to carbonyl centres will undoubtedly continue due to the importance of such reactions. It is evident that the presense of one, or two, carbon-heteroatom bonds adjacent to a carbonyl group allows for a high level of diastereoselectivity, with some predictability. As the number of examples of diastereoselective reactions grows, a greater understanding of the interplay of electronic and steric factors results, and further insight is gained in this area of organic chemistry.

Chapter 4 References

1. Wigfield, D.C. *Tetrahedron* **1979**, *35*, 449.
2. Reetz, M. T.; Stanchev, S.; Haning, H. *Tetrahedron* **1992**, *48*, 6813.
3. Eliel, E. L.; Morris-Natschke, S *J. Am. Chem. Soc.* **1984**, *106*, 2937.
4. Amstutz, R.; Seiler, P.; Seebach, D.; Schweizer, B. Dunitz, J. D. *Angew. Chem., Int .Ed. Engl.* **1980**, *19*, 53.
5. Cram, D. J.; Kopecky, K. R. *J. Am. Chem. Soc.* **1959**, *81*, 2748.
6. Sonoda, S.; Houchigai, H.; Asaoka, M.; Takie, H. *Tetrahedron Lett.* **1992**, *33*, 3145.
7. Corey, E. J.; Boaz, N. W. *Tetrahedron Lett.* **1985**, *26*, 6015. Lewis acid catalyzed congugate addition of silyl ketene acetals to γ-oxygen cycloenones has been reported to occur *syn* to the silyl group: Danishefsky, S.J.; Simoneau, B. *J. Am. Chem. Soc.* **1989**, *111*, 2599.
8. Wilson, G. E., Jr.; Huang, M. G.; Schloman, W. W., Jr. *J. Org. Chem.* **1968**, *33*, 2133.
9. Bulman-Page, P. C.; Ley, S. V.; Morton, J. A.; Williams, D. J. *J. Chem. Soc., Perkin 1* **1981**, 457.
10. Allinger, N. L. *J. Am. Chem. Soc.* **1977**, *99*, 8127.
11. Dewar, M. J. S.; Zoebisch, E. G.; Healy, E. F.; Stewart, J. J. P. *J. Am. Chem. Soc.* **1985**, *107*, 3902.
12. Anh, N. T. *Top. Curr. Chem.* **1980**, *88*, 145.
13. Bondi, A. *J. Phys. Chem.* **1964**, *68*, 441.
14. CRC Handbook of Chemistry and Physics, 75th Edition, David R. Lide, Ed.; CRC Press: New York, 1995.
15. a) Brown, H. C.; Dickason, W. C. *J. Am. Chem. Soc.* **1970**, *92*, 709. b) Klein, J.; Dunkelblum, E.; Eliel, E. L.; Senda, Y. *Tetrahedron Lett.* **1968**,

6127. c) Brown, H. C.; Krishnamurthy, S. *J. Am. Chem. Soc.* **1972**, *94*, 7159. d) Lansbury, P. T.; MacLeay, R. E. *J. Org. Chem.* **1963**, *28*, 1940.

16. Collin, J.; Namy, J.-L.; Kagan, H. B. *Nouv. J. Chim.* **1986**, *10*, 229.
17. Li, H.; le Noble, W. J. *Recl. Trav. Chim. Pay-Bas* **1992**, *111*, 199.
18. a) Brown, H. C. *J. Org. Chem.* **1957**, *22*, 439. b) Wu, Y.-D.; Houk, K. N. *J. Am.Chem. Soc.* **1987**, *109*, 908
19. Cieplak, A. S. *J. Am. Chem. Soc.* **1981**, *103*, 4540.
20. a) Hehre, W. J.; Ditchfield, R.; Pople, J. A. *J. Chem. Phys.* **1972**, *56*, 2257. b) Hariharan, P. C.; Pople, J. A. *Chem. Phys. Lett.* **1972**, *66*, 217.
21. Hach, C. C.; Banks, C. V.; Diehl, H. *Org. Synth. IV.* **1963**, 229.
22. Wrobel, J.; Cook, J. M. *Synth. Commun.* **1980**, *10*, 333.
23. Cherest, M.; Felkin, H.; Prudent, N. *Tetrahedron Lett.* **1968**, 2199, 2205.
24. Maruoka, K.; Takayuki, I.; Yamamoto, H. *J. Am. Chem. Soc.* **1985**, *107*, 4573.
25. Imamoto, T.; Takiyama, N.; Nakamura, K.; Hatajima, T.; Kamiya, Y. *J. Am. Chem. Soc.* **1989**, *111*, 4392.
26. Utimoto, K.; Nakamura, A.; Matsubara, S. *J. Am. Chem. Soc.* **1990**, *112*, 8189.
27. Ashby, E. C. *Pure Appl. Chem.* **1980**, *52*, 545.
28. Liotta, C. L.; Burgess, E. M.; Eberhardt, W. H. *J. Am. Chem. Soc.* **1984**, *106*, 4849.
29. a) Adcock, W.; Cotton, J.; Trout, N. A. *J. Org. Chem.* **1994**, *59*, 1867. b) Hahn, J. M.; le Noble, W. J. *J. Am. Chem. Soc.* **1992**, *114*, 1916. c) Li, H.; Mehta, G.; Padma, S.; le Noble, W. J. *J. Org. Chem.* **1991**, *56*, 2007. d) Bodepudi, V.; le Noble, W. J. *J. Org. Chem.* **1991**, *56*, 2001. e) Chung, W. S.; Turro, N. J.; Srivastava, S.; Li, H.; le Noble, W. J. *J. Am. Chem. Soc.* **1988**, *110*, 7882.

30. Senda, Y.; Morita, M.; Itoh, H. *J. Chem. Soc., Perkin Trans. 2* **1996**, 221.

31. Gung, B. W.; Wolf, M. A. *J. Org. Chem.* **1996**, *61*, 232.

32. Laube, T.; Hollenstein, S. *J. Am. Chem. Soc.* **1992**, *114*, 8812.

33. a) Kelly, D. P.; Aherne, K.; Delgada, F.; Giansiracusa, J. T.; Jensen, W. A.; Karavokiros, R. A.; Mantello, R. A.; Reum, M. E. *J. Am. Chem. Soc.* **1993**, *115*, 12010. b) Laube, T.; Stiltz, H. U. *J. Am. Chem. Soc.* **1987**, *109*, 5876. c) ref. 31.

34. Wu, Y.-D.; Tucker, J. A.; Houk, K. N. *J. Am. Chem. Soc.* **1991**, *113*, 5018.

35. Macaulay, J. B.; Fallis, A. G. *J. Am. Chem. Soc.* **1990**, *112*, 1136.

36. a) Srivastava, S.; le Noble, W. J. *J. Am. Chem. Soc.* **1987**, *109*, 5874. b) Johnson, C. R.; Tait, B. D.; Cieplak, A. S. *J. Am. Chem. Soc.* **1987**, *109*, 5875.

37. Francis, M. B.; Gung, B. W. *Tetrahedron Lett.* **1995**, *36*, 2579.

38. a) Meyers, A. I.; Wallace, R. H. *J. Org. Chem.* **1989**, *54*, 2509. b) Meyers, A. I.; Romine, J. L.; Fleming, S. A. *J. Am. Chem. Soc.* **1988**, *110*, 7245.

39. Yadav, V.; Fallis, A. G. *Can. J. Chem.* **1991**, *69*, 779.

40. Fleming, I. *Frontier Orbitals and Organic Chemical Reactions*; Wiley: New York, 1976.

41. a) Coxon, J. M.; Luibrand, R. T. Tetrahedron Lett. 1993, 34, 7097. b) Kaselj, M.; Adcock, J. L.; Luo, H.; Zhang, H.; Li, H.; le Noble, W. J. *J. Am. Chem. Soc.* **1995**, *117*, 7088.

42. March, J. *Advanced Organic Chemistry, 3rd Edition*; Wiley: New York, 1981.

43. a) Politzer, P.; Landry, S. J. Warnheim, T. *J. Phys. Chem.* **1982**, *86*, 4767. b) Francl, M. M. *J. Phys. Chem.* **1985**, *89*, 428.

44. a) Kesura, G. M.; Kajtar-Peredy, M.; Naray-Szabo, G. *Tetrahedron Lett.* **1994**, *35*, 9255. b) Pudzianowski, A. T.; Barrish, J. C.; Spergel, S. H.

Tetrahedron Lett. **1992**, *33*, 293. c) Sjoberg, P.; Politzer, P. *J. Phys. Chem.* **1990**, *94*, 3959.

45. Wipf, P.; Kim, Y. *J. Am. Chem. Soc.* **1994**, *116*, 11678.
46. a) Shapiro, R. H.; Heath, M. J. *J. Am. Chem. Soc.* **1967**, *89*, 5734.
47. Prepared by the treatment of 3-bromopropanol with *tert*-butyldimethylchlorosilane, triethylamine and DMAP
48. Mancuso, A. J.; Huang, S.-L.; Swern, D. *J. Org. Chem.* **1978**, *43*, 2480.
49. All spectra data for ketone **129** was consistant with reported data employing an alternate synthesis: Paquette, L. A.; Negri, J. T.; Rogers, R. D. *J. Org. Chem.* **1992**, *57*, 3947.
50. Volante, R. P. *Tetrahedron Lett.* **1981**, *22*, 3119.
51. Dess, D. B.; Martin, J. C. *J. Org. Chem.* **1983**, *48*, 4155.
52. Dimethylsulfoxonium methylide was prepared according to Corey (Corey, E. J.; Chaykovsky, M. *J. Am. Chem. Soc.* **1965**, *87*, 1353.) and used as a 1 M solution in THF.

Experimental

General Considerations

All commercial starting materials were purchased from Aldrich Chemical Company unless stated otherwise. All reactions were carried out under an atmosphere of dry nitrogen or argon, unless stated otherwise, in oven-dried glassware equipped with a magnetic stirring bar and rubber septa. Standard inert atmosphere techniques were used in handling all air and/or moisture-sensitive compounds. 'Drying' during the work-up procedure refers to drying with anhydrous magnesium sulfate ($MgSO_4$). 'Concentration' during work-up refers to concentration *in vacuo* using a Buchi R110 Rotovapour, unless stated otherwise.

Petroleum ether refers to the fraction of light petroleum ether that distils between 40 and 60 °C and was redistilled prior to use. Tetrahydrofuran (THF) was dried over sodium/benzophenone and distilled under an atmosphere of dry nitrogen. Dichloromethane (CH_2Cl_2) was dried over calcium hydride and distilled under an atmosphere of dry nitrogen. Benzene and toluene were dried over sodium. All other solvents and reagents were purified by standard techniques or used as supplied. Brine refers to a saturated aqueous solution of sodium chloride.

Analytical thin layer chromatography (TLC) was performed on E. Merck Kieselgel 60 F_{254} aluminum-backed silica gel plates. Visualization was accomplished with ultraviolet light, iodine vapour, treatment with 2.5% ethanolic solution of *p*-anisaldehyde containing 3% aqueous H_2SO_4 (w/v) or a 5% solution of ammonium molybdate in 10% aqueous H_2SO_4 (w/v) and subsequent heating. Conventional (drip) and flash chromatography were performed with E. Merck silica gel 60 (70-230 and 230-400 mesh, respectively) or with E. Merck neutral alumina.

Optical rotations were recorded on an Perkin-Elmer 241 polarimeter operating at 589 nm.

Melting points were determined in capillary tubes with a Thomas-Hoover Uni-Melt apparatus and are uncorrected.

All Infrared (IR) spectra were recorded on a Bomem Michelson 100 Fourier transform or Perkin-Elmer 341 infrared spectrometers neat on sodium chloride plates or with chloroform solution cells unless stated otherwise.

Proton nuclear magnetic resonance (^{1}H NMR) spectra were recorded on Varian Gemini 200 (200 MHz), Varian XL-300 (300 MHz) and Bruker AMX500 (500 MHz) spectrometers. Carbon nuclear magnetic resonance (^{13}C NMR) spectra were recorded at 50 MHz (Varian Gemini 200), 75 MHz (Varian XL-300) and 125 MHz (Bruker AMX500). Residual non-dueterated $CDCl_3$ was used as an internal reference and all chemical shifts are quoted in parts per million downfield from tetramethylsilane. Coupling constants (*J*) are given hertz and signal splitting patterns are described as singlet (s), doublet (d), tripiet (t) and multiplet (m).

Gas chromatography (GC) was performed on a Varian 6000 gas chromatograph equipped with a 25 m x 0.25 mm i.d. silicone gum capillary column. Gas chromatography-mass spectrometry (GC-MS) was performed with a Hewlett Packard 5890 Series II gas chromatograph using a Hewlett Packard HP-1 (crosslinked methyl silicon gum, 12 m x 0.2 mm x 0.33 μm film thickness) capillary column connected to a Hewlett Packard 5971A mass selective detector. Low resolution mass spectroscopy (LRMS) was performed on a V.G. Micromass 7070 HS mass spectrometer with an electron beam energy of 70 eV (electron impact ionization). High resolution mass spectroscopy (HRMS) was performed on a Kratos Concept-IIA mass spectrometer with an electron beam energy of 70 eV.

Microanalyses were performed at M-H-W Laboratories, Phoenix, Arizona, USA or were performed in-house.

Computational studies were performed on Apple Power Macintosh 8100/100 and Silicon Graphics Indigo^2 computers using CAChe MOPAC 6.02 and Wavefuction Spartan SGI V 4.0.4 GL software packages, respectively.

Experimental Concerning Chapter 2

6-Methoxy-1,3-benzoxathiol-2-one (25)

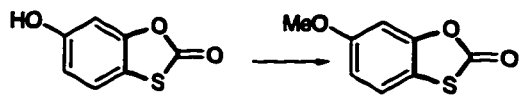

24 25

6-Hydroxy-1,3-benzoxathiol-2-one (11.0 g, 65.8 mmol), after drying under high vacuum (3 hours, 0.1 Torr), was dissolved in tetrahydrofuran (120 mL) and added dropwise to a stirred tetrahydrofuran (50 mL) suspension of sodium hydride (3.0 g, 85% dispersion , 0.11 mol) under argon maintained at 0 °C. After 1 hour, iodomethane (15.0 g, 105 mmol) was added, and the mixture heated to reflux for 45 minutes. The reaction was cooled, quenched by dropwise addition of acetic acid, concentrated *in vacuo*, water added (200 mL), and the organic phase extracted with ether (3 x 50 mL). The combined organic extracts were dried, filtered, concentrated *in vacuo* and the product purified by crystallization from ether-hexane (1:1) to give methyl ether **25** as thick needles (9.6 g, 81%); mp 63-64 °C; IR ($CHCl_3$, cm^{-1}) 1750, 1605, 1275, 1025; ^1H NMR (200 MHz, $CDCl_3$) δ 7.23 (d, J = 8.6 Hz, 1H, H- Ar), 6.84 (d, J = 2.2 Hz, 1H, H-Ar), 6.80 (dd, J = 8.6, 2.2 Hz, 1H, H-Ar), 3.79 (s, 3H, CH_3-O); ^{13}C NMR (50 MHz, $CDCl_3$) δ 169.8, 159.9, 149.9, 122.6, 113.3, 111.9, 98.4, 55.6, HRMS Calcd for $C_8H_6O_3S$ (M^+): 182.0037, Found 182.0040.

6-Methoxy-1,3-benzoxathiol-2-(*Z*)-(carbomethoxy)-ene (26)

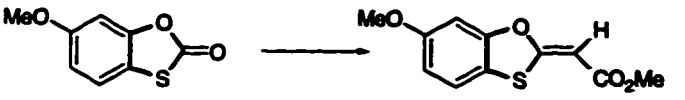

25 26

The methoxy derivative **25** (2.11 g, 11.6 mmol) was dissolved in dry toluene (150 mL), methyl (triphenylphosphoranylidene)acetate (5.01 g, 15.0 mmol) added and the reaction heated to reflux under argon for 30 hours. The reaction was cooled, filtered, and the filtrate concentrated *in vacuo* and purified by flash chromatrography on silica gel (dichloromethane). Combination of the pure fractions, concentration and crystallization from ether resulted in ester **26** as wool-like needles (2.0 g, 73%); mp 156-157 °C; IR ($CHCl_3$, cm^{-1}) 1677, 1571, 1347, 1194; ^1H NMR (200 MHz, $CDCl_3$) δ 7.25 (d, J = 8.6 Hz, 1H, H-Ar), 6.76 (d, J = 2.2 Hz, H-Ar), 6.72 (dd, J = 8.6, 2.2 Hz, H-Ar), 5.83 (s, 1H, H-C=), 3.79 (s, 3H, CH_3-O), 3.75 (s, 3H, CH_3-O); ^{13}C NMR (50 MHz, $CDCl_3$) δ 172.9, 168.7, 159.6, 153.2, 121.8, 115.1, 110.9, 97.8, 88.4, 55.6, 51.2; HRMS Calcd for $C_{11}H_{10}O_4S$ (M^+): 238.0299, Found 238.0302; Anal. Calcd for $C_{11}H_{10}O_4S$: C, 55.45; H, 4.23; S, 13.46. Found: C, 55.30; H, 4.17; S, 13.59.

6-Methoxy-1,3-benzoxathiol-2-(*E*)-(carbomethoxy)-ene (55)

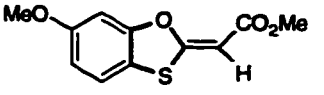

55

The minor isomer of the above reaction was isolated as thick needles (0.63 g, 4.0%); mp 156-157 °C; IR ($CHCl_3$, cm^{-1}) 1685, 1580, 1270, 1150; ^1H NMR (200 MHz, $CDCl_3$) δ 6.96 (d, J = 8.6 Hz, 1H, H-Ar), 6.69 (d, J = 2.2 Hz, H-Ar), 6.54 (dd, J

= 8.6, 2.2 Hz, H-Ar), 5.13 (s, 1H, H-C=), 3.58 (s, 3H, CH_3-O), 3.54 (s, 3H, CH_3-O); ^{13}C NMR (50 MHz, $CDCl_3$) δ 168.6, 164.0, 159.2, 154.5, 121.0, 111.9, 110.9, 97.9, 87.8, 55.1 50.3; HRMS Calcd for $C_{11}H_{10}O_4S$ (M+): 238.0299, Found 238.0289.

Dimethyl 2-bromomalonate (38)

$CH_2(CO_2Me)_2$ (37) ⟶ $Br\text{-}CH(CO_2Me)_2$ (38)

A tetrahydrofuran solution of dimethyl malonate (**37**, 132 g, 1.00 mol) under argon at room temperature was treated with *N*-bromosuccinamide (178 g, 1.00 mol) followed by *p*-toluenesulfonic acid (0.5 g, 2.6 mmol). Stirring was continued for 14 hours at which time the mixture was heated to reflux for 14 hours. After cooling and concentration the residue was distilled under vacuum (0.8 Torr) resulting in pure diester **38** as a colourless liquid (20 g, 9.3%) bp 89-99 °C, 0.8 Torr; ^1H NMR (200 MHz, $CDCl_3$) δ 4.83 (s, 1H, H-C-Br), 3.80 (s, 6H, CH_3-O); ^{13}C NMR (50 MHz, $CDCl_3$) δ 165.1, 53.9, 41.4.

Dimethyl (triphenylphosphoranylidene)malonate (35)

$CH_2(CO_2Me)_2$ (37) ⟶ $Ph_3P{=}C(CO_2Me)_2$ (35)

A cooled (0 °C) solution of benzene (400 mL) containing triphenylphosphine (60.0 g, 229 mmol) was treated slowly with bromine (38.4 g, 0.240 mmol in 150 mL carbon tetrachloride. To this solution was added a solution of triethylamine (65 g, 0.64 mol) in benzene (200 mL) followed by dimethyl malonate (30.2 g, 229 mmol). Stirring was continued for 1 hour at room temperature and then the reaction mixture was heated gently under reflux for 20 minutes. After concentration, the residue was

recrystallized from tetrahydrofuran : hexane (5:1) to give ylide **35** as yellow prisms (32 g, 36%) mp 180-182 °C; ^{1}H NMR (200 MHz, $CDCl_3$) δ 7.68 (m, 6H, H-Ar), 7.47 (m, 9H, H-Ar), 3.29 (s, 6H, methyl); ^{13}C NMR (50 MHz, $CDCl_3$) δ 168.6, 133.4, 133.2, 131.9, 131.8, 128.7, 128.4, 127.3, 125.4, 50.0; LRMS Calcd for $C_{23}H_{21}O_4P$ (M^+): 392, Found 392.

2-Hydroxy-4-methoxyphenyl disulfide (42)

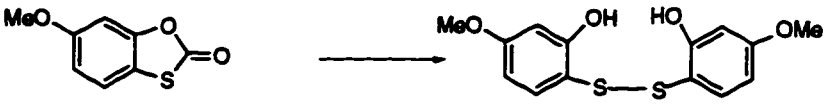

25 **42**

A tetrahydrofuran solution (50 mL) of dimethyl malonate (4.40 g, 33.3 mmol) under argon was cooled to 10 °C and treated with sodium amide (1.5 g, 38 mmol) in portions over a 5 minute period. After 15 minutes of stirring, oxathiolane **25** (1.5 g, 8.2 mmol) was added in portions. Stirring was continued for 30 minutes followed by careful addition of a saturated aqueous ammonium chloride solution. The mixture was heated under reflux for 15 minutes, cooled, diluted with ethyl acetate/hexane (100 mL, 1:1), washed with water (50 mL), brine (50 mL), dried and concentrated *in vacuo*. The residue was purified by silica gel chromatography (50% diethyl ether in hexane) to give the disulfide **42** as a yellow solid which crystallized from diethyl ether : hexane (1:1) resulting in yellow prisms (1.0 g, 80%) mp 92-93 °C; IR ($CHCl_3$, cm^{-1}) 3456, 1605, 1572, 1332, 1248; ^{1}H NMR (200 MHz, $CDCl_3$) δ 7.09 (d, J = 8.6 Hz, 1H, H-Ar), 6.52 (d, J = 2.7 Hz, 1H, H-Ar), 6.39 (dd, J = 8.6, 2.7 Hz, 1H, H-Ar), 6.31 (s, 1H, H-O), 3.78 (s, 3H, CH_3-O); ^{13}C NMR (50 MHz, $CDCl_3$) δ , 164.0, 158.5, 137.4, 111.2, 108.1, 100.4, 55.4; LRMS Calcd for $C_{14}H_{114}O_4S_2$ (M^+): 310, Found 310.

6-Methoxy-1,3-benzoxathiol-2-(*Z*)-(carbomethoxy)-ene-*S*-oxide (46)

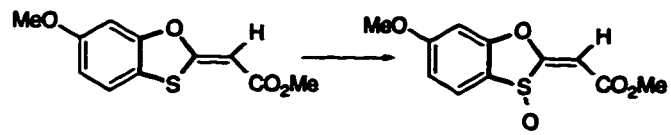

26 46

A dichloromethane solution (100 mL) of sulfide **26** (1.83 g, 7.69 mmol) was cooled to 0 °C and portions of *m*-chloroperbenzoic acid (3.0 g, 9.6 mmol, 55%) added over 15 minutes. After 25 minutes, a 5% aqueous sodium thiosulphate solution (50 mL) was added and the mixture stirred for 30 minutes. After separation of the organic layer, washing with 5% sodium bicarbonate (3 x 50 mL) and water (100 mL), the solution was dried, concentrated *in vacuo* and the residue chromatographed on silica gel (eluted with 100% dichloromethane to 100% diethyl ether). The resultant white solid was recrystallized from ether to give sulfoxide **46** as plates (1.2 g, 62%) mp 171-172 °C; IR ($CHCl_3$, cm^{-1}) 1720, 1600, 1440, 1330; ^1H NMR (200 MHz, $CDCl_3$) δ 7.75 (d, J = 8.6 Hz, 1H, H-Ar), 6.79 (dd, J = 8.6, 2.2 Hz, 1H, H-Ar), 6.68 (d, J = 2.2 Hz, 1H, H-Ar), 6.21 (s, 1H, H-C=), 3.85 (s, CH_3-O, 3H), 3.84 (s, 3H, CH_3-O); ^{13}C NMR (50 MHz, $CDCl_3$) δ 172.7, 165.4, 165.1, 157.2, 128.6, 119.5, 112.1, 104.7, 97.8, 55.9, 52.4; HRMS Calcd for $C_{11}H_{10}O_5S$ (M^+): 254.0249, Found 254.0229; Anal. Calcd for $C_{11}H_{10}O_5S$: C, 51.96; H, 3.96; S, 12.61. Found: C, 51.87; H, 4.18; S, 12.73.

6-Methoxy-1,3-benzoxathiol-2-(*Z*)-(carbomethoxy)-ene-(*S*)-*S*-oxide (+)-46

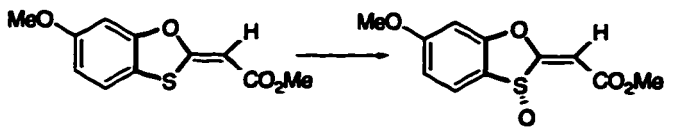

26 (+)-46

Diisopropyl-(L)-tartrate (7.42 mL, 35.3 mmol) was dissolved in dichloromethane (150 mL) at room temperature and treated with titanium(IV) isopropoxide (5.26 mL, 17.6 mmol) followed immediately by water (0.32 mL, 17.7 mmol). After stirring for 30 minutes under argon, sulfide **26** (4.20 g, 17.6 mmol), dissolved in dichloromethane (100 mL), was added and the mixture stirred for an additional 10 minutes. The reaction was cooled to 0 °C and after 5 minutes, cumene hydroperoxide (6.5 mL, 35 mmol, 80% solution) was added *via* syringe over 5 minutes. Stirring was continued for 2 hours at 0 °C, 17 hours at room temperature and the reaction mixture placed directly on a silica gel column and successively eluted with dichloromethane, 30% ether in dichloromethane and finally 100% ether to give the sulfoxide **(+)-46** (4.3 g, 96%). Crystallization from methanol gave the pure enantiomer (3.30 g, 74%); $[\alpha]_D^{22}$ = +497° (c = 2.8, $CHCl_3$), ee ≥ 99% (^1H NMR with Europium(III) tris[3-(heptafluoropropylhydroxymethylene)-(+)-camphorato]); mp 171-172 °C; IR ($CHCl_3$, cm^{-1}) 1720, 1600, 1440, 1330, 1070; ^1H NMR (200 MHz, $CDCl_3$) δ 7.75 (d, *J* = 8.6 Hz, 1H, H-Ar), 6.79 (dd, *J* = 8.6, 2.2 Hz, 1H, H-Ar), 6.68 (d, *J* = 2.2 Hz, 1H, H-Ar), 6.21 (s, 1H, H-C=C), 3.85 (s, 3H), 3.84 (s, 3H); ^{13}C NMR (50 MHz, $CDCl_3$) δ 172.7, 165.4, 165.1, 157.2, 128.6, 119.5, 112.1, 104.7, 97.8, 55.9, 52.4; HRMS Calcd for $C_{11}H_{10}O_5S$ (M^+): 254.0249, Found 254.0229; Anal. Calcd for $C_{11}H_{10}O_5S$: C, 51.96; H, 3.96; S, 12.61. Found: C, 51.87; H, 4.18; S, 12.73.

6-Methoxy-1,3-benzoxathiol-2-(*E*)-(carbomethoxy)-ene-*S*-oxide (56)

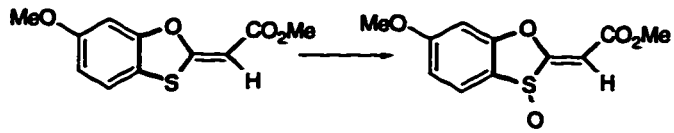

55 56

A dichloromethane solution (20 mL) of sulfide **55** (504 mg, 2.12 mmol) was cooled to 0 °C and *m*-chloroperbenzoic acid (733 mg, 2.33 mmol, 55%) added. After 25 minutes, a 5% aqueous sodium thiosulphate solution (50 mL) was added and the mixture stirred for 30 minutes. After separation of the organic layer and washing with 5% aqueous sodium bicarbonate solution (3 x 50 mL) and water (50 mL), the solution was dried, concentrated *in vacuo* and the residue chromatographed on silica gel (20% diethyl ether in dichloromethane). The resultant white solid was recrystallized from ether to give sulfoxide **56** as colourless plates (0.25 g, 46%) mp 138-140 °C; IR ($CHCl_3$, cm^{-1}) 1710, 1595, 1430, 1270; ^1H NMR (200 MHz, $CDCl_3$) δ 7.69 (d, J = 8.6 Hz, 1H, H-Ar), 6.79 (dd, J = 8.6, 2.2 Hz, 1H, H-Ar), 6.77 (d, J = 2.2 Hz, 1H, H-Ar), 6.04 (s, 1H, H-C=), 3.81 (s, CH_3-O, 3H), 3.76 (s, 3H, CH_3-O); ^{13}C NMR (50 MHz, $CDCl_3$) δ 170.5 165.8, 163.2, 159.1 128.4 118.3, 112.7, 104.5, 98.2, 56.0, 52.0; HRMS Calcd for $C_{11}H_{10}O_5S$ (M^+): 254.0249, Found 254.0234.

*Thermal Diels-Alder Reaction of Sulfoxide **46** with Cyclopentadiene:*

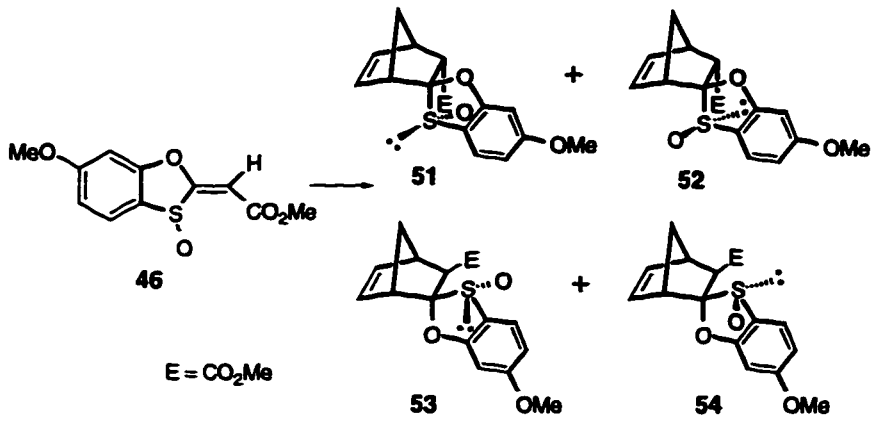

A *m*-xylene solution (120 mL) of sulfoxide **46** (3.70 g, 14.6 mmol) and cyclopentadiene (2.0 g, 30 mmol) under argon was refluxed for 15 hours. The reaction mixture was cooled, concentrated *in vacuo* and chromatographed on silica gel (2% to 10% diethyl ether in dichloromethane) and resulted in the isolation of four cycloadducts (98% combined):

(1*S, 2*R**, 3*R**, 4*R**)-3-Carbomethoxybicyclo[2.2.1]hept-5-ene-2-one 2'-hydroxy-3'-mercaptoanisyl-(*S**)-*S*-oxide acetal (51)**

crystallized from methanol as prisms (1.4 g, 44%) mp 165-166 °C; IR ($CHCl_3$, cm^{-1}) 1740, 1605, 1485, 1335, 1070; ^1H NMR (500 MHz, $CDCl_3$) δ 7.66 (d, *J* = 8.6 Hz, 1H, H-Ar), 6.77 (dd, *J* = 5.6, 3.1 Hz, 1H, H-C=C), 6.68 (dd, *J* = 8.6, 2.3 Hz, H-Ar), 6.65 (d, *J* = 2.3 Hz, 1H, H-Ar), 6.03 (dd, *J* = 5.6, 3.2 Hz, 1H, H-C=C), 3.83 (s, 3H, CH_3-O), 3.64 (s, 3H, CH_3-O-C=O), 3.56 (d, *J* = 3.1 Hz, 1H, H-C-C=O), 3.22 (br s, 1H, H-C bridgehead), 2.52 (br s, 1H, H-C bridgehead), 1.97 (br d, *J* = 9.1 Hz, 1H, H-C bridge *anti*), 1.82 br dd, *J* = 9.1, 3.4 Hz, H-C bridge *syn*); ^{13}C NMR (75 MHz, $CDCl_3$) δ 171.3, 165.2, 160.2, 139.8, 130.8, 128.4, 122.2, 116.7, 110.7, 97.8, 55.7,

52.2, 51.8, 51.2, 48.4, 45.4; HRMS Calcd for $C_{16}H_{16}O_5S$ (M^+): 320.0718, Found 320.0707; Anal. Calcd for $C_{16}H_{16}O_5S$: C, 59.99; H, 5.03; S, 10.01. Found: C, 59.95; H, 5.15; S, 10.02.

(1*S, 2*R**, 3*R**, 4*R**)-3-Carbomethoxybicyclo[2.2.1]hept-5-ene-2-one 2'-hydroxy-3'-mercaptoanisyl-(*R**)-*S*-oxide acetal (52)**

colourless oil (1.2 g, 25%) IR ($CHCl_3$, cm^{-1}) 1740, 1600, 1485, 1290, 1075; ^1H NMR (300 MHz, $CDCl_3$) δ 7.59 (d, *J* = 8.6 Hz, 1H, H-Ar), 6.61 (d, *J* = 2.3 Hz, 1H, H-Ar), 6.56 (d, *J* = 2.3 Hz, H-Ar), 6.50 (dd, *J* = 5.5, 3.1 Hz, 1H, H-C=C), 6.45 (dd, *J* = 5.2, 3.1 Hz, 1H, H-C=C), 3.79 (s, 3H, CH_3-O), 3.47 (br s, 1H, H-C bridgehead), 3.43 (br s, 3H, CH_3-O-C=O), 3.26 (br s, 1H, H-C bridgehead), 3.17 (d, *J* = 3.3 Hz, 1H, H-C-C=O), 2.01 (br d, *J* = 9.2 Hz, 1H, H-C bridge *anti*), 1.87 (br d, *J* = 9.2, Hz, H-C bridge *syn*); ^{13}C NMR (75 MHz, $CDCl_3$) δ 169.9, 165.1, 160.9, 139.3, 134.1, 127.4, 122.6, 117.3, 110.1, 97.6, 58.4, 55.7, 51.6, 49.8, 45.9, 44.8; HRMS Calcd for $C_{16}H_{16}O_5S$ (M^+): 320.0718, Found 320.0671.

(1*S, 2*S**, 3*S**, 4*R**)-3-Carbomethoxybicyclo[2.2.1]hept-5-ene-2-one 2'-hydroxy-3'-mercaptoanisyl-(*R**)-*S*-oxide acetal (53)**

colourless oil (1.0 g, 23%) IR ($CHCl_3$, cm^{-1}) 1740, 1610, 1485, 1290, 1070; ^1H NMR (500 MHz, $CDCl_3$) δ 7.67 (d, *J* = 8.6 Hz, 1H, H-Ar), 6.65 (dd, *J* = 8.6, 2.2 Hz, 1H, H-Ar), 6.62 (dd, *J* = 5.5, 3.1 Hz, 1H, H-C=C) 6.55 (d, *J* = 2.2 Hz, H-Ar), 6.07 (dd, *J* = 5.4, 3.1 Hz, 1H, H-C=C), 3.78 (s, 3H, CH_3-O), 3.68 (s, 3H, CH_3-O-C=O) 3.17 (br s, 1H, H-C bridgehead), 2.84 (d, *J* = 3.1 Hz, 1H, H-C-C=O), 2.68 (br d, *J* = 10 Hz, 1H, H-C bridge *anti*) 2.58 (br s, 1H, H-C bridgehead), 1.76 (br d, *J* = 9.2, Hz, H-C bridge *syn*); ^{13}C NMR (75 MHz, $CDCl_3$) δ 172.2, 165.1, 162.0, 140.4, 134.0, 128.2, 122.7, 114.7, 110.5, 97.5, 55.7, 52.5, 50.9, 48.1, 47.0, 46.2; HRMS Calcd for $C_{16}H_{16}O_5S$ (M^+): 320.0718, Found 320.0688.

(1*S, 2*S**, 3*S**, 4*R**)-3-Carbomethoxybicyclo[2.2.1]hept-5-ene-2-one 2'-hydroxy-3'-mercaptoanisyl-(*S**)-*S*-oxide acetal (54)**

crystallized as prisms from ether (0.30 g, 6.4%) mp 239-241 °C; IR ($CHCl_3$, cm^{-1}) 1735, 1600, 1480, 1290, 1160; ^1H NMR (500 MHz, $CDCl_3$) δ 7.64 (d, J = 8.6 Hz, 1H, H-Ar), 6.64 (dd, J = 8.6, 2.3 Hz, 1H, H-Ar), 6.57 (dd, J = 5.6, 3.1 Hz, 1H, H-C=C) 6.51 (d, J = 2.3 Hz, H-Ar), 6.37 (dd, J = 5.6, 3.1 Hz, 1H, H-C=C), 3.80 (s, 3H, CH_3-O), 3.51 (s, 3H, CH_3-O-C=O) 3.67 (br s, 1H, H-C bridgehead), 3.35 (br s, 1H, H-C bridgehead), 2.51 (d, J = 3.2 Hz, 1H, H-C-C=O), 2.10 (br d, J = 10.2 Hz, 1H, H-C bridge *anti*), 1.84 (br ddd, J = 10.2, 3.5, 3.4 Hz, H-C bridge *syn*); ^{13}C NMR (75 MHz, $CDCl_3$) δ 171.4, 165.5, 162.2, 140.0, 134.6, 127.7, 121.2, 114.8, 110.6, 97.3, 56.6, 55.6, 51.6, 48.1, 46.4, 45.5; HRMS Calcd for $C_{16}H_{16}O_5S$ (M^+): 320.0718, Found 320.0673.

General Procedure for $ZnCl_2$ and $SnCl_2$ Catalyzed Diels-Alder reactions:

A slight excess of the Lewis acid was added to a dry benzene solution (30 mL) containing the sulfoxide **46** under argon at room temperature. After stirring for 1 hour, cyclopentadiene was added and the reaction continued for the indicated time and temperature The reaction mixture was then diluted with benzene (50 mL), washed with saturated aqueous sodium bicarbonate (3 x 50 mL), water (2 x 50 mL), brine (2 x 50 mL), dried and concentrated *in vacuo*. To remove polymeric material, the crude product was purified on a short silica gel column eluted with 10% tetrahydrofuran in dichloromethane. All chemically pure fractions were combined and concentrated *in vacuo* to give a white solid, recrystallized from diethyl ether, to give adducts **51** and **53** as determined by ^1H NMR and GC-MS.

Following the general procedure, sulfoxide xx (677 mg, 2.67 mmol) in benzene (30 mL) under argon at room temperature was treated with $ZnCl_2$ (409 mg, 3.00 mmol). After stirring for 1 hour, the mixture was cooled to 0 °C and cyclopentadiene (308 mg, 4.67 mmol) was added and stirring continued for 18 hours. After purification, a mixture of adducts **51** and **53** (0.83 g, 98%) were isolated in a ratio of 2.6:1, respectively.

Following the general procedure, sulfoxide **46** (0.11 g, 0.44 mmol) in dichloromethane (30 mL) under argon at room temperature was treated with zinc chloride (69 mg, 0.50 mmol). After stirring for 1 hour, the mixture was cooled to 0 °C and cyclopentadiene (59 mg, 0.89 mmol) was added and stirring continued for 38 hours. After purification, a mixture of adducts **51** and **53** (0.14 mg, 97%) were isolated in a ratio of 3.1:1, respectively.

Following the general procedure, sulfoxide **46** (77 mg, 0.30 mmol) in dichloromethane (25 mL) under argon at room temperature was treated with zinc chloride (45 mg, 0.33 mmol). After stirring for 15 minutes, the mixture was cooled to -78 °C and cyclopentadiene (46 mg, 0.70 mmol) was added and stirring continued for 5 hours. Monitoring the reaction by NMR and TLC indicated no reaction and hence, the reaction was allowed to warm to room temperature overnight. After purification, a mixture of adducts **51** and **53** (47 mg, 94%) was isolated in a ratio of 3.1:1, respectively.

*Other Lewis Acid Catalyzed Diels-Alder Reactions of **46** with Cyclopentadiene*

A dichloromethane solution (25 mL) of sulfoxide **46** (0.12 g, 0.47 mmol) at -78 °C under argon was added to a solution composed of a mixture of diethylaluminum chloride (1.5 mL, 0.29 M, 0.43 mmol) in dichloromethane and titanium(IV) chloride

(64 μL, 0.34 M, 0.02 mmol) in dichloromethane under argon at -78 °C. Cyclopentadiene (0.33 g, 5.0 mmol) was added and the mixture stirred at -78 °C for 19 hours. The mixture was allowed to warm to room temperature over 5 hours, followed by purification by silica gel chromatography (25% diethyl ether in dichloromethane) to result in a mixture of adducts **51** and **53** (0.13 g, 87%) in a ratio of 2.5:1, respectively.

Boron trichloride (0.36 mL, 1.0 M, 0.36 mmol) was added to a cold (-78 °C) dichloromethane solution (20 mL) of sulfoxide **46** (93 mg, 0.37 mmol). Cyclopentadiene (0.27 g, 4.1 mmol) was added and the reaction stirred at -78 °C for 5 hours. The solution was washed with 5% aqueous sodium bicarbonate (3 x 50 mL), water (2 x 50 mL), dried, concentrated *in vacuo* and chromatographed on silica gel (25% diethyl ether in dichloromethane) to give a single Diels-Alder adduct **51** (0.14 g, 88%) by ^{1}H NMR.

Following the procedure described above for the boron trichloride-catalyzed Diels-Alder reaction, optically active sulfoxide **(+)-46** (0.87 g, 3.4 mmol) in dichloromethane (150 mL) at -78 °C was treated with boron trichloride (3.4 mL, 1.0 M, 3.4 mmol) followed by cyclopentadiene (2.7 g, 41 mmol) after 15 minutes of stirring. After stirring at -78 °C for 16 hours, the reaction was worked up and purified to afford **(+)-52** as a colourless oil (843 mg, 77%); $[\alpha]_D^{22}$ = +102° (c = 1.7, $CHCl_3$), ee ≥ 99% (^{1}H NMR with Europium(III) tris[3-(heptafluoropropylhydroxymethylene)-(+)-camphorato]); IR ($CHCl_3$, cm^{-1}) 1740, 1600, 1485, 1290, 1075; ^{1}H NMR (300 MHz, $CDCl_3$) δ 7.59 (d, *J* = 8.6 Hz, 1H, H-Ar), 6.61 (d, *J* = 2.3 Hz, 1H, H-Ar), 6.56 (d, *J* = 2.3 Hz, H-Ar), 6.50 (dd, *J* = 5.5, 3.1 Hz, 1H, H-C=C), 6.45 (dd, *J* = 5.2, 3.1 Hz, 1H, H-C=C), 3.79 (s, 3H, CH_3-O), 3.47 (br s, 1H, H-C bridgehead), 3.43 (br s, 3H, CH_3-O-C=O), 3.26 (br s, 1H, H-C bridgehead), 3.17 (d, *J* = 3.3 Hz, 1H, H-C-C=O),

2.01 (br d, J = 9.2 Hz, 1H, H-C bridge *anti*), 1.87 (br d, J = 9.2, Hz, H-C bridge *syn*); ^{13}C NMR (75 MHz, $CDCl_3$) δ 169.9, 165.1, 160.9, 139.3, 134.1, 127.4, 122.6, 117.3, 110.1, 97.6, 58.4, 55.7, 51.6, 49.8, 45.9, 44.8; HRMS Calcd for $C_{16}H_{16}O_5S$ (M^+): 320.0718, Found 320.0695

(1*S, 2*R**, 3*R**, 4*R**)-3-Carbomethoxybicyclo[2.2.1]hept-5-ene-2-one 2'-hydroxy-3'-mercaptoanisyl acetal (73)**

The sulfoxide **51** (689 mg, 2.15 mmol) was dissolved in dichloromethane (30 mL) and dry pyridine (0.81 mL, 9.9 mmol) was added. The solution was cooled to 10 °C and phenyl phosphorodichloridate (1.5 mL, 10 mmol) added dropwise. After 45 minutes, dichloromethane (100 mL) was added and the solution washed with sat. sodium bicarbonate, (25 mL), brine (50 mL), water (2 x 50 mL), dried, concentrated *in vacuo* and chromatographed (100% benzene) to afford oxathiolane **73** crystallized from methanol as prisms (0.63 g, 96%) mp 64-65 °C; IR ($CHCl_3$, cm^{-1}) 1725, 1600 1475, 1340, 1150; ^1H NMR (300 MHz, $CDCl_3$) δ 6.92 (d, J = 8.7 Hz, 1H, H-Ar), 6.58 (dd, J = 5.6, 3.0 Hz, 1H, H-C=C), 6.45 (d, J = 2.4 Hz, H-Ar), 6.43 (dd, J = 8.7, 2.4 Hz, 1H, H-Ar), 6.16 (dd, J = 5.6, 3.4 Hz, 1H, H-C=C), 3.75 (s, 3H, CH_3-O), 3.61 (s, 3H, CH_3-O-C=O), 3.50 (d, J = 3.1 Hz, 1H, H-C-C=O), 3.25 (br s, 1H, H-C bridgehead), 3.11 (br s, 1H, H-C bridgehead), 1.93 (br d, J = 9.1 Hz, 1H, H-C bridge *anti*), 1.74 (br d, J = 9.1, Hz, H-C bridge *syn*); ^{13}C NMR (75 MHz, $CDCl_3$) δ 172.3, 158.8, 155.9, 140.4, 132.5, 121.3, 117.2, 108.0, 107.5, 97.8, 60.3, 55.5, 54.4, 51.5, 46.6, 44.8;

HRMS Calcd for $C_{16}H_{16}O_4S$ (M^+): 304.0769, Found 304.0776; Anal. Calcd for $C_{16}H_{16}O_4S$: C, 63.16; H, 5.26. Found: C, 63.01; H, 5.15.

Following the procedure for sulfoxide reduction described above, optically active sulfoxide **(+)-46** (747 mg, 2.33 mmol) was dissolved in dichloromethane (30 mL), dry pyridine (0.85 mL, 10 mmol) was added and the solution cooled to 10 °C. Following the addition of phenyl phosphorodichloridate (1.5 mL, 10 mmol), the mixture was stirred for 45 minutes and diluted with dichloromethane (100 mL). The mixture was purified to afford a white solid (713 mg). Recrystallization from methanol afforded **(+)-73** as fine needles (0.63 g, 89%); $[\alpha]_D^{22}$ = +77° (c = 2.0, $CHCl_3$), ee ≥ 99% (^{1}H NMR with Europium(III) tris[3-(heptafluoropropylhydroxymethylene)-(+)-camphorato]); IR ($CHCl_3$, cm^{-1}) 1725, 1600 1475, 1340, 1150; ^{1}H NMR (300 MHz, $CDCl_3$) δ 6.90 (d, *J* = 8.7 Hz, 1H, H-Ar), 6.58 (dd, *J* = 5.6, 3.0 Hz, 1H, H-C=C), 6.47 (d, *J* = 2.4 Hz, H-Ar), 6.44 (dd, *J* = 8.7, 2.4 Hz, 1H, H-Ar), 6.16 (dd, *J* = 5.6, 3.4 Hz, 1H, H-C=C), 3.75 (s, 3H, CH_3-O), 3.59 (s, 3H, CH_3-O-C=O), 3.51 (d, *J* = 3.1 Hz, 1H, H-C-C=O), 3.25 (br s, 1H, H-C bridgehead), 3.15 (br s, 1H, H-C bridgehead), 1.93 (br d, *J* = 9.1 Hz, 1H, H-C bridge *anti*), 1.73 (br d, *J* = 9.1, Hz, H-C bridge *syn*); ^{13}C NMR (75 MHz, $CDCl_3$) δ 172.3, 158.8, 155.9, 140.4, 132.5, 121.3, 117.2, 108.0, 107.5, 97.8, 60.3, 55.5, 54.4, 51.5, 46.6, 44.8; HRMS Calcd for $C_{16}H_{16}O_4S$ (M^+): 304.0769, Found 304.0701; Anal. Calcd for $C_{16}H_{16}O_4S$: C, 63.16; H, 5.26. Found: C, 63.29; H, 5.09.

Alternative I_2 Method:

The sulfoxide **46** (1.09 g, 3.41 mmol) was dissolved in dichloromethane (30 mL) and triphenylphosphine (2.0 g, 7.4 mmol) was added. The solution was refluxed under argon for 1 hour and a crystal of iodine (*ca.* 5 mg) added. After refluxing for 20 hours, the mixture was cooled, concentrated *in vacuo* and purified by silica gel

chromatography (100% benzene). The combined fractions were concentrated *in vacuo* to give oxathiolane **73** (0.96 g, 93%) as a white solid.

(1*S, 2*S**, 3*S**, 4*R**)-3-Carbomethoxybicyclo[2.2.1]hept-5-ene-2-one 2'-hydroxy-3'-mercaptoanisyl-(*R**)-*S*-(*p*-toluensulfonimidyl) acetal (74)**

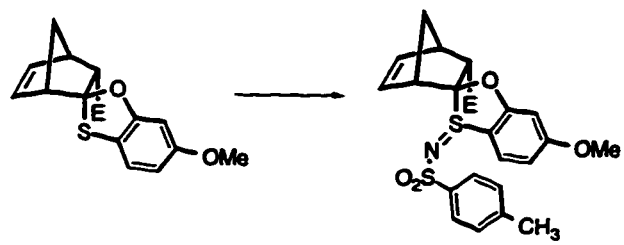

73 **74**

Norbornene **73** (89 mg, 0.29 mmol) was dissolved in methanol (5 mL) and Chloroamine-T (180 mg, 0.64 mmol) in a methanol : water (1:1, 2 mL total) solution was added in one portion. The reaction was stirred for 15 minutes at room temperature and sodium sulfite (200 mg, 1.58 mmol) was added. After 15 minutes of stirring, the reaction mixture was concentrated *in vacuo*. The residue was dissolved in benzene and washed with saturated aqueous sodium bicarbonate (50 mL), water (25 mL), dried, concentrated *in vacuo* and filtered through silica gel (eluted with dichloromethane) to give the sulfinylimine **74** (113 mg, 82%) mp 180-184 °C (dec.); IR ($CHCl_3$, cm^{-1}) 1730, 1600 1480, 1315, 1155, 1135, 955; ^1H NMR (200 MHz, $CDCl_3$) δ 7.67 (d, J = 8.1 Hz, 2H), 7.20 (m, 2H), 7.01 (d, J = 9.2 Hz, 1H), 6.52 (m, 3H), 6.35 (dd, J = 5.7, 3.3 Hz, 1H, H-C=C), 3.77 (s, 3H, CH_3-O), 3.75 (br s, 1H), 3.52 (s, 3H, CH_3-O-C=O), 3.31 (br s, 1H), 3.18 (d, J = 3.3 Hz, 1H), 2.35 (s, 3H, CH_3-Ar), 2.05 (br d, J = 9.6 Hz, 1H), 1.90 (br d, J = 9.6 Hz, 1H); ^{13}C NMR (50 MHz, $CDCl_3$) δ 169.4, 165.4, 161.1, 142.1, 141.7, 141.0, 132.2, 129.2, 129.2, 126.5,126.1, 126.1,

116.1, 114.5, 111.2, 98.0, 60.4, 55.7, 52.2, 49.7, 45.7, 45.3, 21.2; HRMS Calcd for $C_{23}H_{23}O_6NS_2$ (M^+): 473.0967, Found 473.1005.

3-Carbomethoxybicyclo[2.2.1]hept-5-ene-2-one (75 and 76)

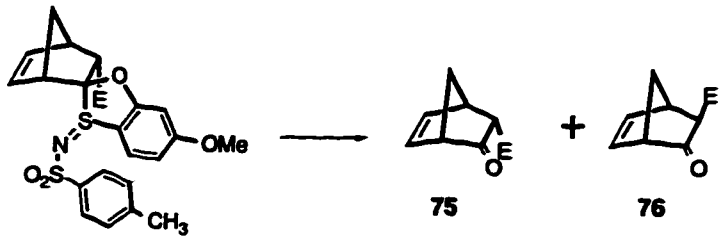

A tetrahydrofuran solution (10 mL) of sulfinylimine **74** (281 mg, 0.59 mmol) containing water (1 mL) and acetic acid (1 mL) was stirred at room temperature for 14 h. The mixture was diluted with benzene (50 mL), washed with water (2 x50 mL), dried and concentrated *in vacuo* to give a mixture of the keto esters **75** and **76** (94 mg, 95%) in a 3:2 ratio as determined by ^1H NMR. Complete separation of the keto esters by silica gel chromatography (3% ethyl acetate in petroleum ether) was not possible.

***endo* adduct: (1*S**, 3*S**, 4*R**)-3-Carbomethoxybicyclo[2.2.1]hept-5-ene-2-one (75)**

colourless oil (56 mg, 60%); IR (neat, cm^{-1}) 2997, 2953, 1760, 1729, 1317, 1129; ^1H NMR (200 MHz, $CDCl_3$) δ 6.70 (dd, J = 5.5, 2.7 Hz, 1H, H-C=C), 5.99 (dd, J = 4.4, 3.4 Hz, 1H, H-C=C), 3.63 (s, 3H, CH_3-O), 3.26 (br s, 1H, H-C bridgehead), 3.10 (br s, 1H, H-C bridgehead), 3.09 (d, J = 3.1 Hz, 1H, H-C-C=O), 2.06 (br d, J = 9.5 Hz, 1H, H-C bridge *anti*), 1.86 (d, J = 9.5 Hz, 1H, H-C bridge *syn*); ^{13}C NMR (50

MHz, $CDCl_3$) δ , 204.8, 169.1, 142.3, 128.4, 55.7, 52.9, 52.1, 47.9, 42.6; HRMS Calcd for $C_9H_{10}O_3$ (M^+): 166.0629, Found 166.0623.

exo adduct: (1*S, 3*R**, 4*R**)-3-Carbomethoxybicyclo[2.2.1]hept-5-ene-2-one (76)**

colourless oil (38 mg, 40%); IR (neat, cm^{-1}) 2995, 2955, 1760, 1730, 1315, 1130; ^1H NMR (200 MHz, $CDCl_3$) δ 6.52 (dd, J = 5.6, 2.9 Hz, 1H, H-C=C), 6.16 (dd, J = 4.4, 3.2 Hz, 1H, H-C=C), 3.66 (s, 3H, CH_3-O), 3.39 (br s, 1H, H-C bridgehead), 3.02 (br s, 1H, H-C bridgehead), 2.81 (d, J = 3.7 Hz, 1H, H-C-C=O), 2.42 (br d, J = 9.9 Hz, 1H, H-C bridge *syn*), 2.13 (d, J = 9.9 Hz, 1H, H-C bridge *anti*); ^{13}C NMR (50 MHz, $CDCl_3$) δ , 207.3, 169.4, 142.5, 133.2, 54.8, 52.3, 50.3, 47.9, 43.9; HRMS Calcd for $C_9H_{10}O_3$ (M^+): 166.0629, Found 166.0634.

*Thermal Diels-Alder Reactions of E-sulfoxide **56** with Cyclopentadiene*

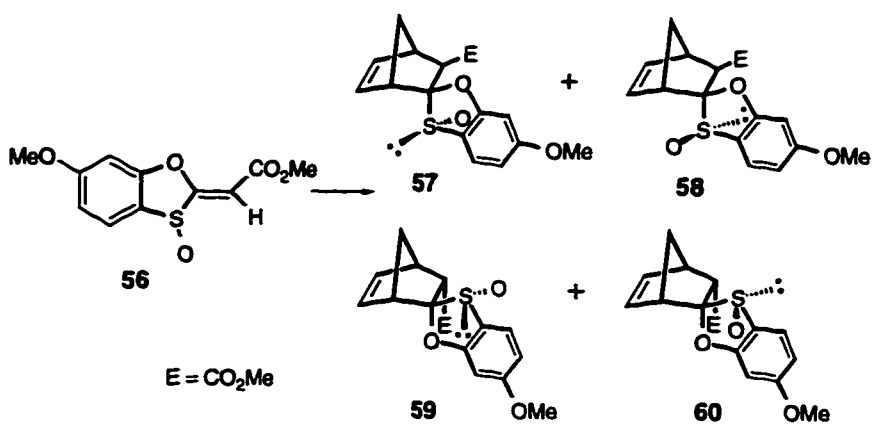

A *m*-xylene solution (15 mL) of sulfoxide **56** (128 mg, 0.506 mmol) and cyclopentadiene (53 mg, 0.8 mmol) under argon was stirred for 2 hours at room temperature and then refluxed for 14 hours. The reaction mixture was cooled, concentrated *in vacuo* and chromatographed on silica gel (20% diethyl ether in

dichloromethane) and resulted in the isolation of four Diels-Alder adducts (122 mg, 95%):

(1*S, 2*R**, 3*S**, 4*R**)-3-Carbomethoxybicyclo[2.2.1]hept-5-ene-2-one 2'-hydroxy-3'-mercaptoanisyl-(*S**)-*S*-oxide acetal (57)**

crystallized as prisms from ether (61.2 mg, 50.1%) mp 179-180 °C; IR ($CHCl_3$, cm^{-1}) 1740, 1600, 1585, 1330, 1150, 1080; ^1H NMR (300 MHz, $CDCl_3$) δ 7.68 (d, *J* = 8.7 Hz, 1H, H-Ar), 6.67 (dd, *J* = 8.7, 2.3 Hz, 1H, H-Ar), 6.54 (d, *J* = 2.3 Hz, H-Ar) 6.47 (dd, *J* = 5.8, 3.4 Hz, 1H, H-C=C) , 6.16 (dd, *J* = 5.8, 3.1 Hz, 1H, H-C=C), 3.80 (s, 3H, CH_3-O), 3.63 (s, 3H, CH_3-O-C=O) 3.49 (d, *J* = 2.4 Hz, 1H, H-C-C=O) 3.31 (br s, 1H, H-C bridgehead), 2.67 (br s, 1H, H-C bridgehead), 2.48 (br d, *J* = 9.3 Hz, H-C bridge *syn*), 2.00 (br ddd, *J* = 9.3, 4.0, 1.6 Hz, 1H, H-C bridge *anti*); ^{13}C NMR (75 MHz, $CDCl_3$) δ 170.8, 165.2, 161.2, 140.7, 134.4, 128.8, 120.4, 115.5, 110.8, 97.3, 55.8, 52.2, 49.6, 48.7, 45.5, 44.2; HRMS Calcd for $C_{16}H_{16}O_5S$ (M^+): 320.0718, Found 320.0707.

(1*S, 2*R**, 3*S**, 4*R**)-3-Carbomethoxybicyclo[2.2.1]hept-5-ene-2-one 2'-hydroxy-3'-mercaptoanisyl-(*R**)-*S*-oxide acetal (58)**

colourless oil (5.9 mg, 4.9%) mp 179-180 °C; IR (neat cm^{-1}) 1735, 1605, 1585, 1320, 1150, 1075; ^1H NMR (300 MHz, $CDCl_3$) δ 7.66 (d, *J* = 8.7 Hz, 1H, H-Ar), 6.66 (dd, *J* = 8.7, 2.3 Hz, 1H, H-Ar), 6.56 (d, *J* = 2.3 Hz, H-Ar) 6.40 (dd, *J* = 5.8, 3.4 Hz, 1H, H-C=C) , 6.13 (dd, *J* = 5.8, 3.1 Hz, 1H, H-C=C), 3.80 (s, 3H, CH_3-O), 3.30 (s, 3H, CH_3-O-C=O), 2.83 (d, *J* = 2.4 Hz, 1H, H-C-C=O) 3.42 (br s, 1H, H-C bridgehead), 3.34 (br s, 1H, H-C bridgehead), 2.40 (br d, *J* = 10 Hz, H-C bridge *syn*), 1.97 (br d, *J* = 10 Hz, 1H, H-C bridge *anti*); ^{13}C NMR (75 MHz, $CDCl_3$) δ 171.2, 165.3, 161.2, 145.7, 129.4, 127.9, 120.1, 115.9, 112.8, 97.8, 55.0, 51.2, 50.3, 49.9, 45.9, 44.7; HRMS Calcd for $C_{16}H_{16}O_5S$ (M^+): 320.0718, Found 320.0737.

(1*S, 2*S**, 3*R**, 4*R**)-3-Carbomethoxybicyclo[2.2.1]hept-5-ene-2-one 2'-hydroxy-3'-mercaptoanisyl-(*R**)-*S*-oxide acetal (59)**

colourless oil (36.1 mg, 29.6%); IR (neat, cm^{-1}) 1738, 1600, 1580, 1325, 1150, 1070; ^1H NMR (300 MHz, $CDCl_3$) δ 7.72 (d, *J* = 8.6 Hz, 1H, H-Ar), 6.85 (dd, *J* = 5.5, 3.1 Hz, 1H, H-C=C), 6.68 (dd, *J* = 8.6, 2.2 Hz, 1H, H-Ar), 6.11 (dd, *J* = 5.5, 3.2 Hz, 1H, H-C=C), 4.12 (d, *J* = 3.4 Hz, 1H, H-C-C=O), 3.79 (s, 3H, CH_3-O), 3.58 (s, 3H, CH_3-O-C=O) 3.29 (br s, 1H, H-C bridgehead), 2.96 (br s, 1H, H-C bridgehead), 1.76 (br s, 2H, H-C bridge); ^{13}C NMR (75 MHz, $CDCl_3$) δ 170.1, 165.3, 161.8, 140.8, 130.5, 128.9, 119.9, 115.1, 110.7, 97.1, 55.7, 52.0, 49.0, 48.2, 46.2, 45.1; HRMS Calcd for $C_{16}H_{16}O_5S$ (M^+): 320.0718, Found 320.0706.

(1*S, 2*R**, 3*R**, 4*R**)-3-Carbomethoxybicyclo[2.2.1]hept-5-ene-2-one 2'-hydroxy-3'-mercaptoanisyl-(*S**)-*S*-oxide acetal (60)**

crystallized as needles from ether (11 mg, 9.7%) mp 109-111 °C; IR ($CHCl_3$, cm^{-1}) 1735, 1600, 1290, 1155 1080, 1030; ^1H NMR (300 MHz, $CDCl_3$) δ 7.71 (d, *J* = 8.6 Hz, 1H, H-Ar), 6.66 (dd, *J* = 8.7, 2.3 Hz, 1H, H-Ar), 6.43 (d, *J* = 2.3 Hz, H-Ar) 6.77 (dd, *J* = 5.6, 3.0 Hz, 1H, H-C=C) , 6.28 (dd, *J* = 5.6, 3.3 Hz, 1H, H-C=C), 3.80 (s, 3H, CH_3-O), 3.75 (br s, 1H, H-C bridgehead), 3.36 (br s, 1H, H-C bridgehead), 3.25 (s, 3H, CH_3-O-C=O), 2.83 (d, *J* = 2.4 Hz, 1H, H-C-C=O), 1.79 (br d, *J* = 9.4 Hz, H-C bridge *syn*), 1.75 (br dd, *J* = 9.4, 3.5 Hz, 1H, H-C bridge *anti*); ^{13}C NMR (75 MHz, $CDCl_3$) δ 169.1, 165.4, 163.1, 140.3, 131.6, 128.5, 120.7, 114.2, 110.5, 96.6, 55.7, 54.2, 51.4, 47.2, 46.1, 46.1; HRMS Calcd for $C_{16}H_{16}O_5S$ (M^+): 320.0718, Found 320.0722.

(1 *R*, 4 *R*)-Bicyclo[2.2.1]hept-5-ene-2-one [(+)-77]

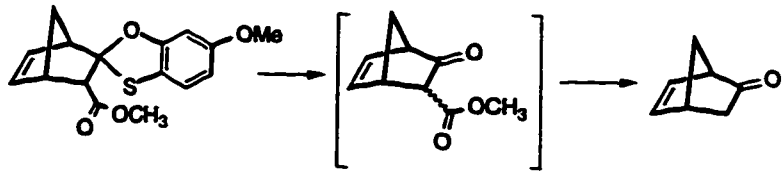

(+)-73 (+)-77

Norbornene **(+)-73** (633 mg, 2.08 mmol) was dissolved in methanol (20 mL) and Chloroamine-T solution (1.0 g, 4.4 mmol) in 2 mL of a MeOH:H_2O (1:1) solution was added in one portion. The reaction was stirred for 15 minutes at room temperature, solid sodium sulfite (650 mg, 5.2 mmol) added, and after 15 minutes of stirring, the reaction mixture was concentrated *in vacuo*. The residue was dissolved in tetrahydrofuran (30 mL) containing water (3 mL) and acetic acid (3 mL) and stirred at room temperature for 14 hours. The mixture was diluted with benzene (100 mL), washed with water (2 x50 mL), dried and concentrated *in vacuo* to give a mixture of the keto esters **75** and **76** in a 3:2 ratio as determined by ^{1}H NMR. The crude residue was dissolved in acetonitrile (30 mL) and treated with chlorotrimethylsilane (325 mg, 3.0 mmol), stirred at room temperature for 15 minutes and sodium iodide (0.45 mg, 3.0 mmol) was added. The solution was refluxed for 3 hours and water (5 ml) was added *via* syringe. After refluxing for a further 2 hours, the solution was cooled and the mixture concentrated carefully at atmospheric pressure. The residue was dissolved in ether, extracted with ether (3 x 30 mL) and the combined organic layers washed with saturated aqueous sodium bicarbonate (50 mL), water (50 mL) and brine (50 mL). After drying, the mixture was carefully concentrated i*n vacuo* (50 Torr, room temperature) and further purified by Kugelrohr distillation (25 Torr) at a temperature setting of 75 °C to afford norbornenone **(+)-77** as a colourless oil (108 mg, 48%); $[\alpha]_D^{22}$ = +893° (c = 1.9, $CHCl_3$); IR ($CHCl_3$, cm^{-1}) 1760, 1600, 1465, 1050; ^{1}H NMR (200 MHz, $CDCl_3$) δ 6.48 (dd, *J* = 5.6, 2.8 Hz, 1H, H-C=C), 6.03 (ddd,

J = 5.6, 4.2, 0.8 Hz, H-C=C), 3.10 (b s, 1H, H-C bridgehead), 2.92 (br s, 1H, H-C bridgehead), 2.10 (br m, 1H), 1.95-1.65 (br m, 3H); ^{13}C NMR (50 MHz, $CDCl_3$) δ 215.6, 143.0, 130.5, 55.8, 50.9, 40.0, 37.2; LRMS Calcd for C_7H_8O (M^+): 108 , Found 108.

(*RS*)-Bicyclo[2.2.1]hept-5-ene-2-one (77)

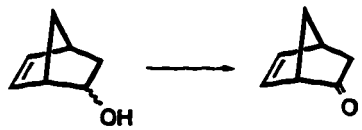

77

5-norbornen-2-ol (5.0 g, 40 mmol, mixture of *endo* and *exo*) was dissolved in dichloromethane (200 mL) at room temperature and treated with pyridinium dichromate (17 g, 45 mmol). The mixture was stirred for five days at room temperature, filtered through a short silica gel column and further purified by silica gel chromatohraphy (3% ethyl acetate in petroleum ether) to give ketone **77** as a colourless oil (1.1 g, 22%); IR ($CHCl_3$, cm-1) 1760, 1600, 1465, 1050; ^1H NMR (200 MHz, $CDCl_3$) δ 6.48 (dd, J = 5.6, 2.8 Hz, 1H, H-C=C), 6.03 (ddd, J = 5.6, 4.2, 0.8 Hz, H-C=C), 3.10 (b s, 1H, H-C bridgehead), 2.92 (br s, 1H, H-C bridgehead), 2.10 (br m, 1H), 1.95-1.65 (br m, 3H); ^{13}C NMR (50 MHz, $CDCl_3$) δ 215.6, 143.0, 130.5, 55.8, 50.9, 40.0, 37.2; LRMS Calcd for C_7H_8O (M^+): 108 , Found 108.

Experimental concerning Chapter 4

(*RS*)-1-Oxa-4-thiaspiro[4.5]decan-6-one (97)

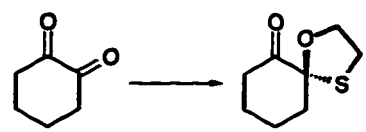

94 97

A mixture of 1,2-cyclohexanedione (5.0 g, 44 mmol), 2-mercaptoethanol (3.1 mL, 44 mmol) and *p*-toluenesulfonic acid (1.0 g, 4.4 mmol) in benzene (100 mL) was heated to reflux under a Dean-Stark apparatus. After 15 hours, the dark red solution was washed with a 10% aqueous sodium hydroxide solution and the aqueous phase extracted with ether (2 x 50 mL). The combined organic phases were washed with water (50 mL), brine (50 mL) and dried. Concentration of the resultant solution *in vacuo* followed by silica gel chromatography (33% ether in petroleum ether) gave **97** as a colourless oil (2.7 g, 36%); IR (neat, cm^{-1}) 2945, 1718, 1440, 911, 732; ^1H NMR (200 MHz, $CDCl_3$) δ 4.41-4.30 (m, H-C-O, 1H), 4.30-4.12 (m, H-C-O, 1H), 3.05-2.95 (m, H-C-S, 2H), 2.80-1.50 (series of m, 8H); ^{13}C NMR (50 MHz, $CDCl_3$) δ 205.5, 95.8, 71.9, 40.3, 38.7, 32.8, 25.9, 24.9; HRMS Calcd for $C_8H_{12}O_2S$ (M^+): 172.0559, Found 172.0562; Anal. Calcd for $C_8H_{12}O_2S$: C, 55.78; H, 7.02. Found: C, 55.79; H, 6.94.

Alternative Preparation of ***97***

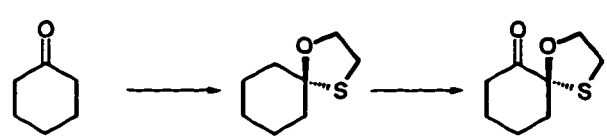

93 95 97

A ethereal (500 mL) solution of cyclohexanone **93** (13.0 g, 132 mmol) under nitrogen was treated with 2-mercaptoethanol (9.25 mL, 132 mmol) and heated to reflux. After 1 hour, boron trifluoride etherate (16.2 mL, 132 mmol) was added with a dropping funnel over 10 minutes and the mixture maintained at reflux for a further hour. The mixture was then cooled, washed with 5% aqueous sodium bicarbonate (2 x 50 mL) and brine (50 mL), dried and concentrated *in vacuo*. The residue was distilled under vacuum (0.2 Torr) to afford **97** as a colourless oil (19 g, 92%); bp 43-44 °C, 0.2 Torr; IR (neat, cm^{-1}) 2945, 1718, 1440, 911, 732; ^1H NMR (200 MHz, $CDCl_3$) δ 4.18 (t, J = 5.6 Hz, H-C-O, 2H), 3.03 (t, J = 5.6 Hz, H-C-S, 2H), 1.98-1.70 (series of m, 6H), 1.61-1.20 (series of m, 4H); ^{13}C NMR (50 MHz, $CDCl_3$) δ 104.1, 71.6, 39.8, 39.1, 33.4, 23.9, 22.1, 21.2; HRMS Calcd for $C_8H_{14}OS$ (M^+): 158.0766, Found 158.0769.

A solution of sulfuryl chloride (2.7 g, 20 mmol) in carbon tetrachloride (10 mL) under nitrogen was added using a dropping funnel to a stirred solution of 1-oxa-4-thiaspiro[4.5]decane (**95**) (1.6 g, 10 mmol) in carbon tetrachloride (50 mL) at 0 °C over a period of 1 hour. A solution of triethylamine (2.8 mL, 20 mmol) in carbon tetrachloride (10 mL) was added with a dropping funnel to the solution at 0 °C. The mixture was allowed to warm to room temperature, filtered, washed with water (3 x 50 mL) and concentrated *in vacuo*. Silica gel (5 g) and water (5 mL) were added and the mixture was stirred for 3 hours. The mixture was filtered, washed with water (50 mL) dried, and concentrated *in vacuo*. Purification by Kugelrohr distillation under vacuum (0.7 Torr) gave **97** as a colourless oil (0.40 g, 23%); bp 74-77 °C, 0.7 Torr.

General Procedure for Grignard and Methyllithium Reactions

A slight excess (1.1 equivalents) of the Grignard reagent or methyllithium was added dropwise to an ethereal or tetrahydrofuran solution of the ketone at the

indicated temperature. The reaction was monitored by GC-MS and was then treated with an aqueous saturated ammonium chloride solution after the indicated time and the aqueous phase extracted with ether. The combined organic phases were washed with brine and dried. Concentration of the resultant solution *in vacuo*, followed by silica gel chromatography (elution with 20% ethyl acetate in hexanes) resulted in the isolation of the product alcohols.

(*RS*)-6-Methyl-1-oxa-4-thiaspiro[4.5]decan-6-ol (102)

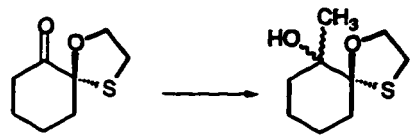

97 102

Following the general procedure, ketone **97** (393 mg, 2.28 mmol) in ether (10 mL) under argon at 0 °C was treated dropwise with methyllithium (1.8 mL, 1.4 M, 2.5 mmol). After stirring for 30 minutes and work-up, the mixture was purified to give alcohol **102** (326 mg, 76%) as a colourless oil (single diastereomer); IR (neat, cm^{-1}) 3473, 2921, 1448, 1367, 1112; ^1H NMR (200 MHz, $CDCl_3$) δ 4.40 (m, H-C-O, 1H), 4.15 (m, H-C-O, 1H), 2.99 (m, H-C-S, 2H), 2.19-1.32 (series of m, 9H), 1.30 (s, methyl, 3H); ^{13}C NMR (50 MHz, $CDCl_3$) δ 104.3, 74.2, 71.5, 39.8, 36.7, 33.1, 23.9, 22.0, 21.1; HRMS Calcd for $C_9H_{16}O_2S$ (M^+): 188.0870, Found 188.0869; Anal. Calcd for $C_9H_{16}O_2S$: C, 57.42; H, 8.57; Found: C, 57.35; H, 8.44.

Following the general procedure, ketone **97** (124 mg, 0.72 mmol) in ether (10 mL) under argon at 0 °C was treated dropwise with methylmagnesium bromide (260 μL, 3.0 M, 0.79 mmol). After stirring for 1 hour and work-up, the mixture was purified to give alcohols **102** (107 mg, 79%, 69% de).

Following the general procedure, ketone **97** (151 mg, 0.87 mmol) in ether (10 mL) under argon at 0 °C was treated dropwise with methylmagnesium chloride (320 µL, 3.0 M, 0.96 mmol). After stirring for 1 hour and work-up, the mixture was purified to give alcohols **102** (127 mg, 78%, 78% de).

General Procedure for Reduction Reactions

A slight excess (1.1 equivalents) of the reducing agent was added dropwise to a solution of the ketone in the indicated solvent under argon at the indicated temperature. The reaction was monitored by GC-MS and was then treated with an aqueous saturated ammonium chloride solution after the indicated time and the aqueous phase extracted with ether. The combined organic phases were washed with brine and dried. Concentration of the resultant solution *in vacuo*, followed by silica gel chromatography (elution with 50% ether in petroleum ether) resulted in the isolation of the product alcohols.

(*RS*)-1-Oxa-4-thiaspiro[4.5]decan-6-ol (103)

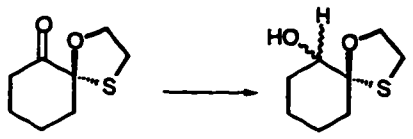

97 **103**

Following the general procedure, ketone **97** (143 mg, 0.83 mmol) in methanol (20 mL) at room temperature was treated with sodium borohydride (35 mg, 0.91 mmol) and stirred for 2 hours. Purification resulted in an inseparable mixture (50% de) of alcohol **103** (134mg, 93%) as a colourless oil (the ^{1}H NMR signals overlapped considerably. The NMR data below are the prominent signals

taken from spectra containing both diastereomers); IR (neat, cm^{-1}) 3436, 2909, 1445, 1250, 1082; ^1H NMR (200 MHz, $CDCl_3$) δ 4.41 (m, H-C-O, 1H), 4.12 (m, H-C-O, 1H), 3.65 (m, H-C-OH, 1H), 3.05 (m, H-C-S, 2H), 2.36-1.14 (series of m, 9H); ^{13}C NMR (50 MHz, $CDCl_3$) δ 101.6, 74.0, 70.7, 38.1, 34.0, 33.0, 23.9, 22.9; HRMS Calcd for $C_8H_{14}O_2S$ (M^+): 174.0714, Found 174.0988; Anal. Calcd for $C_8H_{14}O_2S$: C, 55.13; H, 8.10; Found: C, 55.20; H, 8.24.

Following the general procedure, ketone **97** (107 mg, 0.62 mmol) in tetrahydrofuran (15 mL) under argon at 0 °C was treated dropwise with lithium borohydride (340 μL, 2.0 M, 0.68 mmol). After stirring for 45 minutes and work-up, the mixture was purified to give alcohol **103** (98 mg, 91%, 64% de).

Following the general procedure, ketone **97** (133 mg, 0.77 mmol) in tetrahydrofuran (20 mL) under argon at 0 °C was treated with lithium aluminum hydride (32 mg, 0.68 mmol). After stirring for 30 minutes and work-up, the mixture was purified to give alcohol **103** (111 mg, 83%, 79% de).

Following the general procedure, ketone **97** (111 mg, 0.64 mmol) in tetrahydrofuran (15 mL) under argon at -78 °C was treated dropwise with diisobutylaluminum hydride (470 μL, 1.5 M, 0.70 mmol). After stirring for 90 minutes and work-up, the mixture was purified to give alcohol **103** (99 mg, 89%, 81% de).

Following the general procedure, ketone **97** (103 mg, 0.60 mmol) in ether (20 mL) under argon at 0 °C was treated with lithium tri-*tert*-butoxyaluminum hydride (0.17 g, 0.66 mmol). After stirring for 2 hours and work-up, the mixture was purified to give alcohol **103** (90 mg, 86%, 79% de).

Following the general procedure, ketone **97** (100 mg, 0.58 mmol) in tetrahydrofuran (20 mL) under argon at 0 °C was treated dropwise with lithium tri-*sec*-butylborohydride (640 µL, 1.0 M, 0.64 mmol). After stirring for 2 hours and work-up, the mixture was purified to give alcohol **103** (66 mg, 65%, 83% de).

2-Cyclopentylidenecyclopentanone (106)

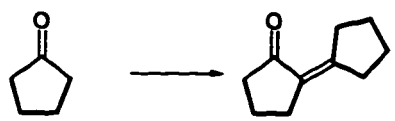

104 **106**

Cyclopentanone (50 g, 0.59 mol) and potassium hydroxide (30 g, 0.54 mol) were dissolved in water (300 mL) and the solution heated to reflux for 16 hours. After separation of the organic phase, the aqueous phase was extracted with ether (3 x 100 mL). The combined organic phases were washed with saturated aqueous sodium bicarbonate solution, brine (100 mL) and then dried. Concentration *in vacuo* , followed by fractional distillation (20 Torr) afforded **106** as a colourless oil (35 g, 40%); bp 142-144 °C, 20 Torr; IR (neat, cm^{-1}) 2915, 1707, 1639, 1415, 1251, 1171; ^1H NMR (200 MHz, $CDCl_3$) δ 2.71 (br m, 2H), 2.49 (br m, 2H), 2.24 (br m, 4H), 1.85 (m, J = 7.4 Hz, 2H), 1.64 (br m, 4H); ^{13}C NMR (50 MHz, $CDCl_3$) δ 207.2, 158.5, 127.8, 39.7, 34.2, 32.4, 29.4, 26.8, 25.1, 19.9; HRMS Calcd for $C_{10}H_{14}O$ (M^+): 150.1045, Found 150.1045; Anal. Calcd for $C_{10}H_{14}O$: C, 79.95; H, 9.39; Found: C, 79.81; H, 9.11.

1,2-Cyclopentanedione (107)

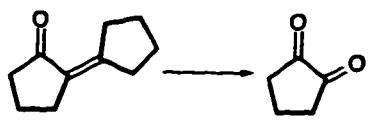

106 107

2-Cyclopentylidenecyclopentanone **106** (3.0 g, 20 mmol) was dissolved in methanol (40 mL) under nitrogen and cooled to -78 °C. A stream of ozone was bubbled through the solution for approximately 1 hour. The reaction was monitored by the use a bubbler which contained an aqueous solution of sodium iodide connected to the reaction flask. A darkening in colour of this solution indicates excess ozone. At this point, methyl sulfide (2.6 mL, 36 mmol) was added and the stirred mixture allowed to warm slowly to room temperature overnight. The methanol was removed *in vacuo* and the resultant oil chromatographed on silica gel (100% ethyl acetate) to afford **107** as a colourless oil (1.6 g, 83%); IR (neat, cm^{-1}) 3205, 2940, 1685, 1480, 955, 910; ^1H NMR (200 MHz, $CDCl_3$) δ 6.58 (t, J = 1.2 Hz, H-C=C, 1H), 6.50 (br s, H-O-C=C, 1H), 2.55-2.40 (br m, 4H); ^{13}C NMR (50 MHz, $CDCl_3$) δ 204.8, 153.3, 130.6, 32.1, 21.6; HRMS Calcd for $C_5H_6O_2$ (M^+): 98.0368, Found 98.0374.

(*RS*)-1-Oxa-4-thiaspiro[4.4]nonan-6-one (108)

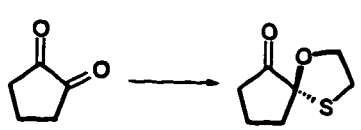

107 108

A mixture of 1,2-cyclopentanedione **107** (1.0 g, 10 mmol), 2-mercaptoethanol (700 µL) and *p*-toluenesulfonic acid (5.6 mg, 4.4 mmol) in benzene (20 mL) was heated to reflux under a Dean-Stark apparatus. After 6 hours, the dark green solution was washed with a 10% aqueous sodium hydroxide

solution and the aqueous phase extracted with ether (2 x 50 mL). The combined organic phases were washed with water (50 mL), brine (50 mL) and dried. Concentration of the resultant solution *in vacuo* followed by Kugelrohr distillation gave **108** as a colourless oil (174 mg, 24%); bp 80-100 °C, 0.2 Torr; IR (neat, cm^{-1}) 2950, 1750, 1122, 1050, 778; ^1H NMR (200 MHz, $CDCl_3$) δ 4.51 (m, H-C-O, 1H), 4.28 (m, H-C-O, 1H), 3.20 (m, H-C-S, 2H), 2.55-1.60 (series of m, 6H); ^{13}C NMR (50 MHz, $CDCl_3$) δ 213.0, 95.0, 72.1, 34.9, 33.1, 32.2, 17.7; HRMS Calcd for $C_7H_{10}O_2S$ (M^+): 158.0402, Found 158.0403; Anal. Calcd for $C_7H_{10}O_2S$: C, 53.14; H, 6.37; S, 20.26. Found: C, 53.18; H, 6.18; S, 20.25.

(5*R, 6*S**)-6-Methyl-1-oxa-4-thiaspiro[4.4]nonan-6-ol (109a)** and **(5*R**, 6*R**)-6-Methyl-1-oxa-4-thiaspiro[4.4]nonan-6-ol (109b)**

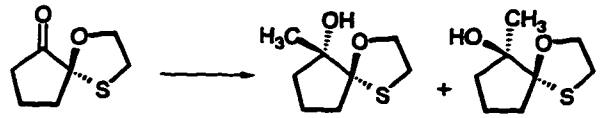

108 **109a** **109b**

Following the general procedure, ketone **108** (113 mg, 0.71 mmol) in ether (15 mL) under argon at 0 °C was treated dropwise with methyllithium (560 μL, 1.4 M, 0.78 mmol). After stirring for 45 minutes and work-up, the mixture was purified to give alcohol **109a** (89 mg, 72%) and alcohol **109b** (9 mg, 7%) as colourless oils:

alcohol **109a**: IR (neat, cm^{-1}) 3475, 2917, 1444, 1361, 1097; ^1H NMR (200 MHz, $CDCl_3$) δ 4.39 (m, H-C-O, 1H), 4.07 (m, H-C-O, 1H), 2.96 (m, H-C-S, 2H), 2.31 (br s, H-O-C, 1H), 2.21-1.50 (series of m, 6H), 1.41 (s, methyl, 3H); ^{13}C NMR (50 MHz, $CDCl_3$) δ 106.5, 81.4, 71.3, 37.9, 36.4, 33.1, 20.8, 18.8; HRMS Calcd for $C_8H_{14}O_2S$ (M^+): 174.0714, Found 174.0721; Anal. Calcd for $C_8H_{14}O_2S$: C, 55.14; H, 8.10. Found: C, 55.20; H, 8.01.

alcohol **109b**: IR (neat, cm^{-1}) 3473, 2915, 1444, 1365, 1108; ^1H NMR (200 MHz, $CDCl_3$) δ 4.35 (m, H-C-O, 1H), 4.21 (m, H-C-O, 1H), 3.02 (m, H-C-S, 2H), 2.43-1.48 (series of m, 7H), 1.55 (s, methyl, 3H); ^{13}C NMR (50 MHz, $CDCl_3$) δ 103.5, 79.7, 70.4, 38.3, 37.1, 33.3, 24.5, 17.8; HRMS Calcd for $C_8H_{14}O_2S$ (M^+): 174.0714, Found 174.0719.

Following the general procedure, ketone **108** (110 mg, 0.69 mmol) in tetrahydrofuran (15 mL) under argon at 0 °C was treated dropwise with methyllithium (560 μL, 1.4 M, 0.78 mmol). After stirring for 30 minutes and work-up, the mixture was purified to give alcohols **109a** and **109b** (98 mg, 82% combined).

Following the general procedure, ketone **108** (104 mg, 0.66 mmol) in ether (20 mL) under argon at 0 °C was treated dropwise with methylmagnesium bromide (240 μL, 3.0 M, 0.73 mmol). After stirring for 45 minutes and work-up, the mixture was purified to give alcohols **109a** and **109b** (103 mg, 90% combined).

Following the general procedure, ketone **108** (114 mg, 0.72 mmol) in tetrahydrofuran (20 mL) under argon at 0 °C was treated dropwise with methylmagnesium bromide (270 μL, 3.0 M, 0.79 mmol). After stirring for 1 hour and work-up, the mixture was purified to give alcohols **109a** and **109b** (111 mg, 89% combined).

Following the general procedure, ketone **108** (101 mg, 0.64 mmol) in tetrahydrofuran (20 mL) under argon at -78 °C was treated dropwise with methylmagnesium bromide (230 μL, 3.0 M, 0.70 mmol). After stirring for 3 hours and work-up, the mixture was purified to give alcohols **109a** and **109b** (48 mg, 43% combined).

Following the general procedure, ketone **108** (100 mg, 0.63 mmol) in ether (20 mL) under argon at 0 °C was treated dropwise with methylmagnesium chloride (230 μL, 3.0 M, 0.69 mmol). After stirring for 90 minutes and work-up, the mixture was purified to give alcohols **109a** and **109b** (72 mg, 66% combined).

Following the general procedure, ketone **108** (107 mg, 0.67 mmol) in ether (20 mL) under argon at 0 °C was treated dropwise with methylmagnesium iodide (240 μL, 3.0 M, 0.74 mmol). After stirring for 1 hour and work-up, the mixture was purified to give alcohols **109a** and **109b** (103 mg, 88% combined).

(5*R, 6*S**)-1-Oxa-4-thiaspiro[4.4]nonan-6-ol (110)** and **(5*R**, 6*R**)-1-Oxa-4-thiaspiro[4.4]nonan-6-ol (111)**

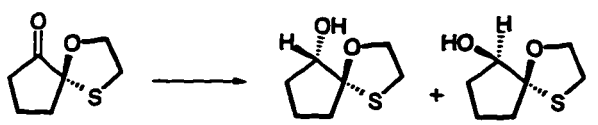

108 110 111

Following the general procedure, ketone **108** (211 mg, 1.31 mmol) in methanol (25 mL) at room temperature was treated with sodium borohydride (55 mg, 1.4 mmol). After stirring for 1 hour and work-up, the mixture was purified to give alcohol **110** (110 mg, 52%) and alcohol **111** (58 mg, 28%) as colourless oils:

alcohol **110**: IR (neat, cm^{-1}) 3474, 2910, 1409, 1111; ^1H NMR (200 MHz, $CDCl_3$) δ 4.20-3.91 (series of m, H-C-O, 2H), 3.76 (br s, H-C-OH, 1H), 3.06 (m, H-C-S, 2H), 2.33-1.44 (series of m, 7H); ^{13}C NMR (50 MHz, $CDCl_3$) δ 100.7, 70.7, 36.1, 33.6, 33.2, 30.2, 18.9; HRMS Calcd for $C_7H_{12}O_2S$ (M^+): 160.0557, Found 160.0544; Anal. Calcd for $C_7H_{12}O_2S$: C, 52.47; H, 7.55. Found: C, 52.37; H, 7.53.

alcohol **111**: IR (neat, cm^{-1}) 3473, 2920, 1410, 1125; ^1H NMR (200 MHz, $CDCl_3$) δ 4.14 (m, H-C-O, 1H), 3.98 (m, H-C-O, 1H), 3.75 (br s, H-C-OH, 1H), 3.01

(m, H-C-S, 2H), 2.30 (br s, H-O-C, 1H), 2.16-1.50 (series of m, 6H); ^{13}C NMR (50 MHz, $CDCl_3$) δ 105.4, 70.5, 36.3, 33.6, 33.2, 31.1, 20.4; HRMS Calcd for $C_7H_{12}O_2S$ (M^+): 160.0557, Found 160.0547.

Following the general procedure, ketone **108** (100 mg, 0.63 mmol) in tetrahydrofuran (20 mL) under argon at 0 °C was treated dropwise with lithium borohydride (350 μL, 2.0 M, 0.69 mmol). After stirring for 30 minutes and work-up, the mixture was purified to give alcohols **110** and **111** (90 mg, 89% combined).

Following the general procedure, ketone **108** (115 mg, 0.73 mmol) in ether (20 mL) under argon at 0 °C was treated with lithium aluminum hydride (30 mg, 0.80 mmol). After stirring for 30 minutes and work-up, the mixture was purified to give alcohols **110** and **111** (98 mg, 84% combined).

Following the general procedure, ketone **108** (106 mg, 0.67 mmol) in tetrahydrofuran (20 mL) under argon at -78 °C was treated dropwise with diisobutylaluminum hydride (490 μL, 1.5 M, 0.74 mmol). After stirring for 90 minutes and work-up, the mixture was purified to give alcohols **110** and **111** (80 mg, 74% combined).

Following the general procedure, ketone **108** (104 mg, 0.66 mmol) in ether (25 mL) under argon at -78 °C was treated dropwise with diisobutylaluminum hydride (490 μL, 1.5 M, 0.74 mmol). After stirring for 1 hour and work-up, the mixture was purified to give alcohols **110** and **111** (73 mg, 69% combined).

Following the general procedure, ketone **108** (113 mg, 0.71 mmol) in dichloromethane (20 mL) under argon at -78 °C was treated dropwise with

diisobutylaluminum hydride (520 μL, 1.5 M, 0.78 mmol). After stirring for 2 hours and work-up, the mixture was purified to give alcohols **110** and **111** (82 mg, 72% combined).

Following the general procedure, ketone **108** (107 mg, 0.68 mmol) in ether (20 mL) under argon at 0 °C was treated with lithium tri-*tert*-butoxyaluminum hydride (190 mg, 0.75 mmol). After stirring for 90 minutes and work-up, the mixture was purified to give alcohols **110** and **111** (82 mg, 75% combined).

Following the general procedure, ketone **108** (122 mg, 0.77 mmol) in tetrahydrofuran (20 mL) under argon at 0 °C was treated dropwise with lithium tri-*sec*-butylborohydride (850 μL, 1.0 M, 0.85 mmol). After stirring for 2 hours and work-up, the mixture was purified to give alcohols **110** and **111** (80 mg, 65% combined).

Following the general procedure, ketone **108** (111 mg, 0.70 mmol) in ether (20 mL) under argon at 0 °C was treated dropwise with sodium bis(2-methoxyethoxy)aluminum hydride (225 mg, 70% w/w soln., 0.77 mmol). After stirring for 1 hour and work-up, the mixture was purified to give alcohols **110** and **111** (86 mg, 77% combined).

(*RS*)-Acenapthenequinone-(1-oxa-4-thiaspiro[4.4]nonan-6-one) (114)

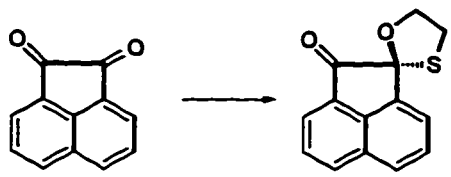

113 114

A mixture of acenapthenequinone **113** (2.0 g, 11 mmol), 2-mercaptoethanol (860 µL, 12 mmol) and pyridinium *p*-toluenesulfonate (140 mg, 0.56 mmol) in benzene (50 mL) was heated to reflux under a Dean-Stark apparatus. After 12 hours, the reaction mixture was concentrated *in vacuo* and chromatography of the residue on neutral alumina (100% ether) gave **114** as an orange solid (2.3 g, 88%); mp 84-85 °C; IR (KBr disc, cm^{-1}) 3057, 2946, 1727, 908; ^1H NMR (200 MHz, $CDCl_3$) δ 8.11 (d, J = 8.2 Hz, H-Ar, 1H), 7.92 (m, H-Ar, 2H), 7.72 (m, H-Ar, 3H), 4.92-4.79 (m, H-C-O, 1H), 4.68-4.56 (m, H-C-O, 1H), 3.78-3.66 (m, H-C-S, 1H), 3.55-3.43 (m, H-C-S, 1H); ^{13}C NMR (50 MHz, $CDCl_3$) δ 200.8, 141.0, 136.1, 131.7, 130.3, 129.6, 128.9, 128.4, 126.1, 122.5, 121.7, 92.3, 73.1, 34.4; HRMS Calcd for $C_{14}H_{10}O_2S$ (M^+): 242.0402, Found 242.0416; Anal. Calcd for $C_{14}H_{10}O_2S$: C, 69.40; H, 4.16; S, 13.23 Found: C, 69.43; H, 4.23; S, 13.30.

(5*R,6*S**)-Acenapthenequinone-(6-methyl-1-oxa-4-thiaspiro[4.4]nonan-6-ol) (115) and (5*R**, 6*R**)-Acenapthenequinone-(6-methyl-1-oxa-4-thiaspiro[4.4]nonan-6-ol) (116)**

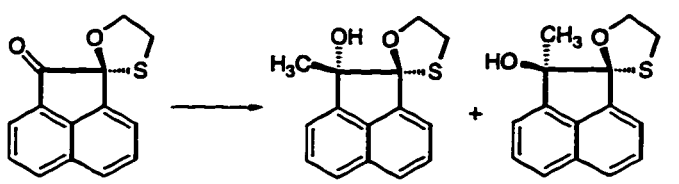

114 **115** **116**

Following the general procedure, ketone **114** (0.38 g, 1.5 mmol) in ether (50 mL) under argon at 0 °C was treated dropwise with methyllithium (2.2 mL, 1.4 M, 1.6 mmol). After stirring for 45 minutes and work-up, the mixture was purified to give alcohol **115** (315 mg, 78%) as a white solid and alcohol **116** (19 mg, 5%) as a colourless oil:

alcohol **115**: mp 85-86 °C; IR (KBr disc, cm^{-1}) 3475, 3053, 2941, 1337, 1088; ^1H NMR (200 MHz, $CDCl_3$) δ 7.75-7.40 (series of m, H-Ar, 6H), 4.66-4.56 (m, H-C-O-C, 1H), 4.46-4.32 (m, H-C-O-C, 1H), 3.57 (s, H-O, 1H), 3.42-3.22 (m, H-C-S, 2H), 1.56 (s, methyl, 3H); ^{13}C NMR (50 MHz, $CDCl_3$) δ 146.2, 141.3, 134.1, 131.1, 129.1 (2C), 126.0, 124.9, 120.9, 119.6, 109.0, 84.8, 73.3, 34.8, 24.6; HRMS Calcd for $C_{15}H_{14}O_2S$ (M^+): 258.0714, Found 258.0734; Anal. Calcd for $C_{15}H_{14}O_2S$: C, 69.74; H, 5.46; S, 12.41. Found: C, 69.95; H, 5.40; S, 12.39.

alcohol **116**: IR (neat, cm^{-1}) 3449, 3057, 2946, 1443, 1003; ^1H NMR (200 MHz, $CDCl_3$) δ 7.80-7.47 (series of m, H-Ar, 6H), 4.41-4.19 (m, H-C-O-C, 2H), 3.50-3.21 (m, H-C-S; H-O, 3H), 1.62 (s, methyl, 3H); ^{13}C NMR (50 MHz, $CDCl_3$) δ 145.3, 141.2, 134.0, 131.3, 129.1, 129.2, 126.1, 125.1, 120.8, 119.4, 109.1, 84.7, 73.0, 34.7, 24.1; HRMS Calcd for $C_{15}H_{14}O_2S$ (M^+): 258.0714, Found 258.0722.

Following the general procedure, ketone **114** (153 mg, 0.63 mmol) in tetrahydrofuran (20 mL) under argon at 0 °C was treated dropwise with methyllithium (495 μL, 1.4 M, 0.69 mmol). After stirring for 1 hour and work-up, the mixture was purified to give alcohols **115** and **116** (144 mg, 84% combined).

Following the general procedure, ketone **114** (131 mg, 0.54 mmol) in ether (20 mL) under argon at -78 °C was treated with zinc chloride (73 mg, 0.54 mmol) and stirred for 2 hours. The mixture was then treated dropwise with methyllithium (425 μL, 1.4 M, 0.59 mmol). After stirring for 2 hours and work-up, the mixture was purified to give alcohols **115** and **116** (139 mg, 91% combined).

Following the general procedure, ketone **114** (120 mg, 0.49 mmol) in toluene (60 mL) under argon at -78 °C was treated dropwise with a solution of methylaluminum bis(2,6-di-*tert*-butyl-4-methylphenoxide, MAD (1.2 mL, 0.4 M, 0.49

mmol) [MAD was prepared as follows: to a solution of 2,6-di-*tert*-butyl-4-methylphenol (44 g, 0.20 mol) in toluene (200 mL) at room temperature under argon was added dropwise trimethylaluminum (50 mL, 2.0 M, 0.1 mol) and stirred for 1 hour. MAD was used without further purification]. After stirring for 15 minutes, methyllithium (385 μL, 1.4 M, 0.54 mmol) was added dropwise and stirring continued for 2 hours. Work-up and purification of the mixture gave alcohols **115** and **116** (110 mg, 87% combined).

Following the general procedure, ketone **114** (139 mg, 0.57 mmol) in toluene (60 mL) under argon at -78 °C was treated dropwise with methylaluminum bis(2,6-di-*tert*-butyl-4-methylphenoxide (2.9 mL, 0.4 M, 1.2 mmol) and stirred for 30 minutes. Methyllithium (450 μL, 1.4 M, 0.62 mmol) was then added dropwise and stirring continued for an additional 2 hours. Work-up and purification of the reaction mixture gave alcohols **115** and **116** (116 mg, 79% combined).

Following the general procedure, ketone **114** (122 mg, 0.50 mmol) in ether (20 mL) under argon at 0 °C was treated dropwise with methylmagnesium chloride (180 μL, 3.0 M, 0.55 mmol). After stirring for 1 hour and work-up, the mixture was purified to give alcohols **115** and **116** (103 mg, 80% combined).

Following the general procedure, ketone **114** (123 mg, 0.50 mmol) in ether (25 mL) under argon at 0 °C was treated dropwise with methylmagnesium bromide (180 μL, 3.0 M, 0.55 mmol). After stirring for 90 minutes and work-up, the mixture was purified to give alcohols **115** and **116** (109 mg, 85% combined).

Following the general procedure, ketone **114** (130 mg, 0.53 mmol) in ether (20 mL) under argon at 0 °C was treated dropwise with methylmagnesium iodide

(200 μL, 3.0 M, 0.59 mmol). After stirring for 90 minutes and work-up, the mixture was purified to give alcohols **115** and **116** (113 mg, 82% combined).

Following the general procedure, ketone **114** (139 mg, 0.57 mmol) in ether (20 mL) under argon at 0 °C was treated with zinc chloride (77 mg, 0.57 mmol) and stirred for 1 hour. The mixture was then treated dropwise with methylmagnesium bromide (210 μL, 3.0 M, 0.62 mmol). After stirring for 2 hours and work-up, the mixture was purified to give alcohols **115** and **116** (126 mg, 86% combined).

Cerium trichloride (332 mg, 0.89 mmol) was heated slowly with stirring to 140 °C under vacuum (*ca.* 0.1 Torr) and this temperature maintained overnight. The solid was cooled under argon to room temperature and treated with tetrahydrofuran (4 mL), stirred for an additional 3 hours and cooled to 0 °C, at which point methylmagnesium bromide (290 μL, 3.0 M, 0.89 mmol) was added dropwise. The mixture was stirred for 30 minutes at 0 °C for 90 minutes at room temperature and then treated with a tetrahydrofuran solution (3 mL) of ketone **114** (144 mg, 0.59 mmol) and stirred for 30 minutes. The reaction mixture was then treated with 10% aqueous acetic acid (10 mL), followed by work-up and purification to give alcohols **115** and **116** (143 mg, 94% combined).

Methylmagnesium bromide (350 μL, 3.0 M, 1.1 mmol) was added to tetrahydrofuran (10 mL) under argon at 0 °C. This mixture was added to a suspension of ytterbium trichloride (605 mg, 1.56 mmol) in tetrahydrofuran (5 mL) at 0 °C. This mixture was stirred at 0 °C for 2 hours, cooled to -78 °C and treated with a tetrahydrofuran solution (2.0 mL) of ketone **114** (127 mg, 0.52 mmol). After stirring for three hours and work-up, the reaction was purified to give alcohols **115** and **116** (119 mg, 89% combined).

(5*R,6*S**)-Acenapthenequinone-(1-oxa-4-thiaspiro[4.4]nonan-6-ol) (117) and (5*R**, 6*R**)-Acenapthenequinone-(1-oxa-4-thiaspiro[4.4]nonan-6-ol) (118)**

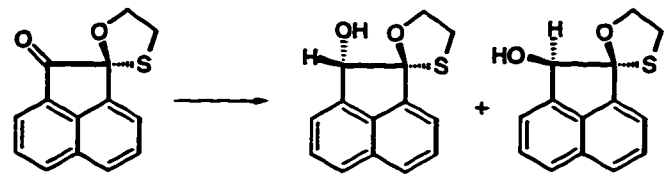

114 117 118

Following the general procedure, ketone **114** (205 mg, 0.84 mmol) in methanol (25 mL) at room temperature was treated with sodium borohydride (35 mg, 0.92 mmol). After stirring for 90 minutes and work-up, the mixture was purified to give alcohol **117** (39 mg, 19%) as a colourless oil and **118** (118 mg, 58%) as a white solid:

alcohol **117**: IR (neat, cm^{-1}) 3305, 3049, 2965, 1341, 1097; ^1H NMR (200 MHz, $CDCl_3$) δ 7.85-7.51 (series of m, H-Ar, 6H), 5.56 (d, J = 10.0 Hz, H-C-OH, 1H), 4.49 (m, H-C-O-C, 2H), 3.40-3.32 (m, H-C-S, 2H), 2.99 (d, J = 10.0 Hz, H-O, 1H); ^{13}C NMR (50 MHz, $CDCl_3$) δ 140.5, 139.8, 134.9, 130.5, 128.4 (2C), 125.8, 124.6, 121.1, 120.6, 107.1, 81.7, 71.2, 34.6; HRMS Calcd for $C_{14}H_{12}O_2S$ (M^+): 258.0714, Found 258.0734; Anal. Calcd for $C_{14}H_{12}O_2S$: C, 68.82; H, 4.95; S, 13.12. Found: C, 69.79; H, 4.76; S, 13.26.

alcohol **118**: mp 92-94 °C; IR (KBr disc, cm^{-1}) 3325, 3036, 2960, 1335, 1086; ^1H NMR (200 MHz, $CDCl_3$) δ 7.82-7.46 (series of m, H-Ar, 6H), 5.29 (d, J = 9.0 Hz, H-C-OH, 1H), 4.68-4.57 (m, H-C-O-C, 1H), 4.34-4.21 (m, H-C-O-C, 1H), 3.53-3.22 (m, H-C-S; H-O, 3H); ^{13}C NMR (50 MHz, $CDCl_3$) δ 141.4, 140.2, 134.9, 130.4, 128.1 (2C), 125.7, 124.5, 120.9, 120.8, 107.4, 82.1, 71.7, 35.0; HRMS Calcd for $C_{14}H_{12}O_2S$ (M^+): 258.0714, Found 258.0719.

Following the general procedure, ketone **114** (120 mg, 0.49 mmol) in tetrahydrofuran (20 mL) under argon at 0 °C was treated dropwise with lithium borohydride (270 μL, 2.0 M, 0.54 mmol). After stirring for 1 hour and work-up, the mixture was purified to give alcohols **117** and **118** (102 mg, 86% combined).

Following the general method, ketone **114** (141 mg, 0.58 mmol) in ether under argon at 0 °C was treated dropwise with zinc borohydride (5.0 mL, 0.14 M, 0.69 mmol) [Zinc borohydride was prepared as follows: a mixture of anhydrous zinc chloride (4.0 g, 29 mmol) in ether (50 mL) was refluxed for 4 hours. The mixture was carefully decanted and added dropwise to a stirred suspension of sodium borohydride (2.7 g, 69 mmol) in ether (150 mL) at room temperature. The mixture was stirred overnight, decanted and used without further purification]. After stirring for 30 minutes and work-up, the mixture was purified to give alcohols **117** and **118** (89 mg, 63% combined).

Following the general procedure, ketone **114** (121 mg, 0.50 mmol) in ether (20 mL) under argon at 0 °C was treated with lithium aluminum hydride (21 mg, 0.55 mmol). After stirring for 30 minutes and work-up, the mixture was purified to give alcohols **117** and **118** (99 mg, 82% combined).

Following the general procedure, ketone **114** (105 mg, 0.43 mmol) in tetrahydrofuran (20 mL) under argon at -78 °C was treated dropwise with diisobutylaluminum hydride (315 μL, 1.5 M, 0.47 mmol). After stirring for 1 hour and work-up, the mixture was purified to give alcohols **117** and **118** (90 mg, 86% combined).

Following the general procedure, ketone **114** (105 mg, 0.43 mmol) in ether (20 mL) under argon at -78 °C was treated dropwise with diisobutylaluminum hydride (315 µL, 1.5 M, 0.47 mmol). After stirring for 1 hour and work-up, the mixture was purified to give alcohols **117** and **118** (78 mg, 75% combined).

Following the general procedure, ketone **114** (100 mg, 0.41 mmol) in dichloromethane (20 mL) under argon at -78 °C was treated dropwise with diisobutylaluminum hydride (300 µL, 1.5 M, 0.45 mmol). After stirring for 1 hour and work-up, the mixture was purified to give alcohols **117** and **118** (79 mg, 79% combined).

Following the general procedure, ketone **114** (123 mg, 0.50 mmol) in ether (20 mL) under argon at 0 °C was treated with lithium tri-*tert*-butoxyaluminum hydride (140 mg, 0.55 mmol). After stirring for 1 hour and work-up, the mixture was purified to give alcohols **117** and **118** (84 mg, 69% combined).

Following the general procedure, ketone **114** (117 mg, 0.48 mmol) in tetrahydrofuran (20 mL) under argon at 0 °C was treated with lithium tri-*sec*-butylborohydride (530 µL, 1.0 M, 0.53 mmol). After stirring for 2 hours and work-up, the mixture was purified to give alcohols **117** and **118** (94 mg, 80% combined).

Following the general procedure, ketone **114** (114 mg, 0.47 mmol) in ether (20 mL) under argon at 0 °C was treated dropwise with sodium bis(methoxyethoxt)aluminum hydride (150 µL, 70% w/w soln., 0.52 mmol). After stirring for 1 hour and work-up, the mixture was purified to give alcohols **117** and **118** (93 mg, 81% combined).

3-Bromo-1-*tert*-butyldimethylsiloxypropane (124)

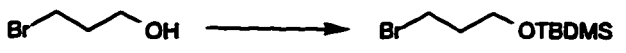

124

A solution of 3-bromopropanol (5.0 g, 36 mmol), in dichloromethane (150 mL) at room temperature under nitrogen was treated with 2,4,6-collidine (11 mL, 80 mmol). The solution was stirred for 10 minutes at which point *t*-butyldimethylsilyltrifluoromethanesulfonate (9.9 mL, 43 mmol) was added. Stirring was continued for 1 hour and the reaction mixture was treated with saturated aqueous ammonium chloride solution. The phases were separated and the aqueous layer extracted with dichloromethane (2 x 50 mL). The combined organic phases were washed with brine and dried. Concentration *in vacuo* followed by Kugelrohr distillation of the residue afforded **124** as a colourless oil (7.6 g, 84%); bp 70-80 °C, 0.2 Torr; IR (neat, cm^{-1}) 2910, 1467, 1255, 1094, 948, 837; ^1H NMR (200 MHz, $CDCl_3$) δ 3.73 (t, J = 5.8 Hz, H-C-Br, 2H), 3.51 (t, J = 6.4 Hz, H-C-O), 2.03 (m, H-C-C, 2H), 0.89 (s, *t*-butyl, 9H), 0.06 (s, dimethyl, 6H); ^{13}C NMR (50 MHz, $CDCl_3$) δ 60.4, 35.6, 30.7, 25.9, 25.8, 18.3, -5.4; HRMS Calcd for $C_5H_{12}OSiBr$ (M^+-57): 194.9841, Found 194.9839.

Cyclopentanone *p*-toluenesulfonhydrazone (123)

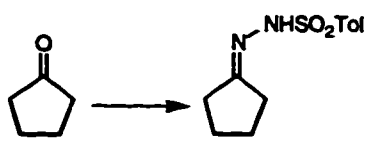

104 123

A solution of *p*-toluenesulfonhydrazide (25 g, 0.13 mol) in methanol (300 mL) was treated with cyclopentanone **104** (9.3 g, 0.12 mol) and stirred at room

temperature for 24 hours. The resultant precipitate was filtered, washed with cold (0 °C) methanol (75 mL), and recrystallized from ethanol to give hydrazone **123** as a white solid (19 g, 70 %); mp 184 °C (dec.); IR ($CHCl_3$, cm^{-1}) 3217, 2967, 1164, 908; ^1H NMR (200 MHz, $CDCl_3$) δ 7.83 (d, *J* = 8.4 Hz, H-Ar, 2H), 7.66 (br s, H-N, 1H), 7.28 (d, *J* = 8.4 Hz, H-Ar, 2H), 2.40 (s, H-C-Ar, 3H), 2.30 (t, *J* = 7.0 Hz, H-C-C=N, 2H), 2.11 (t, *J* = 7.0 Hz, H-C=N, 2H), 1.82-1.61 (m, 4H); ^{13}C NMR (50 MHz, $CDCl_3$) δ 168.1, 143.8, 135.5, 129.5, 127.9, 33.3, 27.9, 24.7, 24.6, 21.5; LRMS Calcd for $C_{12}H_{16}N_2O_2S$ (M^+): 252, Found 252; Anal. Calcd for $C_{12}H_{16}N_2O_2S$: C, 57.12; H, 6.39; N, 11.10 Found: C, 57.26; H, 6.36; N, 11.23.

1-(3-*tert*-Butyldimethylsiloxypropyl)cyclopentene (125)

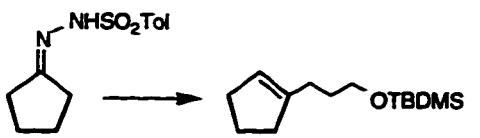

123 **125**

A solution of tosylhydrazone **123** (3.0 g, 12 mmol) in *N,N,N',N'*-tetramethylethylenediamine (30 mL) under argon at -78 °C was treated with *n*-butyllithium (19 mL, 2.5 M, 48 mmol). The solution was allowed to warm to room temperature during which time gas evolution is observed. The mixture was returned to -78 °C when gas evolution ceased. The mixture was then treated with bromide **124** (2.9 g, 12 mmol) added dropwise. The mixture was stirred at -78 °C for 1 hour, allowed to warm to room temperature, stirred for an additional 2 hours and treated with water (10 mL). The mixture was extracted with ether (3 x 150 mL) and the combined extracts were washed with water (3 x 400 mL), 1N hydrochloric acid (3 x 75 mL), saturated aqueous sodium bicarbonate solution (3 x 75 mL) and brine (3 x 75 mL) prior to drying and concentration. The residue was

chromatographed on silica gel (elution with10% ether in petroleum ether) to afford cyclopentene **125** as a colourless oil (1.4 g, 48%); IR (neat, cm^{-1}) 2915, 1455, 1306, 1005, 937; ^1H NMR (200 MHz, $CDCl_3$) δ 5.22 (m, H-C=C, 1H), 3.51 (t, $J = 6.4$ Hz, H-C-O, 2H), 2.24-1.48 (series of m, 10H), 0.89 (s, *t*-butyl, 9H), 0.06 (s, dimethyl, 6H); ^{13}C NMR (75 MHz, $CDCl_3$) δ 144.5, 123.3, 63.1, 35.2, 32.5, 31.0, 27.4, 26.0, 23.5, 18.4, -5.3; HRMS Calcd for $C_{10}H_{19}OSi$ (M^+-57): 183.1206, Found 183.1210.

(1*R**, 5*R**)-1-(3-*tert*-Butyldimethylsiloxypropyl)-6-oxabicyclo[3.1.0]hexane (126)

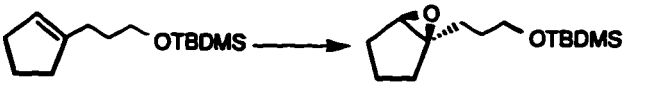

125 126

A solution of cyclopentene **125** (0.70 g, 2.9 mmol) in dichloromethane (50 mL) containing sodium bicarbonate (0.59 g, 7.0 mmol) was cooled to 0 °C and treated with *m*-chloroperbenzoic acid (1.1 g, 36 mmol). The reaction mixture was stirred for 1 hour followed by addition of a saturated aqueous sodium sulfite solution (50 mL). The aqueous phase was separated, extracted with ether (3 x 50 mL), and the combined ethereal phases were washed with saturated sodium bicarbonate solution (50 mL) and brine (100 mL) prior to drying and concentration. Silica gel chromatography (elution with 4% ether in petroleum ether) gave epoxide **126** as a colourless oil (61 mg, 82%); IR (neat, cm^{-1}) 2942, 1467, 1253, 1101, 839; ^1H NMR (200 MHz, $CDCl_3$) δ 3.59 (t, $J = 6.4$ Hz, H-C-O-Si, 2H), 3.22 (br s, H-C-O, 1H), 1.99-1.20 (series of m, 10H), 0.87, (s, *t*-butyl, 9H), 0.02, (s, dimethyl, 6H); ^{13}C NMR (50 MHz, $CDCl_3$) δ 67.7, 63.0, 62.6, 29.5, 28.9, 26.0, 19.5, 18.3, -5.3; HRMS Calcd for $C_{13}H_{25}O_2Si$ (M^+-15): 241.1625, Found 241.1647.

(1*R, 5*R**)-1-(3-Hydroxypropyl)-6-oxabicyclo[3.1.0]hexane (127)**

126 127

A solution of epoxide **126** (0.39 g, 1.5 mmol) in tetrahydrofuran (50 mL) was cooled to 0 °C and treated with tetrabutylammonium fluoride (1.5 mL, 1.1M, 1.6 mmol) The reaction mixture was stirred for 30 minutes and then allowed to warm to room temperature. After stirring at room temperature for 1 hour, water (50 mL) was added. The aqueous phase was extrated with ether (3 x 50 mL) and the combined ethereal phases were washed with brine (75 mL), dried and concentrated *in vacuo.* Purification of the residue by silica gel chromatography (elution with ether) resulted in the isolation of epoxyalcohol **127** as a colourless oil (0.17g, 78%); IR (neat, cm^{-1}) 3389, 2923, 1434, 1054; ^1H NMR (200 MHz, $CDCl_3$) δ 3.63 (br m, H-C-OH, 2H), 3.29 (br s, H-C-O, 1H), 2.15 (br s, H-O, 1H), 2.09-1.30 (series of m, 10H); ^{13}C NMR (50 MHz, $CDCl_3$) δ 67.8, 63.0, 62.5, 29.5, 28.6, 28.3, 27.5, 19.4; HRMS Calcd for $C_8H_{14}O_2$ (M^+): 142.0994, Found 142.1016; Anal. Calcd for $C_8H_{14}O_2$: C, 67.57; H, 9.92. Found: C, 67.44; H, 9.75.

(5*R, 6*S**)-1-Oxaspiro[4.4]nonan-6-ol (128)**

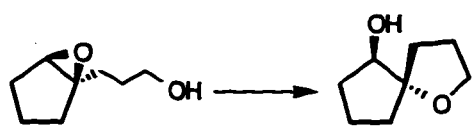

127 128

An ethereal (75 mL) solution of epoxyalcohol **127** (0.17 g, 1.2 mmol) under argon at -78 °C was treated with boron trifluoride etherate (0.16 mL, 1.3 mmol). The

reaction mixture was stirred at -78 °C for 1 hour and saturated aqueous ammonium chloride solution (10 mL) was added. The aqueous phase was extracted with ether (3 x 100 mL) and the combined organic phases were washed with brine (50 mL), dried and concentrated *in vacuo*. Purification of the residue by silica gel chromatography (elution with 50% ether in petroleum ether) gave cyclopentanol **128** as a colourless oil (0.13 g, 75%); IR (neat, cm^{-1}) 3431, 2928, 1443, 1305, 1069; ^1H NMR (200 MHz, $CDCl_3$) δ 3.88 (m, H-C-OH, 1H), 3.77 (t, J = 6.7 Hz, H-C-O-C, 2H), 2.33 (br s, H-O-C, 1H), 2.16-1.38 (series of m, 10H); ^{13}C NMR (50 MHz, $CDCl_3$) δ 93.5, 78.3, 68.6, 35.7, 32.8, 30.6, 27.1, 20.5; HRMS Calcd for $C_8H_{14}O_2$ (M^+): 142.0994, Found 142.1010.

1-Oxaspiro[4.4]nonan-6-one (129)

128 **129**

A cold (-78 °C) solution of oxalyl chloride (30 μL, 0.33 mmol) in dichloromethane (5 mL) under argon was treated with dimethylsulfoxide (53 μL, 0.73 mmol). After 2 minutes of stirring, a solution of cyclopentanol **128** (36 mg, 0.25 mmol) in dichloromethane (3 mL) was introduced, followed 15 minutes later with triethylamine (0.13 mL, 0.93 mmol). The mixture was allowed to warm to 0 °C and stirred at this temperature for 30 minutes. The mixture was then diluted with ether (25 mL), washed with water, 10% aqueous hydrochloric acid solution (25 mL), brine 50 mL, dried and concentrated. The residue was purified by silica gel chromatography (elution with ether) to give cyclopentanone **129** as a colourless oil (30 mg, 84%); IR (neat, cm^{-1}) 3477, 2925, 1747, 1153, 1055; ^1H NMR (200 MHz,

$CDCl_3$) δ 3.94 (t, J = 6.4 Hz, H-C-O, 2H), 2.26-1.65 (series of m, 10H); ^{13}C NMR (50 MHz, $CDCl_3$) δ 218.5, 86.5, 69.0, 35.8, 35.2, 32.3, 25.9, 18.1; HRMS Calcd for $C_8H_{12}O_2$ (M^+): 140.0838, Found 140.0843; Anal. Calcd for $C_8H_{12}O_2$: C, 68.55; H, 8.63;.Found: C, 68.79; H, 8.67.

Alternate preparation:

1-(4,5-Dihydro-2-furyl)cyclobutanol (143)

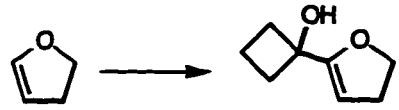

143

A solution of freshly distilled 2,3-dihydrofuran (1.05 g, 15.0 mmol) in tetrahydrofuran (75 mL) under argon was cooled to -78 °C and treated with *t*-butyllithium (10 mL, 1.7 M, 17 mmol). The reaction mixture was warmed to 0 °C for 30 minutes before being returned to -78 °C at which point cyclobutanone (1.01 g, 14.3 mmol) in tetrahydrofuran (10 mL) was introduced using a canula needle. The mixture was stirred for a further 2.5 hours and then allowed to warm to room temperature and treated with saturated aqueous sodium bicarbonate solution (50 mL). The organic phase was separated, the aqueous phase was extracted with ether (3 x 50 mL), and the combined organic phases washed with brine (2 x 50 mL), dried, concentrated and Kugelrohr distilled to give cyclobutanol **143** as a colourless oil (1.65, 82%); bp 85-100 °C, 0.2 Torr; IR (neat, cm^{-1}) 3390, 2934, 1660, 1384, 1244, 1140, 944; ^1H NMR (200 MHz, $CDCl_3$) δ 4.78 (t, J = 0.8 Hz, H-C=C, 1H), 4.30 (t, J = 7.0 Hz, H-C-O, 2H), 2.59 (dt, J = 7.0 Hz, 0.8 Hz, H-C-C=C, 2H), 2.37 (s, H-O-C, 1H), 2.30-1.45 (series of m, 6H); ^{13}C NMR (75 MHz, $CDCl_3$) δ 160.5, 93.9, 71.6, 70.5, 34.5, 29.9, 12.7; HRMS Calcd for $C_8H_{12}O_2$ (M^+): 140.0838, Found 140.0840.

143 129

A solution of cyclobutanol **143** (1.50 g, 10.7 mmol) in dichloromethane (40 mL) was added to a stirred suspension of Dowex 50X4-400 ion-exchange resin (1.43 g after washing with dichloromethane and drying) in dichloromethane (480 mL) at room temperature. The mixture was stirred at room temperature for 20 hours and then filtered through Celite. Concentration of the filtrate *in vacuo* gave cyclopentanone **129** as a colourless oil (1.30 g, 91%) which was used without further purification.

(5*R**, 6*S**)-1-Thiospiro[4.4]nonan-6-ol (132)

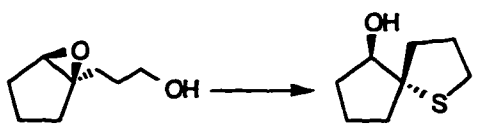

127 132

A solution of triphenylphosphine (3.2 g, 12 mmol) in tetrahydrofuran (100) mL at 0 °C under argon was treated with diethyl azodicarboxylate (2.1 g, 12 mmol) and stirred at 0 °C for 30 minutes during which time a white precipitate formed. To this mixture was added dropwise a tetrahydrofuran solution (50 mL) containing epoxyalcohol 127 (0.86 g, 6.1 mmol) and thiolacetic acid (0.91 mL, 12 mmol) and stirring continued for 1 hour. The mixture was then allowed to warm to room temperature and stirred for an additional 2 hours. The solvent was removed *in vacuo* and the residue dissolved in methanol (40 mL) and treated with a 20% aqueous sodium bicarbonate solution (20 mL) and heated to reflux. The mixture

was maintained at this temperature for 90 minutes, cooled, diluted with ether (200 mL) and the organic layer separated. The aqueous layer was washed with ether (2x 100 mL) and the combined organic layers washed with aqueous 5% hydrochloric acid (50 mL), water (50 mL), brine (50 mL), dried and concentrated *in vacuo*. The residue was diluted with ether (50 mL), cooled to -78 °C and treated dropwise with boron trifluoride etherate (3.0 mL, 24 mmol) and stirred for 1 hour. The mixture was treated with aqueous saturated ammonium chloride solution (20 mL) and allowed to warm to room temperature. The aqueous layer was extracted with ether (2 x 100 mL) and the combined organic phases were washed with brine (100 mL), dried and concentrated *in vacuo*. Purification of the residue by silica gel chromatography (elution with 50% ether in petroleum ether) gave tetrahydrofuran **132** as a colourless oil (0.70 g, 73%); IR (neat, cm^{-1}) 3440, 2931, 1660, 1315, 1105; ^1H NMR (200 MHz, $CDCl_3$) δ 4.02 (m, H-C-OH, 1H), 2.88 (m, H-C-S, 2H), 2.16-1.45 (series of m, 11H); ^{13}C NMR (75 MHz, $CDCl_3$) δ 78.9, 67.1, 38.9, 35.1, 33.0, 31.2, 30.4, 19.7; HRMS Calcd for $C_8H_{14}OS$ (M^+): 158.0765, Found 158.0764.

1-Thiaspiro[4.4]nonan-6-one (133)

132 **133**

A solution of tetrahydrothiophene **132** (0.35 g, 2.2 mmol) in dichloromethane (15 mL) at room temperature under argon was treated with Dess-Martin periodinane (1.0 g, 2.4 mmol) [prepared according to: Dess, P. B.; Martin, J. C. *J. Org. Chem.* **1983**, *48*, 4155] in dichloromethane (10 mL). After stirring for 30 minutes, ether (50 mL) was added and the entire mixture added to an aqueous

10% sodium hydroxide solution (20 mL). The organic layer was washed with aqueous saturated sodium bicarbonate (50 mL), water (50 mL), brine (50 mL), and dried. The solvent was removed *in vacuo* and the residue purified by Kugelrohr distillation (bp 75-90 °C, 0.2 Torr) to give ketone **133** as a colourless oil (0.29 g, 83%); IR (neat, cm^{-1}) 2943, 1742, 1133, 1065; ^1H NMR (200 MHz, $CDCl_3$) δ 2.98 (t, J = 5.6 Hz, H-C-S, 2H), 2.53-1.77 (series of m, 10H); ^{13}C NMR (75 MHz, $CDCl_3$) δ 217.9, 69.9, 39.8, 35.0, 33.2, 31.1, 30.7, 20.2; HRMS Calcd for $C_8H_{12}OS$ (M^+): 156.0608, Found 156.0612; Anal. Calcd for $C_8H_{12}OS$: C, 61.50; H, 7.74; Found: C, 61.55; H, 7.73.

(5*R**, 6*R**)-6-Methyl-1-oxaspiro[4.4]nonan-6-ol (134)

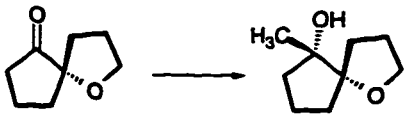

129 **134**

Following the general procedure, ketone **129** (122 mg, 0.87 mmol) in ether (20 mL) under argon at 0 °C was treated dropwise with methyllithium (680 μL, 1.4 M, 0.96 mmol). After stirring for 1 hour and work-up, the mixture was purified to give alcohol **134** (122 mg, 90%) as a colourless oil; IR (neat, cm^{-1}) 3465, 2912, 1438, 1369, 1096; ^1H NMR (200 MHz, $CDCl_3$) δ 3.71 (m, H-C-O, 2H), 2.01-1.51 (series of m, 11H), 1.13 (s, methyl, 3H); ^{13}C NMR (75 MHz, $CDCl_3$) δ 93.2, 81.8, 68.0, 38.6, 36.3, 29.5, 26.5, 21.1, 18.9; HRMS Calcd for $C_9H_{16}O_2$ (M^+): 156.1149, Found 156.1157; Anal. Calcd for $C_9H_{16}O_2$: C, 69.19; H, 10.32; Found: C, 69.39; H, 10.04.

Following the general procedure, ketone **129** (77 mg, 0.55 mmol) in ether (25 mL) under argon at 0 °C was treated dropwise with methylmagnesium bromide (160 μL, 3.0 M, 0.47 mmol). After stirring for 1 hour and work-up, the mixture was purified to give alcohol **134** (80 mg, 93%).

(5*R, 6*R**)-1-Oxaspiro[4.4]nonan-6-ol (130)** and
(5*R, 6*S**)-1-Oxaspiro[4.4]nonan-6-ol (128)**

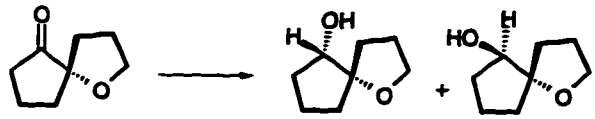

129 **130** **128**

Following the general procedure, ketone **129** (152 mg, 1.08 mmol) in methanol (30 mL) at room temperature was treated with sodium borohydride (45 mg, 1.2 mmol). After stirring for 90 minutes and work-up, the mixture was purified to give alcohol **130** (122 mg, 80%) and alcohol **128** (14 mg, 9%) as colourless oils:

alcohol **130**: IR (neat, cm^{-1}) 3427, 2926, 1447, 1300, 1066; ^1H NMR (200 MHz, $CDCl_3$) δ 3.72 (m, H-C-O, 2H), 3.53 (m, H-C-OH, 1H), 2.42 (d, J = 5.4 Hz, H-O-C, 1H), 2.00-1.33 (series of m, 10H); ^{13}C NMR (50 MHz, $CDCl_3$) δ 90.4, 76.8, 68.1, 35.1, 34.6, 31.9, 26.3, 19.6; HRMS Calcd for $C_8H_{14}O_2$ (M^+): 142.0993, Found 142.1007; Anal. Calcd for $C_8H_{14}O_2$: C, 67.57; H, 9.92. Found: C, 67.51; H, 9.88.

alcohol **128**: IR (neat, cm^{-1}) 3424, 2927, 1447, 1303, 1065; ^1H NMR (200 MHz, $CDCl_3$) δ 3.82 (br m, H-C-OH, 1H), 3.71 (t, J = 6.7 Hz, H-C-O, 2H), 2.22-1.35 (series of m, 11H); ^{13}C NMR (50 MHz, $CDCl_3$) δ 92.3, 77.4, 67.6, 34.6, 31.9, 29.5, 26.1, 19.4; HRMS Calcd for $C_8H_{14}O_2$ (M^+): 142.0993, Found 142.1013.

Following the general procedure, ketone **129** (117 mg, 0.83 mmol) in tetrahydrofuran (25 mL) under argon at room temperature was treated dropwise

with lithium borohydride (460 μL, 2.0 M, 0.92 mmol). After stirring for 1 hour and work-up, the mixture was purified to give alcohols **130** and **128** (111 mg, 94% combined).

Following the general procedure, ketone **129** (110 mg, 0.78 mmol) in dichloromethane (20 mL) under argon at -78 °C was treated dropwise with diisobutylaluminum hydride (575 μL, 1.5 M, 0.86 mmol). After stirring for 2 hours and work-up, the mixture was purified to give alcohols **130** and **128** (102 mg, 92% combined).

Following the general procedure, ketone **129** (100 mg, 0.71 mmol) in ether (20 mL) under argon at 0 °C was treated with lithium aluminum hydride (30 mg, 0.78 mmol). After stirring for 1 hour and work-up, the mixture was purified to give alcohols **130** and **128** (92 mg, 84% combined).

Following the general procedure, ketone **129** (105 mg, 0.75 mmol) in ether (20 mL) under argon at 0 °C was treated dropwise with zinc borohydride (5.9 mL, 0.14 M, 0.82 mmol). After stirring for 2 hours and work-up, the mixture was purified to give alcohols **130** and **128** (91 mg, 85% combined).

Following the general procedure, ketone **129** (100 mg, 0.71 mmol) in a ether: tetrahydrofuran mixture (1:1, 30 mL total) under argon at -42 °C was treated dropwise with zinc borohydride (5.6 mL, 0.14 M, 0.78 mmol). After stirring for 90 minutes and work-up, the mixture was purified to give alcohols **130** and **128** (52 mg, 52% combined).

(5*R, 6*R**)-6-Methyl-1-thiaspiro[4.4]nonan-6-ol (135)**

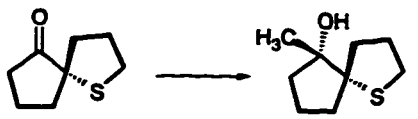

133 135

Following the general procedure, ketone **133** (125 mg, 0.80 mmol) in ether (25 mL) under argon at 0 °C was treated dropwise with methyllithium (630 μL, 1.4 M, 0.88 mmol). After stirring for 1 hour and work-up, the mixture was purified to give alcohol **135** (120 mg, 87%) as a colourless oil; IR (neat, cm^{-1}) 3433, 2931, 1428, 1107; ^1H NMR (200 MHz, $CDCl_3$) δ 2.87 (m, H-C-S, 2H), 2.20-1.53 (series of m, 11H), 1.17 (s, methyl, 3H); ^{13}C NMR (75 MHz, $CDCl_3$) δ 72.5, 66.3, 38.7, 35.0, 33.2, 31.5, 30.3, 21.4, 20.1; HRMS Calcd for $C_9H_{16}OS$ (M^+): 172.0925, Found 172.0935; Anal. Calcd for $C_9H_{16}OS$: C, 62.74; H, 9.36. Found: C, 62.69; H, 9.17.

Following the general procedure, ketone **133** (110 mg, 0.70 mmol) in ether (25 mL) under argon at 0 °C was treated dropwise with methylmagnesium bromide (255 μL, 3.0 M, 0.77 mmol). After stirring for 1 hour and work-up, the mixture was purified to give alcohol **135** (96 mg, 80%).

(5*R, 6*S**)-1-Thiaspiro[4.4]nonan-6-ol (136)** and **(5*R**, 6*R**)-1-Thiaspiro[4.4]nonan-6-ol (132)**

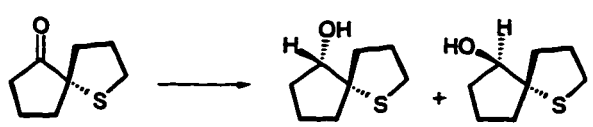

133 136 132

Following the general procedure, ketone **133** (250 mg, 1.60 mmol) in methanol (50 mL) at room temperature was treated with sodium borohydride (67

mg, 1.76 mmol). After stirring for 90 minutes and work-up, the mixture was purified to give alcohol **136** (200 mg, 79%) and alcohol **132** (25 mg, 10%) as colourless oils:

alcohol **136**: IR (neat, cm^{-1}) 3442, 2933, 1320, 1112; ^1H NMR (200 MHz, $CDCl_3$) δ 4.08 (m, H-C-OH, 1H), 2.81 (m, H-C-S, 2H), 2.11-1.45 (series of m, 11H); ^{13}C NMR (50 MHz, $CDCl_3$) δ 78.8, 67.2, 38.2, 34.9, 32.9, 31.3, 30.3, 20.0; HRMS Calcd for $C_8H_{14}OS$ (M^+): 158.0765, Found 158.0758; Anal. Calcd for $C_8H_{14}OS$: C, 60.71; H, 8.92. Found: C, 60.62; H, 8.88.

alcohol **132**: IR (neat, cm^{-1}) 3440, 2931, 1315, 1105; ^1H NMR (200 MHz, $CDCl_3$) δ 4.02 (m, H-C-OH, 1H), 2.88 (m, H-C-S, 2H), 2.16-1.45 (series of m, 11H); ^{13}C NMR (50 MHz, $CDCl_3$) δ 78.9, 67.1, 38.9, 35.1, 33.0, 31.2, 30.4, 19.7; HRMS Calcd for $C_8H_{14}OS$ (M^+): 158.0758, Found 158.0745.

Following the general procedure, ketone **133** (107 mg, 0.68 mmol) in tetrahydrofuran (20 mL) under argon at room temperature was treated dropwise with lithium borohydride (375 μL, 2.0 M, 0.75 mmol). After stirring for 1 hour and work-up, the mixture was purified to give alcohols **136** and **132** (101 mg, 94% combined).

Following the general procedure, ketone **133** (77 mg, 0.49 mmol) in dichloromethane (20 mL) under argon at -78 °C was treated dropwise with diisobutylaluminum hydride (360 μL, 1.5 M, 0.54 mmol). After stirring for 90 minutes and work-up, the mixture was purified to give alcohols **136** and **132** (63 mg, 81% combined).

Following the general procedure, ketone **133** (103 mg, 0.66 mmol) in ether (25 mL) under argon at 0 °C was treated with lithium aluminum hydride (27 mg,

0.72 mmol). After stirring for 30 minutes and work-up, the mixture was purified to give alcohols **136** and **132** (85 mg, 81% combined).

Following the general procedure, ketone **133** (98 mg, 0.63 mmol) in ether (25 mL) under argon at 0 °C was treated dropwise with zinc borohydride (4.9 mL, 0.14 M, 0.69 mmol). After stirring for 1 hour and work-up, the mixture was purified to give alcohols **136** and **132** (86 mg, 86% combined).

General Procedure for Epoxidation and Subsequent Reduction Reactions

A stirred suspension of trimethylsulfoxonium iodide in tetrahydrofuran under argon at 0 °C was treated dropwise with *n*-BuLi [trimethylsulfoxonium iodide was prepared as follows: A solution of methylsulfoxide (30 mL, 0.42 mol) in iodomethane (60 mL, 0.96 mol) was heated to reflux and maintained at this temperature for 15 hours. The resultant white solid was washed with chloroform, dried under high vacuum and used without further purification]. After stirring for 5 minutes, a solution of the ketone in tetrahydrofuran was added dropwise and the mixture stirred at 0 °C for 30 minutes and stirred further for the indicated time at room temperature. Water was then added to quench any unreacted reagent and the aqueous phase extracted with ether. The combined organic phases were analyzed by GC-MS, washed with water, brine, dried and concentrated *in vacuo*. Purification of the residue by silica gel chromatography (elution with 25% ether in petroleum ether) gave the resultant epoxides. The epoxide which had formed in the greatest yield was diluted with ether, cooled to 0 °C under argon and treated with lithium aluminum hydride. After stirring for the indicated amount of time, the reaction mixture was treated with an aqueous solution of saturated ammonium chloride and the organic phase analyzed by GC-MS.

(3*S, 4*R**)-Acenapthenequinone-(1,5-dioxa-8-thia-dispiro[2.0.4.3]undecane) (141) and (3*R**, 4*R**)-Acenapthenequinone-(1,5-Dioxa-8-thia-dispiro[2.0.4.3]undecane) (142)**

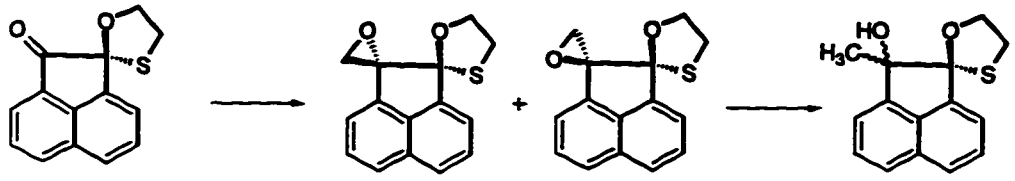

114 141 142

Following the general procedure, a stirred suspension of trimethylsulfoxonium iodide (0.42 g, 1.9 mol) in tetrahydrofuran (30 mL) under argon at 0 °C was treated dropwise with *n*-butyllithium (690 µL, 2.5 M, 1.7 mmol). After stirring for 5 minutes, a solution of ketone **114** (0.38 g, 1.5 mmol) in tetrahydrofuran (5 mL) was added dropwise and the mixture stirred for 30 minutes at 0 °C. The reaction was warmed to room temperature and stirred for an additional 30 minutes. Work-up and purification gave epoxides **141** (330 mg, 82%) and **142** (24 mg, 6%) as colourless oils:

epoxide **141**: IR (neat, cm^{-1}) 3050, 2972, 1494, 1250, 1069; ^1H NMR (200 MHz, $CDCl_3$) δ 7.74 (m, H-Ar, 2H), 7.55 (m, H-Ar, 3H), 7.21 (m, H-Ar, 1H), 4.40 (m, H-C-$O_{oxathiolane}$, 2H), 3.63 (d, J = 5.4 Hz, H-C-$O_{epoxide}$, 1H), 3.41-3.22 (series of m, 3H); ^{13}C NMR (50 MHz, $CDCl_3$) δ 142.8, 136.5, 136.1, 130.2, 128.5, 128.4, 125.5, 125.3, 120.4, 117.8, 99.4, 73.0, 70.4, 55.4, 34.6; HRMS Calcd for $C_{15}H_{12}O_2S$ (M^+): 256.0557, Found 256.0551.

epoxide **142**: IR (neat, cm^{-1}) 3050, 2968, 1495, 1255, 1061; ^1H NMR (200 MHz, $CDCl_3$) δ 7.76 (m, H-Ar, 2H), 7.49 (m, H-Ar, 3H), 7.22 (m, H-Ar, 1H), 4.42 (m, H-C-$O_{oxathiolane}$, 2H), 3.59 (d, J = 5.5 Hz, H-C-$O_{epoxide}$, 1H), 3.51-3.20 (series of m, 3H); ^{13}C NMR (50 MHz, $CDCl_3$) δ 130.8, 129.1, 129.0, 128.9, 126.4, 126.1, 125.8,

123.6, 121.8, 118.3, 97.3, 72.7, 58.3, 35.6, 31.5; HRMS Calcd for $C_{15}H_{12}O_2S$ (M^+): 256.0557, Found 256.0549.

A solution of epoxide **141** (0.10 g, 0.39 mmol) in ether (15 mL) under argon at room temperature was treated with lithium aluminum hydride (22 mg, 0.58 mmol), and the mixture heated to reflux and maintained at this temperature for 2 hours. The mixture was then cooled, treated with an aqueous solution of saturated ammonium chloride, and the organic phase analyzed by GC-MS.

(3*S, 4*R**)-1,5-Dioxa-8-thia-dispiro[2.0.4.3]undecane (139)** and **(3*R**, 4*R**)-1,5-Dioxa-8-thia-dispiro[2.0.4.3]undecane (140)**

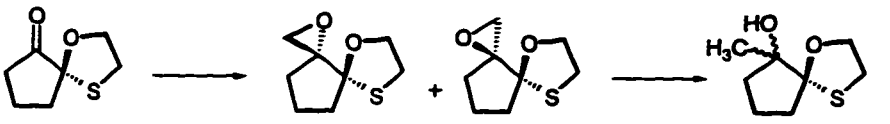

108 139 140

Following the general procedure, a stirred suspension of trimethylsulfoxonium iodide (0.26 g, 1.2 mmol) in tetrahydrofuran (15 mL) under argon at 0 °C was treated dropwise with *n*-butyllithium (435 µL, 2.5 M, 1.1 mmol). After stirring for 5 minutes, a solution of ketone **108** (156 mg, 0.99 mmol) in tetrahydrofuran (5 mL) was added dropwise and the mixture stirred for 30 minutes at 0 °C. The reaction was warmed to room temperature and stirred for an additional 2 hours. Work-up and purification gave epoxides **139** (139 mg, 82%) and **140** (15 mg, 9%) as colourless oils:

epoxide **139**: IR (neat, cm^{-1}) 2980, 1388, 1245, 1022; ^1H NMR (200 MHz, $CDCl_3$) δ 4.41 (m, H-C-$O_{oxathiolane}$, 2H), 3.61 (d, J = 5.5 Hz, H-C-$O_{epoxide}$, 1H), 3.08 (m, 3H), 2.37-1.52 (series of m, 6H); ^{13}C NMR (50 MHz, $CDCl_3$) δ 99.7, 71.8, 71.3, 50.2, 37.2, 29.4, 21.0, 20.4; HRMS Calcd for $C_8H_{12}O_2S$ (M^+): 172.0557, Found 172.0555.

epoxide **140**: IR (neat, cm^{-1}) 2967, 1401, 1225, 1109; ^1H NMR (200 MHz, $CDCl_3$) δ 4.38 (m, H-C-$O_{oxathiolane}$, 1H), 4.10 (m, H-C-$O_{oxathiolane}$, 1H), 3.60 (d, J = 5.5 Hz, H-C-$O_{epoxide}$, 1H), 3.11 (m, 3H), 2.22-1.48 (series of m, 6H); ^{13}C NMR (50 MHz, $CDCl_3$) δ 98.3, 71.4, 69.4, 48.3, 39.2, 30.2, 20.1, 19.2; HRMS Calcd for $C_8H_{12}O_2S$ (M^+): 172.0557, Found 172.0561.

A solution of epoxide **139** (0.10 g, 0.59 mmol) in ether (10 mL) under argon at room temperature was treated with lithium aluminum hydride (33 mg, 0.87 mmol), and the mixture heated to reflux and maintained at this temperature for 1 hour. The mixture was then cooled, treated with an aqueous solution of saturated ammonium chloride, and the organic phase analyzed by GC-MS.

(3*R**, 4*R**)-1,5-Dioxa-dispiro[2.0.4.3]undecane (137)

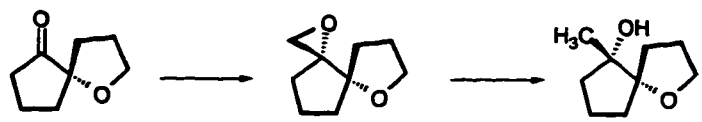

129 **137** **134**

Following the general procedure, a stirred suspension of trimethylsulfoxonium iodide (0.31 g, 2.2 mmol) in tetrahydrofuran (15 mL) under argon at 0 °C was treated dropwise with *n*-butyllithium (820 µL, 2.5 M, 2.0 mmol). After stirring for 5 minutes, a solution of ketone **129** (260 mg, 1.8 mmol) in tetrahydrofuran (5 mL) was added dropwise and the mixture stirred for 30 minutes at 0 °C. The reaction was warmed to room temperature and stirred for an additional 3 hours. Work-up and purification gave epoxide **137** (0.32 g, 93%) as a colourless oil; IR (neat, cm^{-1}) 2977, 1372, 1245, 1039; ^1H NMR (200 MHz, $CDCl_3$) δ 3.70-3.59 (series of m, 4H), 2.04-1.48 (series of m, 10H); ^{13}C NMR (50 MHz,

$CDCl_3$) δ 91.4, 88.3, 73.4, 71.5, 32.1, 32.0, 21.4, 20.9, 19.9; HRMS Calcd for $C_9H_{14}O_2$ (M^+): 154.0993, Found 154.0990.

A solution of epoxide **137** (107 mg, 0.69 mmol) in ether (10 mL) under argon at room temperature was treated with lithium aluminum hydride (40 mg, 1.0 mmol), and the mixture heated to reflux and maintained at this temperature for 1 hour. The mixture was then cooled, treated with an aqueous solution of saturated ammonium chloride, and the organic phase analyzed by GC-MS.

Appendix

X-ray Crystallographic Data

	compound		
	51	**112**	**114**
formula	$C_{16}H_{10}SO_5$	$C_{18}H_{18}NSO_3$	$C_{14}H_{12}SO_2$
formula weight	320.26	328.40	242.24
crystal system	monoclinic	orthorombic	monoclinic
space group	P 21/a	P bca	C 2/c
a (Å)	10.472 (3)	15.576 (18)	21.796 (5)
b (Å)	12.446 (3)	22.002 (9)	10.904 (4)
c (Å)	12.4374 (16)	9.682 (5)	11.335 (2)
B (deg.)	108.418 (14)	104.349 (15)	91.845 (16)
V (Å^3)	1537.6 (6)	1385.4 (8)	2692.5 (12)
D (g/cm^3)	1.453	1.315	1.388
Z value	4	8	8
Rf; Rw	0.117; 0.97	0.086; 0.048	0.061;0.050

X-ray Crystallographic Data

	compound	
	115	**118**
formula	$C_{15}H_{14}SO_2$	$C_{14}H_{12}SO_2$
formula weight	258.33	244.31
crystal system	monoclinic	monoclinic
space group	P 21/c	P 21/n
a (Å)	14.143 (4)	7.854 (5)
b (Å)	5.594 (3)	7.901 (3)
c (Å)	16.1288 (24)	18.979 (6)
B (deg.)	108.583 (15)	90.718 (40)
V ($Å^3$)	1209.5 (7)	1177.08 (5)
D (g/cm^3)	1.419	1.379
Z value	4	4
Rf; Rw	0.032; 0.026	0.048; 0.069